On the Cosmology of String Axions

Dissertation
zur Erlangung des Doktorgrades
an der Fakultät für Mathematik, Informatik und Naturwissenschaften
Fachbereich Physik
der Universität Hamburg

vorgelegt von

Nicole Righi

Hamburg
2022

Gutachter/innen der Dissertation:	Dr. Alexander Westphal Prof. Dr. Jan Louis
Zusammensetzung der Prüfungskommission:	Prof. Dr. Dieter Horns Prof. Dr. Jan Louis Prof. Dr. Geraldine Servant Prof. Dr. Timo Weigand Dr. Alexander Westphal
Vorsitzende/r der Prüfungskommission:	Prof. Dr. Dieter Horns
Datum der Disputation:	22.06.2022
Vorsitzender Fach-Promotionsausschuss PHYSIK:	Prof. Dr. Wolfgang J. Parak
Leiter des Fachbereichs PHYSIK:	Prof. Dr. Günter H. W. Sigl
Dekan der Fakultät MIN:	Prof. Dr. Heinrich Graener

Eidesstattliche Versicherung / Declaration on oath

Hiermit versichere ich an Eides statt, die vorliegende Dissertationsschrift selbst verfasst und keine anderen als die angegebenen Hilfsmittel und Quellen benutzt zu haben.

Hamburg, den 17.05.2022

Unterschrift der Doktorandin / des Doktoranden

Abstract

In this thesis, we discuss various aspects of the phenomenology of axion fields originating from the compactification of type IIB superstring theory. First, we give an overview of moduli stabilisation and string axions. Starting from their origin as p-form gauge potentials integrated over p-cycles of the internal manifold, we discuss how they behave as four-dimensional effective fields and how they relate with certain swampland conjectures, namely the axionic version of the Weak Gravity Conjecture and the Festina Lente bound. Moreover, we study the effective theory of thraxions, i.e. ultralight axionic modes living in warped throats of Calabi-Yau manifolds.

Then, we move to cosmology and in particular we focus on inflation and dark matter, two open issues which could find a solution once axions are taken into account. After reviewing the inflationary dynamics and some of the main proposals of axion inflation, we proceed to discuss how to realise hybrid inflation with axions supplying also a way to UV-complete the model. Moreover, and we provide a new approach to winding inflation, where the inflationary sector and dynamics arise from the complex structure moduli and are governed by certain topological invariants of the Calabi-Yau.

Finally, we give a string-theoretical explanation of fuzzy dark matter as made of ultralight axions coming from type IIB compactifications. We show how it is possible to obtain such light axions in the type IIB axiverse including also thraxions, and we relate them with the present observational constraints. This allows us to both restrict the parameter space where future experiments could possibly detect string axions, and to use the observational bounds to put constraints on the UV theory and the compact dimensions.

Zusammenfassung

In dieser Dissertation behandeln wir verschiedene Aspekte der Phänomenologie von Axionen, welche in Kompaktifizierungen der Typ IIB Stringtheorie auftreten. Zunächst geben wir einen Überblick über die Modulistabilisierung und Axionen in der Stringtheorie. Ausgehend von Ihrem Ursprung als Integral von p-Form Eichpotentialen über p-Zykel der internen Mannigfaltigkeit diskutieren wir, wie sich Axionen als vierdimensionale effektive Felder verhalten und wie sie mit bestimmten Swampland Vermutungen wie der Weak Gravity Conjecture und dem Festina Lente Bound in Verbindung stehen. Weiterhin analysieren wir die effektive Theorie ultraleichter axionischer Moden in warped throat Regionen von Calabi-Yau Mannigfaltigkeiten, sogenannter Thraxionen.

Anschließend wenden wir uns der Kosmologie zu, mit besonderem Augenmerk auf die Probleme der kosmologischen Inflation und der dunklen Materie, welche möglicherweise in der Axionphysik eine Lösung finden könnten. Nachdem wir die inflationäre Dynamik und einige Modelle der Axion-Inflation beschreiben, erörtern wir, wie hybrid inflation mittels Axionen realisiert werden kann und schlagen eine UV-Vervollständigung dieses Modells vor. Außerdem präsentieren wir einen neuen Ansatz für winding inflation Modelle, in welchem der inflationäre Sektor und dessen Dynamik aus den Moduli der komplexen Struktur einer Calabi-Yau entspringt und durch topologische Invarianten dieser bestimmt wird.

Schlussendlich liefern wir eine stringtheoretische Erklärung von fuzzy dark matter, in welcher diese aus ultraleichten Axionen in Typ IIB Kompaktifizierungen besteht. Wir zeigen auf, wie es möglich ist, solche leichten Axionen im IIB Axiversum zu realisieren und untersuchen die Kompatibilität mit aktuellen experimentellen Beobachtungen. Dies ermöglicht es uns den Parameterbereich einzuschränken, in welchem zukünftige Experimente möglicherweise String-Axionen finden könnten. Weiterhin können wir die UV-Theorie sowie die kompakten Raumdimensionen hierdurch einschränken.

This thesis is based on the publications:

Festina Lente bound for axions
V. Guidetti, N. Righi, G. Venken, A. Westphal
arXiv: *to appear*

Fuzzy dark matter candidates from String Theory [1]
M. Cicoli, V. Guidetti, N. Righi, A. Westphal
arXiv: 2110.02964 [hep-th]

Thraxions: towards full string models [2]
F. Carta, A. Mininno, N. Righi, A. Westphal
JHEP 01 (2022) 082, arXiv: 2110.02963 [hep-th]

Gopakumar-Vafa hierarchies in winding inflation and uplifts [3]
F. Carta, A. Mininno, N. Righi, A. Westphal
JHEP 05 (2021) 271, arXiv: 2101.07272 [hep-th]

Harmonic hybrid inflation [4]
F. Carta, N. Righi, Y. Welling, A. Westphal
JHEP 12 (2020) 161, arXiv: 2007.04322 [hep-th]

Ai miei genitori.

Contents

1 Introduction to Axion Cosmology **1**

2 String Axions **5**

2.1 Compactification and low-energy EFT 6

2.1.1 Calabi-Yau compactification and moduli spaces 7

2.1.2 Branes and fluxes 12

2.1.3 Kähler moduli stabilisation 13

2.2 Closed string axions 16

2.3 String axions and the swampland 17

2.3.1 Festina Lente bound for axions 21

2.4 Thraxions 23

2.4.1 Thraxions in flux compactification 23

2.4.2 Moduli stabilisation 29

2.4.3 General structure of the superpotential in the presence of thraxions 30

2.4.4 Vanishing conditions of the $\mathcal{O}(\varepsilon)$ cross terms and application to KKLT 32

2.4.5 Behaviour of the $\mathcal{O}(\varepsilon)$ thraxion mass cross terms in LVS 35

2.4.6 Mass scales for thraxion setups in KKLT and LVS 36

2.4.7 Comments about the 10d origin of the cross terms 38

3 Inflation in String Theory and Axions as Inflatons **41**

3.1 Basics of inflation 42

3.2 Inflation in String Theory 46

3.3 Axions as inflatons 47

3.3.1 Natural inflation and field space alignment 48

3.3.2 Axion monodromy inflation 49

3.4 Harmonic hybrid inflation 52

3.4.1 Effect of instanton-induced phases 55

3.4.2 $\mathbb{Z}_2$ symmetry breaking effects 56

3.4.3 Comments about eternal inflation and vacuum decay 61

3.4.4 Towards a String Theory embedding 62

3.5 Winding inflation and de Sitter uplift 65

3.5.1 Inflationary sector 68

3.5.2 De Sitter uplift 70

3.5.3 Combining inflation and uplift 71

3.6 Discussion 75

4 Fuzzy Dark Matter from String Axions **78**
4.1 Basics of dark matter . . . 78
4.2 String origin of ultralight axionic DM candidates . . . 82
4.2.1 LVS: FDM from C_4 axions . . . 85
4.2.2 LVS: FDM from C_2 axions . . . 90
4.2.3 FDM from Thraxions: KKLT & LVS? . . . 96
4.3 Overall predictions and comparison with experimental constraints . . . 100
4.4 Discussion . . . 102

5 Conclusions and Outlook **105**

Appendix A Complete Intersection Calabi-Yaus **108**

Appendix B Concrete Calabi-Yau Orientifolds Supporting Thraxions **114**

Appendix C A database of GV invariants for CICYs **120**

Appendix D String Axion Appendices **124**
D.1 Closed string axions: Sf computations . . . 124
D.2 Open string axions computations . . . 126
D.3 Additional corrections for C_4 axions . . . 128
D.4 Anharmonicity and isocurvature bounds . . . 130

Bibliography **141**

Chapter 1

Introduction to Axion Cosmology

> *È geniale questa cosa che i giorni finiscono. È un sistema geniale. I giorni e poi le notti. E di nuovo i giorni. Sembra scontato, ma c'è del genio. E là dove la natura decide di collocare i propri limiti, esplode lo spettacolo. I tramonti.* [1]
>
> — Alessandro Baricco, *Oceano Mare*

A general prediction of String Theory is the presence of axions in the low-energy effective theory. In this context, axions have several fascinating properties. For example, they show properties of the ultraviolet (UV)-completed theory at the level of testable Physics. Furthermore, axions also serve as promising candidates to solve fascinating puzzles in Cosmology. It is remarkable that at the moment of writing we still lack for evidence of their existence, while many clues point in that direction. Their (ultra)light masses and feeble interactions with the Standard Model make them almost invisible, and the experimental effort to detect them grows every year, spanning from astrophysical observations to lattice simulations. At the same time, these properties are precisely the reason they are appealing for stringy-inspired model building.

The phenomenological features of string axions (i.e. axion fields that derive from ten-dimensional superstring theories) crucially depend on the details of the *compactification*, namely on the way the extra dimensions get 'integrated out' to obtain a low-energy theory, leaving traces of their presence in our four-dimensional universe. Hence, in my opinion, it is of great importance to study the axionic parameter space predicted by String Theory. This allows for targeted searches, as well as to gather hints on the details of the compactification based on experimental bounds. This thesis adopts this perspective and is thus devoted to show the deep connections between string axions and the universe. Before turning to String Theory and Cosmology, we review the genesis of axions as fields endowed with a *shift symmetry*. This unique feature will follow us throughout our discussions.

QCD axions

Quantum chromodynamics (QCD) suffers from the so-called strong-CP problem. This originates from the fact that the QCD Lagrangian allows for a total derivative term of the form

$$\mathcal{L}_{\rm QCD} \supset \frac{g^2}{32\pi^2}\theta\, F_{\mu\nu}\tilde{F}^{\mu\nu}\,, \tag{1.1}$$

[1] It is brilliant this thing that days end. It is a brilliant system. Days and then nights. And then days again. It seems obvious, but there is genius. And there, where nature decide to place its own limits, the view explodes. The sunsets.

where $F_{\mu\nu}$ is the gluonic field strength whose trace runs over the colour SU(3) indices, g is the strong coupling constant and $\theta \in [0, 2\pi]$ is a parameter coming from the non-trivial structure of the QCD vacuum [5]. The problem lies in the value that θ should take. The Lagrangian term in (1.1) is odd under CP since it violates parity but conserves charge symmetry, and so it produces CP-violating effects, such as a non-vanishing electric dipole moment d_n of the neutron. If $\theta \sim \mathcal{O}(1)$, the value of d_n produced by (1.1) is $\sim 10^{10}$ times larger than the experimental upper bounds. In order to be consistent with observations, θ should be smaller than 10^{-10}. If there were only CP-conserving strong interactions, then θ could be simply set to zero. The actual issue arises when we consider also the electroweak sector, since it violates CP. The Lagrangian term for weak interactions takes the form $\mathcal{L}_w = \bar{q}_{i,R} M_{ij} q_{j,L}$+h.c. and in order to diagonalise the mass matrix, one has to perform a chiral rotation of the quark fields. This rotation does affect the QCD vacuum as well, as it changes the parameter θ in (1.1) as $\theta = \tilde{\theta} + \arg\det M$, where $\tilde{\theta}$ is the bare parameter. It is now clear that a value of $\theta < 10^{-10}$ represents a fine-tuning problem called the strong-CP problem.

A possible solution to the strong-CP problem was proposed in 1977 by Roberto Peccei and Helen Quinn [6] and developed further the year after by Steven Weinberg [7] and Frank Wilczek [8]. In their work, Peccei and Quinn (PQ) showed that, by introducing a new global $\mathrm{U}(1)_{\mathrm{PQ}}$ symmetry that is spontaneously broken, θ can be dynamically set to zero. Then Weinberg and Wilczek independently pointed out that such a global symmetry also implies the presence of a (pseudo) Nambu-Goldstone (pNG) boson, i.e. an *axion*. Therefore, the introduction of the $\mathrm{U}(1)_{\mathrm{PQ}}$ symmetry in the theory replaces the static angle with a dynamical field. This procedure is called misalignment mechanism and can be summarized as follows. First, after the spontaneous breaking of the $\mathrm{U}(1)_{\mathrm{PQ}}$ symmetry, θ is promoted to a dynamical field $\theta(x)$ with a kinetic term in the Lagrangian of the form

$$\mathcal{L}_{\mathrm{kin}} = \frac{1}{2} f^2 \left(\partial\theta(x)\right)^2 ,$$

where f has the dimension of a mass and is known as the *axion decay constant*. Since conventionally a scalar field has mass dimension one, we can canonically normalise $a(x) \equiv \theta(x) f$. The contribution to the total Standard Model Lagrangian given by $a(x)$ reads

$$\mathcal{L} = \frac{1}{2} \left(\partial a(x)\right)^2 + \frac{g^2}{32\pi^2} \frac{a(x)}{f} F_{\mu\nu} \tilde{F}^{\mu\nu} . \tag{1.2}$$

Remarkably, (1.2) exhibits a continuous shift symmetry for the axion under $a(x) \to a(x) + fc$, c being a constant. This symmetry is preserved at the perturbative level and for energies bigger than Λ_{QCD}. However, when non-perturbative (QCD instanton) effects switch on at Λ_{QCD}, the shift symmetry is broken explicitly and a receives a periodic potential of the form

$$V = \Lambda_{\mathrm{QCD}}^4 \left(1 - \cos\left(\frac{a}{f}\right)\right) .$$

Minimising the potential with respect to a gives the Peccei-Quinn solution: at $\langle a(x)\rangle = 0$, θ is set to zero dynamically, forcing the theory to be CP-symmetric. The proof of CP-conservation of the instanton-corrected action is known as the Vafa-Witten theorem [9], which guarantees that the instanton potential is minimised at the CP-conserving value. Hence, the QCD axion mass is given by $m = \Lambda_{\mathrm{QCD}}^2 / f$.

A combination of collider and astrophysical experiments has given some rigid constraints to the value of f for the QCD axion, which turns out to be typically rather high, of order $10^9 \lesssim f \lesssim 10^{12}$ GeV, while the value of the non-perturbative scale is much lower, namely $\Lambda_{\mathrm{QCD}} \sim 200$ MeV. In the

relation above, the lower bound is given by astrophysical observations, whereas the upper bound comes from dark matter overproduction for $\theta \sim \mathcal{O}(1)$ (which means that the upper bound could be relaxed if $\theta \ll 1$). Therefore, we can see that the axion has a parametrically small mass and from the last term in (1.2) it follows that it exhibits very feeble interactions. Such a light particle can have very interesting implications in Cosmology. Since it is stable on cosmological timescales, if an axionic population had been produced in the early universe, it would have survived until nowadays, allowing for a possible detection. Moreover, at very high energies, an axion could drive an epoch of primordial expansion in the universe. We will delve further on these interesting aspects in Chapter 4 and Chapter 3 respectively.

pNG vs. fundamental axions

So far, we have discussed a particular, semi-classical axion, the QCD one. However, in this thesis we will be mostly interested in a slightly different type of axions. In the language introduced lately in the literature [10], we will distinguish pNG bosons from *fundamental axions*. A pNG boson can be parametrised as the complex phase of a scalar field, while a fundamental axion is the imaginary part of a complex modulus. The latter is purely originating from String Theory as a *closed string axion*, and it is present in all string compactifications. Actually, in a general Calabi-Yau compactification, hundreds of them can be present. One source of such fundamental axions are higher-dimensional p-form gauge potentials ($p \geq 1$), with the fields arising from the integral of gauge potentials over p-cycles of the compact dimensions.

This distinction is useful in the context of Quantum Gravity: for a pNG boson, there is a point in the field space where the decay constant can vanish, and this point can be described by within the low-energy EFT. On the contrary, for a fundamental axion the point where the decay constant shrinks to zero corresponds to an infinite volume limit, where the effective description breaks down and hence cannot be reached in a consistent effective theory [11, 12]. It is also conjectured that string axions cannot acquire trans-Planckian decay constants while keeping the theory under control [13–16]. This conjecture goes under the name of *Weak Gravity Conjecture* (WGC)[2] and belongs to a class of Swampland conjectures [17] that aim to distinguish effective theories which can be UV-completed to Quantum Gravity from those which cannot. While these conjectures are still under inspection, if true they would put severe constraints also on the phenomenology of string axions. Conversely, experimental bounds on axion-like particles and possible future astrophysical signatures would prove or modify appropriately the conjectures, allowing for a better understanding of the correct UV completion.

Outline

Since fundamental axions will play a prominent role in Chapters 3 and 4, in Chapter 2 we review how they arise from String Theory in the low-energy effective theory and we describe their properties as effective particles. We will focus on the so-called type IIB string *axiverse* [18] which arises by compactifying type IIB superstring theory on a Calabi-Yau (CY) threefold equipped with internal cycles. We choose to work in this corner of the string landscape as its formulation is at weak coupling in the string coupling g_s, allowing for perturbative control. Indeed, this setup is one of the most studied in the literature, and this will allow us to perform detailed computations and derive solid conclusions. Nevertheless, when possible we will try to highlight the connections with the other superstring theories, in particular of their four-dimensional *moduli spaces*, see Section 2.1. After deriving the axionic $4d$ EFT, we explore

[2]The name derives from the original formulation: in every consistent low energy EFT of gravity and electromagnetism there should exist at least one light charged particle with mass m and U(1) charge e such that $m \lesssim eM_P$, i.e. gravity should always be the weakest force. We dedicate Section 2.3 to this topic and its relation with axions.

it in Section 2.3 in the context of the Swampland program, where we give an explicit derivation of the WGC for axions, and we propose a new EFT criterion, namely the *axionic Festina Lente* bound. Finally, we present a detailed study on compactification in the presence of warped throats hosting axionic modes dubbed *thraxions*. While their $4d$ effective theory is complex and requires further study, their phenomenology is appealing and they widen the predicted parameter space of type IIB string axiverse.

In Chapter 3 we start developing the Cosmology of string axions, beginning with *inflation*. With the term inflation, we refer to an epoch of accelerated expansion that is believed to have occurred when the universe was around 10^{-32} seconds old. These fractions of a second are actually crucial to explain the universe we observe today, however we lack a precise description of what exactly happened during this epoch and which particle(s) were responsible for such unique dynamics. Indeed, given that inflation should have taken place at high energies,[3] it must be deeply tied with quantum-gravitational effects. Therefore, after giving an overview of inflation and its relation with String Theory in Section 3.2, we introduce some of the most prominent models of axion inflation, namely KNP alignment and axion monodromy. After that, in Section 3.4 we first present a new way to obtain hybrid inflation with string axions, then in Section 3.5 we discuss how the topological data of the extra dimensions can help in realising inflationary directions, as well as a positive cosmological constant.

After studying the early history of our universe, in Chapter 4 we move to present days and delve into the problem of the missing visible mass, i.e. the famous *dark matter*. We first explain how 'dark matter came to matter' [19] and how ultralight axions can be good dark matter candidates, in particular as *fuzzy dark matter*. After reviewing why String Theory naturally populates the universe with these axions, we inspect how closed string axions and thraxions relate with current astrophysical bounds. Finally, we also comment on the compactifications that could provide the right candidates, and how likely they are in the string landscape.

To close this introduction, let us point out how exciting it is that so many experiments are now looking for (string) axions, and what great amount of knowledge about the UV completion a detection would bring us. In the end, axions may yet turn out to be the missing link towards testing String Theory.

[3] If it happened at all, but in this thesis we will assume that an inflationary epoch has occurred at some point in the history of our universe

Chapter 2

String Axions

Ask me, then, if I believe in the spirit of the things as they were used, and I'll say yes. They're all here. All the things which had uses. All the mountains which had names. And we'll never be able to use them without feeling uncomfortable. And somehow the mountains will never sound right to us; we'll give them new names, but the old names are there, somewhere in time, and the mountains were shaped and seen under those names. The names we'll give to the canals and mountains and cities will fall like so much water on the back of a mallard. No matter how we touch Mars, we'll never touch it. And then we'll get mad at it, and you know what we'll do? We'll rip it up, rip the skin off, and change it to fit ourselves."

— Ray Bradbury, *The Martian Chronicles*

A generic prediction of string phenomenology models is the presence of axion-like particles in the low energy spectrum below the compactification scale. They arise in the compactification process as the Kaluza-Klein zero modes of $10d$ antisymmetric tensor fields by taking integrals of higher p-form gauge potentials on p-cycles of the internal space. The number and properties of these particles are determined essentially by the ten-dimensional origin, hence by the topology of the internal manifold. In this chapter, we will focus on closed string axions: we will show how they generically arise from compactifying the higher dimensional theory, and we will describe their features in the $4d$ effective supergravity description.

Some unique properties of string axions make them interesting from a phenomenological point of view [18,20–23], for example in the context of inflation, or as possible dark matter constituents. Moreover, their features are of central prominence in the Swampland program [11,17], especially in the context of the Weak Gravity Conjecture [13]. Hence, axions represent a promising class of particles which could provide information about the underlying theory of quantum gravity at the level of testable physics. Many of the next-generation experiments will partially cover the parametric space where string axions are expected to live. In addition, thanks to the discovery of gravitational waves [24], there is now a completely new window where one could detect their effect on gravitational phenomena, such as the superradiance instability of binary black holes (BHs) [23] (for recent progress in linking large-scale CY database scans with the BH superradiance constraints for axions see e.g. [25]).

In this chapter, we discuss how string axions appear in the $4d$ effective theory. We first give an

overview of the compactification from $10d$ down to $4d$, mostly focusing on type IIB string theory, but highlighting the connections to the other superstring theories. Then we describe the spectrum obtained from compactifying on a Calabi-Yau threefold, focusing especially on axions fields. Then, we discuss some properties that these fields should satisfy in the IR in order to have a consistent UV completion, i.e. we present a part of the swampland program which concern axions. Finally, we introduce a newly-discovered class of axionic modes, called thraxions, and we give a $4d$ effective treatment in the context of moduli stabilisation.

2.1 Compactification and low-energy EFT

We start by considering type IIB superstring theory in $10d$, $\mathcal{N}=2$. The $10d$ action in Einstein frame is given by

$$S_{\rm IIB}=\frac{1}{2\kappa_{10}^2}\int \mathrm{d}^{10}x\sqrt{-G}\left(R-\frac{1}{2}\left|\frac{\partial\tau}{\mathrm{Im}\,\tau}\right|^2-\frac{|G_3|^2}{2\mathrm{Im}\,\tau}-\frac{1}{4}|\tilde{F}_5|^2\right)+\frac{1}{8i\kappa_{10}^2}\int\frac{C_4\wedge G_3\wedge\bar{G}_3}{\mathrm{Im}\,\tau}\,, \tag{2.1}$$

where G_3 is the complex three-form $G_3=F_3-\tau H_3$ and $\tau=C_0+ie^{-\phi}$ is the axio-dilaton, and we use the notation $|F_p|^2=(p!)^{-1}F_{M_1\dots M_p}F^{M_1\dots M_p}$. The field strengths are defined in terms of the gauge potentials as

$$H_3=dB_2\,,\quad F_3=dC_2\,,\quad \tilde{F}_5=dC_4-\frac{1}{2}dC_2\wedge dB_2+\frac{1}{2}B_2\wedge dC_2\,. \tag{2.2}$$

Self-duality of $\tilde{F}_5$ must be supplemented by hand to the equations of motion. In addition to supersymmetry, the theory enjoys p-form gauge invariance and invariance under an $\mathrm{SL}(2,\mathbb{R})$ symmetry which leaves the metric and C_4 invariant and acts on the remaining fields as

$$\tau\to\frac{a\tau+b}{c\tau+d}\,,\qquad \begin{pmatrix}C_2\\B_2\end{pmatrix}\to M\begin{pmatrix}C_2\\B_2\end{pmatrix}\,,\quad M=\begin{pmatrix}a&b\\c&d\end{pmatrix}\,,\quad (ad-cb=1)\,. \tag{2.3}$$

This $\mathrm{SL}(2,\mathbb{R})$ symmetry is exact at the classical level, but gets broken down to its subgroup $\mathrm{SL}(2,\mathbb{Z})$ at the quantum level. This subgroup is conjectured to be preserved in the full non-perturbative type IIB string theory.

The presence of this duality group can be beautifully explained in the context of F-theory [26–29]. The transformation (2.3) is identical to the modular transformation of an elliptic curve with complex structure τ, i.e. a torus. The transformation (2.3) leaves the shape of the torus invariant. This allows us to give a 12-dimensional interpretation of type IIB where the $\mathrm{SL}(2,\mathbb{R})$ duality is geometrized and where the type IIB field τ represents the complex structure modulus of a torus. The point of view of F-theory makes also manifest why in type IIB branes are present. When the field τ encircles the brane, it undergoes a monodromy $\tau\to\tau+1$ which can be understood as (2.3) with

$$M=\begin{pmatrix}1&1\\0&1\end{pmatrix}\,. \tag{2.4}$$

Hence this monodromy is detecting the presence of a D7-brane, as a D7-brane is a magnetic source for C_0. By consistency of (2.3), this monodromy is also acting on the 2-form potentials. It is therefore natural to include D-branes and O-planes in type IIB, as they are fully encoded in the F-theory geometrical setup. We will in fact need them to break supersymmetry in $4d$. However, before doing this, we should lower the number of dimensions. In the next section, we show the most studied way to do so.

2.1.1 Calabi-Yau compactification and moduli spaces

Type IIB string theory is a consistent theory in $10d$ with $\mathcal{N} = 2$ supersymmetry, i.e. 32 supercharges. Given that we are interested in its phenomenology, we have to first find a way to reduce the number of dimensions down to the four we observe. This translates into finding a solution for the $10d$ equations of motion with non-trivial Riemann tensor, that nevertheless solve the vacuum Einstein's equations $R_{MN} = 0$, i.e. the $6d$ extra dimensions must be a Ricci-flat manifold. A non-trivial class of such manifolds actually exists and is called Calabi-Yau threefold.

Consider a complex manifold X of $\dim_{\mathbb{C}} = 3$ where we can define three complex coordinates z^m, each parametrizing a patch, such that on all overlaps of the patches the transition functions are holomorphic. We choose the metric $g_{m\bar{n}}$ on the complex manifold to be Hermitian with associate tensor

$$J \equiv i g_{m\bar{n}} \mathrm{d}z^m \wedge \mathrm{d}\bar{z}^{\bar{n}} \,, \tag{2.5}$$

which is a nowhere-vanishing $(1,1)$-form called *Kähler form*. If J is a closed form, i.e. $\mathrm{d}J = 0$, our manifold X is Kähler and the metric can be expressed locally in terms of a Kähler potential K as $g_{m\bar{n}} = \partial_m \bar{\partial}_{\bar{n}} K(z, \bar{z})$, such that $J = i\partial\bar{\partial}K$. Note that K is not uniquely defined, as under a Kähler transformation $K \to K + f(z) + \bar{f}(\bar{z})$, where f and $\bar{f}$ are holomorphic and anti-holomorphic functions, the metric $g_{m\bar{n}}$ is invariant.

We are actually looking for a particular subclass of Kähler manifolds, namely those that have vanishing Ricci tensor. We can define the closed Ricci $(1,1)$-form on a Kähler manifold as

$$\mathcal{R} = -i\partial\bar{\partial} \log\left(\det g\right) \,. \tag{2.6}$$

It is now useful to introduce the notion of total Chern class of a manifold M as

$$c(M) = 1 + \sum_j c_j(M) = \det(1 + \mathcal{R}) = 1 + \operatorname{tr}\mathcal{R} + \operatorname{tr}\left(\mathcal{R} \wedge \mathcal{R} - 2(\operatorname{tr}\mathcal{R})^2\right) + \dots \,, \tag{2.7}$$

where the k-th Chern class $c_k(M)$ is an element of the de Rham cohomology group $H^k(M)$. If the first Chern class is vanishing, then X is a Ricci-flat Kähler manifold. Therefore, we call CY a Kähler manifold with vanishing first Chern class.

Admitting a Kähler metric with vanishing Ricci curvature is equivalent to having a reduced holonomy group contained in $\mathrm{SU}(n)$, $n \leq 3$. Hence, we can globally define a covariantly constant spinor ψ on X as the unique $1d$ subspace that is left invariant upon parallel transport around any loop.[1] In the case of CY threefolds, it is useful to demand that the holonomy group is exactly SU(3). Knowing the holonomy group of a manifold allows us to compute how many supercharges survive the compactification. A CY with SU(3) holonomy preserves $1/4$ of the $10d$ supersymmetry, hence compactifying type II on a CY threefold leads to a $4d$ theory with 8 supercharges, i.e. $\mathcal{N} = 2$ supersymmetry, while e.g. heterotic superstring theory on a CY threefold preserves $\mathcal{N} = 1$ in $4d$. Considering subgroups of SU(3) leads to more supercharges in $4d$, therefore asking for the maximal holonomy group allowed guarantees having the minimal amount of supersymmetry in $4d$.

[1] This occurs when we require the factorization $\mathbb{R}^{10} = \mathbb{R}^{1,3} \times X$. The associated group decomposition reads $\mathrm{SO}(1,9) \supset \mathrm{SO}(1,3) \times \mathrm{SO}(6)$, with corresponding decomposition of spinors $\mathbf{16} \to (\mathbf{2}, \mathbf{4}) \oplus (\bar{\mathbf{2}}, \bar{\mathbf{4}})$. Then, since $\mathrm{SO}(6) \cong \mathrm{SU}(4)$, the spinors ψ and $\bar{\psi}$ are the $\mathbf{4}$ and $\bar{\mathbf{4}}$ of SU(4). Decomposing ψ into the irreducible representations of SU(3), we have $\mathbf{4} \to \mathbf{3} \oplus \mathbf{1}$. We have thus obtained a manifold with a singlet, which is the unique covariantly constant spinor on the CY.

We can use the spinor to define a holomorphic, closed $(3,0)$-form as

$$\Omega = \Omega_{mnr} \mathrm{d}z^m \wedge \mathrm{d}z^n \wedge \mathrm{d}z^r \quad \text{where} \quad \Omega_{mnr} \sim \bar{\psi}\, \Gamma_{mnr} \psi \,. \tag{2.8}$$

Therefore, this form is unique and nowhere-vanishing, and it is a special feature of a CY. The Kähler form and the holomorphic 3-form are not independent, but satisfy

$$J \wedge J \wedge J = \frac{3i}{4} \Omega \wedge \overline{\Omega} \,, \qquad J \wedge \Omega = 0 \,. \tag{2.9}$$

Compactifying on a CY threefold is useful because it preserves a certain amount of supersymmetry in $4d$. Moreover, we can derive some features of the low-energy theory from its topology. This is due to the fact that the harmonic forms on X corresponds to the elements of the Dolbeault cohomology groups $H^{p,q}_{\bar{\partial}}(X)$. The elements of $H^{p,q}_{\bar{\partial}}(X)$ are defined as the set of closed (p,q)-forms quotiented out by the set of exact (p,q)-forms, where (p,q) denotes the number of holomorphic and anti-holomorphic differentials of the harmonic forms. In particular, the dimension of the group is given by $\dim H^{p,q}_{\bar{\partial}}(X) \equiv h^{p,q}$, which is called Hodge number. In a simply-connected CY threefold, the only independent Hodge numbers are $(h^{1,1}, h^{2,1})$.[2] The Euler characteristic is then given by the simple relation $\chi(X) = 2(h^{1,1} - h^{2,1})$.

Now, we can ask whether there exists infinitesimal deformations of the metric $\delta g = \delta g_{m\bar{n}} \mathrm{d}z^m \mathrm{d}\bar{z}^{\bar{n}} + \delta g_{mn} \mathrm{d}z^m \mathrm{d}z^n + \text{c.c.}$ such that $g + \delta g$ is still a Ricci-flat Kähler metric. By choosing the gauge $\nabla(\delta g) = 0$ to fix the diffeomorphism invariance, it turns out that the conditions on $\delta g_{m\bar{n}}$ and δg_{mn} are decoupled, so that there are two independent classes of deformations.

First, the gauge choice imposes $\Delta \delta g_{m\bar{n}} = 0$ on the mixed-indices contribution, implying that $\delta g_{m\bar{n}}$ has to be a harmonic $(1,1)$-form. Moreover, the components of $\delta g_{m\bar{n}}$ leads to deformations of the Kähler form (2.5). The Kähler form can be expanded in a basis of harmonic forms ω_i, $i = 1, \ldots, h^{1,1}$, as $J = t^i(x)\omega_i$, where the $t^i(x)$ are real scalar fields called *Kähler moduli*. In order to make sure that the t^i are such that the corrected metric is still positive definite, we impose the so-called Kähler cone conditions

$$\int_C J > 0 \,, \quad \int_S J \wedge J > 0 \,, \quad \int_X J \wedge J \wedge J > 0 \,, \tag{2.10}$$

for all complex curves (or 2-cycles) $\Sigma^{(2)}$ and surfaces (or 4-cycles) $\Sigma^{(4)}$ on the CY X. The 2- and 4-cycles $(\Sigma^{(2)}, \Sigma^{(4)})$ constitute an integral basis for the homology groups $H_2(X)$ respectively $H_4(X)$ and are the Poincaré duals to the basis of 4- and 2-forms $(\tilde{\omega}^j, \omega_i)$. The Kähler form takes values inside a strongly convex polyhedral cone spanned by the Kähler moduli, and its interior is known as the Kähler cone or Kähler moduli space $\mathcal{M}_K$, which has dimension equal to $h^{1,1}$. By defining the topological quantities known as (triple) intersection numbers

$$k_{ijk} \equiv \int_X \omega_i \wedge \omega_j \wedge \omega_k \,, \tag{2.11}$$

we can see from (2.10) that the t^i are the volumes of the 2-cycles, while the volume of 4-cycles are defined as $\tau_i \equiv k_{ijk} t^j t^k / 2$, and the last integral gives the volume of the CY, namely[3]

$$\mathcal{V}(X) \equiv \frac{1}{6} k_{ijk} t^i t^j t^k \,. \tag{2.12}$$

[2] This statement can be shown as follows. First, $h^{p,q} = h^{q,p}$ from complex conjugation, while Hodge star duality implies $h^{p,q} = h^{3-p,3-q}$ and it is guaranteed by the existence and uniqueness of the top-form. $h^{3,0} = 1$ because the holomorphic 3-form is unique. $h^{0,0} = 1$ because X is compact and connected. Assuming simply-connectedness implies trivial fundamental group, i.e. by Hurewicz's theorem $h^{0,1} = 0$.

[3] Note from (2.9) that we can also define the CY volume as $\mathcal{V}(X) \sim \int_X \Omega \wedge \bar{\Omega}$. For this reason, the holomorphic 3-form is also called the volume form, and it is clear now physically why it should be unique.

Since $\mathcal{M}_K$ is a Kähler manifold, it admits a Kähler metric which reads

$$K_K = -2\ln(\mathcal{V}) \,. \tag{2.13}$$

If the number of generators ω_i of the Kähler cone is equal to the dimensionality of the cone, the Kähler cone is said to be simplicial. Otherwise, the number of generators outnumbers the dimensionality of the cone, and the Kähler cone is non-simplicial. The dual cone of the Kähler cone is a cone within the vector space of 2-cycles of the CY, and it is called the Mori cone. In other words, the Mori cone is the set of all 2-cycles satisfying the condition $\int_{\Sigma^{(2)}} \omega_i \geq 0$ for all generators ω_i of the Kähler cone. Note that if the Kähler cone is simplicial, the Mori cone is also simplicial, and vice versa.

By contrast, the metric deformation of pure indices δg_{mn} violates hermiticity, and it must hence be accompanied by a change in complex structure. It can be shown that δg_{mn} must be a harmonic $(2,0)$-form to preserve Ricci-flatness, just as for mixed-indices deformations. However, $h^{2,0} = 0$ for a CY, hence to count these complex structure deformations, we put $H^{2,0}(X)$ in one-to-one correspondence to $H^{2,1}(X)$ via Ω as follows

$$\chi = \Omega^{\bar{p}}_{mn} \delta g_{\bar{p}\bar{q}} \mathrm{d}z^m \mathrm{d}z^n \mathrm{d}\bar{z}^{\bar{q}} \,. \tag{2.14}$$

Let us consider a basis of 3-forms (α^a, β_a), $a = 0, \ldots, h^{2,1}$, satisfying

$$\int_X \alpha^a \wedge \beta_b = \int_{\mathcal{A}^b} \alpha^a = -\int_{\mathcal{B}^a} \beta^b = \delta^a_b \,, \tag{2.15}$$

i.e. it is a symplectic basis. The 3-forms are the Poincaré duals to the so-called $\mathcal{B}$ and $\mathcal{A}$-cycles that form a basis of the third homology group which is symplectic, implying that the 3-surfaces intersect as $\mathcal{A}_a \cap \mathcal{B}^b = -\mathcal{B}^b \cap \mathcal{A}_a = \delta_a{}^b$. The complex structure moduli space $\mathcal{M}_{cs}$ is special Kähler, and there is a natural set of $h^{2,1}+1$ special complex coordinates on it which can be defined as

$$z^a \equiv \int_{\mathcal{A}_a} \Omega \,, \quad \mathcal{F}_a(z) \equiv \int_{\mathcal{B}^a} \Omega \,, \tag{2.16}$$

which allows us to express the unique, holomorphic form as $\Omega = z^a \alpha_a - \mathcal{F}_b \beta^b$. It is useful to write the above periods in terms of the *period vector*

$$\Pi = \begin{pmatrix} z^a \\ \mathcal{F}_a(z) \end{pmatrix} . \tag{2.17}$$

Since the z^a are homogeneous complex projective coordinates on $\mathcal{M}_{cs}$, we can normalize Ω such that $z^0 = 1$ away from $z^0 = 0$. Hence, from now on $a = 1, \ldots, h^{2,1}$. The periods $\mathcal{F}_a(z)$ are determined in terms of the z^a by the *prepotential* $\mathcal{F}(z)$ via $\mathcal{F}_a(z) = \partial_{z^a}\mathcal{F}(z)$ and $\mathcal{F}_0 = 2\mathcal{F}(z) - z^a \partial_{z^a}\mathcal{F}(z)$.

We take (2.16) (appropriately rescaled) as the definition of *complex structure moduli* z^a. Hence, we can define the metric on $\mathcal{M}_{cs}$ as [30]

$$g_{a\bar{b}} = \frac{\partial^2 K_{cs}}{\partial z^a \partial \bar{z}^{\bar{b}}} \,, \quad \text{where} \quad K_{cs} = -\ln\left(i \int_X \Omega \wedge \bar{\Omega} \right) = -\ln\left(i\bar{z}^a \mathcal{F}_a - i z^a \bar{\mathcal{F}}_a \right) . \tag{2.18}$$

For later purposes, we introduce the exact expression for K_{cs}. At large complex structure (LCS) we can

write the prepotential as $\mathcal{F}(z) = \mathcal{F}_{\text{pert}}(z) + \mathcal{F}_{\text{inst}}(z)$ with

$$\begin{aligned} \mathcal{F}_{\text{pert}} &= -\frac{1}{6}\tilde{k}_{abc} z^a z^b z^c + \frac{1}{2} a_{ab} z^a z^b + b_a z^a + c\,, \\ \mathcal{F}_{\text{inst}} &= \frac{1}{(2\pi i)^3} \sum_{\beta} n^0_\beta \, \text{Li}_3\left(e^{2\pi i \beta_a z^a}\right)\,, \end{aligned} \tag{2.19}$$

where Li_k is the polylogarithm function. This expression refers to the mirror CY $\tilde{X}$, hence $\tilde{k}_{abc}$ are the triple intersection numbers of the mirror and the sum runs over effective curves in the mirror [31, 32]. The constants a, b are rational numbers, and $c = -\frac{\zeta(3)}{(2\pi i)^3}\chi(X)$. The n^0_β are the genus 0 Gopakumar-Vafa (GV) invariants, which count the number of holomorphic curves of genus 0 in a given homology class $[\beta]$ of $\tilde{X}$.

To describe the prepotential we had to introduce the concept of mirror of a CY. Mirror symmetry [33] is a symmetry which corresponds to the interchange of the third cohomology class of a manifold with the even cohomologies of the putative mirror one. In particular, for a CY X this means that there exists a mirror CY $\tilde{X}$ given by a map called mirror map which exchanges complex structure and Kähler moduli between X and $\tilde{X}$ (hence, X and its mirror are in general topologically different manifolds). Mirror symmetry can then be seen as the statement that type IIB compactifyied on X is mirror-symmetric to type IIA on $\tilde{X}$. Since the moduli spaces are interchanged, it means that the prepotentials are identical. This allows us to compute the metric on the Kähler part of the moduli space of type IIA (which receives both perturbative and worldsheet instantons corrections) by relating the type IIA prepotential via the mirror map to the type IIB prepotential which can be computed classically.

The complex structure moduli space of type IIB is classically exact because it is the space of vector multiplets. Upon compactificaton on a CY, type IIB gives a low-energy effective theory in $4d$ whose spectrum is composed of $\mathcal{N} = 2$ multiplets. In particular, their massless bosonic components are shown in table 2.1, where S is the $4d$ axio-dilaton and the reduction of the $10d$ metric yields the $4d$ metric $g_{\mu\nu}$, the graviphoton 1-form V^0 and of course $h^{2,1}$ complex structure moduli z^a and $h^{1,1}$ Kähler moduli t_i. All the other fields appear as coefficients in the expansion of the $10d$ forms in terms of harmonic forms of X as

$$B_2 = \hat{B}_2(x) + b_i(x)\omega^i\,, \quad C_2 = \hat{C}_2(x) + c_i(x)\omega^i\,, \quad C_4 = d^i(x)\tilde{\omega}_i + d'_i\omega^i + V^a \wedge \alpha_a + A'_b \wedge \beta^b\,, \tag{2.20}$$

where the 2-forms $\hat{B}_2$ and $\hat{C}_2$ can be dualised to two axions b_0, c_0. Moreover, there are $2h^{1,1}$ model-dependent axions b_i, c_i, while from C_4 we get the axions d^i and the ones dual to the 2-form d'_i, which must be identified from the self-duality of the 5-form field strength, hence giving in total $h^{1,1}$ C_4-axions. The V^a are 1-forms entering the vector multiplet. Therefore, we have that $\mathcal{M}_K \equiv \mathcal{M}_h$ and $\mathcal{M}_{cs} \equiv \mathcal{M}_V$, where $\mathcal{M}_h$ and $\mathcal{M}_V$ are the hyper and vector multiplet moduli spaces respectively. Therefore, for mirror symmetry, in type IIA we have $\mathcal{M}_{cs} \equiv \mathcal{M}_h$ and $\mathcal{M}_K \equiv \mathcal{M}_V$.

Note that, since the dilaton ϕ appears in the universal hypermultiplet, $\mathcal{M}_h^{\text{IIB}}$ receives (perturbative and non-perturbative) corrections in g_s. In contrast to this, the vector multiplet moduli space is exact

	number	components
gravity multiplet	1	$g_{\mu\nu}$, V^0
vector multiplets	$h^{2,1}$	z^a, V^a
Kähler hypermultiplets	$h^{1,1}$	t_i, b_i, c_i, d^i
universal hypermultiplet	1	$S = C_0 + ie^{-\phi}$, b_0, c_0

Table 2.1: $4d$, $\mathcal{N} = 2$ multiplets and their bosonic field content [34].

at string-tree level. The same is true in type IIA where the dilaton is again part of $\mathcal{M}_h^{\rm IIA}$, while this is not the case for heterotic string theory, where the dilaton enters the vector multiplet moduli space. Let us consider type IIA string theory compactified on $\tilde{X}$, where the metric on $\mathcal{M}_V^{\rm IIA}$ receives perturbative and non-perturbative worldsheet corrections in α'. Under mirror symmetry, this is mapped to type IIB on X, where $\mathcal{M}_V^{\rm IIB}$ is classically exact. On the contrary, $\mathcal{M}_V^{\rm het}$ in the heterotic theory is given by the $h^{1,1}$ Kähler moduli plus the heterotic axio-dilaton S_h, and in order to have $4d$, $\mathcal{N}=2$ the heterotic theory has to be compactified on K3 $\times T^2$. The existence of a duality between heterotic and type IIA actually imposes the structure of a K3 fibration onto $\tilde{X}$ [35] and in particular implies $h^{1,1}(\tilde{X}) \geq 2$. Due to the product structure of the moduli space in $\mathcal{N}=2$ and the fact that the dilaton resides in different multiplets in the two theories, it is possible to compare the heterotic $\mathcal{M}_V$ in a weak coupling expansion with the $\mathcal{M}_V$ of the type IIA vacuum at large volume. The duality between type IIA and heterotic maps the volume of the base space of X to the heterotic dilaton, in the limit of large volume of the base or equivalently weak heterotic string coupling [36]. Via the mirror map, we can then relate these limits to the LCS limit in type IIB. The beautiful structure connecting the moduli spaces that we have just briefly summarised is the $4d$, $\mathcal{N}=2$ realization of the fact that type II and heterotic superstrings (as well as type I) are manifestations of the same underlying theory.

We have discussed at the beginning of the section how type IIB can be seen as the weak coupling limit of F-theory, where the latter is defined with a twelve-dimensional formulation as type IIB with varying axio-dilaton. We can therefore consider F-theory compactified on a CY fourfold elliptically fibred over a three complex dimensional base manifold. However, this gives in $4d$ only $\mathcal{N}=1$ supersymmetry. This is because type IIB is actually the weak coupling *orientifold* limit of F-theory: in fact, in F-theory the presence of D-branes and O-planes is encoded in the geometry, while in type IIB they should be introduced. Indeed, once in type IIB an *orientifold projection* is taken into account, half of the supersymmetry is broken and we are left with $\mathcal{N}=1$.

In particular, in type IIB given a manifold with discrete $\mathbb{Z}_2$ symmetry group σ with even-dimensional fixed point locus (i.e. with O3/O7-planes), we can project the degrees of freedom of our theory onto the sector invariant under $(-1)^{F_L}\Omega_p\sigma$, where Ω_p denotes worldsheet parity, F_L is the left-moving fermion number. In order to preserve some supersymmetry, σ must be holomorphic, hence the cohomology groups split into even and odd eigenspaces as $H^{p,q} = H^{p,q}_+ \oplus H^{p,q}_-$. At the level of the spectrum, this means that we are projecting out half of the fields, and the leftovers must be repackaged in $\mathcal{N}=1$ multiplets. The $\mathcal{N}=2$ gravity multiplet loses the vector and the universal hypermultiplet loses two of its axions, b_0 and c_0. The Kähler hypermultiplets are split into $h^{1,1}_+$ chiral multiplets composed by (t_i, d^i) and $h^{1,1}_-$ axion chiral multiplets (c_α, b_α) and in particular, we are left with the following invariant 2- and 4-form fields:

$$B_2 = b^\alpha(x)\omega_\alpha\,, \quad C_2 = c^\alpha(x)\omega_\alpha\,, \quad C_4 = d^i(x)\tilde{\omega}_i\,. \tag{2.21}$$

where $i=1,\dots,h^{1,1}_+$, $\alpha=1,\dots,h^{1,1}_-$. The complex structure deformations divide into $h^{2,1}_-$ complex structure chiral multiplets and $h^{2,1}_+$ vector multiplets (see table 2.2). Now, we need to rearrange the invariant scalar degrees of freedom into the bosonic components of chiral multiplets of $\mathcal{N}=1$ supersymmetry. The proper coordinates of the moduli space turn out to be $h^{1,1}_-$ 2-form fields G_α, $h^{1,1}_+$ Kähler moduli T_i, $h^{2,1}_-$ complex structure moduli z^a and the axio-dilaton S [34]:

$$S = C_0 + i\,e^{-\phi}\,, \quad G_\alpha = c_\alpha - S b_\alpha\,, \quad T_i = \tau_i + i\,d_i + \frac{i\,\kappa_{i\alpha\beta}}{2\left(S-\bar{S}\right)} G^\alpha \left(G-\bar{G}\right)^\beta\,. \tag{2.22}$$

where $\tau_i \equiv \frac{1}{2}k_{ijk}t^j t^k$ while κ_{ijk} and $\kappa_{i\alpha\beta}$ are the triple intersection numbers between all even 4-cycles

	number	components
gravity multiplet	1	$g_{\mu\nu}$
chiral multiplet	1	$S = C_0 + ie^{-\phi}$
Kähler chiral multiplets	$h^{1,1}_+$	t_i, d^i
chiral multiplets	$h^{1,1}_-$	b_i, c_i
vector multiplets	$h^{2,1}_+$	V^a_+
c. s. chiral multiplets	$h^{2,1}_-$	z^a_-, b_0, c_0

Table 2.2: $4d$, $\mathcal{N} = 1$ multiplets and their bosonic field content in O3/O7-orientifold compactifications [34].

the i-th orientifold-even 4-cycle and a pair of orientifold-odd 4-cycles. We immediately see that the axionic content of the theory coming from closed string modes is given by the fields C_0, c_α, b_α, d_i, whose number hence depends on the geometrical structure of the extra dimensions.

To leading order in g_s and α', the resulting low-energy Kähler potential reads

$$K = -2\ln\left(\mathcal{V}(T+\bar{T})\right) - \ln\left(S-\bar{S}\right) - \ln\left(i\int_X \Omega(z)\wedge\bar{\Omega}(\bar{z})\right), \tag{2.23}$$

where $\mathcal{V}$ depends implicitly on the real part of the complexified Kähler moduli T. The low-energy effective theory that we have arrived to is actually a supergravity theory. The F-term $4d$ supergravity scalar potential is given in terms of a Kähler potential K and a superpotential W (in units of M_P) by

$$V = e^K\left[K^{I\bar{J}}\mathcal{D}_I W \mathcal{D}_{\bar{J}}\bar{W} - 3|W|^2\right], \tag{2.24}$$

where $\mathcal{D}_I W \equiv \partial_I W + K_I W$ is the Kähler covariant derivative and the indices I, J run over all moduli. Hence, since for now W is identically vanishing, all the fields we discussed so far are flat directions in their moduli spaces.

2.1.2 Branes and fluxes

The inclusion of supersymmetry-breaking orientifold planes comes at a cost. In particular, O7-planes carry negative magnetic charge under C_0 (and negative tensions), which we must cancel by including also a number of D7-branes. Actually, the inclusion of branes also generates a potential for the Kähler moduli and the axions, which would be otherwise parametrising flat directions of the moduli space. Moreover, each D-brane comes along with a U(1) gauge theory that lives on its worldvolume, while placing a number of branes on top of each other give rise to non-Abelian gauge theories. Because we will need all these features, we now review the basics of branes and fluxes in type IIB CY compactification.

The dynamics of a Dp-brane is described by the DBI action together with a Chern-Simons action which read

$$\begin{aligned} S_{\rm DBI} &= -T_p\int_\Sigma \mathrm{d}^{p+1}\xi\, e^{-\phi}\sqrt{-\det\left(g+B_2+2\pi\alpha' F_2\right)}\,, \\ S_{\rm CS} &= \mu_p\int_\Sigma C_{p+1}e^{2\pi\alpha' F_2+B_2}\,, \end{aligned} \tag{2.25}$$

where F_2 is the gauge field living on the brane, T_p is the tension and μ_p the RR-charge of the brane. The inclusion of branes implies a modification of the chiral Kähler coordinates [37], as one now should deal also with the open string moduli, which are moduli corresponding to the strings stretching between branes parametrising the positions of the branes in the internal manifold. In the F-theory perspective,

these are actually just normal geometric moduli of the fourfold.

However, usually *fluxes* take care of these moduli, stabilising them at high energy scales. In particular, let us focus on background fluxes: we can add 3-form fluxes F_3 and H_3 on 3-cycles. By combining them into the 3-form fluxes $G_3 \equiv F_3 - SH_3$, it was shown in [38] by Giddings, Kachru and Polchinski (GKP) that the F-terms of the complex structure and the axio-dilaton possess a common solution locus where the fluxes G_3 only have components of Hodge type $(0,3)$ and $(2,1)$, i.e. they are imaginary self-dual (ISD) $\star_6 G_3 = iG_3$. The vanishing of the $(1,2)$ and $(3,0)$ components corresponds to $h^{2,1}+1$ conditions on $h^{2,1}$ complex structure moduli and the axio-dilaton. Therefore, the complex structure moduli and the axio-dilaton are stabilized by turning on background fluxes, since the latter generate the Gukov-Vafa-Witten (GVW) superpotential [39]

$$W \sim \int_X G_3 \wedge \Omega \,. \tag{2.26}$$

Let us note here that due to the modified Bianchi identity, 3-form fluxes carry D3-brane charge which must be cancelled by other localized objects. This leads to the tadpole cancellation condition

$$\frac{1}{(2\pi)^4(\alpha')^2}\int_X F_3 \wedge H_3 + N_{D3} - \frac{1}{4}N_{O3} = 0\,, \tag{2.27}$$

where N_{D3} and N_{O3} are the net number of positive and negative D3-charge sources respectively. Via the ISD condition, one can show that the flux contribution is always positive, hence requiring the presence of an object with negative D3-charge.

Since now we have a superpotential, the supergravity potential is non-trivial and reads

$$e^{-K}V = K^{S\bar{S}}\mathcal{D}_S W \mathcal{D}_{\bar{S}}\bar{W} + K^{z\bar{z}}\mathcal{D}_z W \mathcal{D}_{\bar{z}}\bar{W} + \left(K^{i\bar{j}}K_i K_{\bar{j}} - 3\right)|W|^2\,. \tag{2.28}$$

The parenthesis is actually vanishing as K at tree level satisfies the no-scale identity [40], implying the existence of a classical no-scale structure of the potential for the Kähler moduli, which are therefore still flat directions. The potential (2.28) is positive semidefinite and allows us to fix the complex structure moduli in a supersymmetric way, i.e. with $F_I = \mathcal{D}_I W = 0$. In fact, whether supersymmetry is preserved or not also depends on the choice of the G_3 fluxes: if G_3 is of the $(2,1)$-type then supersymmetry is unbroken, while a G_3 of the $(0,3)$-type breaks the supersymmetry. In both cases, one gets a Minkowski vacuum at tree level.

2.1.3 Kähler moduli stabilisation

The $4d$ effective field theory coming from string compactification contains many scalar fields, which parametrise the size and the shape of the extra dimensions. Since the moduli appear at tree-level as massless and uncharged scalar fields which, thanks to their effective gravitational coupling to all ordinary particles, they would mediate some as of now undetected long-range fifth forces. For this reason, it is necessary to develop a potential for these particles in order to give them a mass. This problem goes under the name of moduli stabilisation.

The flatness of the F-term scalar potential for the Kähler moduli can be cured by considering perturbative and non-perturbative corrections to the Kähler potential and the superpotential. For the superpotential, only non-perturbative ones are allowed in the Kähler moduli T due to the non-renormalisation theorem [41]. These corrections can be generated either by Euclidean D3-brane instantons [42] or by gaugino condensation effect happening in the worldvolume theories of stacks of D7-branes wrapping

rigid divisors [43, 44]. Both these contributions take the form

$$W_{\rm np} = \sum_i A_i e^{-a_i T_i} \,, \tag{2.29}$$

where $a_i = 2\pi$ for ED3-branes and $a_i = 2\pi/h^\vee(G_i)$ for the gaugino condensation case. Here $h^\vee(G_i)$ is the dual Coxeter number of the gauge group G_i on the i-th stack of D7-branes. The 1-loop Pfaffians A_i depend on the stabilisation of the complex structure moduli. Additionally, there might be higher instanton corrections, but these can be neglected as long as $a_i T_i > 1$.

In general, the Kähler potential receives corrections both in string loop expansion and in α', where the leading α'^3 correction comes from the ten-dimensional R^4-term, and induce the so called BBHL correction parametrised by the constant ξ [45]. The corrected Kähler potential is then

$$K = -2\ln\left(\mathcal{V} + \frac{\hat{\xi}}{2}\right) + \delta K_{g_s} + \delta K_{\mathcal{O}(\alpha'^4)} = K_0 + \delta K_{g_s} + \delta K_{\alpha'} \,, \tag{2.30}$$

where $\hat{\xi}$ is a constant which controls the strength of α' corrections and is given by $\hat{\xi} = \xi/g_s^{3/2}$,

$$\xi = \frac{-\chi(X)\zeta(3)}{2(2\pi)^3} \,, \tag{2.31}$$

and $\chi(X)$ is the Euler characteristic of the CY 3-fold. In (2.30) by δK_{g_s} (resp. $\delta K_{\alpha'}$) we collectively mean all the string loop corrections [46–48] to the Kähler potential (resp. all α' corrections). In the $\mathcal{N} = 1$ case, this correction was shown to be the leading one to contribute thanks to the extended no-scale cancellation of $\mathcal{O}(\alpha'^2)$ and the subdominance of higher terms [48].[4]

Let us specialize the F-term supergravity potential by including the perturbative and non-perturbative corrections of eqs. (2.29) and (2.30). If we assume that the complex structure moduli and the axio-dilaton are stabilized at higher energy scales, they contribute only as a constant both in K and in W. In particular, we can write the superpotential after complex structure and axio-dilaton stabilisation as $W = W_0 + W_{\rm np}$, where W_0 is a constant determined by the VEVs of the stabilised fields from the tree-level W. Therefore, we can consider the potential for the Kähler moduli only, and we can split it into three terms, namely

$$\begin{aligned} &V = V_{\rm np_1} + V_{\rm np_2} + V_{\alpha'} \quad \text{where} \\ &V_{\rm np_1} = e^K K^{j\bar{k}}\, \partial_{T_j} W \partial_{\bar{T}_k} \bar{W} \,, \quad V_{\rm np_2} = e^K K^{j\bar{k}} \left[\bar{W}\partial_{T_j} W \partial_{\bar{T}_k} K + h.c.\right] \,, \\ &V_{\alpha'} \sim 3\hat{\xi}\frac{\hat{\xi} + 7\hat{\xi}\mathcal{V} + \mathcal{V}^2}{(\mathcal{V} - \hat{\xi})(2\mathcal{V} - \hat{\xi})^2}|W|^2 \,. \end{aligned} \tag{2.32}$$

Hence, we can rewrite V as [50]

$$\begin{aligned} V = &e^K \left[\sum_{\alpha,\beta} K^{T_\alpha \bar{T}_\beta} a_\alpha A_\alpha a_\beta A_\beta e^{-a_\alpha T_\alpha - a_\beta \bar{T}_\beta}\right] \\ &- e^K \left[\sum_{\alpha,\beta} K^{T_\alpha \bar{T}_\beta} \left(a_\alpha A_\alpha e^{-a_\alpha T_\alpha} \bar{W} \partial_{\bar{T}_\beta} K + a_\beta A_\beta e^{-a_\beta \bar{T}_\beta} W \partial_{T_\alpha} K\right)\right] \\ &+ 3\hat{\xi}\frac{\hat{\xi} + 7\hat{\xi}\mathcal{V} + \mathcal{V}^2}{(\mathcal{V} - \hat{\xi})(2\mathcal{V} - \hat{\xi})^2}|W|^2 \,. \end{aligned} \tag{2.33}$$

[4] Note that in the $\mathcal{N} = 1$ case with O7-planes one should trade $\chi(X)$ with $\chi_{\rm eff}(X) = \chi(X) + 2\int_X D^3_{O7}$ in $\hat{\xi}$ [49].

Over the years, many proposals of moduli stabilisation in controlled regimes have been put forward. Since in this thesis we deal only with the *KKLT* [51] mechanism and the *Large Volume Scenario* (*LVS*) [52], we will review only these two ideas. Let us anticipate here that both these proposals give rise to (supersymmetric and non-supersymmetric respectively) AdS minima, and whether the minima can be *uplifted* to dS is an active field of research.

KKLT involves a competition between the tree-level superpotential W_0 and non-perturbative corrections. To do so, and to render α' corrections unimportant, W_0 should be made very small via a tuning of fluxes. In particular, by considering $h^{1,1} = 1$, K only at tree level and the first non-perturbative correction in W one finds that the F-term is

$$\mathcal{D}_T W = -aA\, e^{-aT} - 3\,\frac{A\, e^{-aT} + W_0}{T+\bar{T}}\,, \tag{2.34}$$

which has a solution for $T \sim \ln(-W_0)/a$, where T should have a VEV at moderately large value for a controlled minimum. Indeed, this is consistent only if $|W_0| \ll 1$. The vacuum energy is supersymmetric and is given by

$$V_{\rm AdS} = -3e^K |W|^2 \sim -\frac{3}{(T+\bar{T})^3}|W_0|^2\,. \tag{2.35}$$

It was proposed already in [51] that this negative vacuum can be uplifted by including $\overline{\rm D3}$-branes placed at the tip of a warped throat. The vacuum energy of the anti-brane is positive and scales as $\omega_0^4/(T+\bar{T})^{-2}$, where ω_0 is the IR warp-factor of the throat [53]. By tuning fluxes appropriately so that $\omega_0^4 \sim |W_0|^2$, the anti-brane potential dominates over (2.35), thus giving the possibility for dS vacua of tunable cosmological constant.

Note that due to the fact that KKLT AdS vacuum is supersymmetric, fields belonging to the same multiplet get stabilised at the same energy level by the same non-perturbative effects. For example, Kähler moduli and their axionic supersymmetric partners have the same mass, which is generically of the same order as the gravitino mass, i.e. $e^{K/2}|W_0|\, M_P$. This fact could actually be a drawback for phenomenology, as it seems rather difficult to obtain in this way a spectrum of particles with different mass scales. We will delve further into this topic in Chapter 4. A supersymmetry-breaking AdS vacuum could therefore in principle allow for more varieties of scales in the effective theory. The LVS procedure can address exactly this problem, as we review in what follows.

As its name suggests, LVS moduli stabilisation allows the volume of the extra dimensions to be stabilised at exponentially large values, creating a natural hierarchy between energy scales that can be parametrised by inverse powers of the overall volume. This is particularly convenient for phenomenology, since it allows us to perform moduli stabilisation step by step, at different energies. LVS stabilizes the Kähler moduli via an interplay between α' corrections to K and non-perturbative corrections to W. In order to keep control on α' corrections, the overall CY volume $\mathcal{V}$ must be stabilized at exponentially large values. As a result, $|W_0| \sim \mathcal{O}(1)$. However, some topological requirements are needed. First, inside the α' correction in (2.30), the Euler number of the CY must be negative, i.e. $h^{2,1} > h^{1,1} > 1$. This in turn ensures that ξ is positive and so that, as $\mathcal{V}$ tends to infinity, the potential goes to zero from below in the LVS scaling regime (2.37) discussed below. LVS produces an AdS minimum which is no longer supersymmetric. Second, there must be present at least one blow-up mode, $\tau_s \subset T_s$, corresponding to a 4-cycle modulus resolving a pointlike singularity. In the limit $\mathcal{V} \to \infty$, all $\tau_i \to \infty$ but τ_s. This modulus should be the one inducing the leading non-perturbative corrections to W, namely $W_{\rm np} \sim e^{-a_s T_s}$. Of course all moduli could appear in $W_{\rm np}$, but in the above limit their contribution is subleading.

Being interested in large 4-cycles parametrising the overall volume of extra dimensions, we can

consider the (weak) Swiss-cheese parametrisation of the volume, namely

$$\mathcal{V} = \left(f_{3/2}(\tau_i) - \tau_s^{3/2}\right) \qquad i = 1, \dots, h^{1,1} - 1\,, \tag{2.36}$$

where $f_{3/2}$ is a function of degree 3/2 in τ_i that we assume to be given by a single term for simplicity and τ_s is a diagonal contractible blow-up cycle. Given this simplifying assumptions and considering non-perturbative corrections to W only related to the small cycle T_s, LVS stabilisation is able to fix three directions in the Kähler moduli space, namely the overall volume $\mathcal{V}$, the small cycle τ_s and the C_4 axion d_s at

$$\langle\tau_s\rangle^{3/2} \simeq \frac{\hat{\xi}}{2}\,, \qquad e^{-a_s\langle\tau_s\rangle} \simeq \frac{\sqrt{\tau_s}\,|W_0|}{a_s A_s \mathcal{V}}\,, \qquad d_s = \frac{k\pi}{a_s}\,, \tag{2.37}$$

where $k \in \mathbb{Z}$. From the previous equations, we see that the LVS minimum lies at exponentially large volume $\mathcal{V} \sim e^{a_s\tau_s} \gg 1$ and does not require any fine-tuning on the tree-level superpotential $W_0 \sim 1 \div 100$. Non-perturbative effects do not destabilise the flux-stabilised complex structure moduli and the dilaton. Moreover, supersymmetry is mostly broken by the F-terms of the Kähler moduli and the gravitino mass is exponentially suppressed with respect to M_P, as $m_{3/2} \sim \mathcal{V}^{-1} M_P$. This can give low-energy supersymmetry naturally. Moreover, one can show that all the other relevant scales of the theory scale with inverse powers of the bulk volume, as e.g. in Planck units the string scale is $M_s \sim \mathcal{V}^{-1/2}$ while the KK scale reads $M_{\rm KK} \sim \mathcal{V}^{-2/3}$.

LVS models are characterised by a non-supersymmetric AdS minimum of the scalar potential at exponentially large volume, which reads

$$V_{\rm AdS} = -\mathcal{O}(1)\frac{g_s|W_0|^2\sqrt{\ln(\mathcal{V})}}{\mathcal{V}^3}\,, \tag{2.38}$$

hence we must find a way to uplift this negative minimum to a dS vacuum. This can be done by switching on magnetic fluxes on D7-branes [54], adding anti-D3-branes [51, 55–62], hidden sector T-branes [63], non-perturbative effects at singularities [64], non-zero F-terms of the complex structure moduli [65] or via the winding mechanism coming from a flat direction in the complex-structure moduli space [3, 66]. We dedicate to the latter proposal Section 3.5. Note that the uplift to de Sitter does not destabilise the axions, as *generically* the fields responsible for the uplift are the Kähler moduli.

Axions are stabilised basically in the same way we just described for the moduli. This is true in particular for the C_4 axions d, which are the supersymmetric partners of the Kähler moduli t. Some additional ingredients should be considered for the odd axions, such as requiring the stack of branes to be magnetised, or by considering perturbative effects in the DBI action. In what follows and in the rest of this thesis, we will focus on this topic, namely how to generate a potential for string axions and what this implies on our universe.

2.2 Closed string axions

In String Theory, axion-like particles coming from closed string modes arise from the integration of p-form gauge field potentials over p-cycles of the compact space. In what follows we consider type IIB string compactifications where axions arise from the integration of the NS-NS 2-form B_2 and R-R 2-form C_2 over 2-cycles, Σ_2^α, or from the integration of the R-R 4-form C_4 over 4-cycles, Σ_4^i, namely

$$b_\alpha = \frac{1}{(2\pi)^2\alpha'}\int_{\Sigma_2^\alpha} B_2\,, \quad c_\alpha = \frac{1}{(2\pi)^2\alpha'}\int_{\Sigma_2^\alpha} C_2\,, \quad d_i = \frac{1}{(2\pi)^4(\alpha')^2}\int_{\Sigma_4^i} C_4\,, \tag{2.39}$$

and another axion is given by the R-R 0-form C_0. Since axion fields arise as harmonic zero modes of p-forms gauge potentials on p-cycles of the compactification space, at the perturbative level the $10d$ gauge invariances of the p-form gauge fields descend to continuous shift symmetries of their associated p-form axions in $4d$ $\Phi_i \sim \Phi_i + c$, $c \in \mathbb{R}$. The kinetic part of the $4d$ Lagrangian contains the following terms associated to the axions:

$$\mathcal{L} \supset \frac{g_{ij}}{2} \partial_\mu \Phi^i \partial^\mu \Phi^j \,, \tag{2.40}$$

where $g_{ij} = 2\frac{\partial^2 K}{\partial T^i \partial \bar{T}^j}$ for C_4 axions, $g_{ij} = 2\frac{\partial^2 K}{\partial G^i \partial \bar{G}^j}$ for C_2 and B_2 axions, and K is the Kähler potential of the theory. In order to work with canonically normalised fields, we need to diagonalise the Kähler metric and find the axion metric eigenvalues λ_i and eigenvectors $\tilde{\Phi}_i$. After that, we define the canonically normalised axion fields as $\phi_i = \sqrt{\lambda_i}\tilde{\Phi}_i M_P$ (restoring proper powers of M_P) where [18]

$$\mathcal{L}_{\text{kin}} \supset \frac{\lambda_i M_P^2}{2} \partial_\mu \tilde{\Phi}_i \partial^\mu \tilde{\Phi}_i = \frac{1}{2} \partial_\mu \phi_i \partial^\mu \phi_i \,. \tag{2.41}$$

In the case of massless axions, it is quite common to refer to $\hat{f}_i = \sqrt{\lambda_i}\, M_P$ as the axion decay constant. This derives from the fact that the couplings of the physical axions with all other fields scale as $\propto 1/\hat{f}$ after canonically normalising the axions. So far we have only considered massless axions but, as with the rest of the moduli, these fields need to be stabilised.

Axions acquire a mass through the non-perturbative quantum corrections in (2.29) that break their continuous shift symmetry down to their discrete subgroup. The typical form of the potential arising from a single non-perturbative correction reads

$$V(\phi_i) = \Lambda_i^4 \cos(a_i \Phi_i) \,, \tag{2.42}$$

where $a_i = 2\pi/N_i$, with $N_i \in \mathbb{N}^+$ being the rank of the gauge group living on the branes, and Λ is a dynamically-generated scale proportional to the instanton action. In general, to work with physical fields, we need to find the field basis that diagonalises both the mass matrix and the field space metric. Note that this is not always possible, and in general one is able to diagonalise only either the kinetic terms or the potential.

In the simplest case where the Kähler metric is approximately diagonal ($\Phi_i \sim \tilde{\Phi}_i$) and we have a single non-perturbative correction, computing the decay constant becomes rather simple. Since the field periodicity corresponds to that of the potential, the stabilised axion decay constant, f_i, derives from

$$\begin{aligned} a_i\, \Phi_i \quad &\to \quad a_i\, \Phi_i + 2\pi\, k \qquad \text{implying that} \\ \phi_i \quad &\to \quad \phi_i + 2\pi f_i\, k \qquad \text{where} \qquad f_i = \sqrt{\lambda_i}\, \tfrac{M_P}{a_i} = \tfrac{\hat{f}_i}{a_i} \,. \end{aligned} \tag{2.43}$$

We have seen how string axions behave in the effective field theory. In the next section, we discuss how the effective theory should behave in order for the axions to have a consistent UV completion.

2.3 String axions and the swampland

The WGC [67] suggests that there must exist (some) charged states whose charge-to-mass ratio is larger than that of an extremal black hole in the theory, implying that gravity should be the weakest force. Since axions can be seen as 0-form gauge fields, the WGC should hold for them as well. The axionic

version of the WGC states that there must be an instanton whose action satisfies

$$Sf \lesssim \alpha M_P \,, \tag{2.44}$$

where α is an $\mathcal{O}(1)$ constant depending on the extremality bound entering the formulation of the conjecture. However, general extremal solutions for instantons have not been found yet, therefore the precise value of α is known only for special cases (see e.g. [68–71]). Let us mention here that in the literature many versions of the WGC were proposed up to date (see e.g. [16] for a recent review). First, we can mainly distinguish between 'strong' and 'mild' forms of the WGC. By strong WGC we mean that *all* the axions present in a given model will acquire their dominant instanton potential from instantons satisfying the WGC bound. Instead, with mild WGC we refer to the statement that the WGC-satisfying instantons may give subleading contributions to the non-perturbative axion potential. This means that the mild WGC allows for some axions to acquire the leading potential from instantons with an effective $Sf > 1$.

Let us now study the relation between the decay constant and the instanton action of the closed-string axion-like particles. The general refined statement for the WGC for p-forms with gauge coupling $e_{p;d}$ in d dimensions in the absence of a dilaton background reads [14]

$$\frac{p(d-p-2)}{d-2}\, T_p^2 \leq e_{p;d}^2\, q^2 M_{P;d}^{d-2} \,, \tag{2.45}$$

where T_p is the tension of the charged $(p-1)$-brane with integer charge q, and $M_{P;d}$ is the Planck mass in d-dimensions. Such relation is degenerate for 0-forms (axions), hence it does not directly apply. In order to get a statement for axions, we are forced to rely on an indirect computation. Extending an argument proposed in [70], we give a new derivation of the bound on Sf for axions in type IIB by relating the quantity Sf to the charge-to-mass ratio of a particle in type IIA, to which (2.45) applies. A similar computation was carried out in [69] using T-duality. As we will show, we do not need the use of T-duality, as we will express the needed relations in terms of purely geometrical quantities which are independent of the underlying theory used. In what follows, we first derive a geometrical relation for a charged particle by wrapping a Dp-brane on a p-cycle. Then, we show that we can get the same geometrical quantity from a D$(p-1)$-brane wrapping the same cycle, hence producing instanton 'charged' under an axion in the non-compact space. Therefore, following [70], a bound for the particle carries through to the axion via the purely geometrical relation.

We start with a theory in $10d$ with Dp-branes wrapped on a p-cycle Σ^p of the CY, namely

$$\frac{1}{4\kappa_{10}^2}\int_{M_4\times X} e^{\frac{3-p}{2}\phi} F_{p+2}\wedge \star^{(E)} F_{p+2} + \mu_p \int_{Dp \text{ on } \Sigma^p} C_{p+1} \,. \tag{2.46}$$

Upon compactification on the CY, this action leads to the Maxwell theory for a charged particle in $4d$ from the reduction of the C_{p+1} gauge potential, as we show in what follows. First, we introduce a symplectic basis of harmonic p-forms ω_i of the p-th cohomology of X. Such basis satisfies

$$\int_X \omega_i \wedge \star\omega_j = K_{ij} \,, \tag{2.47}$$

where K_{ij} is the metric on the space of p-forms and is proportional to the Kähler metric. Note that K_{ij} depends on the CY volume and on powers of α'. Then, we can expand the $(p+2)$-form flux and the $(p+1)$-form potential in terms of the symplectic basis as $F_{p+2} = F_2^i \wedge \omega_i$ and $C_{p+1} = A_1^i \wedge \omega_i$. The $4d$

action is then obtained by integrating on X. By defining the integral charges as

$$q_i^{\Sigma^p} = \int_{\Sigma^p} \omega_i \,, \tag{2.48}$$

we can write our $4d$ theory as

$$\frac{M_P^2\, e^{\frac{3-p}{2}\phi}}{4V_X} \int_{M_4} K_{ij} F_2^i \wedge \star F_2^j + \mu_p \int A_1^i q_i^{\Sigma^p} \,, \tag{2.49}$$

where we used the relation $\kappa_{10}^2 = V_X/M_P^2$ and V_X is the CY volume in Einstein frame. Since only a certain linear combination of gauge fields is sourced by the particle with charge $q_i^{\Sigma^p}$, we can define the field A_1 and its field strength $F_2 = dA_1$ as $A_1 = A_1^i K^{ij} q_j^{\Sigma^p}$ and $F_2 = F_2^i K^{ij} q_j^{\Sigma^p}$. The $4d$ action then reads

$$\frac{M_P^2 |q^{\Sigma^p}|^2\, e^{\frac{3-p}{2}\phi}}{4V_X} \int_{M_4} F_2 \wedge \star F_2 + \mu_p\, |q^{\Sigma^p}|^2 \int A_1 \,, \tag{2.50}$$

where we introduced the notation $|q^\Sigma|^2 = K^{ij} q_i^\Sigma q_j^\Sigma$. In order to extract the $4d$ gauge coupling, we should normalise the gauge potential such that the final action reads

$$S_4 \supset \frac{1}{2e^2} \int_{M_4} F_2 \wedge \star F_2 + \int_{0-brane} A_1 \,. \tag{2.51}$$

Therefore, the gauge coupling should be given by

$$\frac{1}{e^2} = \frac{e^{\frac{3-p}{2}\phi} M_P^2}{2\mu_p^2 V_X |q^{\Sigma^p}|^2} \,. \tag{2.52}$$

The particle descending from the brane wrapped on Σ^p has mass squared given by

$$m^2 = \mu_p^2\, e^{\frac{p-3}{2}\phi}\, V_{\Sigma^p}^2 \,, \tag{2.53}$$

where V_{Σ^p} is the volume of the p-cycle. Finally, the ratio of the mass of the particle and the gauge coupling reads

$$\frac{e^2 M_P^2}{m^2} = \frac{2V_X |q^{\Sigma^p}|^2}{V_{\Sigma_p}^2} \,. \tag{2.54}$$

By imposing the WGC relation (2.45) for a 1-form in $4d$, we have that

$$\frac{e^2 M_P^2}{m^2} \geq \frac{1}{2} \,. \tag{2.55}$$

Note that, in order to have a particle in $4d$ we should wrap Dp-branes on p-cycles, where $p = 2,\, 3,\, 4$ since we are working with CY manifolds. This means in turn that we are implicitly working in type IIA, where D2- and D4-branes are present, or in type IIB with D3-branes wrapped on 3-cycles.

Our goal now is to derive a geometrical relation similar to the one displayed in (2.54) but for 0-forms. Hence, we slightly change our starting setup, and we consider the very same cycle Σ^p wrapped this time by D$(p-1)$-branes, i.e.

$$\frac{1}{4\kappa_{10}^2} \int_{M_4 \times X} e^{\frac{4-p}{2}\phi} F_{p+1} \wedge \star F_{p+1} + \mu_{p-1} \int_{D(p-1) \text{ on } \Sigma^p} C_p \,. \tag{2.56}$$

Indeed, upon compactification on the CY X, we get the action of an axion in $4d$. As before, we can define a basis of harmonic p-forms ω_i of X and expand the $(p+1)$-field strength and the p-form gauge

potential as $F_{p+1} = F_1^i \wedge \omega_i$ and $C_p = \theta^i \wedge \omega_i$, where the θ^i are our 0-forms. Using the definition of integral charges of (2.48) and compactifying on X, we get in $4d$

$$\frac{M_P^2\, e^{\frac{4-p}{2}\phi}}{4V_X} \int_{M_4} K_{ij} F_1^i \wedge \star F_1^j + \mu_{p-1}\, q_i^{\Sigma^p} \theta^i \,. \tag{2.57}$$

In order to consider again the right linear combination of fields, we further redefine the field θ and its field strength $F_1 = d\theta$ as $\theta = \theta^i K^{ij} q_j^{\Sigma^p}$ and $F_1 = F_1^i K^{ij} q_j^{\Sigma^p}$. The $4d$ action then reads

$$\frac{M_P^2 |q^{\Sigma^p}|^2\, e^{\frac{4-p}{2}\phi}}{4V_X} \int_{M_4} F_1 \wedge \star F_1 + \mu_{p-1}\, |q^{\Sigma^p}|^2 \theta \,, \tag{2.58}$$

where we used again the notation $|q^\Sigma|^2 = K^{ij} q_i^\Sigma q_j^\Sigma$. After redefining the axionic field such that the final action is canonically normalized, we obtain

$$S_4 \supset \frac{f^2}{2} \int_{M_4} F_1 \wedge \star F_1 + \theta \,, \tag{2.59}$$

where the first part of the r.h.s. is the kinetic term of the axion and hence it should be multiplied by the decay constant f, which we defined to be

$$f^2 = \frac{e^{\frac{4-p}{2}\phi} M_P^2}{2\mu_{p-1}^2 V_X |q^{\Sigma^p}|^2} \,. \tag{2.60}$$

For an axion we have that the mass is replaced by the instanton action S from the wrapped D$(p-1)$-brane as

$$S^2 = \mu_{(p-1)}^2\, e^{\frac{p-4}{2}\phi}\, V_{\Sigma^p}^2 \,. \tag{2.61}$$

Finally, we arrive at the expression for Sf in terms of purely geometrical quantities, namely

$$\frac{M_P}{Sf} = \frac{\sqrt{2V_X}\, |q^{\Sigma^p}|}{V_{\Sigma^p}} \,. \tag{2.62}$$

Note that the r.h.s. is the same geometrical ratio that we found previously for a particle (cf. (2.54)). For $p = 2$, 4, this computation is valid in type IIB, while for $p = 3$ we are working in type IIA.

The main point of our computations is the following: the bound (2.55) is actually a bound on geometrical quantities and does not contain any information on the starting $10d$ theory, i.e.

$$\frac{2V_X |q^{\Sigma^p}|^2}{V_{\Sigma_p}^2} \geq \frac{1}{2} \,. \tag{2.63}$$

Therefore, as long as the cycle is the same, we are entitled to apply these bounds on the axion as well, as we managed to express the quantity Sf in the same language as the particle. This finally leads to the bound

$$\frac{M_P}{Sf} \geq \frac{1}{\sqrt{2}} \,, \tag{2.64}$$

where the lower bound is the WGC bound for axions coming from dimensional reduction (see e.g. [16]). Note that our derivation does not rely on T-duality, but only on the fact that both the relation for the particle and the one for the axion are expressed in terms of the same geometrical quantities of the CY.

2.3.1 Festina Lente bound for axions

Using the same logic, we are able to extend the Festina Lente (FL) bound to axions. In [72, 73], it was discovered that for charged black holes in (approximate) de Sitter space with Hubble constant H to decay consistently, one expects an additional constraint called the FL bound. This bound states that all charged particles with mass m and U(1) gauge coupling e must obey [72]

$$\frac{eM_P^2}{m^2} \lesssim \frac{M_p}{H}\,, \tag{2.65}$$

where the '$\sim$' accounts for an $\mathcal{O}(1)$ constant. Unfortunately, this bound does not geometrize nicely. However, the gauge theory must be at weak coupling $e < 1$. This then implies the weaker bound

$$\frac{e^2M_P^2}{m^2} \lesssim \frac{M_p}{H}\,, \tag{2.66}$$

which as we shall see does geometrize in a clean way. The bound (2.66) can also be directly derived from ensuring black holes in de Sitter behave consistently under FL for dipoles rather than charged particles [73]. Let us explain how this works in some more detail.

The bound which we will dualize to axions is the dipole version of the FL bound. While the production of electric (magnetic) dipoles clearly cannot discharge an electrically (magnetically) charged black hole, such dipoles locally screen the electric field. A dipole with moment μ in a theory with gauge coupling e gains an energy $-\mu E$ ($-\mu B$) when favourably aligned in an external electric field. One then expects an instability against rapid production of dipole for a particle of mass m when $-\mu E > m$. Filling in the field strength for the maximally charged Nariai black hole [74, 75],[5] one obtains

$$\mu \lesssim \frac{m}{eM_PH}\,. \tag{2.67}$$

The dipole moment μ is set by eL, with L the length scale of the dipole. As we are dealing with fundamental particles, we take this to be the Compton length of the particle $L = 1/m$. From this, then (2.66) follows. The same result can be derived analogously for magnetic dipoles. Hence, we can simply apply (2.66) to (2.63) and we get an allowed window for the value of Sf, namely

$$\frac{1}{\sqrt{2}} \leq \frac{M_P}{Sf} \lesssim \sqrt{\frac{M_P}{H}}\,, \tag{2.68}$$

where the lower bound is the usual WGC bound for axions coming from dimensional reduction, while the upper bound is the new FL bound for axions (aFL). We have found that all instantons with action S coupled to an axion with decay constant f must obey the aFL bound, which reads

$$Sf \gtrsim \sqrt{M_PH} \sim V^{1/4}\,, \tag{2.69}$$

with V the vacuum energy density.

Having found the bound for a single axion from dimensional reduction, it would be interesting to extend it to a setup where multiple axions are present, as was put forward for the WGC [68]. Therefore, we consider a theory with N canonically-normalized axion fields ϕ_i, $i = 1, \ldots, N$, such that their kinetic

[5] The (charged) Nariai black hole is a particular Schwarzschild solution in de Sitter background, whose horizon coincides with the de Sitter one.

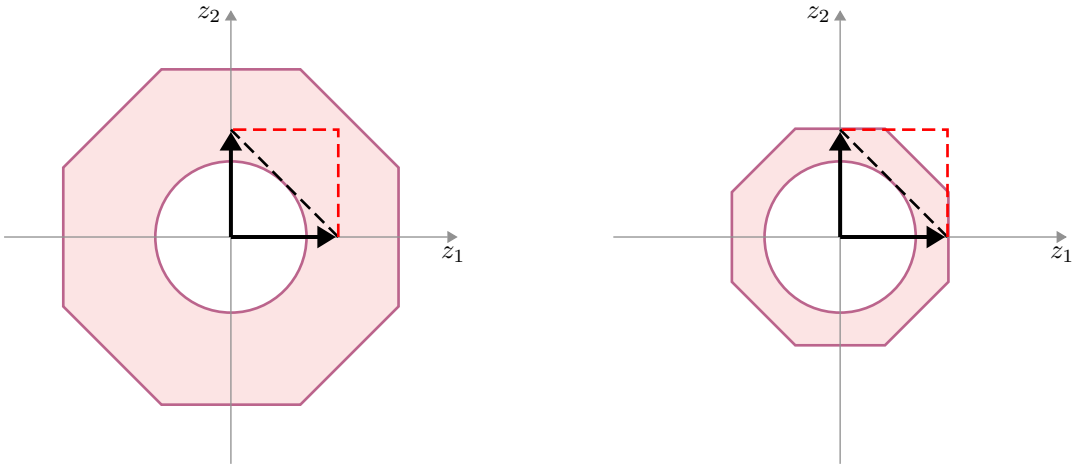

Figure 2.1: Convex hull (inner circle) and convex nut (outer polygon). On the left, the charge vectors satisfy both, while on the right we have a violation of the aFL bound. Indeed, charge vectors need to be big enough for all extremal dyonic black holes (inner circle) to decay, so that the black dotted line lies outside the circle. If we also impose aFL and in a situation where the outer shell is very thin, having very big charge vectors could violate the aFL bound.

terms are given in the canonical form. Then, the potential takes the form

$$V \sim \sum_a A_a e^{-S_a} \cos\left(\sum_i \frac{\phi_i}{f_{ai}}\right) , \tag{2.70}$$

where the index a runs over the number of instantons contributing to the action. The analogue of the charge-to-mass ratio vectors is [68]

$$\mathbf{z}_{ai} = \sum_i \frac{M_P}{f_{ai} S_a} \mathbf{e}_i \, , \tag{2.71}$$

where the $\mathbf{e}_i$ form an orthonormal basis of the vector space. The WGC translates into the requirement that the convex hull spanned by the vectors $\mathbf{z}_{ai}$ should contain the N-dimensional unit ball, i.e. $\mathbf{z}_{ai} > 1$.

The generalization to multi-U(1)s of the FL bound puts an upper bound on every vector. Consider a $\mathrm{U}(1)^N$ gauge theory. We denote the couplings as g_i, $i = 1, .., N$. Let the theory have M species of charged particles with masses m_a, $a = 1, .., M$ and q_{ia} charges under the U(1). The multi-U(1) version of the (dipole version of the) FL bound states [73]

$$m_a^2 > \mathcal{O}(1) \sum_i q_{ai}^2 \, g_i^2 \, H M_P \, . \tag{2.72}$$

By defining the charge-to-mass ratio vector of the a-th particle charged under the i-th U(1) as $\mathbf{z}_{ai} \equiv \frac{g_i q_{ia} M_P}{m_a}$, we can rewrite (2.72) as the upper bound

$$\mathbf{z}_{ai} < \sqrt{\frac{M_P}{H}} \, . \tag{2.73}$$

Hence, from (2.68), we get a window for every vector, namely

$$1 < \mathbf{z}_{ai} < \sqrt{\frac{M_P}{H}} \, . \tag{2.74}$$

From the derivation of the previous section, this holds also for a theory with many axions, where $\mathbf{z}_{ai}$ is now given by (2.71). Note that the relation in (2.74) means that the vectors should stay outside the

extremal region constrained by the WGC, and also they should lie inside a 'nut' originating from *all* the $\mathbf{z}_{ai}$ of the theory. The danger then exists that if the allowed window between the extremal region and the nut is very thin, the WGC convex hull will be unable to satisfy the aFL bound (see figure 2.1). In particular, in presence of N axions and considering the 'largest' elementary axionic charge, i.e. $\vec{q} = \vec{1}$, we have that $||\mathbf{z}_a|| = \sqrt{N}$. We then find that generically we must have

$$N < \frac{M_P}{H}\,, \tag{2.75}$$

which produces a bound on the number of allowed axions. For this bound to be very constraining, we need to have a mild hierarchy between H and M_P.

2.4 Thraxions

Thraxions, or throat-axions [76], are a recently discovered class of ultralight axionic modes arising whenever the CY admits a system of multiple warped throats (multi-throats) sharing some common 3-cycle $\mathcal{B}$, near a conifold point in complex structure moduli space. In such a case, it is in fact possible to reduce the 2-form R-R and NS potentials C_2 and B_2 on the family of sectional $S^2 \subset \mathcal{B}$, generating new axions as the lowest-lying radial Kaluza-Klein (KK) mode in the low energy effective theory. These axions were found to be parametrically lighter than any other particle in the spectrum. Their mass squared is suppressed by six times the warp factor $\omega_{\rm IR}$ of the throats, while the warped-throat KK modes of, e.g. the throat complex-structure modulus, receive a double suppression only. Since the thraxions own such unique features, it is important to explore their behaviour in a fully stabilized setup in order to connect them with axion phenomenology.

The aim of this section is to discuss two relevant questions that were left behind in the original paper [76]. First, we study the effect of a non-vanishing thraxion VEV at the level of the SU(3)-structure torsion classes of the compactification space. We find that for a non-vanishing VEV, the compactification space fails to be CY and becomes simply a complex manifold. We understand this as a breakdown of the imaginary self-dual condition of the G_3-flux, and we relate quantitatively the size of the thraxion VEV with the size of the ISD breaking. Second, we study the interplay between thraxions and Kähler moduli stabilisation. In particular, we find that in general the thraxion potential receives potentially non-vanishing corrections which lift the mass squared to $\sim \omega_{\rm IR}^3$ only. After explaining why this is the case, we show that these cross terms in general do not vanish in multi-throats consisting of at least three joined throats. Conversely, in the simplest class of double-throats, avoiding the cross terms reduces to essentially a single concretely realizable condition on the periods of double-throats.

2.4.1 Thraxions in flux compactification

Let us consider type IIB superstring theory compactified on a compact CY threefold X whose volume is sufficiently larger than the string scale. Let $H_3(X)$ be the third homology group of X with integer coefficients. We fix an integral basis for $H_3(X)$ consisting of $2h^{2,1}+2$ 3-cycles $\mathcal{A}_i$, $\mathcal{B}^j$, $i,j = 1,\dots h^{2,1}+1$. Generic pointlike singularities of X arise at specific codimension 1 loci in $\mathcal{M}_{cs}$, where one of the complex structure moduli z_i vanishes. Such singularities are called conifold points [77, 78].

It is important to discuss now a crucial difference regarding conifold singularities in a compact CY, compared to a non-compact one. In a non-compact setting, it is possible to have a conifold singularity in which a single one of the complex structure moduli z_i vanishes. From (2.16) this implies that a single $\mathcal{A}$-cycle vanishes. On the other hand, in a compact setting a conifold singularity is only possible if two

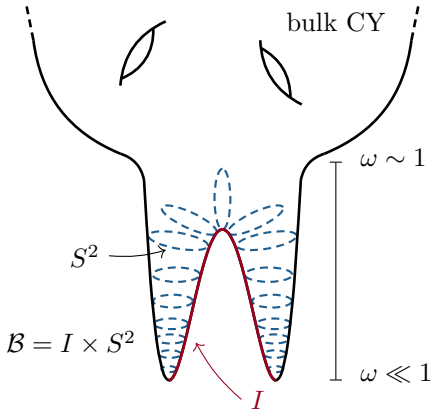

Figure 2.2: Example of a double-throat system with one thraxion.

or more $\mathcal{A}$-cycle related in homology shrink to zero volume [79].[6] Throughout this section, we will call this latter case *multi-conifold*, to distinguish it with the non-compact case in which a single $\mathcal{A}$-cycle vanishes.

Let us consider a multi-conifold singularity on X in which a set of n $\mathcal{A}$-cycles vanish, and they satisfy m homology relations of the form $p_i^I[\mathcal{A}]_i = 0$. This leaves only $n-m$ $\mathcal{A}_i$-cycles independent. For each one of them, there is a symplectic dual $\mathcal{B}_i$-cycle. Geometrically, this $\mathcal{B}_i$-cycle interpolates between d_i singular points. The numerical value of d_i can be determined as a function of the homology relations coefficients p_i^I, essentially determining which independent $\mathcal{B}_i$-cycle intersects which of the original n $\mathcal{A}_i$-cycles. We depict this schematically in Figure 2.2, for the simplified case of $n = 2,\ m = 1$. Note that in this picture, for ease of exposition, we draw two finite-size long throats rather than two conifold points. We will see later that this is the relevant setup once fluxes are turned on and the orientifold projection breaking to $\mathcal{N} = 1$ is imposed. As it can be seen from Figure 2.2, for $n = 2,\ m = 1$, the interpolating $\mathcal{B}$-cycle is, as a topological space, homeomorphic to $I \times S^2$, where I is a finite size interval connecting the two singular points. The situation generalizes easily for $n, m > 1$. In such a case, the $n-m$ interpolating 3-cycles will be topologically homeomorphic to $Y_{d_i}^i \times S^2$ where $i = 1, \dots n-m$, and Y_{d_i} is the complete graph with d_i nodes.

We now *define* the thraxion field as the dimensional reduction of the R-R 2-form gauge potential on the interpolating family of S^2 sphere discussed above, namely

$$c \coloneqq \int_{S^2} C_2 \,. \tag{2.76}$$

Hence, on the deformed side $c = c(r)$ does not constitute a true harmonic zero mode, but the lowest radial KK-mode in the multi-throat. Moreover, the decay constant can be computed from dimensional reduction of the $F_3 \wedge \star F_3$ term over the sectional S^2 on which c is defined and then plug the expansion of C_2 in harmonic forms. In this way, one can show that f depends explicitly on inverse powers of the warp factor. The result can be found in appendix D of [76]. Here it is shown also how the decay constant gets an effective enhancement by the flux quantum. This will be important for thraxions phenomenology, as we will discuss in Section 4.2.3.

Given a conifold singularity, it is often also possible to perform a small resolution of it, producing

[6] The reason for this arises from the subset of conifold singularities which admit a resolution phase. In such a case, the fact that a single 3-cycle shrinks to zero size will induce a breaking of the Kähler condition on the resolution side of the transition.

extra 2-cycles.[7] Going from the deformed to the resolved phase is known as a conifold transition [80]. Let us call $\tilde{X}$ the manifold on the resolution side. In a conifold transition, in a compact setting, the Hodge numbers change as $\tilde{h}^{1,1} > h^{1,1}$, $\tilde{h}^{2,1} < h^{2,1}$. In particular, on the resolved side, there will be $\Delta h^{1,1} = \tilde{h}^{1,1} - h^{1,1}$ extra resolution 2-cycles compared to the deformed side. This number of 2-cycles is equal to the number of the homology relations among the conifolds in the deformed side. On the resolved side, thraxions correspond to massless axions coming from the integrals of the 2-form over these $\Delta h^{1,1}$ independent resolutions $\mathbb{P}^1$. It is believed that the presence of conifold singularities and conifold transitions is very generic. It has been conjectured that all the CY manifolds are connected with each other by a web of conifold transitions [80,81]. It has also been shown that this statement holds true in numerous closed classes of examples [82–87]. Therefore, the existence of thraxions is a generic prediction of any IIB CY compactification, at least at the $\mathcal{N} = 2$ level.

We now consider the introduction of an orientifold projection, and fluxes, in order to break supersymmetry to $\mathcal{N} = 1$. For concreteness, we focus on the case in which the orientifold projection has O3/O7 fixed loci. From the point of view of representation theory of the $4d$, $\mathcal{N} = 1$ SUSY algebra, thraxions are the lowest component of a scalar chiral superfield G^I, $I = 1, \dots, m$. Clearly, not all CY orientifolds supports the presence of thraxions: for example, many orientifolds are such that $h^{1,1}_- = 0$. In order for thraxions to be present in a $\mathcal{N} = 1$ setup, at least two crucial conditions must hold true:

- The orientifold projection must leave the conifold transition intact.
- In the quotient space, a multi-conifold with interpolating $\mathcal{B}$-cycles must still exist.

It has been shown in [88] that orientifolds supporting thraxions exist within the set of complete intersection CYs. Having included an orientifold, for reasons of both tadpole cancellation and moduli stabilisation, we will consider the addition of 3-form fluxes. Flux quanta are defined as

$$M_i = \frac{1}{(2\pi)^2\alpha'} \int_{\mathcal{A}_i} F_3 \quad \text{and} \quad K_i = -\frac{1}{(2\pi)^2\alpha'} \int_{\mathcal{B}_i} H_3 \,. \tag{2.77}$$

As shown in [38, 89], generic choices of the fluxes stabilize the complex structure moduli and the axio-dilaton. Furthermore, if $K_i \gg g_s M_i$, the complex structure modulus associated to the cycle $\mathcal{A}_i$ will be stabilized close to the conifold point,

$$|z_i| = \exp\left(-2\pi \frac{K_i}{g_s M_i}\right) \ll 1 \,. \tag{2.78}$$

Everywhere in this section we will work under this assumption, which we request to hold independently for each pair of flux quanta K_i, M_i.

When the complex structure moduli are stabilized close to the conifold point, the multi-conifold system described in the previous paragraphs is replaced with a system of long multiple throats, which arise due to the backreaction of fluxes on the geometry. Within the throats, the metric is well approximated by the Klebanov-Tseytlin [90] solution

$$ds^2 = \omega(r)^2 \eta_{\mu\nu} dx^\mu dx^\nu + \omega(r)^{-2} \left(dr^2 + 2^2 ds_{T^2_{1,1}}\right) , \quad \omega(r)^2 \sim \frac{r^2}{g_s M \alpha'} \log\left(\frac{r}{r_{\rm IR}}\right)^{-\frac{1}{2}} , \tag{2.79}$$

where r is the radial coordinate, $\omega(r)$ is the warp factor. The solution ceases to hold at a UV cutoff $r_{\rm UV}$, where the multi-throat is attached to the bulk geometry, and also at a IR cutoff $r_{\rm IR}$ near the

[7] This is not always the case. A famous example of a compact CY admitting a conifold singularity without resolution branch is the mirror quintic [79].

bottom of the throats. For $r \lesssim r_{\rm IR}$ the metric is given by the full Klebanov-Strassler (KS) solution [91]. An exponential hierarchy, as the one in Randall-Sundrum model [38, 92], is thus engineered by $\omega_{\rm IR} \equiv \omega(r_{\rm IR}) \sim r_{\rm IR}/r_{\rm UV} \sim |z^{1/3}|$.

We will now review in more detail how the complex structure moduli stabilisation operates in this setup. For concreteness, we focus on a subset of $n \leq h^{2,1}_-$ complex structure moduli associated to n $\mathcal{A}$-cycles subject to m homology relations. The superpotential coupling the thraxion fields G^I to the complex structure moduli can be derived from the GVW superpotential [39] and it reads [76]

$$W = \sum_{k=1}^{n} \left(M_k \frac{z_k}{2\pi i} \log z_k - \tau K_k z_k \right) - \sum_{I=1}^{m} \frac{G^I}{2\pi} \mathcal{P}_I + \hat{W}_0(z) + \mathcal{O}(z_k^2)\,, \tag{2.80}$$

where $\hat{W}_0(z)$ is a holomorphic function denoting contributions from other cycles and $\mathcal{P}_I$ are the m relations for the n complex structure moduli z_i, $\mathcal{P}_I \equiv \sum_{k=1}^{n} \sum_{I=1}^{m} p^k_I z_k$. The n complex structure moduli are thought to be all independent. The fact that they are subject to m relations is imposed dynamically, once the thraxions G^I are set on-shell by their equation of motion. In particular, the fields G^I act as Lagrange multipliers, imposing the homology relations among the complex structure moduli.

On the other hand, the Kähler potential for the complex structure moduli reads

$$\begin{aligned} K_{\rm cs}(z_i, \bar{z}_i) &= -\log\left(-i \int \Omega \wedge \bar{\Omega}\right) = -\log\left(i g_K(z) - \overline{g_K(z)} + \sum_{I=1}^{n-m} i \bar{z}_I G^I + \text{ c.c.} \right) \\ &= -\log\left(i g_K(z) - \overline{g_K(z)} + \sum_{i=1}^{n} \left[\frac{|z_i|^2}{2\pi} \log(|z_i|^2) + i \bar{z}_i g^i(z) - i z_i \overline{g^i(z)} \right] \right)\,, \end{aligned} \tag{2.81}$$

where $g_K(z)$ is a holomorphic function encoding contributions from the periods of $h^{2,1}_- - n$ complex structure moduli of the bulk CY, while the $g_i(z)$ are related to the periods of the complex structure moduli of the multi-throat. Being interested in small z_i we can Taylor expand these functions as

$$g_k(z) = g_{K,0} + \sum_j g^i_{K,1} z_i + \mathcal{O}(z^2)\,, \quad g^i(z) = g^i_0 + \sum_j g^{ij} z_j + \mathcal{O}(z^2)\,. \tag{2.82}$$

It is also possible to expand $\hat{\hat{W}}(z)$ as

$$\hat{\hat{W}}(z) = g_{W,0} + \sum_{i=1}^{n} g^1_{W,1} z_i + \mathcal{O}(z^2)\,, \quad \text{and define } \hat{W}_0 \equiv g_{W,0} + \sum_{i=1}^{n} M_i g^i_0 \tag{2.83}$$

to be the superpotential containing all the contributions of order $\mathcal{O}(z^0)$. By computing the F-terms for the complex structure moduli z_i using (2.80), one can relate the VEV of the n moduli to the VEV of the thraxions, as[8]

$$\begin{aligned} z_k &= z_{0,k}\, e^{i \sum_I \frac{p^I_k G^I}{M_k}} \quad \text{where} \\ z_{0,k} &= e^{-1 - 2\pi \frac{K_k}{g_s M_k}} e^{-\frac{2\pi i}{M_k} \left(\sum_j g_1^{kj} + g^k_{W,1} - i \frac{\tilde{g}^k_0 \hat{W}_0}{2 \mathrm{Im}\, g_{K,0}} \right)} + \mathcal{O}\left(e^{-4\pi \frac{K_k}{g_s M_k}} \right)\,. \end{aligned} \tag{2.84}$$

We remark that at the current level of the discussion, the thraxion fields themselves are *not* stabilized yet. Therefore, the complex structure moduli themselves are yet not stabilized, but simply expressed in terms of the VEV of the thraxion and flux quanta. By plugging (2.84) in (2.80), we find the effective

[8] In (2.84) we have already set C_0 to zero.

superpotential for the thraxions we will be using in the stabilisation procedure. Let us consider the effective thraxion superpotential for n throats and m thraxions [76]:

$$W_{\rm eff} = \hat{W}_0 - \sum_{k=1}^{n} \varepsilon_k e^{i\sum_{I=1}^{m} p_I^k G^I/M_k} \,, \tag{2.85}$$

where

$$\varepsilon_k \equiv \frac{M_k}{2\pi i} z_{0,k} \left(1 - \frac{2\pi}{M_k} \frac{\hat{W}_0 \overline{\tilde{g}_0^k}}{\mathfrak{a}}\right) . \tag{2.86}$$

We also introduced $\tilde{g}_0^k = g_0^k - \overline{g_{K,1}^k}$, $\mathfrak{a} \equiv -2{\rm Im}\,(g_{K,0})$. We remark that the physical deformation parameters are the z_k defined in (2.84). As we will analyse later, a non-vanishing VEV for G^I is necessary to generate a potential for the thraxions, but whenever they are not stabilized at zero, the CY condition is broken. Indeed, generically G^I does not need to stabilize at zero.

By using some approximations, one can simplify (2.85). In particular, in the explicit examples discussed later, we will always work with a simplified superpotential. As in [76], supposing that only $g_{W,0}$ and $g_{K,0}$ are non-vanishing, the definitions of $z_{0,k}$, ε_k and $\hat{W}_0$ simplify.[9] For the case in which there is only one thraxion in one multi-throat system composed of n throats, by using a symmetrical choice of M_k and K_k fluxes, it is possible to rewrite (2.85) as

$$W_{\rm thr}(G) = W_0 + n_p \varepsilon \left(1 - \cos\left(G/M\right)\right) \,, \tag{2.87}$$

where n_p is the number of KS throats in the multi-throat system, and we have defined $W_0 \equiv \hat{W}_0 - n_p\,\varepsilon$. In this way, we recover the general axion effective potential. When there are k multi-throats in the CY, each one hosting a single thraxion, the superpotential can approximately be written as q copies of (2.85), namely

$$W_{\rm thr}(G^I) = W_0 + \sum_{I=1}^{q} \varepsilon_I \left(1 - \cos\left(G^I/M_I\right)\right) \,, \tag{2.88}$$

where we have absorbed the number of KS throats inside each system in the definition of ε_I.

So far we reviewed the complex structure moduli stabilisation in presence of thraxions. One is then left with discussing the problem of moduli stabilisation for the thraxions themselves and for the Kähler moduli. The total Kähler potential actually reads

$$K\left(G, \bar{G}, T, \bar{T}, z, \bar{z}\right) = K_{\rm cs}(z, \bar{z}) + K_{\rm thr}(G - \bar{G}, T + \bar{T}) \,, \tag{2.89}$$

where $K_{\rm cs}$ has been introduced in (2.81), while $K_{\rm thr}$ is a Kähler potential coupling the thraxions to Kähler moduli. We assume that one can invert the relation between the 2- and 4-cycle moduli to write the Kähler potential $K_{\rm thr}$ for the T and G fields as

$$\begin{aligned} &K_{\rm thr} = -2\log\left(F\right) \,, \quad \text{where} \\ &F = \sum_{\alpha=1}^{h^{1,1}_+} \sum_{a,b=1}^{h^{1,1}_-} c_\alpha \left(T_\alpha + \bar{T}_\alpha - \frac{g_s}{4}\kappa_{\alpha a b}\left(G^a - \bar{G}^a\right)\left(G^b - \bar{G}^b\right)\right)^{3/2} \,. \end{aligned} \tag{2.90}$$

However, we stress that the discussion we will carry out in what follows does not need to assume any explicit expression for the Kähler potential. The F-term supergravity potential can be computed from (2.24). Let us consider for simplicity the case of a single thraxion. Thanks to the no-scale property

[9] Such approximation imposes that $\hat{W}_0$ and all the non-logarithmic terms in (2.81) are constants.

of $K_{\rm thr}$, one can show that the F-term potential scales as

$$V\left(G,\bar{G}\right) \propto \left|\partial_G W\left(G\right)\right|^2 . \tag{2.91}$$

Hence, the potential for the thraxion gets a double suppression in the $\varepsilon \sim z_0 \sim \omega_{\rm IR}^3$ parameter. In turn, by construction this implies that the mass-squared of the G field is of order $\omega_{\rm IR}^6 \ll 1$, making the thraxion an extremely light particle. This effect generalizes trivially for the case of multiple thraxions.

So far, the Kähler moduli sector is left as a flat direction of the potential. We have considered only tree-level contributions to the superpotential, which come from the presence of thraxions in the theory. In what follows, we will study if and how the potential for thraxions gets modified by the inclusion of perturbative and non-perturbative quantum effects proportional to the Kähler moduli.

First, we discuss the backreaction on the geometry given by the presence of thraxions. Fluxes and localized objects in general backreact on spacetime, causing the compactification manifold X to cease to be CY, yet still maintaining a SU(3) structure. Geometrical properties of the backreacted compactification manifold can be understood by an analysis of its SU(3) torsion classes.

In order for a thraxion to exist there must be present in X at least one warped multi-throat region, with at least one homology relation among the shrinking β-cycles. This setting implies the presence of quantized $(2,1)$-form background fluxes. Hence, there is an amount of $H_3^{(6)}\Big|_0$, $F_3^{(6)}\Big|_0$ stabilizing the whole complex structure moduli sector and warp factor. On top of this background flux configuration, turning on the thraxion corresponds to turning on 'a bit' of C_2 at the IR ends of the multi-throat, with profile in the throat radial direction. Thus, turning on the thraxion corresponds to turning on 'a bit' of pure[10] $\Delta F_3^{(6)}$ but *without* any accompanying $H_3^{(6)}$. Hence, the extra thraxion-flux $\Delta F_3^{(6)}$ is non-ISD because the complex structure moduli of the multi-throat simply cannot adjust their VEVs in order to be ISD again with respect to the new configuration. This is impossible for the following reason. If they could adjust their VEVs to be ISD again, this would imply that the thraxion potential vanishes. However, this was shown to be impossible since the $10d$ equations of motion of the perturbed multi-throat analysed in [76] forbid it, once the multi-throat is embedded in a compact CY. The system cannot relax back to vanishing vacuum energy at finite thraxion-flux. Schematically, this can be denoted as:

$$(\text{ISD} \;\Rightarrow\; V=0 \wedge \partial_{z^i} V = 0 \;\forall i) \quad \Rightarrow \quad (V \neq 0 \vee \partial_{z^i} V \neq 0 \;\Rightarrow\; \text{non-ISD}) . \tag{2.92}$$

The effect of the ISD-violation on the torsion classes of the compactification is non-negligible. The main backreaction from the thraxion will be its non-ISD nature, which distorts the torsion classes of the manifold. In glossing over the multiple 3-cycles of an actual CY we can see, that by writing this extra thraxion-flux $\Delta F_3^{(6)} \equiv \varepsilon\, F_3^{(6)}\Big|_0$ the classical ISD relation changes as

$$\begin{aligned} 2abH_3^{(6)} &= 2a(b_0+\delta b)\, H_3^{(6)}\Big|_0 = -e^{\phi}(a^2-(b_0+\delta b)^2)\star_6 F_3^{(6)}\Big|_0 \\ &= -e^{\phi}(a^2-b_0^2)\star_6 F_3^{(6)}\Big|_0 + e^{\phi}\varepsilon\star_6 F_3^{(6)}\Big|_0 . \end{aligned} \tag{2.93}$$

Plugging in $a = ib_0$ this becomes

$$\begin{aligned} 2ib_0^2\, H_3^{(6)}\Big|_0 + 2ib_0\delta b\, H_3^{(6)}\Big|_0 &= e^{\phi}(2b_0^2+2b_0\delta b+\delta b^2)\star_6 F_3^{(6)}\Big|_0 \\ &= e^{\phi}2b_0^2\star_6 F_3^{(6)}\Big|_0 + e^{\phi}\varepsilon\star_6 F_3^{(6)}\Big|_0 . \end{aligned} \tag{2.94}$$

[10] The thraxion-induced F_3-flux lives on a 3-cycle in the throat part of the $(2,1)$-homology of the CY, and thus has to be locally of the same cohomology type as the ISD background fluxes.

Cancelling out identical pieces, we see that $\delta b = \sqrt{\varepsilon}$, that is, the thraxion-sourced extra $\Delta F_3^{(6)} = \mathcal{O}(\varepsilon)$ deforms the ISD relation $a = ib_0$ to $a \neq ib$ with deformation $\mathcal{O}(\varepsilon^{1/2})$. Hence, the flux with turned-on thraxion is non-ISD in such a way, that $W_3 \neq 0$ because now $a \neq \pm ib$. According to [93] the thraxion thus 'wrecks' the CY in the qualitatively worst fashion, leaving just a complex manifold. Still, the extreme scale suppression of the thraxion sector due to warping may leave this just-complex non-CY manifold in some sense 'near' the original conformal CY, where the word 'near' awaits an appropriate definition of distance in torsion deformation space and the space of 4d effective actions from KK reduction, which is beyond the scope of this discussion.

2.4.2 Moduli stabilisation

The GKP-type flux compactification that we considered so far discusses the stabilisation of complex structure moduli in presence of thraxions. We are still left with the problem of Kähler moduli stabilisation, which we will address in this section. Whenever thraxions are present, there are two sources of no-scale breaking, which contribute to Kähler moduli stabilisation: one is the usual F-term scalar potential coming from the introduction of non-perturbative corrections to the superpotential, while the other one is the CY breaking potential of the thraxions reviewed above. In [76], an initial study of the mixing between these two effects was discussed. However, no detailed analysis was carried out.

We will study the backreaction on the thraxion potential (2.91) when we appropriately stabilize the Kähler moduli via the leading stabilisation mechanisms. As a main result, we find a 2-fold statement. On one hand, *generically* the six-fold warp suppression is spoiled, once the thraxion-carrying multi-throat consists of at least 3 connected throats. On the other hand, for double-throats there exist classes of CY flux compactifications where the six-times warp suppression survives Kähler moduli stabilisation. The survival of the full warp suppression depends on the Kähler moduli stabilisation, potentially inducing a cross term which is proportional to the warp factor cubed only. Consequently, the mass gets lifted whenever this cross term does not vanish. The mass squared of the warped-throat KK modes scales as $\omega_{\rm IR}^2$. Moreover, we will show below that while the stabilized Kähler moduli are parametrically lighter than the warped KK modes, the thraxion is still parametrically lighter than the Kähler moduli. Hence, it remains the lightest state inside the throat. The mass-spectrum is still *effectively* gapped.

The survival of the full warp suppression depends on the Kähler moduli stabilisation, potentially inducing a cross term which is proportional to the warp factor cubed only. Consequently, the mass gets lifted whenever this cross term does not vanish. The mass squared of the warped-throat KK modes scales as $\omega_{\rm IR}^2$. Moreover, we will show below that while the stabilized Kähler moduli are parametrically lighter than the warped KK modes, the thraxion is still parametrically lighter than the Kähler moduli. Hence, it remains the lightest state inside the throat. The mass-spectrum is still *effectively* gapped. Nevertheless, we find that in certain classes of setups the $\mathcal{O}(\varepsilon)$ cross term (which is responsible for lifting the mass) gets cancelled by Kähler moduli stabilisation. This happens when we set the C_4 axion to its minimum.

Let us specialize the F-term potential in (2.33) for the T and G fields. The pieces corresponding to the G fields only and the mixing of G and T are subleading in ε. Indeed, in the following analysis we can disregard the $G\bar{G}$ contribution since it will lead to a double-warp suppressed term as in (2.91). For a general treatment of the potential, we should add also the cross terms between the Kähler moduli and the G fields. However, it was shown in [34] that the Kähler metric for these components is proportional to b^a. If the VEV of b^a at the minimum is at most order ε as defined in (2.86), they can be neglected in this analysis because they will produce terms of order $\mathcal{O}(\varepsilon^2)$. If the VEV of b^a at the minimum is larger

than ε, they must be considered. For the sake of expositions, we will now assume that the VEV of b^a vanishes at the minimum. This assumption is generically satisfied when D-terms are included [94–96]. The vanishing VEV of b^a implies then that the Kähler metric is block diagonal. We do not expect that a different VEV for b^a would change the consequences of our discussion.

The terms that might lift the thraxion mass are those that break the no-scale condition of the potential and the perturbative corrections in α', i.e. $V_{\text{np}_2} + V_{\alpha'}$. This allows us to focus only on the terms in (2.33), since there will be no contributions to the potential coming from the mixing between the G^a fields and the Kähler moduli T_α once $b^a = 0$. By decomposing the superpotential and the Kähler moduli in real and imaginary parts, i.e.

$$W = \text{Re}\,(W) + i\text{Im}\,(W) \equiv W^R + iW^I\,, \quad T_\alpha = \text{Re}\,(T_\alpha) + i\text{Im}\,(T_\alpha) \equiv T_\alpha^R + iT_\alpha^I\,, \tag{2.95}$$

we rewrite $V_{\text{np}_2} + V_{\alpha'}$ as follows:

$$\begin{aligned} V_{\text{np}_2} + V_{\alpha'} = \; e^K \Bigg[& 2\sum_{\alpha,\beta} K^{T_\alpha \bar{T}_\beta} W^R a_\alpha A_\alpha e^{-a_\alpha T_\alpha^R} \partial_{\bar{T}_\beta} K \cos\left(a_\alpha T_\alpha^I\right) \\ & -2\sum_{\alpha,\beta} K^{T_\alpha \bar{T}_\beta} W^I a_\alpha A_\alpha e^{-a_\alpha T_\alpha^R} \partial_{\bar{T}_\beta} K \sin\left(a_\alpha T_\alpha^I\right) \Bigg] \\ & + 3\xi \frac{\xi^2 + 7\xi\mathcal{V} + \mathcal{V}^2}{(\mathcal{V}-\xi)(2\mathcal{V}+\xi)^2} \left(\left(W^R\right)^2 + \left(W^I\right)^2\right)\,. \end{aligned} \tag{2.96}$$

In Section 2.4.3, we will see that eq. (2.96) can endanger the double suppression of the thraxion potential found in [76] and displayed in (2.91). Generically, the superpotential for the thraxions will generate linear terms in the warp factor in presence of Kähler moduli. However, we propose two ways in which such situation does not occur and the six-time warp suppression is recovered. In Section 2.4.4 we show that by allowing for tuning of fluxes and topological properties of the CY, the linear term in ε vanishes. In Section 2.4.5 we comment on how an exponentially large CY volume stabilized à la LVS could compete with ε. For particular cases, this makes the linear term in ε subdominant with respect to the ε^2 ones.

2.4.3 General structure of the superpotential in the presence of thraxions

In this section, we argue that the potential in (2.96) actually generates cross terms that are linear in the warp factor $\varepsilon \sim \omega_{\text{IR}}^3$. We consider a setup of n multi-throats, each one hosting a number m_k of thraxions, $k = 1, \dots n$. The superpotential reads:[11]

$$W_{\text{eff}} = \hat{W}_0 - \sum_{k=1}^{n} \varepsilon_k e^{i\sum_{\mathfrak{I}=1}^{m_k} p_{\mathfrak{I}}^k G^{\mathfrak{I}}/M_k} + \sum_\alpha A_\alpha e^{-a_\alpha T_\alpha}\,. \tag{2.97}$$

It is possible to divide the superpotential in real and imaginary part, defining

$$\begin{aligned} \hat{W}_0 &= \text{Re}\,(\hat{W}_0) + i\text{Im}\,(\hat{W}_0) = \hat{W}_0^R + i\hat{W}_0^I\,, \quad \varepsilon_k = \text{Re}\,(\varepsilon_k) + i\text{Im}\,(\varepsilon_k) = \varepsilon_k^R + i\varepsilon_k^I\,, \\ G^{\mathfrak{I}} &= \text{Re}\,(G^{\mathfrak{I}}) + i\text{Im}\,(G^{\mathfrak{I}}) = G_R^{\mathfrak{I}} + iG_I^{\mathfrak{I}}\,, \quad T_\alpha = \text{Re}\,(T_\alpha) + i\text{Im}\,(T_\alpha) = T_\alpha^R + iT_\alpha^I\,, \end{aligned} \tag{2.98}$$

[11] In this section we use $\mathfrak{I}$ as index to count the number of thraxions, because we reserve I to be the index indicating the imaginary part of a complex function.

so that

$$\begin{aligned} W =& \hat{W}_0^R + \sum_\alpha A_\alpha e^{-a_\alpha T_\alpha^R} \cos\left(a_\alpha T_\alpha^I\right) - \sum_k \varepsilon_k^R e^{-\sum_{\mathfrak{I}} p_{\mathfrak{I}}^k \frac{G_I^{\mathfrak{I}}}{M_k}} \cos\left(\sum_{\mathfrak{I}} p_{\mathfrak{I}}^k \frac{G_R^{\mathfrak{I}}}{M_k}\right) \\ &+ \sum_k \varepsilon_k^I e^{-\sum_{\mathfrak{I}} p_{\mathfrak{I}}^k \frac{G_I^{\mathfrak{I}}}{M_k}} \sin\left(\sum_{\mathfrak{I}} p_{\mathfrak{I}}^k \frac{G_R^{\mathfrak{I}}}{M_k}\right) \\ & i\left(\hat{W}_0^I - \sum_\alpha A_\alpha e^{-a_\alpha T_\alpha^R} \sin\left(a_\alpha T_\alpha^I\right) - \sum_k \varepsilon_k^R e^{-\sum_{\mathfrak{I}} p_{\mathfrak{I}}^k \frac{G_I^{\mathfrak{I}}}{M_k}} \sin\left(\sum_{\mathfrak{I}} p_{\mathfrak{I}}^k \frac{G_R^{\mathfrak{I}}}{M_k}\right)\right. \\ &\left. - \sum_k \varepsilon_k^I e^{-\sum_{\mathfrak{I}} p_{\mathfrak{I}}^k \frac{G_I^{\mathfrak{I}}}{M_k}} \cos\left(\sum_{\mathfrak{I}} p_{\mathfrak{I}}^k \frac{G_R^{\mathfrak{I}}}{M_k}\right)\right) \\ =& W^R + iW^I \,. \end{aligned} \tag{2.99}$$

We can try to explicitly compute ε_k introducing

$$\begin{aligned} \tilde{g}_{0,k} &= \mathrm{Re}\left(\tilde{g}_{0,k}\right) + i\mathrm{Im}\left(\tilde{g}_{0,k}\right) = \tilde{g}_{R,0}^k + i\tilde{g}_{I,0}^k \,, \\ g_1^{jk} &= \mathrm{Re}\left(g_1^{jk}\right) + i\mathrm{Im}\left(g_1^{jk}\right) = g_{R,1}^{jk} + ig_{I,1}^{jk} \,, \\ g_{W,1}^k &= \mathrm{Re}\left(g_{W,1}^k\right) + i\mathrm{Im}\left(g_{W,1}^k\right) = g_{R,W,1}^k + ig_{I,W,1}^k \,. \end{aligned} \tag{2.100}$$

In this way we can define $z_{0,k} = |R_{0,k}|e^{i\varphi_{0,k}}$, where

$$\begin{aligned} |R_{0,k}| &= \exp\left[-2\pi\frac{K^k}{g_s M_k} + \frac{2\pi}{M_k}\left(\sum_j M_j g_{I,1}^{jk} + g_{I,W,1}^k + \tilde{g}_{R,0}^k \frac{\hat{W}_{R,0}}{\mathfrak{a}} + \tilde{g}_{I,0}^k \frac{\hat{W}_{I,0}}{\mathfrak{a}}\right) - 1\right] \,, \\ \varphi_{0,k} &= -\frac{2\pi}{M_k}\left(\sum_j M_j g_{R,1}^{jk} + g_{R,W,1}^k - \tilde{g}_{R,0}^k \frac{\hat{W}_{I,0}}{\mathfrak{a}} + \tilde{g}_{I,0}^k \frac{\hat{W}_{R,0}}{\mathfrak{a}}\right) \,. \end{aligned} \tag{2.101}$$

Finally, ε_k becomes

$$\begin{aligned} \varepsilon_k =& \varepsilon_k^R + i\varepsilon_k^I \\ =& \frac{M_k}{2\pi}|R_{0,k}|\sin(\varphi_{0,k}) - \frac{1}{\mathfrak{a}}|R_{0,k}|\left(\tilde{g}_{R,0}^k \hat{W}_0^R + \tilde{g}_{I,0}^k \hat{W}_0^I\right)\sin(\varphi_{0,k}) \\ & - \frac{1}{\mathfrak{a}}|R_{0,k}|\left(\tilde{g}_{R,0}^k \hat{W}_0^I - \tilde{g}_{I,0}^k \hat{W}_0^R\right)\cos(\varphi_{0,k}) \\ & + i\left(-\frac{M_k}{2\pi}|R_{0,k}|\cos(\varphi_{0,k}) + \frac{1}{\mathfrak{a}}|R_{0,k}|\left(\tilde{g}_{R,0}^k \hat{W}_0^R + \tilde{g}_{I,0}^k \hat{W}_0^I\right)\cos(\varphi_{0,k})\right. \\ & \left. - \frac{1}{\mathfrak{a}}|R_{0,k}|\left(\tilde{g}_{R,0}^k \hat{W}_0^I - \tilde{g}_{I,0}^k \hat{W}_0^R\right)\sin(\varphi_{0,k})\right) \,. \end{aligned} \tag{2.102}$$

Assuming that complex structure moduli stabilisation in the bulk is done at energies high enough that do not interfere with the stabilisation of the Kähler moduli, we can take the functions g in (2.102) to be approximately zeros except for $g_{W,0}$ and $g_{K,0}$. This approximation was done in Section 3.2.3 of [76], however, in Section 2.4.4, we show that this assumption is necessary, together with other assumptions, in order to get the six-times suppression of the thraxion masses. As a consequence, ε_k^R in (2.102) vanishes.

Another possible assumption is that $\hat{W}_0$ is purely real,[12] so that, finally, (2.99) becomes

$$\begin{aligned} W = \hat{W}_0^R + \sum_\alpha A_\alpha e^{-a_\alpha T_\alpha^R} \cos\left(a_\alpha T_\alpha^I\right) + \sum_k \varepsilon_k^I e^{-\sum_\mathfrak{I} p_\mathfrak{I}^k \frac{G_I^\mathfrak{I}}{M_k}} \sin\left(\sum_\mathfrak{I} p_\mathfrak{I}^k \frac{G_R^\mathfrak{I}}{M_k}\right) \\ - i\left(\sum_\alpha A_\alpha e^{-a_\alpha T_\alpha^R} \sin\left(a_\alpha T_\alpha^I\right) + \sum_k \varepsilon_k^I e^{-\sum_\mathfrak{I} p_\mathfrak{I}^k \frac{G_I^\mathfrak{I}}{M_k}} \cos\left(\sum_\mathfrak{I} p_\mathfrak{I}^k \frac{G_R^\mathfrak{I}}{M_k}\right)\right) . \end{aligned} \tag{2.103}$$

Recall that in (2.96), we have ignored the cross terms proportional to b^a because we will evaluate the potential at the minimum. We note that a linear term in ε survives in the scalar potential. Because of this linear dependence of V in ε we expect that generically the thraxion mass scales linearly with the warp factor.

One could argue that, in the case in which the minimum is realized at $T_\alpha^I = \kappa\pi/a_\alpha$, such linear dependence of V in ε vanishes, as in this case the whole second line of equation (2.96) vanishes.[13] However, we remark that this is not the case, as the W^R term in (2.103) will still carry a linear dependence in ε. Moreover, we generically do not expect T^I to stabilize at such VEV. Despite this, we will see in the next section that in some specific models the opposite is true and T^I stabilizes at zero. We will expand on this point later.

2.4.4 Vanishing conditions of the $\mathcal{O}(\varepsilon)$ cross terms and application to KKLT

We showed that *generically*, the thraxion potential receives non-trivial contributions of order $\mathcal{O}(\varepsilon)$ from Kähler moduli stabilisation, which spoil their characteristic six-time-warp suppressed scale. However, in some cases, such contributions to the scalar potential can vanish. In this section we first perform the KKLT moduli stabilisation procedure with a simplified thraxion superpotential. Then, we comment on some possible ways to cancel the terms of the potential which are linear in ε.

Consider a setup of n multi-throats, each one hosting m_k thraxions, $k = 1, \dots n$. Suppose that the k-th multi-throat has n_k interpolating $\mathcal{A}$-cycles and $\mathcal{B}$-cycles. Then, we allow the following simplifications:

- $m_k = 1, \forall k = 1, \dots n$.
- For each multi-throat system, the flux quanta are chosen with the same magnitude, i.e. $|K_{i,k}| = c_k,\ |M_{i,k}| = d_k,\ \forall\, i = 1, \dots n_k$ and given fixed integer numbers $c_k,\ d_k$.
- The homology relation defining the single thraxion present in the multi-throat is of the form $\sum_j [\mathcal{A}_j] = 0$, namely $p_j^k = 1,\ \forall j, k$.
- All ε_k are equal.

It is straightforward to show that under these assumptions the superpotential (2.85) in a single multi-throat system plus the non-perturbative corrections takes the form

$$W = W_0 + \varepsilon\left(1 - \cos\left(\frac{G}{M}\right)\right) + \sum_\alpha A_\alpha e^{-a_\alpha T_\alpha} , \tag{2.104}$$

where $\varepsilon = \varepsilon^R + i\varepsilon^I$.[14] In order to include the thraxion in the KKLT scenario, we use the superpotential of eq. (2.104). As a concrete example, we consider the stabilisation of one Kähler modulus in presence

[12] This assumption is not strictly necessary, but it could be another way to simplify the expression. Note that W_0 from the complex structure moduli stabilisation is related to $\hat{W}_0$ by a shift of a function depending on ε_k. The requirement that $\hat{W}_0$ is completely real, means that we are allowing for small imaginary parts for W_0.

[13] Moreover, the piece proportional to $(W^I)^2$ also will not have a linear term in ε.

[14] Note that we reabsorbed the factor proportional to n in the definition of ε.

of one thraxion. The Kähler potential is

$$K_{\rm thr} = -3\log\left(F\right)\,, \quad \text{where} \;\; F = T + \bar{T} - \frac{g_s}{4}\kappa_{+--}\left(G-\bar{G}\right)^2\,. \tag{2.105}$$

After stabilizing b to zero, the F-term scalar potential reads [97]

$$\begin{aligned} e^{-K_{\rm c.s.}}\cdot V = &\frac{aA^2e^{-2aT^R}\left(aT^R+3\right)}{6(T^R)^2} - \frac{|\varepsilon|^2}{6(T^R)^2M^2g_s\kappa_{+--}}\sin\left(\frac{c}{M}\right)^2 \\ &+ \frac{aA}{2(T^R)^2}\mathrm{Re}\left[\bar{W}_0e^{-aT} + \bar{\varepsilon}\,e^{-aT}\left(1-\cos\frac{c}{M}\right)\right]\,. \end{aligned} \tag{2.106}$$

We have some new pieces compared to the usual KKLT potential without thraxions. The first one is the $G\bar{G}$ term found in (2.91): it scales as $\varepsilon^2 \sim \omega_{\rm IR}^6$. Instead, the cross term is new, it is induced by the presence of no-scale breaking effects and it scales as $\varepsilon \sim \omega_{\rm IR}^3$. Thus, even in the easiest toy model, we obtain a term which lifts the double suppression of the thraxion mass to a single suppression.

Now, we investigate if we can remove the cross term and restore the six-time warp suppression. Consider adding to the bullet list above the additional requirement:

- All ε_k are imaginary, i.e. $\varepsilon_k^R = 0$.

Hence, we see already from the toy model that with this additional request, the cross term cancels when the C_4 axion is stabilized to its minimum. In general, we can show this process as follows. We can expand (2.104) with $\varepsilon^R = 0$ in its real and imaginary parts as

$$\begin{aligned} W =& W_0 + \sum_\beta A_\beta e^{-a_\beta T_\beta^R}\cos\left(a_\beta T_\beta^I\right) + \varepsilon^I\sin\left(\frac{c}{M}\right)\sinh\left(\frac{b}{g_sM}\right) \\ &- i\left(\sum_\beta A_\beta e^{-a_\beta T_\beta^R}\sin\left(a_\beta T_\beta^I\right) + \varepsilon^I\left(\cos\left(\frac{c}{M}\right)\cosh\left(\frac{b}{g_sM}\right)-1\right)\right) \\ =& W^R + iW^I\,. \end{aligned} \tag{2.107}$$

First, we see that, when $b = 0$, W^R does not contain ε^I, so the cross terms that were present in Section 2.4.3 cancel out. Moreover, it is possible to see that T_β^I stabilizes at $\kappa\pi/a_\beta$, with $\kappa \in \mathbb{Z}$. The only terms that contain ε^I are those multiplied by W^I. However, they cancel when the potential is evaluated at $T^I = \kappa\pi/a_\beta$. All the terms that could possibly give cross terms are then cancelled and the final potential for the thraxion scales as in (2.91), i.e. with the six-time warp factor.

Now, let us consider the backreaction coming from the presence of a thraxion on the stabilization of b and θ to their vanishing minima. We have already discussed how the potential is minimised when $\langle b^a\rangle \equiv b_0^a = 0$ and $\langle\theta_\alpha\rangle \equiv \theta_{0,\alpha} = 0$. Now, we can consider small fluctuations around these minima, which we parametrise as δb^a and $\delta\theta_\alpha$. By Taylor-expanding around these minima, we can study the potential at the next-to-leading order in $b^a = b_0^a + \delta b^a$ and $\theta_\alpha = \theta_{0,\alpha} + \delta\theta_\alpha$ as follows. Let us consider $V(x) = V_0(x) + \varepsilon V_1(x)$, with $x = b, \theta$, $\varepsilon \ll 1$ and $\alpha = a = 1$. Here $V_1(x)$ is the potential induced by the possible backreaction of the thraxion on the fields, thus it scales as the warp factor. Hence, (writing $x|_{t_0,\,b_0}$ as $x|_0$ to avoid notation cluttering)

$$\begin{aligned} \partial_\theta V =& \;\partial_\theta V_0|_0 + \partial_\theta\partial_b V_0|_0\,\delta b + \partial_\theta^2 V_0\big|_0\,\delta\theta + \varepsilon\;\partial_\theta V_1|_0 + \mathcal{O}(\varepsilon^2)\,, \\ \partial_b V =& \;\partial_b V_0|_0 + \partial_b\partial_\theta V_0|_0\,\delta\theta + \partial_b^2 V_0\big|_0\,\delta b + \varepsilon\;\partial_b V_1|_0 + \mathcal{O}(\varepsilon^2)\,, \end{aligned} \tag{2.108}$$

where the first terms in both the right hand sides vanish when imposing the equations of motion. To

find $\delta\theta$ and δb we have to solve the system

$$\begin{cases} \partial_\theta\partial_b V_0|_0\,\delta b + \partial_\theta^2 V_0\big|_0\,\delta\theta = -\varepsilon\,\partial_\theta V_1|_0 \\ \partial_b\partial_\theta V_0|_0\,\delta\theta + \partial_b^2 V_0\big|_0\,\delta b = -\varepsilon\,\partial_b V_1|_0 \end{cases} \tag{2.109}$$

and the solution is given by

$$\begin{aligned} \delta\theta &= \varepsilon\,\frac{\partial_b V_1|_0\,\partial_\theta\partial_b V_0|_0 - \partial_b^2 V_0\big|_0\,\partial_\theta V_1|_0}{\partial_\theta^2 V_0|_0\,\partial_b^2 V_0|_0 - \partial_\theta\partial_b V_0|_0\,\partial_b\partial_\theta V_0|_0}\,, \\ \delta b &= \varepsilon\,\frac{\partial_b V_1|_0\,\partial_\theta^2 V_0\big|_0 - \partial_b\partial_\theta V_0|_0\,\partial_\theta V_1|_0}{\partial_\theta\partial_b V_0|_0\,\partial_b\partial_\theta V_0|_0 - \partial_\theta^2 V_0|_0\,\partial_b^2 V_0|_0}\,. \end{aligned} \tag{2.110}$$

That is, both fluctuations scale at least as ε. By plugging these results back in the potential, we see that $V(\delta b^a,\,\delta\theta_\alpha) \sim \mathcal{O}(\varepsilon^2)$ or higher. Therefore, the potential for the fluctuations is always of order $\mathcal{O}(\varepsilon^2)$ or higher, meaning it is highly suppressed compared to the potential evaluated in $\langle b^a\rangle = \langle\theta_\alpha\rangle = 0$. This verifies that the stabilisation considered previously is self-consistent.

Many moduli stabilisation scenarios naturally minimise at $b = 0$. However, stabilizing the b field to zero carries about another important consequence that could help to reduce the amount of tuning required to cancel the linear terms in ε. As shown in [76], a non-vanishing VEV for the b field produces a backreaction on the throats as it changes the relative H_3-flux distribution. In other words, this makes all the throats (in the same multi-throat system) of different lengths. In this case, the warp factors, i.e. the ε parameters, acquire all different values. In turn, this means that in the case in which $b = 0$, all the warp factors in the same multi-throat system could be taken to be equal more easily. As $\varepsilon_k \sim e^{-K_k/g_s M_k}$, one still has to require that the ratio of the flux numbers is equal in each throat of the system. Once these two requirements are met, all the warp factors in the same multi-throat system are actually equal. We note here that in a double-throat system, this is always the case. Thanks to the homology relation, we have only one effective $\mathcal{A}$- and $\mathcal{B}$-cycle, hence only one effective flux quantum of F_3 and of H_3.

We comment now on the conditions listed above. The first condition states that in every multi-throat system there must be a single homology relation and therefore a single thraxion. It is interesting to note that in *all* known examples of CY orientifold supporting thraxions, this is always true. Namely, at the moment of writing we do not know of any CY orientifold in which a given multi-throat hosts more than one thraxion. However, in view of how small the set of CICY parents of our CICY orientifold database is compared to other known algorithmically constructable sets of CY 3-folds, it seems unwarranted to assume a priori that manifolds with multi-throats hosting more than one thraxion do not exist.

The second condition implies that all the various throats in the same multi-throat system have the same length. The third condition requires a specific form of the homology relation. Note that one could use a rescaling of the base of 3-cycles $[\mathcal{A}_j] \to n_j[\mathcal{A}_j]$, $[\mathcal{B}_j] \to n_j^{-1}[\mathcal{B}_j]$, $n_j \in \mathbb{Z}\setminus\{0\}$ in order to ensure that such condition is always satisfied. We remark that if we have more than one homology relation, only one of them can be recast in the form $\sum_j[\mathcal{A}_j] = 0$ by rescaling. Hence, for multi-throats carrying more than one thraxion the symmetrization of the multi-throat becomes impossible.

The last condition, $\varepsilon_k^R = 0$, is observed to restore the six-times warp suppression of the thraxion mass. Moreover, for double-throats (provided stabilizing $b = 0$) ensuring $\varepsilon_k^R = 0$ guarantees the enhanced warp suppression of the thraxion mass. Hence, it is interesting to note that in the subclass of flux vacua found in [98], which is determined by the prime condition necessary for well working KKLT vacua (i.e. small W_0), ε is always imaginary to leading order in the conifold modulus z_0.This should not be seen as a physical motivation, but rather as evidence supporting the existence of whole classes of examples

realizing this assumption.

In this section, we argued that under some special conditions, the thraxion mass can still be double-suppressed. However, these requirements are generically difficult to meet in a more complicated scenario in which within a given multi-throat system there is more than one thraxion, or unequal flux ratios.

2.4.5 Behaviour of the $\mathcal{O}(\varepsilon)$ thraxion mass cross terms in LVS

There is another, interesting way which could restore the six-times warp suppression. Such way appears to be quite generic as long as one stabilizes the CY volume $\mathcal{V}$ to exponentially large values, as happens in LVS. In the following, we show how the interplay between large values of $\mathcal{V}$ and small values of ε could favour the terms proportional to ε^2 over the linear ones.

More in detail, by considering a superpotential corrected with (2.29) together with the Kähler potential in (2.30), LVS stabilizes the volume as $\mathcal{V} \sim e^{a_s T_s^R}$. In turn, this means that in the potential, each time a term is proportional to $e^{-n\, a_s T_s^R}$, such term is $\mathcal{O}(\mathcal{V}^{-n})$ times suppressed. The standard LVS potential without the odd sector scales as $\mathcal{O}(\mathcal{V}^{-3})$ [52].[15] Let us now consider the superpotential in (2.97). For $\mathcal{V} \to \infty$, the no-scale breaking potential of eq. (2.33) scales as[16]

$$\begin{aligned} V_{\text{np}_1} &\sim \frac{K^{T_s\bar{T}_s}|\partial_{T_s} W|^2}{\mathcal{V}^2} \sim \mathcal{O}\left(\frac{1}{\mathcal{V}^3}\right) + \dots \\ V_{\text{np}_2} &\sim -\frac{K^{T_s\bar{T}_s} K_{\bar{T}_s}}{\mathcal{V}^2}\, W^R e^{-a_s T_s^R} \cos\left(a_s T_s^I\right) - \frac{K^{T_s\bar{T}_a} K_{\bar{T}_a}}{\mathcal{V}^2} e^{-a_s T_s} \bar{W} \sim \mathcal{O}\left(\frac{1}{\mathcal{V}^3}\right) + \mathcal{O}\left(\frac{\varepsilon}{\mathcal{V}^3}\right) + \dots \\ V_{\alpha'} &\sim \frac{\hat{\xi}|W|^2}{\mathcal{V}^3} \sim \mathcal{O}\left(\frac{1}{\mathcal{V}^3}\right) + \mathcal{O}\left(\frac{\varepsilon}{\mathcal{V}^3}\right) + \dots . \end{aligned} \tag{2.111}$$

However, the $G\bar{G}$ part of the potential has a different scaling, namely

$$V_{G,\bar{G}} = K^{G\bar{G}} \mathcal{D}_G W \mathcal{D}_{\bar{G}} \bar{W} = \frac{K^{G\bar{G}}|\partial_G W|^2}{\mathcal{V}^2} \sim \mathcal{O}\left(\frac{\varepsilon^2}{\mathcal{V}}\right) . \tag{2.112}$$

This piece receives volume-suppression only from e^K, which is partially compensated by the inverse of the Kähler metric $K^{G\bar{G}}$. This results in an $\mathcal{O}(\mathcal{V}^{-1})$ suppression, which is milder than the $\mathcal{O}(\mathcal{V}^{-3})$ dependence of the term proportional to ε in the potential (2.111). Therefore, in LVS the stronger suppression in ε^2 is compensated by a milder one in $\mathcal{V}$ and hence it could happen that the $\mathcal{O}(\varepsilon^2)$ term coming from (2.112) would dominate over the $\mathcal{O}(\varepsilon)$ one. Note that, so far, the discussion is completely general.

In the following, we show this remarkable behavior in a specific example. Then, we comment on the implications of the interplay between ε and $\mathcal{V}$ in two phenomenological applications. For the sake of consistency, we explicitly compute the F-term scalar potential for a CY with one thraxion, $h^{1,1}_+ = 2$ and whose volume takes the standard Swiss-cheese form

$$\mathcal{V} = \left(T_b + \bar{T}_b\right)^{3/2} - \left(T_s + \bar{T}_s - \frac{g_s}{4}\kappa_{s--}\left(G - \bar{G}\right)^2\right)^{3/2} , \tag{2.113}$$

[15] See also [99] for the inclusion of the odd sector in LVS, where the odd axions get a potential from fluxed D3-brane instanton contributions to W, as well as [100] for very recent results on moduli stabilisation with odd axions.

[16] Here and below we make use of the no-scale breaking property of the Kähler potential and of the following standard relations about the Kähler metric, as derived in [34], in the $\mathcal{V} \to \infty$ limit:

$$K_{T_\alpha} \sim t^\alpha \mathcal{V}^{-1} , \quad K^{T_\alpha \bar{T}_\beta} \sim -\mathcal{V}\kappa_{\alpha\beta\gamma} t^\gamma + \tau_\alpha \tau_\beta , \quad K^{T_\alpha \bar{T}_\beta} K_{T_\alpha} \sim -\tau_\beta , \quad K^{G^a \bar{G}^b} \sim -g_s^{-1} \mathcal{V} \left(\kappa_{ab\gamma} t^\gamma\right)^{-1} .$$

Since at this stage we are only interested in the scaling with $\mathcal{V}$, we will drop numerical factors, the signs and the dependence on the 2-cycles. We will restore them when computing the explicit example.

where we assumed that the only non-trivial even-odd-odd triple intersection number is κ_{s--}. We further assume that the thraxion superpotential can take the form of eq. (2.87) and hence the total superpotential for this toy model can be written as

$$W(G,T_s) = W_0 + \varepsilon\,(1-\cos\left(G/M\right)) + A_s e^{-a_s T_s}\,, \tag{2.114}$$

where the leading non-perturbative correction comes from the blow-up modulus τ_s. The field b stabilizes at zero, and in order for its kinetic terms to be positive definite we should have $\kappa_{s--} > 0$. Hence, we get the following potential

$$\begin{aligned} e^{-K_{\rm c.s.}}V = &\frac{2\sqrt{2}a_s^2 A_s^2\, e^{-2a_s\tau_s}\sqrt{\tau_s}}{3\mathcal{V}} + \frac{4a_s A_s W_0 \tau_s e^{-a_s\tau_s}\cos\left(a_s\theta_s\right)}{\mathcal{V}^2} + \frac{3W_0^2\hat{\xi}}{4\mathcal{V}^3} \\ &- \frac{3\varepsilon^2\,\hat{\xi}}{\mathcal{V}^3}\sin\left(\frac{c}{2M}\right)^4 - \frac{\varepsilon^2\sqrt{2}\left(4\mathcal{V}^2 - 2\mathcal{V}\hat{\xi} + \hat{\xi}^2\right)}{12 g_s M^2 \kappa_{s--}\sqrt{\tau_s}\,\mathcal{V}^3}\sin\left(\frac{c}{M}\right)^2 \\ &+ \frac{4i\,\varepsilon\, a_s A_s \tau_s\, e^{-a_s\tau_s}}{\mathcal{V}^2}\left(1-\cos\left(\frac{c}{M}\right)\right)\sin\left(a_s\theta_s\right)\,. \end{aligned} \tag{2.115}$$

Note that for $\varepsilon = 0$ we recover the standard LVS potential and the thraxion enters as a correction in $\mathcal{O}(\varepsilon)$ and $\mathcal{O}(\varepsilon^2)$: the LVS moduli stabilisation proceeds as usual. Also, this turns out to be one of the special cases in which the thraxion is independent of the Kähler moduli stabilisation, as the $\mathcal{O}(\varepsilon)$ term vanishes once the C_4 axion is set to its VEV. However, our main point is the following: in (2.115) the $\mathcal{O}(\varepsilon)$ term is twice more suppressed in $\mathcal{V}$ than one of the $\mathcal{O}(\varepsilon^2)$ ones. Hence, it could happen that these effects balance among each other and the $\mathcal{O}(\varepsilon^2)$ term becomes eventually the leading one.

As a first application, we could investigate whether this situation takes place when we require the thraxion to be the inflaton. Suppose we want to realize an inflationary potential with $V \sim (10^{15}\text{ GeV})^4$, i.e. $V \sim 10^{-12}$ in Planck units. In order for the $\mathcal{O}(\varepsilon^2)$ term to be the leading one and thus to reproduce such scaling, we should have $\mathcal{V} > 250$. This guarantees that the $\mathcal{O}(\varepsilon)$ term is subleading. The value we found for the CY volume fits perfectly within LVS. Therefore, for inflationary applications, we restore the double suppression of the thraxion mass as in its original proposal.

Nevertheless, if we consider the thraxion to be a possible Fuzzy Dark Matter (FDM) candidate as in [1], this balance turns out to be impossible, or very dangerous for LVS. With FDM we refer to a particle taken as a possible dark matter candidate that is so light that its nature is basically wave-like [101]. Such particle should be characterized by a mass of order $m \sim 10^{-22}$ eV and a decay constant of roughly $f \sim 10^{17}$ GeV. In [102], it was shown that for a stringy axion-like particle to be a good FDM candidate, its instanton action (and thus the potential) should scale as $\exp(-S) \sim \exp(-230) \sim 10^{-100}$ in Planck units, see Chapter 4. Requiring the $\mathcal{O}(\varepsilon^2)$ term to be the leading one entails a large size for the CY volume, namely $\mathcal{V} > 10^{20}$. However, such value is incompatible with the low energy phenomenology. Given that the scale of SUSY breaking is $m_{3/2} \sim \mathcal{V}^{-1}M_P$, we would have SUSY at values smaller than 10^{-2} GeV. Therefore, for FDM in a LVS moduli stabilisation, the leading term is always the $\mathcal{O}(\varepsilon)$ one (if it does not get cancelled by the C_4 axion stabilisation).

2.4.6 Mass scales for thraxion setups in KKLT and LVS

We can now apply our results to derive the mass scaling of the low-lying states in setups with volume moduli stabilisation. These light states include the lightest Kähler moduli, the warped KK modes inside the multi-throat carrying the thraxion, and the thraxion itself.

KKLT: Fluxes inside a warped throat generically induce perturbations which scales with powers of r. These perturbations are divided in normalizable and non-normalizable modes. In particular, non-normalizable modes correlate with the ISD breaking fluxes [103]. Since gaugino condensation (necessary to stabilize Kähler moduli) breaks both no-scale and sources non-ISD fluxes [104], its presence activates the non-normalizable perturbation. Following the classification of throat perturbations in [104], we then have the gaugino condensate sourcing a perturbation

$$\delta G_3 \sim \langle \lambda\lambda \rangle \, r^{-3/2} \sim W_0 \, r^{-3/2} \, . \tag{2.116}$$

As discussed in [104] we have to require the coefficients of such perturbations in the UV to be small enough such that at the IR end of the throat they do not become comparable with the background fluxes. In our case we see that the $\langle \lambda\lambda \rangle$-sourced non-ISD flux perturbation becomes $\mathcal{O}(1)$ whenever $r^{3/2} \sim W_0$. Hence, for our perturbation to satisfy the condition of [104] we must ask for $\varepsilon > W_0^2$. We can use this bound to compare the mass of the thraxions to the masses of the other light particles in the compactification. In this section we will focus on KKLT scenarios, while in the following we will discuss similar computations for LVS. From the potential in (2.106), we have that

$$m_{\rm thr}^2 \sim \varepsilon \, \frac{|W_0|}{\mathcal{V}^{4/3}} \sim m_{\rm wKK}^2 \, \varepsilon^{1/3} |W_0| \, , \tag{2.117}$$

where we used the definition $m_{\rm wKK}^2 \sim \varepsilon^{2/3}/\mathcal{V}^{4/3}$ for the mass squared of the warped KK modes. Since $|W_0| \ll 1$ in KKLT and $\varepsilon \leq 1$ by definition, this implies that thraxions stay parametrically lighter than the warped KK modes even if the cross term lifts the thraxion mass-squared to $\mathcal{O}(\varepsilon)$. Moreover, the condition $\varepsilon > W_0^2$ implies that the ratio

$$\frac{m_{\rm thr}^2}{m_{\rm wKK}^2} > |W_0|^{5/3} \tag{2.118}$$

is bounded from below. Then, we should compare the mass of Kähler moduli with the one of thraxions, to ensure that the latter are still the lightest particle in the spectrum. The Kähler modulus mass reads

$$m_\tau^2 \sim \frac{|W_0|^2}{\mathcal{V}^2} \qquad \text{hence} \qquad \frac{m_{\rm thr}^2}{m_\tau^2} \sim \frac{\mathcal{V}^{2/3}\varepsilon}{|W_0|} \sim \varepsilon \, \frac{\log\left(W_0^{-1}\right)}{|W_0|} \, , \tag{2.119}$$

where we used the KKLT relation $\mathcal{V} \sim -\log(|W_0|)^{3/2}$ for the CY volume (in case of single modulus). We see that $m_{\rm thr}^2 < m_\tau^2$ if $\varepsilon < |W_0|$. Therefore, to ensure that the thraxion is lighter than the Kähler modulus and that the IR end of the throat is safe from large corrections, ε should sit in the window $|W_0|^2 < \varepsilon < |W_0|$.

We can also consider the scaling of the gravitino mass $m_{3/2} \sim |W_0||\log(W_0)|^{-3/2}$ in Planck units, then we get the relation

$$\frac{m_\tau^2}{m_{\rm thr}^2} \sim \frac{m_{3/2}}{\varepsilon} \, |\log W_0|^{1/2} \, . \tag{2.120}$$

Therefore, the Kähler modulus is heavier compared to the thraxion if

$$m_\tau^2 > m_{\rm thr}^2 \quad \Longleftrightarrow \quad \frac{m_{3/2}}{M_P} > \frac{\varepsilon}{\sqrt{|\log W_0|}} \, , \tag{2.121}$$

where in the last relation we restored the Planck mass. By requiring that $m_\tau^2 > m_{\rm thr}^2$ together with the relation $\varepsilon > W_0^2$, we have a lower bound on the gravitino mass.

LVS: In this scenario, the thraxion is always lighter than the warped KK modes, as

$$\frac{m^2_{\rm thr}}{m^2_{\rm wKK}} \sim \frac{\varepsilon}{\mathcal{V}^{5/3}}\,. \tag{2.122}$$

Then, we can compare the thraxion mass to the one of the volume-supporting Kähler modulus, as it is the lightest modulus in the LVS spectrum. The mass squared of the big cycle scales as $m^2_{\tau_b} \sim \mathcal{V}^{-3}$. We see that

$$\frac{m^2_{\rm thr}}{m^2_{\tau_b}} \sim \varepsilon\,, \tag{2.123}$$

which means that the thraxion is always lighter.

We note here that both the non-perturbative effect stabilizing τ_s and the $\mathcal{O}(\alpha'^3)$ correction inferred from the 10d R^4 term via the induced correction to the volume moduli Kähler potential break no-scale as well as likely source non-ISD 3-form fluxes. By an analysis similar to the one in the KKLT section above, this will source perturbations in the thraxion multi-throat which will bound ε from below. However, doing this properly while including the perturbations sourced by the $\mathcal{O}(\alpha'^3)$ correction to K is difficult, as the structure of the direct $10d$ origin, schematically represented by terms $\alpha'^3 G_3^2 R^3$ is unknown. Hence, we have to leave a proper analysis for a future time when the corresponding supersymmetric completion of the R^4 term in type IIB string theory will have been determined.

2.4.7 Comments about the 10d origin of the cross terms

We will review here shortly an argument given in [97] concerning the $10d$ origin of the single-warped cross term in the thraxion scalar potential with moduli stabilisation in many cases. The starting point is the observation that as soon as non-perturbative effects like gaugino condensation on a stack of 4-cycle wrapping D7-branes are involved in Kähler moduli stabilisation, these non-perturbative effects tend to generate non-ISD 3-form flux contributions. For simplicity, we now focus on the situation of a double throat. As thraxions are the lowest lying radial KK-mode of C_2 in the double throat, they react sensitively not just to the change of the IR Dirichlet boundary conditions driven by giving thraxion a finite VEV, but to changes of the UV boundary conditions as well. The presence of ISD-breaking non-perturbative effects in the bulk in general will source such UV boundary terms which take the form [97]

$$\delta S[z] = \frac{M_{10}^8}{2}\int d^4x \int \frac{dr}{r}\,(J_{\rm UV}\bar{z} + c.c.)\,. \tag{2.124}$$

If we use for moduli stabilisation e.g. gaugino condensation as the non-perturbative effect, this implies a source $J_{\rm UV} = j\cdot r\,\delta(r - r_{\rm UV})$ with $j \sim \langle\lambda\lambda\rangle$. In the dual holographic description of a perturbed KS throat [104] used to describe each half of the double throat, this corresponds to a dimension $\Delta = 3$ chiral operator. In presence of this UV perturbation the solution for $z(r)$ takes the form [97]

$$z(r) = \frac{1}{4}j\,(r^2 - r_{IR}^2) + z_1 + \frac{1}{2}\frac{r^2 - r_{IR}^2}{r_{\rm UV}^2 - r_{IR}^2}(z_2 - z_1) \tag{2.125}$$

in the first throat, and with $z_1 \leftrightarrow z_2$ in the second throat. If we now insert this back into the 5d effective action for the complex structure modulus $z(r)$ from [76, 97] and corrected by $\delta S[z]$, we get a scalar potential

$$V(c) = |z_1 - z_2|^2 + {\rm Re}\,(\bar{j}(z_1 + z_2)) + \text{ const.} = 4|z_0|^2 - 2{\rm Re}\,(\bar{j}z_0)(1 - \cos(c/M)) + \text{ const.}\,, \tag{2.126}$$

which clearly shows the ISD-violating source j generating the cross term, provided that $\bar{j}z_0$ is not purely imaginary. Moreover, since e.g. $j \sim \langle\lambda\lambda\rangle \sim |W_0|$ in the KKLT scenario, we see that this argument has the features to reproduce the cross term observed in the 4d EFT computation. We leave a more detailed construction of this argument for future work.

Finally, a full treatment of our $4d$ EFT results in a $10d$ setting is difficult at the current time, in particular for the case when we choose LVS to stabilize the Kähler moduli. The reason here consists of the fact that for LVS, the $\mathcal{O}(\alpha'^3)$ correction in the volume moduli Kähler potential contributes to the $\mathcal{O}(\varepsilon)$ cross term in the scalar potential. However, the contributions to the scalar potential at $\mathcal{O}(\alpha'^3)$ were derived from 10d in [45] using the known 10d type IIB α'^3R^4 correction dimensionally reducing to the known $\mathcal{O}(\alpha'^3)$ correction to K, from which in turn via 4d $\mathcal{N}=1$ local supersymmetry [45] inferred the $\mathcal{O}(\alpha'^3)$ to the supergravity F-term scalar potential. The direct $10d$ origin of this correction to V would arise from terms reading schematically as $\mathcal{O}(\alpha'^3)G_3^2R^3$ which are part of the supersymmetric completion of the R^4 term in type IIB in $10d$. This supersymmetric completion, however, unfortunately is to date not completely known already at the needed fifth order. Hence, at least for the case of LVS Kähler moduli stabilisation, a $10d$ discussion of our $4d$ EFT results must await future progress on the supersymmetric completion of the type IIB α'^3R^4 term.

Discussion and conclusions

We presented a detailed study about thraxions beyond the flux compactification level. Specifically, we analysed $4d$, $\mathcal{N}=1$ effective supergravity in presence of thraxions and how the results derived in [76] change when also the Kähler moduli sector is taken into account. We find that in general the thraxion potential receives potentially non-vanishing corrections which lift the mass squared to $\sim \omega_{\rm IR}^3$ only. After explaining why this is the case, we show that these cross terms in general do not vanish in multi-throats consisting of at least three joined throats. Conversely, in the simplest class of double-throats, avoiding the cross terms reduces to essentially a single concretely realizable condition on the periods of double-throats.

By analysing SU(3)-structure's torsion classes, we find that the CY condition is broken due to the breakdown of the ISD condition of the G_3 flux. This leaves us with just a complex manifold. The amount of the breaking is related qualitatively to the value of the thraxion VEV. In turn, if the CY condition is broken already at the KK scale, the use of the 4d supergravity approximation in order to describe the 4d effective theory could be questionable. However, we argue for a sufficiently small thraxion VEV or a decoupling of the thraxion dynamics coming from the high warping, in such a way that the manifold is still (almost) CY. Hence, we can be entitled to use the effective supergravity action and include the Kähler moduli stabilisation.

Then we discussed the relation of thraxions and Kähler moduli in the presence of perturbative and non-perturbative corrections to the Kähler potential and the superpotential. We find that in general Kähler moduli stabilisation spoils the high suppression of the thraxion mass coming from the sixth power of the warp factor. The no-scale breaking terms induce additional contributions to the potential which are proportional to the warp factor cubed only, hence lifting the thraxion mass. However, the thraxion is still the lightest particle in the spectrum, and the spectrum is still effectively gapped.

One may ask what are the consequences of this new thraxion behaviour on the axionic version of the WGC [67]. In [76], it was found a parametric violation of the lattice WGC while the sub-lattice WGC [14, 15, 105] was still satisfied but with a parametrically coarse sub-lattice. The new scaling of the thraxion mass still provides a violation of the lattice WGC but milder by a factor of 2, resulting

in a less coarse sub-lattice needed to satisfy the sublattice WGC. The study of the validity of the EFT whenever the thraxion stabilizes to a VEV different from zero is an important task for future work, as in this situation the CY condition is broken. It would be interesting to see for how long the EFT is still valid before new light states must be integrated-in. Indeed, the violation of the lattice-WGC might be a symptom that some new objects must be considered in order to fully describe the physics of thraxions.

In addition, there may be implications from the finite D3-brane charge tadpole of any given type IIB CY compactification. While we leave a full discussion of this for future work, we observe that: i) metastability of a dS uplift from a single anti-D3-brane implies a lower bound $M \gtrsim \mathcal{O}(10)$ on the R-R 3-form flux on the throat $\mathcal{A}$-cycle. ii) Fixing the thraxion mass scale for some physical application on the other hand fixes the warp factor and thus $K/M \gg 1$. This entails the D3-brane charge tadpole placing an upper bound $M < \sqrt{Q_{D3}(K/M)^{-1}}$, which may get tightened by replacing Q_{D3} by $Q_{D3}^{\text{eff.}} < Q_{D3}$ due to flux stabilisation of the complex structure moduli eating up a part of Q_{D3} [106–108]. Depending on the size of the available tadpole and the number of non-zero fluxes needed to freeze the complex structure moduli, this may effectively limit the achievable warp factor suppression of the thraxion mass scale and/or the existence of meta-stable anti-D3 uplifts.

After our generic discussion, we worked out the conditions sufficient to obtain the original scaling of the thraxion mass with respect to the warp factor. Such cases require the presence of only one thraxion in each multi-throat system, a democratic distribution of fluxes in the throats and a particular homology relation among the interpolating cycles. These requirements need a certain amount of tuning, unless the multi-throats are double-throats. Therefore, which of the two cases is more prevalent in the string landscape will depend significantly on the relative frequencies of double versus higher multi-throats. It is interesting to note here that in the database of the CICY orientifolds built in [88], we always have one thraxion per multi-throat system. Whether this is the case also for other CY sets as e.g. the Kreuzer-Skarke database [109] is an important question that we leave to further study.

We then specialized the discussion of no-scale breaking effects to the specific examples of LVS and KKLT moduli stabilisation approaches. In particular, in LVS the exponentially large values of the CY volume allow us to suppress the cross terms which otherwise would be responsible for lifting the mass. This suppression turns out to be effective only in scenarios where the scalar potential scale is sufficiently high. This in particular includes the interesting case of high-scale inflation.

Given the obvious phenomenological possibilities of thraxion models, as well as their intrinsic theoretical interest, this leaves for the future many interesting open questions we raised here.

Chapter 3

Inflation in String Theory and Axions as Inflatons

The sky above the port was the color of television,
tuned to a dead channel.

— William Gibson, *Neuromancer*

An ongoing series of observational cosmological probes, among them cosmic microwave background (CMB) measurements [110–112], type IA supernova data [113], large-scale structure surveys [114] and baryon acoustic oscillation (BAO) measurements [115], has so far provided increasing evidence for the ΛCDM cosmological standard model. In particular, this includes support for a concurrent late-time accelerating expansion of the universe compatible with a description by de Sitter space with a very small positive cosmological constant and a very early epoch of extremely rapid exponential expansion called inflation. Inflation has become the leading paradigm to explain the homogeneity and isotropy of our universe. The observations by the WMAP [110] and *Planck* [111] satellites, as well as the BICEP/*Keck* telescopes at the South Pole [112], provide us with powerful tools to explore the early stages of the cosmological history and to understand the inflationary epoch. Moreover, beyond serving as tests for many inflationary models proposed throughout the years, these data are also beginning to constrain top-down constructions attempting to embed inflation into a theory of quantum gravity. In fact, inflation is also one of the most promising means to explore the physics at energy scales that require a candidate theory of quantum gravity, such as String Theory. The observational background provides the motivation for continued efforts to search for vacuum solutions (*vacua*) of String Theory as a candidate theory of quantum gravity which can realize both controlled dS vacua and an observationally viable epoch of slow-roll inflation. In many cases, constructing such string vacua involves stabilizing all moduli scalar fields and stringy p-form axion fields using fluxes and orientifold planes up to typically one or two scalar field directions left massless and flat at leading order. For these remaining few flat directions a scalar potential arises from taking into account non-perturbative quantum corrections, in particular if these flat directions are axions for which perturbative corrections are absent.

In this chapter, we show why and how axions can serve as inflatons. First, in Section 3.1 we review the basics of inflation from the effective theory point of view. Then, Section 3.2 discusses the problems of embedding the inflationary dynamics in a UV-completed theory and why considering axions as inflations could alleviate those problems. Therefore, in Section 3.3 we introduce two of the main proposals of

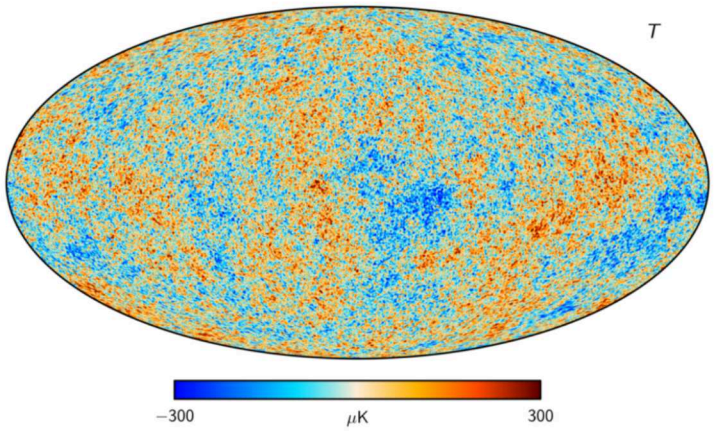

Figure 3.1: Temperature fluctuations in the CMB radiation. Figure taken from [119].

axion inflation, namely alignment and axion monodromy. In particular, for the latter, we provide new phenomenological bounds arising when imposing the Weak Gravity Conjecture and the Festina Lente bound. Finally, we present a new mechanism of axion inflation based on Linde's hybrid inflation in Section 3.4, while in Section 3.5 we show a way to achieve winding inflation via the topological data of the extra dimensions.

3.1 Basics of inflation

With *inflation* we refer to an extended period of quasi-dS evolution, in which the Hubble rate of expansion varies slowly over a Hubble time [116–118]. Inflation is thought to be responsible both for the large-scale homogeneity that we observe today and for the small fluctuations in the CMB that were the seeds for the formation of structures, as galaxies and clusters. In particular, the uniformity of the CMB fluctuations represents an intriguing and challenging puzzle. The CMB is a beautiful picture of a large patch of the universe at the recombination time, at energies around 0.1 eV. If we compare the Hubble radius[1] evaluated nowadays with the one at the time of recombination, we naively infer that the part of the universe we see in the CMB should be made of 10^4 causally disconnected regions: the scales entering the comoving horizon today have been far outside the horizon at CMB decoupling. Then, how could it be possible that the radiation we observe is isotropic to one part in 10^5 (see fig. 3.1)? There should have been a point in the history of the universe when these apparently causally-separated patches have been in contact. For this reason, this homogeneity problem is also called *horizon problem*: the comoving horizon, or the fraction of the universe in causal contact strictly increases with time. This suggests that the horizon problem (as well as other Big Bang puzzles that we have omitted here) could be solved by a very simple and effective idea: have an epoch in the early universe when the comoving Hubble radius was decreasing, so that all past light-cones originating from the CMB patch at the time of recombination intersect before they hit the initial singularity. Therefore, distances greater than the Hubble radius *now* were actually in causal contact early on. We can achieve this by postulating an era before radiation domination, where the universe was dominated by an energy that behaves like the cosmological constant today: this era is referred to as the inflationary epoch. We explain in what follows how this idea works, referring mainly to [120, 121].

[1]The Hubble radius $(aH)^{-1}$ quantifies the distance that can be travelled within an e-fold of cosmological expansion. During the conventional expansion of the universe, it strictly grows with time. By integrating the Hubble radius over the logarithm of the scale factor, we get the comoving horizon, i.e. the maximum distance that a light ray can traverse.

The cosmological principle postulates that the universe is homogeneous and isotropic on large scales, and the CMB is an evidence of this. Such universe can be described with the Friedmann-Lemaitre-Robertson-Walker (FLRW) metric

$$\mathrm{d}s^2 = -\mathrm{d}t^2 + a(t)^2 \left(\frac{\mathrm{d}r^2}{1 - k\, r^2} + r^2 \mathrm{d}\Omega^2 \right) , \tag{3.1}$$

where $a(t)$ is the scale factor that encodes the growth of the (maximally symmetric three-dimensional) spatial slices with time, and the curvature parameter k is vanishing for flat, $\mathbb{R}^3$ spatial slices, positive for S^3-like slices or negative for three-dimensional hyperbolic spaces. In this background and assuming that the stress-energy tensor is that of a perfect fluid with energy density ρ and pressure p, the Einstein's equations become two coupled differential equations called Friedmann equations:

$$H^2 \equiv \left(\frac{\dot{a}}{a} \right) = \frac{\rho}{3} - \frac{k}{a^2} , \qquad \frac{\ddot{a}}{a} = -\frac{1}{6} \left(\rho + 3p \right) , \tag{3.2}$$

where the overdots denote derivatives with respect to t. Note that in (3.2) we have defined the Hubble parameter H which gives the expansion rate of the universe, hence setting the fundamental scale of the FLRW spacetime. The Friedmann equations are not independent: they can be combined into the continuity equation

$$\dot{\rho} = -3H(\rho + p) = -3(1 + w)H\rho \, , \tag{3.3}$$

which upon integration gives $\rho \sim a^{-3(1+w)}$, where $w \equiv p/\rho$ is the equation of state. In order to solve the horizon problem, we saw that the Hubble radius $(aH)^{-1}$ should shrink for a certain period of time. Via the Friedmann equations this leads to

$$\frac{\mathrm{d}}{\mathrm{d}t} \left(\frac{1}{aH} \right) < 0 \quad \Rightarrow \quad \ddot{a} > 0 \quad \Rightarrow \quad \rho + 3p < 0 \, , \tag{3.4}$$

i.e. we have an accelerated expansion given by a violation of the strong energy condition, which implies $w < -1/3$. In particular, a simple way to achieve this is a cosmological constant dominating the very early universe, whose negative pressure is responsible for the accelerated expansion. During this epoch, the scale factor evolves as

$$a\,(t) \sim e^{Ht} \, . \tag{3.5}$$

This represents a so-called quasi-dS situation: exact dS expansion corresponds to a constant (rather than slowly changing) H. The situation just described is what we call inflationary epoch, i.e. the epoch of accelerated expansion that separates the initial singularity from the radiation epoch, that gives an explanation to the homogeneity of the CMB.

The accelerated expansion should however last enough time so that quantum fluctuations in the CMB have time to generate. We can measure this 'slowness' requirement by defining two parameters that keep track of the evolution of the Hubble parameter as follows. From the second Friedemann equation, the acceleration required for the shrinking Hubble sphere implies

$$\varepsilon_H \equiv -\frac{\dot{H}}{H^2} = -\frac{\partial \log H}{\partial N} < 1 \, , \tag{3.6}$$

where we have introduced the number of e-folds N of inflationary expansion, which is expressed in cosmic time via the relation $\mathrm{d}N = H\mathrm{d}t$. Hence, the accelerated expansion lasts as long as the parameter

ε_H stays below the unity. This parameter, together with

$$\eta_H \equiv -\frac{1}{2}\frac{\partial \log \varepsilon_H}{\partial N}\,, \tag{3.7}$$

are called *slow-roll parameters*, and they measure the deviation from an exact dS solution, as the limit $\varepsilon_H \to 0$ corresponds to the dS limit. The first slow-roll parameter ε_H measures the relative change of H in one expansion time of the universe. Similarly, the second slow-roll parameter η_H captures the relative change of ε_H, and $|\eta_H| < 1$ ensures that this change is small, such that we have a quasi-dS scenario.

In the slow-roll, single-field regime, these parameters can be approximated in terms of derivatives of the scalar potential, giving conditions on the shape of the inflationary potential. Consider a scalar field ϕ minimally coupled to gravity with arbitrary potential $V(\phi)$. The classical dynamics for the *inflaton* field $\phi(t)$ in the slow-roll regime with FRLW background is then described by

$$\text{Friedmann eq.} \qquad 3H^2 = \frac{1}{2}\dot{\phi} + V(\phi)\,, \tag{3.8a}$$

$$\text{Klein-Gordon eq.} \quad \ddot{\phi} + 3H\dot{\phi} = -V'(\phi)\,, \tag{3.8b}$$

where the prime denotes the derivatives with respect to ϕ. By combining these equations, we get the potential slow-roll parameter as functions of the scalar potential as

$$\varepsilon \equiv \frac{1}{2}\left(\frac{V'}{V}\right)^2\,, \qquad \eta \equiv \frac{V''}{V} - \left(\frac{V'}{V}\right)^2\,, \tag{3.9}$$

where all the energy scales are in units of M_P. The conditions $\varepsilon < 1$ and $\eta < 1$ guarantee the presence of an inflationary expansion: ε parametrises the presence of the slow rolling phase, as inflation lasts as long as the potential energy dominates over the kinetic energy, $V > \dot{\phi}^2$, i.e. as long as $\varepsilon < 1$. On the same footing, η tells us how long the inflationary phase is lasting: as prolonged inflation is given by the predominance of the Hubble friction over V'', we have a prolonged inflationary epoch as long as the η parameter is less than one. In other words, requiring $\eta < 1$ implies requiring that $m_\phi^2 < 3H^2$. As we will review in Section 3.2, it is generally hard to realise such hierarchy from a UV-completed model.

From the slow-roll parameters, we can define two observables,

$$\text{the spectral tilt} \qquad n_s = 1 + 2\,\eta - 6\,\varepsilon\,, \tag{3.10a}$$

$$\text{the tensor-to-scalar ratio} \quad r = 16\,\varepsilon\,. \tag{3.10b}$$

These should be evaluated at the time when the pivot scale k (i.e. a representative scale among the ones probed by the CMB) exited the horizon. In fig. 3.2 we report the latest prediction from the *Planck* satellite [122] on n_s and r, together with predictions from theoretical models.

The *spectral tilt* parametrises deviations from perfect scale invariance. By taking into account quantum fluctuations during inflation, which effectively become classical once stretched to super-horizon wavelengths, we generate a primordial curvature perturbation $\mathcal{R}$. Its two-point function can be described via its power spectrum, $\mathcal{P}_\mathcal{R}(k) \equiv |\mathcal{R}_k|^2$. It is useful to define the dimensionless power spectrum

$$\Delta^2_\mathcal{R}(k) \equiv \frac{k^3}{2\pi^2}\mathcal{P}_\mathcal{R}(k) = \frac{1}{8\pi^2}\frac{H^4}{M_P^2|\dot{H}|c_s}\,, \tag{3.11}$$

where c_s is the speed of sound and at horizon crossing we have the relation $c_s k = Ha$. Since (3.11) is supposed to be evaluated at horizon crossing, any time dependence of H and c_s translates into a scale

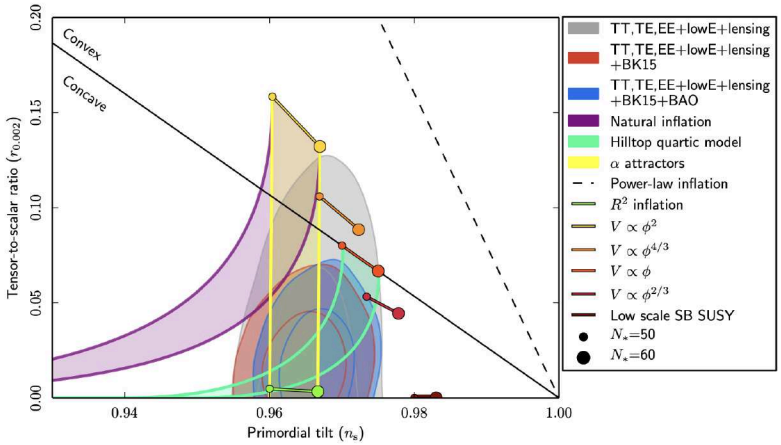

Figure 3.2: *Planck* contours [122] constraining the tensor-to-scalar ratio r and the primordial tilt n_s, with inflationary models evaluated at 50 and 60 e-folds. The pivot scale in the *Planck* data is $k_\star = 0.002$ Mpc^{-1}.

dependence of the power spectrum. That is, scale-invariant fluctuations correspond to $\Delta^2_{\mathcal{R}}(k)$ =const. and the spectral tilt quantifies the deviation from scale invariance since

$$n_s - 1 \equiv \frac{\mathrm{d}\ln\Delta^2_{\mathcal{R}}}{\mathrm{d}\ln k}\,. \tag{3.12}$$

Therefore, from the time-dependence of H during a quasi-dS epoch, we expect a scale dependence of the power spectrum. Indeed, (3.12) and (3.10a) are equivalent once one derives the power spectrum (exchanging the derivative in $\ln k$ with a derivative in the number of e-folds) and plugging the slow roll parameters. Hence, we have a deviation from scale invariance ($n_s \neq 1$) as long as ε is non-vanishing (i.e. H is a function of t), which in turn also implies $\eta \neq 0$.

We expect that both scalar and tensor perturbations of the metric are generated in an expanding background. Hence, a clear prediction of inflation is the presence of primordial gravitational waves. Since the quantization of tensor fluctuations follows the one for scalar fluctuations, we can again define the tensor power spectrum as [123]

$$\Delta^2_h(k) \equiv \frac{k^3}{2\pi^2}\mathcal{P}_h(k) = \frac{12}{\pi^2}\frac{H^2}{M_P^2}\,, \tag{3.13}$$

which we evaluated at horizon crossing already. Note that (3.13) is not a function of $\dot{H}$, but only of the Hubble parameter. Tensor fluctuations are therefore a direct probe of the energy scale at which inflation took place. Finally, we can define the *tensor-to-scalar ratio* r as the ratio between the dimensionless power spectrum of tensor fluctuations $\Delta^2_h(k)$ and the amplitude of scalar fluctuations in order to have an observational constraint on the size of tensor fluctuations, since the amplitude of scalar fluctuations has been measured. In fact, not only we can place an upper bound on the size of tensor fluctuations (since so far we have seen none), but using $\Delta_{\mathcal{R}}(k_\star) = 4.7\times10^{-5}$ in (3.13) one finds [121]

$$H = 3\times10^{-5}\frac{r}{0.1}^{1/2} M_P \quad \Rightarrow \quad E_{\rm inf} \equiv (3H^2M_P^2)^{1/4} = 8\times10^{-3}\frac{r}{0.1}^{1/4} M_P\,. \tag{3.14}$$

Apart from side-products of the inflationary dynamics, we can use the pivot scale to estimate how much our inflationary stage should last. Let us call $\phi_\star$ the point in field space at which the number of

e-folds remaining, away from the critical point $\phi_{\rm end}$, is

$$N_\star = \int_{\phi_{\rm end}}^{\phi_\star} \frac{\mathrm{d}\phi}{\sqrt{2\,\varepsilon}}\,. \tag{3.15}$$

The total number of e-folds needs to be at least $N_\star \sim 50 \div 60$ to solve the early universe problems,[2] as CMB fluctuations are created during four e-folds about 50 e-folds before the end of inflation. Hence, a putative inflationary model should last at least as much. Now, if we assume that ε increases monotonically with ϕ, we can put an upper bound on $N_\star < \Delta\phi/\sqrt{2\,\varepsilon}$. Using (3.10b) and restoring proper powers of M_P, we can write such bound as

$$\frac{\Delta\phi}{M_P} > \sqrt{\frac{r}{8}}\,N_\star\,, \tag{3.16}$$

which is known as the Lyth bound [124]. This bound gives rise to the distinction between two different classes of inflationary models: *large-field* and *small-field* models. In his work, Lyth showed that a slow-roll regime combined with sufficiently-lasting inflation and detectable tensor modes in the CMB (i.e. $r > 0.01$) requires trans-Planckian field displacements. Models achieving a sufficiently long inflationary stage via $\Delta\phi > M_P$ are called large-field models. As we will see in Section 3.2, it is quite difficult to UV-complete these models. We could also have models where the field displacement stays sub-Planckian, and we refer to these as small-field models. However, in general these models are achievable at the price of giving up with detectable tensor modes. Upcoming CMB B-mode polarization searches (CMB-S3: e.g. *Simons Array* [125], *Simons Observatory* [126], BICEP Array [127], CMB-S4 [128–130] and space missions such as e.g. PIXIE [131] or LiteBird [132,133]) will be able to possibly detect tensor modes up to $r \gtrsim 10^{-4}$.

3.2 Inflation in String Theory

The inflationary dynamics clearly takes place in an epoch where Quantum Gravity and the UV-physics could start playing a prominent role, as it is believed that inflation is located at energies around $H \sim 10^{15}$ GeV. Given that inflation talks to the UV-physics, it is natural to ask how does the UV-physics arising near the Planck scales affect the inflationary dynamics. We have already seen that having $\eta < 1$ requires that the mass of the inflaton is lighter than the Hubble scale at the epoch of interest. We explain in the following why this requirement is problematic in a UV-completed theory, and why String Theory is arguably the best candidate that allows us to naturally address these issues arising at energies approaching the Planck scale.

Consider an effective theory of inflation with cutoff $\Lambda > H$. In order to write such theory, we have integrated out all particles with masses above the cutoff scale. Hence, the low energy effective theory bears operators of the form $\mathcal{O}_d/M_P^{d-4}$, where d is the mass dimension of the operator. In the absence of any specific symmetry, we could allow in the EFT Lagrangian for a $d = 6$ Planck-suppressed operator of the form

$$\frac{\mathcal{O}_6}{M_P^2} = \frac{\mathcal{O}_4}{M_P^2}\,\phi^2\,, \tag{3.17}$$

which corrects the inflaton mass as $\Delta m^2 \propto \langle\mathcal{O}_4\rangle/M_P^2$. Thus, in a generic effective theory, the mass of the inflaton is radiatively unstable and runs to the cutoff scale. Moreover, if $\langle\mathcal{O}_4\rangle \sim V$, this radiative correction leads to $\Delta\eta \geq 1$. This is the origin of the so-called *η-problem* [134], and it is the reason we say that inflation is highly UV-sensitive.

[2] We discussed in details only the horizon problem, but other issues are e.g. the flatness problem and the presence of relics that could lead to overclosure of the universe.

From this simple example, we can infer an important consequence. For $\Delta\phi > M_P$, all $\mathcal{O}_{4+2n}$ $(n > 0)$ operators correct η by an order one factor. Therefore, whenever the inflaton traverse a distance of order M_P, the derivatives of the potential receive non-negligible corrections from an infinite series of higher-dimensional Planck-suppressed operators. This spoils the inflationary expansion by drastically reducing its duration. Instead, when $\Delta\phi < M_P$, $\mathcal{O}_{4+2n}$ contributions are suppressed for $n \geq 2$ in $(\Delta\phi/M_P)^{2n-2}$. Hence, the deep distinction between large and small field models is that the UV-sensitivity is much more dramatic for the former ones [135]. It turns out that in large-field models, maintaining the flat potential needed for slow roll is difficult, as quantum corrections are naturally significant on Planckian scales.

The upshot of this discussion is that, in order to embed inflation in a theory of quantum gravity, one needs to ensure that the UV-physics does not induce radiative corrections, or that it bears a mechanism that suppresses them. The most effective mechanism is a symmetry, as we discuss in the next section.

3.3 Axions as inflatons

We have shown before that the η-problem poses a serious challenge to model building. However, we can circumvent such problem by including a symmetry in the potential, or equivalently by considering a UV-completion that naturally produces a symmetry in the four-dimensional effective theory. This would prevent radiative corrections to affect the potential, thus spoiling the prolonged slow-roll phase. Unfortunately, in this case we cannot rely on supersymmetry, as it could be already broken at the inflationary scale.

We could instead consider a potential $V(\phi)$ which is invariant under a shift symmetry $\phi \to \phi + \text{const}$. This can be realised by taking the inflaton to be an axion. The unbroken shift symmetry forbids all non-derivative operators to appear in the Lagrangian, while a weakly broken shift symmetry could in principle give rise to radiatively stable models of large-field inflation. Hence, axions naturally solve the η-problem because their mass is protected by their shift symmetry.

However, for axions a super-Planckian field displacement corresponds to a super-Planckian decay constant f. As explained in Section 2.3, an axion with $f > M_P$ appears to be forbidden by the WGC. Moreover, in all the controlled string-theoretical construction that we know, we are able to get only sub-Planckian decay constants. Indeed, the WGC in its mild form allows for evasions of the bound, which usually happens for higher instantons contributions or effective enhancements. One should then argue why those are the leading effects, and this appears to be challenging while maintaining control on the compactification. In what follows, we introduce the two main proposals to circumvent these obstacles, namely alignment and axion monodromy. Then, we will discuss a model of axion inflation which is of the small-field type but still gives reasonable values for the tensor-to-scalar ratio and can be embeddable in known string compactifications. We call this model *harmonic hybrid inflation*. All these proposals can be derived from String Theory considering closed string axions (see Section 2.2). Finally, we present a model of (in principle) large-field inflation based on a winding mechanism that generates inflation via the phase of complex structure moduli. While a proper explicit model for such proposal is missing, we show that the necessary features can be generically obtained relying on the topology of the compactification manifold. This would render the future model building easier.

For a comprehensive review of inflationary models with axions we refer the reader to e.g. [135–137] and references therein.

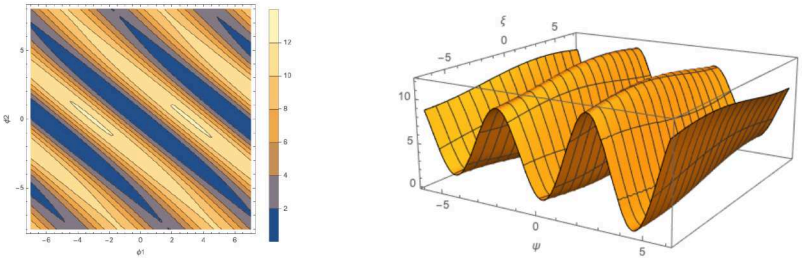

Figure 3.3: Example of KNP alignment with $f_{1,2} = 0.98\,M_P$, $\Lambda_a = 1.5\,M_p$, $\Lambda_b = 1\,M_P$, $c_{2,a} = 1$, $c_{2,b} = 1.4$. The resulting decay constant enhancement for these values is $f_\xi \sim 3.5\,M_P$.

3.3.1 Natural inflation and field space alignment

In axion natural inflation [138], the role of the inflaton is played by an axion field ϕ with a potential

$$V = \Lambda^4 \left[1 - \cos\left(\frac{\phi}{f}\right)\right] . \tag{3.18}$$

In general, this potential originates from weakly breaking the shift symmetry to a discrete subgroup, which can happen either spontaneously or explicitly (from the stringy perspective) by non-perturbative effects induced by the presence of branes and worldsheet instanton wrapping the appropriate cycle (see Section 2.2). Although such a potential is natural from a bottom-up perspective (as it is radiatively stable against one-loop corrections, as we discussed above), one can show that in order to have enough inflation, the decay constant should be super-Planckian. To overcome this problem, Kim, Nilles and Peloso (KNP) proposed a way to achieve a super-Planckian decay constant starting from a sub-Planckian one [139]. The KNP proposal relies on the presence of two axions $\phi_{1,2}$ with decay constants $f_{1,2}$ entering the cosines as linear combinations, namely

$$V = \Lambda_a^4 \left[1 - \cos\left(c_{1a}\frac{\phi_1}{f_1} + c_{2a}\frac{\phi_2}{f_2}\right)\right] + \Lambda_b^4 \left[1 - \cos\left(c_{1b}\frac{\phi_1}{f_1} + c_{2b}\frac{\phi_2}{f_2}\right)\right] . \tag{3.19}$$

The mass matrix has determinant $\det(M^2) = (c_{1b}c_{2a} - c_{1a}c_{2b})/(f_1^2 f_2^2)$, hence when $c_{1a}c_{2b} = c_{1b}c_{2a}$ (i.e. when we have *alignment*) we have a single, flat direction in the potential. However, $\phi_{1,2}$ are not the physical fields. The true physical fields are the eigenvectors of M^2 and are proportional to a linear combination of ϕ_1 and ϕ_2. For ease of exposition, consider $c_{1a} = c_{1b} = 1$ and $\Lambda_a > \Lambda_b$. The physical fields ψ and ξ have masses

$$\begin{aligned} &m_\psi^2 = \Lambda_a^4 \left(\frac{1}{f_1^2} + \frac{c_{2a}^2}{f_2^2}\right) , \quad m_\xi^2 = \Lambda_b^2 \frac{(c_{2a} - c_{2b})^2}{c_{2a}^2 f_1^2 + f_2^2} \\ &\text{for} \quad \psi = \frac{f_1 f_2}{\sqrt{c_{2a}^2 f_1^2 + f_2^2}} \left(\frac{\phi_1}{f_1} + \frac{c_{2a}\phi_2}{f_2}\right) , \quad \xi = \frac{f_1 f_2}{\sqrt{c_{2a}^2 f_1^2 + f_2^2}} \left(\frac{\phi_2}{f_1} - \frac{c_{2a}\phi_1}{f_2}\right) . \end{aligned} \tag{3.20}$$

Hence, for $c_{2a} = c_{2b}$ we have perfect alignment, and ξ is a flat direction of V. Now, if we slightly detune $c_{2a} \simeq c_{2b}$, ξ becomes very light.[3] If this direction is associated with the inflaton field, the inflaton has a suppressed mass m_ξ and hence we have a suppression of the η parameter. Moreover, a suppression in

[3]Note that we should slightly detune these coefficients also because otherwise we would be in the presence of an unbroken shift symmetry, which is conjectured to be forbidden in a consistent theory of Quantum Gravity [140].

m_ξ corresponds to an enhancement in the decay constant, which reads

$$f_\xi = \frac{\left(c_{2a}^2 f_1^2 + f_2^2\right)^{1/2}}{|c_{2b} - c_{2a}|} \,. \tag{3.21}$$

This means that we could have effective super-Planckian field displacements from sub-Planckian decay constants. Indeed, due to the difference in the scales, the physical fields evolve independently and during the proper inflationary stage, $m_\psi \gg H$, hence ψ is settled to its minimum and ξ drives inflation.

Let us note here that the field redefinitions at the core of KNP alignment do not guarantee that the kinetic terms are canonically normalized as well. Usually, the contrary happens, and in general one should better normalize the kinetic terms first, risking spoiling the desired structure for alignment.

The idea behind axion alignment was later implemented for N axions, hence the name *N-flation* [141]. Here, N axions get excited simultaneously and each develops a potential on its own. The Hubble friction operates on the sum of the potential, resulting in an individual enhancement proportional to $\sqrt{N}$. This leads to a super-Planckian collective excitation, while the individual field displacement remains sub-Planckian. However, one can show that loops of the N light axion fields renormalize M_P with a factor that scales as $\sqrt{N}$. Hence, we cannot get parametrically large collective displacements by relying only on a huge number of fields.

Moreover, from the string-theoretical point of view, we can read this as the fact that the overall volume of a CY should not grow linearly with N, otherwise M_P gets corrections proportional N which would cancel the gain from travelling along the collective field trajectory. It was then asserted that suitable cancellations may occur, maintaining a small volume and allowing for parametric enhancement. In [22], this cancellation was called into question, and it was argued that in the large volume limit, axion decay constants should scale as $1/\sqrt{N}$, cancelling the collective enhancement. In the same work, an alternative proposal was pointed out, which was heavily depending on the details of the CY geometry. Later [142] proved that it is unrealistic. Crucially, [142] reports a geometric argument (independent on the number of axions) on why parametric enhancement of the radius of axion moduli space is impossible, finding an upper bound on such quantity. Finally, N-flation is in tension with the axionic version of the Convex Hull WGC [68] (cf. Section 2.3).

Hence, it seems that String Theory forbids enhancement of field displacements based on mechanisms that do not rely on monodromy. For this reason, we devote the next section to such a class of axion inflation models.

3.3.2 Axion monodromy inflation

In order to avoid all the problems affecting large-scale inflationary models that rely on enhancement of the field displacement based on Pythagorean logic, one should find a completely different mechanism that still produces large effective field displacements while maintaining sub-Planckian string-derived quantities. An example of such mechanism is given by *axion monodromy inflation*, which we review in what follows.

When a system reaches a new configuration after being transported around a closed loop in the naive configuration space is said to undergo a monodromy transformation. Something very similar happens to a string axion when non-perturbative effects introduce non-periodic terms in the potential, thus generating a monodromy on top of the harmonic terms. Therefore, we could imagine applying the shift symmetry to the axion for multiple cycles; this produces an effective field displacement in the configuration space that greatly exceeds the fundamental period. Moreover, the leftover discrete shift

symmetry protects the structure of the potential over each cycle, forbidding loop contributions during the trajectory. Hence, large-field inflation is achieved while keeping a sub-Planckian decay constant.

In the original proposal [143, 144], axion monodromy inflation is realized by considering the non-perturbative effect coming from a D5-brane (or an NS5-brane, which basically means applying S-duality) wrapped on an internal 2-cycle Σ.[4] Upon integrating on the cycle, the DBI action produces a linear term for the B_2 axion (or, in the case of the NS5-brane, for the C_2 axion) in the $4d$ potential, which is then no longer a periodic function of the axion. The final effective potential in terms of the canonically normalized field ϕ takes the form

$$V = \mu^3 \phi + \Lambda^4 \cos\left(\frac{\phi}{f}\right) , \tag{3.22}$$

where the periodic part is dominant for small VEVs while it gets exponentially suppressed at large volume, and the monodromy term takes over on large field displacements. Hence, we have effectively a large-field monomial inflation with tiny periodic modulations on top. Note that many other variants of chaotic inflation can arise via monodromy, changing the exponents in the monodromy term [145]. Hence, we can write the general parent of the potential in (3.22) as

$$V = \mu^{4-p} \phi^p + \Lambda^4 \cos\left(\frac{\phi}{f}\right) , \quad \text{where} \quad p \leq 2 \tag{3.23}$$

Despite the fact that all the ingredients are rather common in string compactification, a concrete model realising this idea has proven to be challenging to construct.

Later, it was shown that it is possible to get a potential as the one in (3.22) by generating a similar monodromy and a mass term from background fluxes and their F-term potentials [146]. This would make the actual model building of axion monodromy inflation more feasible. Consider the Chern-Simons coupling $\tilde{F}_p = F_p + B_2 \wedge F_{p-2}$: the action is invariant under the B_2 gauge transformation $B_2 \to B_2 + \mathrm{d}\Lambda_1$ if at the same time $C_{p-1} \to C_{p-1} - \Lambda_1 \wedge F_{p-2}$ holds. Hence, turning on the F_{p-2} flux provides the axion field $b(x)$ with a mass term, i.e. it provides a non-periodic potential for $b(x)$ of the form

$$V \sim \int_X \tilde{F_p}^{\,2} \sim \left(N_p + b(x)\, N_{p-2}\right)^2 , \tag{3.24}$$

where N_p and N_{p-2} denote the flux quanta of F_p and F_{p-2} fluxes that are turned on. Therefore, the field range of $b(x)$ no longer shows periodicity and is a priori unbounded: we have parametrically extended the axion field range along a non-periodic potential coming from fluxes. The full potential then displays a set of non-periodic branches for the axions labelled by N_{p-2}, and the periodicity of the full theory is visible when summing over all branches. The effective potential on each branch picked by F_{p-2} looks like the one in (3.22), where as usual the periodic contribution comes from non-perturbative effects. Moreover, (3.24) gives a string-theoretical derivation of the axion 4-form Lagrangian proposed in [147] as a $4d$ model of axion monodromy inflation, namely

$$\mathcal{L} \sim F_4^2 + (\partial\phi)^2 + \mu\phi F_4 \, . \tag{3.25}$$

An interesting side of axion monodromy inflation is that it produces peculiar phenomenological signatures. For example, the oscillatory corrections on top of the background dynamics imprint a characteristic oscillating signal in all primordial correlation functions. Moreover, the power spectrum also

[4] In order to cancel the tadpole, one should also add a $\overline{\text{D5}}$-brane (or a $\overline{\text{NS5}}$-brane) wrapping a distinct representative of the same homology class of Σ.

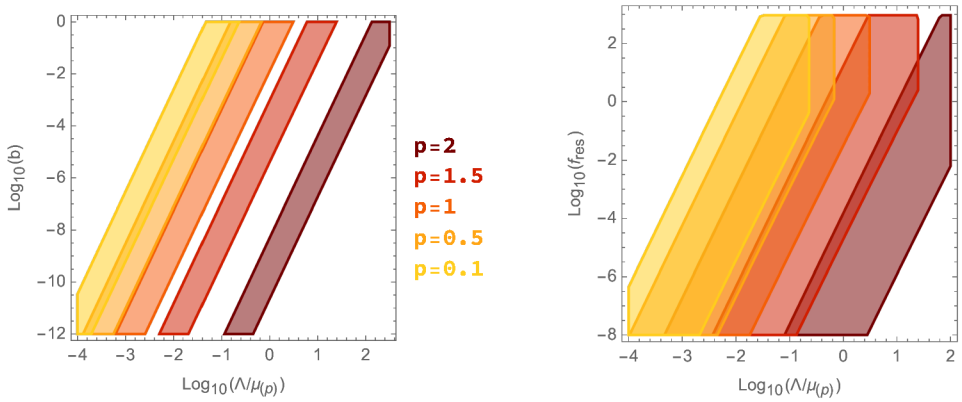

Figure 3.4: Theoretically allowed values of $b_\star$ (left) and $f_{NL}^{\rm res}$ (right) coming from imposing monotonicity of the inflationary potential, i.e., $b_\star < 1$, aFL and WG conjectures, and requiring that $\omega_\star < 10^2$ to match experimental constraints [150]. These results refer to the monomial monodromy potential, fixing the number of e-folding in absence of wiggles to be $N = 50$ and imposing COBE normalization.

carries a signature of the modulations. Calling the monodromy induced term V_0, we can introduce the parameter $b_\star$, which measures the instanton generated wiggles intensity in the inflationary potential,

$$b_\star \equiv \frac{\Lambda^4}{V_0'(\phi_\star) f} \tag{3.26}$$

where $\phi_\star$ is the value of the inflaton as horizon exit. Indeed, to match the experimental constraints on the power spectrum of density perturbation, the oscillating part of the potential must be highly suppressed at the pivot scale.

The monotonicity of the potential and the consistency with observational constraints require $b_\star \ll 1$ for $p \geq 1$ but this condition is believed to hold in the more general case we consider. By taking $b_\star \ll 1$, one can treat the cosine as a perturbation in the power spectrum and show that it can modulate the monomial-generated power spectrum, producing oscillations that can be now searched with e.g. WMAP and *Planck* [148]. These are detected as resonant non-gaussianities [149]

$$f_{NL}^{\rm res} = \frac{3\sqrt{2\pi}}{8} b_\star \, \omega_\star^{3/2} \,, \tag{3.27}$$

where $\star$ denotes evaluation at horizon exit, $\omega_\star = \left(\frac{\sqrt{2\varepsilon_\star} M_P}{f}\right)$ is the resonance frequency and ε is the slow-roll parameter derived from the monodromy potential only.

To get the range of admissible values for $f_{NL}^{\rm res}$ for each value of p, we remove a model degree of freedom imposing COBE normalization[5], i.e.,

$$\sqrt{P_s(N_\star)} \simeq \frac{1}{10\pi} \sqrt{\frac{4}{3} \frac{V_{\Lambda=0}(\phi_\star)}{\varepsilon_\star M_P^4}} \simeq 2 \times 10^{-5} \,. \tag{3.28}$$

Moreover, the wiggles in the potential cannot significantly affect the number of e-folds N unless a massive parameter fine-tuning is performed; therefore, as experimental constraints require $40 < N < 60$, we fix $N = 50$ when $\Lambda = 0$, thus removing another degree of freedom from the model. In this way, we uniquely identify μ and the value of $\phi_\star$. We stress that our results do not significantly change when choosing other N values within the allowed range. Using the upper and lower bounds in (2.68), also imposing the relation $\Lambda^4 = e^{-S}$, we get to the theoretically allowed window for $b_\star$ and $f_{NL}^{\rm res}$, WGC and aFL providing

[5] Which means we fix the size of the curvature perturbations.

the lower and upper bound respectively. We plot these results in Fig. 3.4.

Finally, requiring that the lower bound on $b_\star$ coming from WGC is not in contrast with the condition $b_\star \ll 1$ sets a lower bound on the instanton action $S \gtrsim 25$. It can be easily checked that this relation is almost insensitive to the value of p.

3.4 Harmonic hybrid inflation

Hybrid inflation is a mechanism of slow-roll inflation which achieves the end of the slow-roll phase, driven by one scalar field, through an instability induced by the coupling with another scalar, which then undergoes a rapid 'waterfall' roll to the minimum. The slow-roll phase itself is dominated by a large field-independent vacuum energy, i.e. hybrid inflation 'hybridizes' between 'new' slow-roll inflation and 'old' false-vacuum inflation. Interestingly, this vacuum energy domination implies that hybrid inflation possesses a smallish field displacement corresponding to the last about 60 e-folds of observable inflation, $\Delta\phi_{60} \lesssim M_P$, which nevertheless does not become parametrically small. Hence, hybrid inflation naturally constitutes a mechanism that realises high-scale inflation while accommodating the Swampland Distance Conjecture [11].

Linde's original hybrid inflation model [151] considers two scalar fields ϕ, χ. The terms of the scalar potential relevant for the hybrid mechanism read

$$V = \frac{\lambda}{4}(\chi^2 - v^2)^2 + g\chi^2\phi^2 + \Delta V(\phi)\,, \tag{3.29}$$

where $\Delta V(\phi)$ is the non-constant slow roll potential for the inflaton field ϕ along the $\chi = 0$ direction. Two important features of this model are the presence of two end-of-waterfall minima at $\chi = \pm v$, $\phi = 0$ and the bi-quadratic coupling that provides the stabilisation of $\chi = 0$ beyond the waterfall critical point of ϕ. Such coupling between χ and ϕ induces an effective mass for the waterfall field that depends on the value of the inflaton as

$$m_\chi^2 = -\lambda v^2 + 2g\phi^2 \equiv -M^2 + 2g\phi^2\,. \tag{3.30}$$

This vanishes at the waterfall critical point $\phi = \phi_c \equiv M/\sqrt{2g}$. The dynamics of this model depends on the value of the inflaton with respect to the critical point and can be described as follows. As long as ϕ is larger than the critical value, the field χ is frozen and the system resembles the canonical single-field slow roll driven by the vacuum energy of the universe. This allows for inflation with sub-Planckian field displacements, without the same amount of fine-tuning of the initial conditions as usually required in natural inflation. When ϕ approaches ϕ_c, the field χ starts becoming light and the dynamics corresponds to a two-field one. Finally, when $\phi < \phi_c$, the determinant of the Hessian flips sign, i.e. χ becomes tachyonic and inflation ends rapidly. Indeed, hybrid inflation requires a certain hierarchy between the masses of the two fields, $V_{\phi\phi} \ll M^2$. A UV-completion of such model should be able to explain such feature.

The peculiar way in which hybrid inflation ends allows for the presence of interesting features that could potentially lead to observational signatures. The most prominent one is tachyonic preheating [152, 153], which induces peculiar peaks in the spectrum of primordial gravitational waves [154,155] and could lead to the presence of oscillons [156].

Note that hybrid inflation setups generating the hybrid behaviour by means of a bi-quadratic coupling between the inflaton and the waterfall field usually show a $\mathbb{Z}_2$ symmetry between the two degenerate final vacua of the scalar field trajectory. This $\mathbb{Z}_2$ symmetry leads to domain wall production overclosing the late universe. One should then find a way to break such symmetry and avoid the domain wall

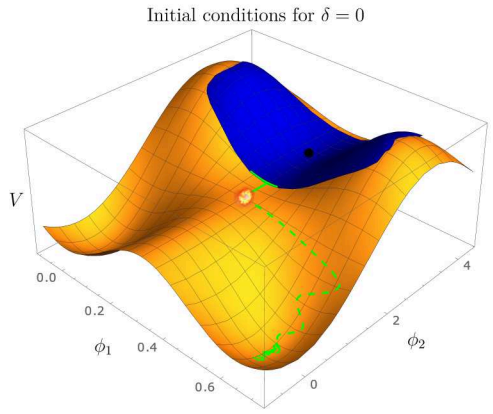

Figure 3.5: Hybrid inflation potential driven by the two axions ϕ_1 and ϕ_2, for $c_2 = 1$, $c_1 = 10$, $\alpha = 0.01$, corresponding to $\tilde{\Lambda}^4 = \frac{1+\alpha}{1-\alpha}\Lambda^4 \simeq 1.02\Lambda^4$. The slow-roll regime develops along the valley parametrized by the ϕ_2 direction, while in the ϕ_1 direction the waterfall is displayed. Black dot: the inflationary saddle point. Blue region: complete region of initial conditions supporting at minimum 60 e-folds of slow-roll inflation. There is no significant fine-tuning of initial conditions in this model. Solid green: slow-roll part of a sample inflationary trajectory providing 60 e-folds of slow-roll inflation before reaching the waterfall critical point. Fireball: explosive growth of tachyonic quantum fluctuation and consequent loss of classical rolling description. Dashed green: would-be classical waterfall evolution neglecting quantum fluctuations for the same sample inflationary trajectory after crossing the waterfall critical point.

problem.

Motivated by the above features, we proposed a regime of hybrid inflation driven by two axions acquiring a purely non-perturbative periodic scalar potential. As explained in Section 2.2, axions are a ubiquitous presence in most models of string compactifications, see e.g. [21–23]. Moreover, string theory axions appear with an exponentially wide spectrum of masses, suggesting some of them as suitable inflaton candidates. With this as guidance, we can guess a two-field axion-like potential of the form

$$V = \Lambda^4 + \tilde{\Lambda}^4 - \left(\tilde{\Lambda}^4 + \Lambda^4 \cos\left(c_1\,\phi_1\right)\right) \cos\left(c_2\,\phi_2\right), \tag{3.31}$$

where Λ and $\tilde{\Lambda}$ are energy scales to be specified later (with $\tilde{\Lambda} > \Lambda$) and the coefficients $c_i \geq 1$ are proportional to the inverse of the axion decay constants f_i in units of M_P. We take the two fields ϕ_1 and ϕ_2 such that their kinetic terms are canonically normalized. Note that ϕ_2 plays the role of the inflaton field and determines the mass of ϕ_1. As ϕ_2 evolves in time, its cosine eventually flips sign and renders ϕ_1 tachyonic. This is exactly the dynamic of the classic hybrid inflation model.

It is instructive to perform a backward comparison of our axion model with the original hybrid inflation model. In (3.29), the potential is given up to quartic terms in the field χ as well as quadratic in ϕ, and the structure of the potential covers both the position of the hybrid inflation valley and the minima. We can now expand the axion potential in (3.31) up to quartic order in ϕ_1, ϕ_2, assuming for simplicity $\tilde{\Lambda}^4 = \Lambda^4$. If we do this expansion around $c_1\phi_1 = \pi$, $\phi_2 = 0$, the resulting scalar potential resembles eq. (3.29) qualitatively, but the two waterfall minima occur at values which are $\mathcal{O}(1)$ shifted from their position at $(c_1\phi_1 = \{0, 2\pi\}, \phi_2 = 0)$ in the full potential (3.31). We conclude, that the higher-order terms of the 'harmonic' cosine terms dictated by the instanton expansion are crucial for the full field space structure of the model, which we are thus motivated to call *harmonic hybrid inflation*.[6]

[6]We note, that in general finding the global minimum and at least a subset of all critical points of such harmonic potentials is non-trivial but achievable using the methods described in appendix A of [4]

We can recast the scalar potential (3.31) in the canonical form

$$V = \Lambda_1^4[1-\cos(c_1\phi_1+c_2\phi_2)] + \Lambda_2^4[1-\cos(c_1\phi_1-c_2\phi_2)] + \Lambda_3^4[1-\cos(c_2\phi_2)]\,, \tag{3.32}$$

by a suitable identification of the parameters, namely $\Lambda_1^4 = \Lambda_2^4 \equiv \Lambda^4/2$, $\Lambda_3^4 \equiv \tilde{\Lambda}^4$. Clearly, the first equivalence is a tuning condition to be fulfilled by any UV realization of the mechanism. For practical use, we also define the following quantities

$$V_0 = \tilde{\Lambda}^4 + \Lambda^4\,, \quad \alpha = \frac{\tilde{\Lambda}^4 - \Lambda^4}{\tilde{\Lambda}^4 + \Lambda^4} \quad \text{and} \quad c = c_2\,. \tag{3.33}$$

In a hybrid inflation model, we require the following three conditions on the parameters to be satisfied:

1. Presence of a dS saddle point in the potential. Inflation will start close to this saddle point in order to inflate a sufficient number of e-folds. This amounts to $\tilde{\Lambda} > \Lambda$. If this condition is violated, a local minimum will develop that traps the inflaton field instead.

2. The dominance of vacuum energy, $\alpha \ll 1$.

3. The inflationary solution should undergo a fast waterfall transition. To achieve this, we additionally assume $c_1 \gg 1$. This drives ϕ_1 much more massive than H inside the valley for values larger than the waterfall critical point $\phi_{2,c} = \pi/(2c)$, but it becomes strongly tachyonic $-m_{\phi_1}^2/H^2 \gg 1$ after the inflationary trajectory crosses this point.

From the dominance of vacuum energy, we have as an immediate benefit the limited field range $\Delta\phi_2 \lesssim M_P$, which implies that harmonic hybrid inflation works with sub-Planckian axion decay constants $f_a \lesssim M_P$. This renders our realization of hybrid inflation with axions consistent with bounds on the axion decay constant from controlled string compactifications [20, 21] as well as from arguments about weak gravity (WGC) [67].

Between the de Sitter saddle point and the waterfall critical point, the waterfall field is stabilized at $\phi_1 = \pi/c_1$ and, after integrating out ϕ_1, the scalar potential takes the effective form

$$V_{\rm inf}(\phi_2) = V_0\,(1-\alpha\cos(c\,\phi_2))\,. \tag{3.34}$$

We evaluate the viability of our model by computing the slow-roll parameters and the inflationary observables. In the slow-roll and single-field regime, the slow-roll parameters can be approximated in terms of derivatives of the scalar potential as in (3.9). In particular, we have that

$$\varepsilon \approx \frac{1}{2}\left(\frac{V_{\rm inf}'}{V_{\rm inf}}\right)^2 = \frac{1}{2}\alpha^2 c^2 \sin^2(c\,\phi_2) + \mathcal{O}(\alpha^4)\,. \tag{3.35}$$

The number ΔN of inflationary e-folds away from the waterfall critical point $\phi_{2,c}$ can be derived from (3.15), where $\phi_{\rm end} \equiv \phi_{2,c}$. By performing the integral and inverting the resulting expression, we find a relation between the field ϕ_2 and the number of e-folds

$$\phi_2(\Delta N) = \frac{2}{c}\arctan\left(e^{\alpha c^2 \Delta N}\right)\,, \tag{3.36}$$

discarding higher order corrections in α. Here we assume we inflate from a point close to the saddle point $\phi_2 = \pi/c$ towards the waterfall critical point $\phi_{2,c} = \pi/2c$ at $\Delta N = 0$, but equivalently inflation could start close to any of the other saddle points $\phi_2 = (\pi + 2\pi n)/c$ towards the transition points

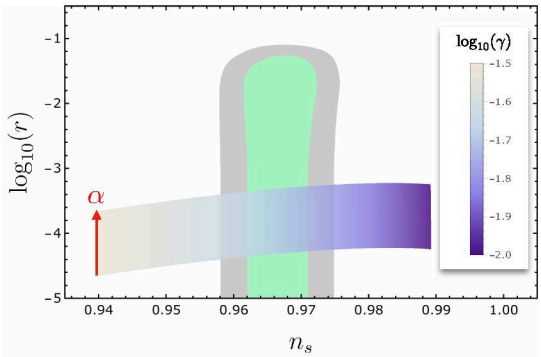

Figure 3.6: Analytical predictions for n_s and r varying $\log_{10}(\gamma) \in [-3, -1.5]$ and $\log_{10}(\alpha) \in [-3, -2]$ (purple-to-white contour) together with the 1σ and 2σ confidence contours found by *Planck* [111] (grey and mint contours, respectively).

$\phi_{2,c} = (2\pi n \pm \pi/2)/c$. The above solution allows us to write the first slow-roll parameter as a function of the e-folds

$$\varepsilon(\Delta N) = 2\,\alpha\,\gamma\,\frac{e^{2\gamma\Delta N}}{\left(1+e^{2\gamma\Delta N}\right)^2}\,, \tag{3.37}$$

where we define $\gamma \equiv \alpha c^2$. The second slow-roll parameter is then given by

$$\eta(\Delta N) \equiv \frac{1}{2\varepsilon}\frac{\partial\varepsilon}{\partial\Delta N} = \gamma\,\frac{1-e^{2\gamma\Delta N}}{1+e^{2\gamma\Delta N}}\,. \tag{3.38}$$

Notice the hierarchy $|\eta| \gg \varepsilon$. Therefore, as usual in small field inflation, the tensor-to-scalar ratio is highly suppressed. The spectral tilt is to a high level of precision determined by the value of γ only (given some value of ΔN). If we take ΔN between 50 and 60 e-folds, the 1σ constraint that $n_s \in [0.9627, 0.9703]$ [111] translates into $\gamma \in [0.0185, 0.0229]$. In other words, the parameters Λ, $\tilde{\Lambda}$ and c are degenerate, however, they need to be fine-tuned such that the resulting n_s falls within the observed window. In fig. 3.6 we show the analytical predictions for n_s and r based on (3.37) and (3.38) with $\Delta N = 60$.As discussed before, α only moves the prediction for r up or down and n_s is very sensitive to the value of γ. As we will consider in a moment, we have to break the symmetry in ϕ_1 in order to avoid the formation of domain walls. Therefore, this toy model is not the end of the story, and we will see that the predictions are also highly sensitive to the amount of symmetry breaking.

3.4.1 Effect of instanton-induced phases

Since axions arising in String Theory enjoy perturbative shift symmetries as non-linear realizations of the underlying $10d$ p-form gauge symmetries, they acquire a scalar potential via non-perturbative instanton effects (unless monodromy-generating sources of stress-energy such as branes or fluxes are present as well). These instanton effects, which generate the scales Λ_i^4 of the periodic axion potentials they induce, possess an ab initio arbitrary complex phase. In string theory realizations, the 1-loop determinants of such instanton contributions entering the scales Λ_i^4 become functions of the moduli VEVs. Since we can tune the VEVs by the choice of quantized background fluxes of p-form field strengths, the value of the phases of the instanton effects is adjustable. Hence, in principle all the three cosines in (3.32) can have a non-vanishing but finite adjustable phase, which was omitted in the discussion so far. However, two phases out of three can be reabsorbed thanks to the shift freedom given by the presence of two axions. In the following, we evaluate how much the inclusion of the remaining phase will change the model and how it will affect the inflationary predictions.

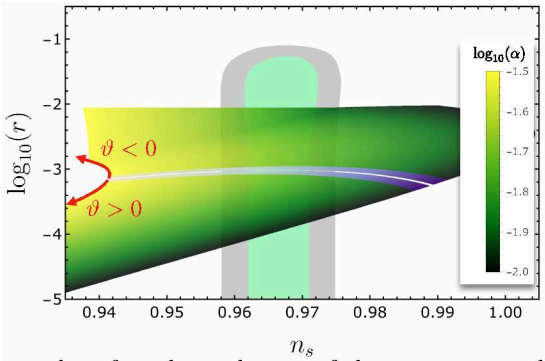

Figure 3.7: Predictions for n_s and r after the inclusion of the instanton-induced phase ϑ. We evaluated which values of the parameters α, ϕ_2 (meaning its starting point on the cosine) and especially ϑ fit best the experimental data. We compare the *Planck* contours with the numerical predictions for n_s and r keeping $c = 1$ fixed while varying $\log_{10}(\alpha) \in [-2.0, -1.5]$ and $\vartheta \in [-1/15, 1/15]$. Notice that here we allow the phase to take both positive and negative values. The purple contour is the region where the analytical approximation for small ϑ holds. This will be useful to compare the modifications from the perfect hybrid due to ϑ with the ones following from the $\mathbb{Z}_2$-symmetry breaking terms (see 3.4.2).

Without loss of generality, we choose to keep the phase ϑ in the single-axion cosine term. Again, during the slow-roll evolution of ϕ_2 we can integrate out ϕ_1. This leaves us with

$$V_{\rm inf}^{(\vartheta)}(\phi_2) = V_0 - \tilde{\Lambda}^4 \cos\left(c_2\phi_2 + \vartheta\right) + \Lambda^4 \cos\left(c_2\phi_2\right) , \tag{3.39}$$

and the equations determining the slow-roll parameters change accordingly. In fact, the first slow-roll parameter becomes to leading order in α and ϑ

$$\varepsilon^{(\vartheta)} \simeq \frac{c_2^2}{2}\left(\alpha \sin(c_2\phi_2) + \frac{1}{2}\vartheta\cos(c_2\phi_2)\right)^2 + \mathcal{O}(\alpha^2\vartheta, \alpha^2\vartheta^2) . \tag{3.40}$$

We require $\vartheta \lesssim 0.1$ in order to have vacuum energy domination during the slow-roll regime. Otherwise, for bigger values of ϑ the hybrid mechanism is spoiled, because the inflaton-dependent part of the scalar potential controls the inflaton dynamics, which in turn drives the model into the large-field regime. The results of the analysis for the inclusion of the phase are displayed in fig. 3.7. There is a whole set of (α, ϑ, ϕ_2) combinations that can actually give good hybrid inflation lasting (at least) 60 e-folds. Below a certain value of α, the value of the phase giving the required n_s becomes basically fixed. Thus, one could balance the values of α and ϑ in order to have the least amount of fine-tuning possible. [7]

3.4.2 $\mathbb{Z}_2$ symmetry breaking effects

At the end of inflation, the hybrid valley false vacuum has to decay into the true vacuum. The onset of this transition is controlled by the inflaton field, which allows for tachyonic growth of the waterfall field as the inflaton crosses the critical point. Tachyonic preheating proceeds similar to a second order phase transition, via a spinodal decomposition. The spinodal time and the average size of the domains have been computed originally in [157, 158] and have been refined beyond the quench approximation in [159–161]. However, in order to avoid the domain wall problem [162] either the tachyonic instability should be avoided or the vacuum degeneracy needs to be broken such that asymmetry generates a

[7] We wish to point out in passing, that it may be possible to get the instanton phases discussed in this section to vanish dynamically in appropriately arranged field theory realizations involving bi- or tri-fundamental matter representations coupled to three non-Abelian gauge groups.

pressure pushing the true vacuum domains to grow with a rate that depends on the surface tension of the domain walls. For the latter option, we need $\Delta V \gg V_0\pi^4/c_1^2$ such that domain walls will not dominate the energy budget in the universe [163]. In order to break the vacuum degeneracy, we necessarily need to break the $\mathbb{Z}_2$ symmetry around the inflationary trajectory. Our model naturally allows for such a breaking by assuming different axion decay constants multiplying ϕ_1. In what follows, we investigate this simple generalization. Additionally, such a setup *generically* removes the tachyonic instability and hence no domain walls are formed in the first place. This drastically changes the physics of preheating, as it does not proceed via the spinodal instability. Instead, a period of parametric resonance [164–166] will most likely follow and the post-inflation phenomenology may be enriched by the formation of two-field oscillons [156].

As discussed above, the two vacua providing the possible endpoints of the waterfall regime have a $\mathbb{Z}_2$ symmetry in the ϕ_1 direction. This leads to the formation of domain walls after inflation. Therefore, we should break the symmetry to avoid such a scenario incompatible with our universe. The simplest way to do so is to generalize the potential (3.32) to the form

$$V = \Lambda_1^4[1-\cos\left(c_1^+\phi_1 + c_2^+\phi_2\right)] + \Lambda_2^4[1-\cos\left(c_1^-\phi_1 - c_2^-\phi_2\right)] + \Lambda_3^4[1-\cos\left(c_2\phi_2\right)]\,. \tag{3.41}$$

Choosing $c_1^+ \neq c_1^-$ will *generically* break the $\mathbb{Z}_2$ vacuum degeneracy, but it also removes the tachyonic instability at the end of inflation and no domain walls are formed. Moreover, preheating does not proceed via tachyonic growth (assuming that $c_1^+ - c_1^-$ is not exponentially close to zero, which we expect to be the case in the possible string embeddings discussed below). To see why the tachyonic instability characteristic for tachyonic preheating disappears, we notice that the inflationary trajectory proceeds along a straight line $\phi_1 = \pi/c_1$ only in the presence of the $\mathbb{Z}_2$ symmetry. When the $\mathbb{Z}_2$ symmetry is broken, the waterfall field ϕ_1 gets stabilized at a value depending on the expectation value of the inflaton field ϕ_2. This is illustrated with the red solid line in fig. 3.8. More precisely, in presence of the unbroken $\mathbb{Z}_2$ symmetry, the signature of the Hessian changes along the inflationary slow-roll trajectory $\phi_1 = \pi/c_1$ from $(-,+)$ to $(+,-)$ at a single point ($\phi_1 = \pi/c_1$, $\phi_2 = \phi_{2,c}$). Once the $\mathbb{Z}_2$ symmetry is broken, we see in fig. 3.8 that the path given by $\partial_{\phi_1} V = 0$ approximating the slow-roll part of the inflaton trajectory enters a region with Hessian of signature $(+,+)$ while turning away and missing the former critical point before re-entering a region with signature $(-,+)$. From this, it is self-evident that the point-like transition from $(+,-)$ to $(-,+)$ signature on a classical trajectory with $\phi_1 = $ const. characteristic of the tachyonic preheating instability is simply gone once the $\mathbb{Z}_2$ symmetry is broken. This means that ϕ_1 never develops the tachyonic preheating instability, except in the presence of a $\mathbb{Z}_2$ symmetry.

We will look at a minimal deformation of this kind, choosing a symmetric deformation $c_1^\pm = c_1(1\pm\delta)$ while keeping $c_2^\pm = c$, $\Lambda_1^4 = \Lambda_2^4 = \Lambda^4/2$ and $\Lambda_3^4 = \tilde{\Lambda}^4$, which should be close but slightly larger than Λ^4. Note that the effect of symmetry breaking becomes larger if we move further away from $\phi_1 = 0$. At the same time, a set of global minima are still located at $\phi_1 = 0$ and $\phi_2 = 2\pi n/c$. From here onwards, we restrict ourselves to inflation in the neighbourhoods of these minima.

We shall now quickly summarize the effects of this $\mathbb{Z}_2$-symmetry breaking before providing the details. Breaking the degeneracy in the minimal fashion described above has consequences. First, the maximum of the potential in ϕ_2 in the hybrid valley around $\phi_1 = \pi/c_1$ is shifted from its original position at $\phi_2^{max}(\delta = 0) = \pi/c$. Next, the symmetry breaking implies that the waterfall regime, involving tachyonic preheating as well, in the strict sense is lost and replaced with a waterfall-like rapid exit from inflation once $\phi_2 < \phi_{2,c}$. Furthermore, the loss of degeneracy implies that there are now two inequivalent inflationary regimes: one starting from $\phi_2 < \phi_2^{max}$ towards $\phi_2 = 0$ and another starting at $\phi_2 > \phi_2^{max}$

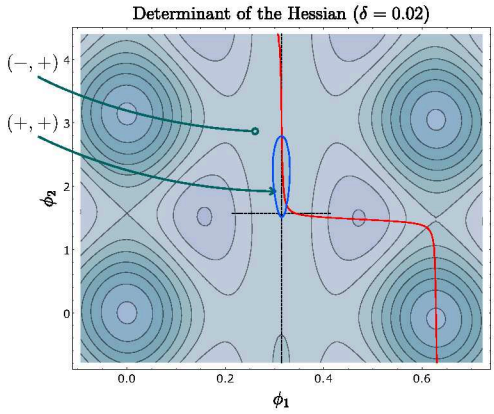

Figure 3.8: Contour plot of the determinant of the Hessian of the deformed potential given in (3.41) with $c_1^{\pm} = c_1(1 \pm \delta)$ and $c_2^{\pm} = c$. We choose the same values of the parameters as in fig. 3.10, namely $\delta = 0.02$, $\alpha = 0.01$, $\gamma = 0.011$ and $c_1 = 10$. The red solid curve shows where the gradient of the potential in the ϕ_1 direction is vanishing, and provides initially a good proxy of the inflationary trajectory. The black cross, on the other hand, shows the vanishing of the gradient in case the $\mathbb{Z}_2$ symmetry would be unbroken, that is, for $\delta = 0$. The highlighted central contour specifies where the determinant of the Hessian changes sign. This contour shrinks to zero size as $\delta \to 0$, while the rest of the contours remain similar.

towards $\phi_2 = 2\pi/c$ in the neighbouring vacuum region. In addition, with increasing δ the field trajectory will become more and more curved in its entirety due to the increasingly broken $\mathbb{Z}_2$ symmetry of the inflationary valley, which will cause sizeable changes in n_s and r. As we will see in fig. 3.9b, using the full numerical analysis, maintaining compatibility with observations forces us to keep $\delta \ll 1$ to maintain a near-hybrid inflation regime.

First, we study analytically a small breaking of the $\mathbb{Z}_2$ symmetry. We start by expanding the potential to linear order in $c_1\phi_1\delta$. The result is

$$V^{(\delta)} = V^{(0)} + c_1\phi_1\delta\,\frac{\Lambda^4}{2}\left(\sin_+ - \sin_-\right) + \mathcal{O}\left((c_1\phi_1\delta)^2\right) . \tag{3.42}$$

Here, $V^{(0)}$ denotes the hybrid potential of (3.32) and we introduced the shorthand notation $\sin_\pm \equiv \sin\left(c_1\phi_1 \pm c\phi_2\right)$. The higher-order terms in the potential are the ones arising from the series expansion at least quadratic in $c_1\phi_1\delta$, the even terms coming with factors of $\cos_\pm$. Hence, we see that choosing $\delta \neq 0$ breaks the $\mathbb{Z}_2$ vacuum degeneracy between the two vacua left and right of the inflationary valley with an amount of $\Delta V \sim (\pi\delta)^2\Lambda^4$, allowing us to avoid the domain wall problem. Repeating the same steps as for the phase ϑ, the effective potential for ϕ_2 in the $c_1\phi_1 = \pm\pi + \mathcal{O}(\delta)$ valley is, to leading order in δ, given by

$$V_{\text{inf}}^{(\delta)} = V_0\left(1 - \alpha\cos(c\phi_2) \mp \alpha\tilde{\delta}\sin(c\phi_2)\right) + \mathcal{O}(\pi^2\delta^2)\,, \tag{3.43}$$

where we defined $\tilde{\delta} \equiv \frac{\Lambda^4}{\Lambda^4+\tilde{\Lambda}^4}\frac{\pi\delta}{\alpha} = \frac{1-\alpha}{2}\frac{\pi\delta}{\alpha}$. Note that the phenomenology will be close to our hybrid inflationary toy model only if $|\pi\delta| \ll \alpha$. For larger $\alpha \lesssim |\pi\delta| \ll 1$ the inflationary trajectory might still be of the hybrid kind, in the sense that inflation happens along a straight line $c_1\phi_1 \approx \pm\pi$ and ends almost instantaneously at a critical value of ϕ_2. However, the potential is twisted and the saddle points are displaced along the ϕ_2 direction. This squeezes or stretches the effective potential and is the reason the phenomenology is substantially modified. We therefore trust the following analytical predictions only in the regime $|\tilde{\delta}| \ll 1$ and we will study larger deformations numerically. From the effective potential

we compute the slow-roll parameter

$$\varepsilon^{(\delta)} \approx \frac{1}{2}c^2\alpha^2\left(\sin(c\phi_2) \mp \tilde{\delta}\cos(c\phi_2)\right)^2 , \tag{3.44}$$

where we neglected corrections of order $\mathcal{O}(\alpha, \tilde{\delta}^2)$ *inside* the round brackets. Moreover, using the expression for $V^{(\delta)}$ we find that ϕ_1 becomes tachyonic at $c\phi_{2,c}^{(\delta)} = 2\pi n \pm \arctan\left(\frac{1}{\pi\delta}\right) \approx c\phi_{2,c}$, i.e. the waterfall transition point is approximately unchanged. Next, by integrating over the slow-roll parameter, we express ϕ_2 as a function of the e-folds. Two branches of solutions emerge

$$\phi_2^{(\delta)}(\Delta N) = \frac{2\arctan\left(e^{\gamma\Delta N}\right)}{c} \pm \frac{\tilde{\delta}}{c}\frac{\left(1-e^{\gamma\Delta N}\right)^2}{1+e^{2\gamma\Delta N}} , \tag{3.45}$$

where as before we defined $\gamma \equiv \alpha c^2$ and we discarded corrections that are of higher order in $\tilde{\delta}$. Moreover, we assume that we start inflation in the neighbourhood of the saddle point close to $c\phi_2 = \pi$ and move towards the critical point close to $c\phi_2 = \pi/2$. The alternative trajectories starting close to $c\phi_2 = -\pi$ moving towards $c\phi_2 = -\pi/2$ have equivalent phenomenology with these two solutions, but with the $\pm$ sign swapped. In light of the numerical analysis, we therefore cover all possible outcomes by solving for the inflationary solution that starts close to $c\phi_2 = c_1\phi_1 = \pi$ where δ takes both positive and negative values. Therefore, we take $\pm$ to be $+$ from here onwards. The first slow-roll parameter is then given by

$$\varepsilon^{(\delta)}(\Delta N) = 2\alpha\gamma\frac{e^{2\gamma\Delta N}\left(1-\tilde{\delta}+e^{2\gamma\Delta N}(1+\tilde{\delta})\right)^2}{\left(1+e^{2\gamma\Delta N}\right)^4} . \tag{3.46}$$

Moreover, the second slow-roll parameter is, to leading order in $\tilde{\delta}$, given by

$$\eta^{(\delta)}(\Delta N) = \gamma\frac{1-e^{2\gamma\Delta N}}{1+e^{2\gamma\Delta N}} + 4\gamma\tilde{\delta}\frac{e^{2\gamma\Delta N}}{\left(1+e^{2\gamma\Delta N}\right)^2} , \tag{3.47}$$

and, as before, provides the dominant contribution to n_s. In fig. 3.9a we plot the analytical predictions. Within the regime of validity of the analytical approximation, the predictions are very sensitive to the value of γ, and only mildly dependent on $\tilde{\delta}$.

Next, we study larger deformations numerically. In order to set appropriate initial conditions we have to identify the location of the saddle point,[8] which we numerically search for in the neighbourhood of $c_1\phi_1 = c\phi_2 = \pi$, given some δ. Even though the potential might get twisted substantially, it turns out we do not need much fine-tuning of the initial conditions. In fig. 3.10 we show an example of a deformed hybrid potential.

We solve for the background solution until the end of inflation using the transport code in [167] and evaluate the Hubble slow-roll parameters at 60 e-folds before the end of inflation to estimate the tensor-to-scalar ratio and the spectral tilt. The results are shown in fig. 3.9b. We confirm that the analytical results capture the predictions well if $\tilde{\delta} \ll 1$, and that in this regime the inflationary observables are only mildly dependent on $\tilde{\delta}$. However, for larger deformations both $\tilde{\delta}$ and γ become important to determine the observables. On the other hand, changing α only shifts the value of r up and down, and therefore the degeneracy between c and α remains within the current CMB limits. However, since we require $c \geq 1$ the observational constraints demand $\alpha \lesssim 0.02$ which translates into the upper bound $r \lesssim 0.01$. Interestingly, even though we are on the boundary of small field and large field inflation, the tensor-to-scalar ratio approaches $r \sim 0.01$ already for deformations $\delta = \mathcal{O}(0.01)$. If in addition we only

[8] For a discussion of finding critical points in a more general scalar potential that is a sum of cosines (and/or sines), but where the coefficients appearing in front of the fields are integers, see appendix A of [4]

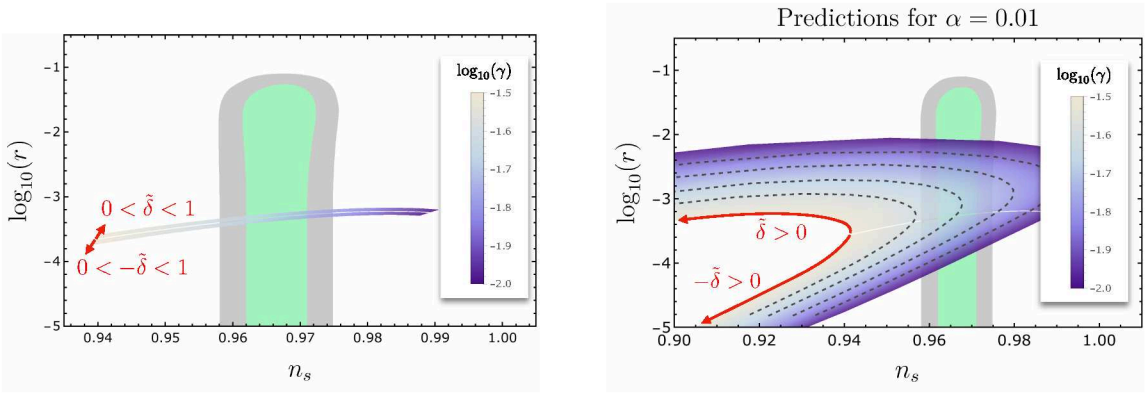

(a) (b)

Figure 3.9: Left: Same as fig. 3.6 but now we compare the *Planck* contours with the analytical predictions for $n_s^{(\delta)}$, $r^{(\delta)}$ and $\log_{10}(\gamma) \in [-2.0, -1.5]$, where we vary $\log_{10}(|\tilde{\delta}|) \in [-2.0, -1.0]$ while fixing $\alpha = 0.01$. The region $\tilde{\delta} > 0$ corresponds to inflationary trajectories with wide initial condition range of the type shown in fig. 3.10 ending up in the false minimum at $\phi_1 = 2\pi/c_1$, $\phi_2 = -\mathcal{O}(\tilde{\delta})$. The complement $\tilde{\delta} < 0$ corresponds to trajectories which in fig. 3.10 start with ϕ_2-values beyond the saddle point with little allowed initial condition space, and end up in the true minimum at $\phi_1 = \phi_2 = 0$.
Right: We compare the *Planck* contours with the numerical predictions for n_s and r computed through the Hubble slow-roll parameters, where we vary $\log_{10}(|\tilde{\delta}|) \in [-2.0, 1.0]$ and $\log_{10}(\gamma) \in [-2.0, -1.5]$, while fixing $\alpha = 0.01$. The black dotted lines correspond to fixed γ to $\{0.013, 0.017, 0.021, 0.025\}$, from right to left, respectively. The region $\tilde{\delta} > 0$ corresponds to inflationary trajectories with wide initial condition range of the type shown in fig. 3.10 ending up in the false minimum at $\phi_1 = 2\pi/c_1$, $\phi_2 = -\mathcal{O}(\tilde{\delta})$. The complement $\tilde{\delta} < 0$ corresponds to trajectories which in fig. 3.10 start with ϕ_2-values beyond the saddle point with little allowed initial condition space, and end up in the true minimum at $\phi_1 = \phi_2 = 0$.

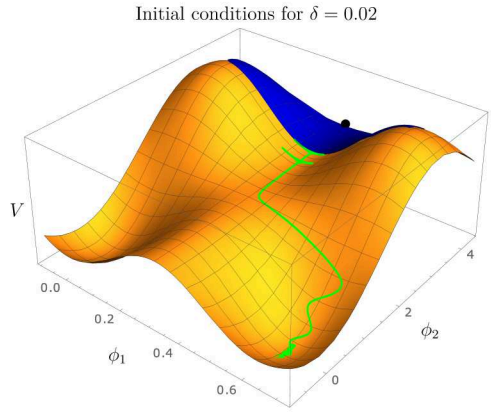

Figure 3.10: We illustrate the amount of fine-tuning of initial conditions in a deformed hybrid potential with $\delta = 0.02$, $\alpha = 0.01$, $\gamma = 0.011$ and $c_1 = 10$. In blue the patch of the potential around the saddle point (black dot) from which at least 60 e-folds of inflation will originate is shown. Moreover, in green two example trajectories of respectively 50 and 60 e-folds are shown. They are separated by $5 - 10\%$ of the total field range of ϕ_2 between the saddle point and the minimum of the potential.

require minimal tuning on the parameters the tensor-to-scalar ratio becomes bounded from below as well, $r \gtrsim 10^{-4}$. Maintaining compatibility with observations and at the same time $c \geq 1$ forces us to keep $\delta = \frac{2\alpha}{(1-\alpha)\pi}\tilde{\delta} \lesssim 3 \times \frac{2\alpha}{(1-\alpha)\pi}$, maintaining a near-hybrid inflation regime. This need to tune δ small represents a requirement for an embedding of the inflationary mechanism into string theory, as there the quantities $c_1^{\pm}$ and $c_2^{\pm}$ will be determined by discrete data of the string compactification such as intersection numbers and p-form flux quanta.

Let us now compare the results for the inclusions of the phases ϑ and $\tilde{\delta}$. By looking at eq.s (3.40)

and (3.44) we see that the phase ϑ coming from the instanton effects generating the potential and the asymmetry $\tilde{\delta}$ which is needed to break the $\mathbb{Z}_2$ vacuum degeneracy produce a similar correction to the first slow-roll parameter. Thus, by comparing the expressions for $\varepsilon^{(\vartheta)}$ and $\varepsilon^{(\delta)}$, we can extract a relation between these phases, which reads

$$\vartheta = -\frac{2\alpha}{1+\alpha}\tilde{\delta} \ . \tag{3.48}$$

The above relation was derived analytically and it holds only for $\vartheta \lesssim \alpha$. This means that in this regime ϑ and $\tilde{\delta}$ are degenerate. The predictions for the tensor-to-scalar ratio and the spectral tilt in the presence of ϑ in this regime (fig. 3.7 the small, central purple contour) and of $\tilde{\delta}$ (fig. 3.9a) are the same once the values of ϑ and $\tilde{\delta}$ are related by the factor of eq. (3.48) (notice also that in fig. 3.7 α is varied and $c = 1$ is fixed while in 3.9a α is fixed while $\gamma \equiv \alpha c^2$ is varied). For $\vartheta > \alpha$ we could not perform the same analytical comparison, thus we cannot prove the degeneracy for all values of our parameters. The complete contours were obtained with the slow-roll approximation in fig. 3.7 whereas for fig. 3.9b we solved the full equations of motion.

3.4.3 Comments about eternal inflation and vacuum decay

The inflationary valley of our harmonic hybrid model by necessity contains an inflationary saddle point with $\varepsilon = 0$, $|\eta| \ll 1$. We can now apply a comparison between the variance $\langle \delta\phi^2 \rangle_q = H^2/(4\pi^2)$ of quantum fluctuations of the light inflaton scalar in near-dS space-time and the classical slow-rolling speed $\dot{\phi} = -V'/(3H)$ to argue for the presence of eternal inflation [168–170] driven by quantum diffusion near the inflationary saddle point in our model. Arguments based on this comparison between quantum diffusion and classical rolling (as reviewed e.g. in [171,172]) show that the relevant criterion $\varepsilon \lesssim V/(12\pi^2)$, $|\eta| < 1$ when applied to exact hybrid inflation ($\delta = 0$), produces a region satisfying it around the saddle point, which is several hundred times wider than the average quantum fluctuation size $H/(2\pi)$. For the exact hybrid limit $\delta = 0$, our models thus supports slow-roll eternal inflation.

However, avoidance of domain walls dictates $\delta \neq 0$ and the scenarios for string theory realization of harmonic hybrid inflation we later discuss indicate that $|\delta| \gtrsim 0.01$. For such values of δ we observe that the region potentially supporting eternal inflation around the inflationary saddle point shrinks drastically. Its width reduces to a few times $H/(2\pi)$, rendering the existence of robust eternal inflation for these $\mathbb{Z}_2$-symmetry broken models doubtful. A much more detailed analysis is clearly necessary. If the outcome were the continued existence of this tension between model viability in the String Theory context and ability to support eternal inflation, this would suggest two possible interpretations: we may either use it as evidence against slow-roll eternal inflation, or conversely, as an opportunity to predict the most likely size of δ once a well-defined measure for eternal inflation is found.

In presence of the $\mathbb{Z}_2$-symmetry breaking, our setup contains a whole set of non-degenerate local minima with vacuum energy splitting of order $V_0\delta^2$, whose vacuum energy increases with increasing ϕ_1-distance from the set of global minima at $\phi_1 = 0$, $\phi_2 = 2\pi n/c$. Between the local minima of this mini-landscape there will be tunnelling instanton transitions described by Coleman and de Luccia (CdL) [173].

We next recall that the inflationary trajectories starting from wide initial conditions always end up in one of the two false minima at $\phi_1 = 2\pi/c_1$, $\phi_2 \simeq 0$ or $\phi_2 \simeq 2\pi/c$. As we expect these slow-roll trajectories due to their large region of initial condition space to dominate the inflationary slow-roll dynamics, we need to tune the vacuum energy of the false minima at ($\phi_1 = 2\pi/c_1$, $\phi_2 \simeq 0$ or $\phi_2 \simeq 2\pi/c$) to match the current-day vacuum energy $\sim 10^{-120} M_P^4$. The adjacent true minima ($\phi_1 = 0$, $\phi_2 = 2\pi n/c$) then are comparatively deep AdS vacua with vacuum energy of order $-V_0\delta^2$. Applying the CdL tunnelling description to these dS-AdS vacuum neighbours, we find that the so-called bounce

action of the CdL instanton scales as $B \sim 1/V_{\text{current c.c.}} \sim 10^{120}$. Hence, tunnelling out of the false post-inflationary minimum into the nearest global AdS minimum is highly suppressed, with a life-time $\tau = \Gamma^{-1} \sim e^B \sim 10^{10^{120}}$ similar to the dS Poincaré recurrence time.

3.4.4 Towards a String Theory embedding

Consider a type IIB string theory compactified to $4d$ on an orientifolded CY three-fold. We assume a choice of 3-form fluxes such that they stabilize the complex structure moduli at a high mass scale while generating an effectively constant superpotential W_0 [38]. As we reviewed in Section 2.1, in the 4d $\mathcal{N}=1$ low-energy theory, O3/O7 planes project the Kähler moduli space in even and odd subspaces with dimensions $h^{1,1}_+$ and $h^{1,1}_-$ respectively. This forces a rearrangement of the scalar degrees of freedom into $h^{1,1}_-$ axion multiplets coming from the 2-forms B_2 and C_2, and $h^{1,1}_+$ complexified Kähler moduli. When considering only the C_4 axions θ_i, the expression for T_i in (2.22) simplifies to

$$T_i = \frac{1}{2} k_{ijk} t^j t^k + i \int_{D_i} C_4 \equiv \tau_i + i\theta_i \,. \tag{3.49}$$

At the classical level and in the absence of branes, each θ_i enjoys a continuous shift symmetry. However, the presence of the O3/O7 orientifold planes induces D3- and D7-brane charges. In order to cancel their tadpole, we must include D3- and D7- branes in the compactification setup. Such branes will break the continuous shift symmetry of θ_i into a discrete one by inducing non-perturbative corrections to the superpotential. Harmonic hybrid inflation can then be obtained if we allow stacks of multiply-wrapped D7 branes on some of the 4-cycles. We will now discuss one mechanism to get the harmonic hybrid potential (3.32) from an LVS embedding.

We start by assuming the volume $\mathcal{V}$ of a CY three-fold to be large compared to l_s and to have the following Swiss-cheese like shape

$$\mathcal{V} \sim \alpha \tau_b^{3/2} - \beta \tau_s^{3/2} - \gamma \tau_{s_1}^{3/2} - \delta \tau_{s_2}^{3/2} \,, \tag{3.50}$$

where α, β, γ, δ are constants depending on the geometry of the manifold. For an explicit example of a CY with such volume, see e.g. [174]. Employing an LVS-type string compactification should allow us to use moduli stabilisation to obtain a mass hierarchy among the axions. This is necessary to reproduce the dynamics of hybrid inflation models in general. However, we consider two additional terms compared to the classic LVS Swiss-cheese volume because θ_b, the axionic partner of τ_b, is almost massless as it receives scalar potential contributions from T_b-dependent non-perturbative corrections which are highly suppressed by the compactification volume, i.e. $m_{\theta_b} \sim \exp(-\mathcal{V}^{2/3}) \sim 0$ [175]. Moreover, when one stabilizes τ_s, it can be shown that its axion θ_s gets stabilized as well, and in such a way that they gain approximately the same mass $m_{\theta_s} \sim m_{\tau_s} \sim m_{3/2}$. Therefore, θ_s is a rather heavy particle and it is frozen during inflation. We then infer that these two axions are not good candidates to reproduce our harmonic hybrid inflation. Thus, we should add two more blow-up moduli and arrange for their axions θ_{s_1}, θ_{s_2} to be ultralight but more massive than the axion corresponding to the base. The axionic mass hierarchy obtained from compactification should be $m_{\theta_b} \ll m_{\theta_{s_2}} < m_{\theta_{s_1}} \lll m_{\theta_s}$.

Then, we allow the tree-level superpotential W_0 to receive non-perturbative corrections W_{np} of the type

$$W = W_0 + A_s e^{-a_s T_s} + A_{s_2} e^{-a_{s_2} T_{s_2}} + A_{s_1} e^{-a_{s_1}\left(n^1_{s_1} T_{s_1} + n^2_{s_1} T_{s_2}\right)} + A_{s_2} e^{-a_{s_2}\left(n^1_{s_2} T_{s_1} + n^2_{s_2} T_{s_2}\right)} \,. \tag{3.51}$$

These corrections can be explained as follows. Consider 4 stacks of D7-branes. One stack wraps the 4-cycle associated to Kähler modulus T_s, and another one wraps the 4-cycle associated to T_{s_2}. These two stacks give rise to the usual non-perturbative corrections to the superpotential from gaugino condensation (i.e. the second line of eq. (3.51)). Then the other two stacks wrap two different cycles which are representative of two different divisor classes, each one being a linear combination of the divisor classes of T_{s_1} and T_{s_2}. Finally, we allow for the D7-branes of these last stacks to wrap the cycle multiple times [96]. This information is encoded in the winding numbers $n^j_{s_i}$ and their inclusion modifies the superpotential corrections as in (3.51).

Here we will anticipate the crucial point of this type of embedding: in order to recover the effective potential (3.32), we will need to require $n^2_{s_2} < 0$. From now on, the negative sign will be extracted. We might worry about this linear combination with negative coefficients, for the following reason: in order for the non-perturbative corrections to the superpotential to arise, the stacks of branes must wrap rigid and ample divisors [44,176]. It is natural to ask if $n^2_{s_2} < 0$ spoils the ampleness condition. We argue that this is not always the case. In fact, the divisors corresponding to the Kähler moduli in the exponents could be themselves linear combinations of toric divisors, and not just toric divisors. Therefore, we may be able to change base and re-write the exponents of eq. (3.51) in a way in which only toric divisors appear, and with positive coefficients. If this is the case, we may be able to satisfy the requirements of rigidity and ampleness. A concrete example of this can be found in [177].

Moduli stabilisation with the LVS mechanism forces

$$\partial_{T_s} W_{np} \sim \frac{W_0}{\mathcal{V}} \,. \tag{3.52}$$

To achieve scale separation between the axions θ_{s_1} and θ_{s_2} with respect to θ_s, we choose $a_{s_1}, a_{s_2}, \tau_{s_1}$ and τ_{s_2} such that

$$\partial_{T_{s_1}} W_{np} \sim \partial_{T_{s_2}} W_{np} \sim \varepsilon \, \frac{W_0}{\mathcal{V}} \,, \tag{3.53}$$

where $\varepsilon < 1$. If $\mathcal{V}^{-1} \ll \varepsilon \ll 1$, then axions get stabilised after the Kähler moduli. The dominant terms for the θ_{s_1}, θ_{s_2} axions are then the ones of order $\mathcal{O}\left(\varepsilon\, \mathcal{V}^{-3}\right)$. It can be shown that these are given by the $T_{s_i}\bar{T}_{s_j}(+\text{ h.c.})$, $i,j = 1,2$, terms in V_{np_2}, namely

$$V_{np_2}\left(\theta_{s_1}, \theta_{s_2}\right) = \frac{1}{\mathcal{V}^2}\left[K_0^{i\bar{j}} W_0 \partial_{T_{s_i}} W_{np} \partial_{\bar{T}_{s_j}} K_0 + h.c.\right] \,. \tag{3.54}$$

Plugging in this equation the derivatives of the superpotential with respect to $s_{1,2}$ and using the fact that $K_0^{i\bar{j}} K_i^0 = -\frac{1}{4}\tau_j$, the potential for the $\theta_{s_1}, \theta_{s_2}$ axions can be written as

$$\begin{aligned} V_{np_2}\left(\theta_{s_1}, \theta_{s_2}\right) = & \frac{2W_0}{\mathcal{V}^2} \tau_{s_2} a_{s_2} A_{s_2} e^{-a_{s_2}\tau_{s_2}} \cos\left(a_{s_2}\theta_{s_2}\right) \\ & + \frac{2W_0}{\mathcal{V}^2} a_{s_1} A_{s_1} \left(n^1_{s_1}\tau_{s_1} + n^2_{s_1}\tau_{s_2}\right) e^{-a_{s_1}\left(n^1_{s_1}\tau_{s_1} + n^2_{s_1}\tau_{s_2}\right)} \cos\left[a_{s_1}\left(n^1_{s_1}\theta_{s_1} + n^2_{s_1}\theta_{s_2}\right)\right] \\ & + \frac{2W_0}{\mathcal{V}^2} a_{s_2} A_{s_2} \left(n^1_{s_2}\tau_{s_1} - n^2_{s_2}\tau_{s_2}\right) e^{-a_{s_2}\left(n^1_{s_2}\tau_{s_1} - n^2_{s_2}\tau_{s_2}\right)} \cos\left[a_{s_2}\left(n^1_{s_2}\theta_{s_1} - n^2_{s_2}\theta_{s_2}\right)\right] \,. \end{aligned} \tag{3.55}$$

Our harmonic hybrid inflation potential of eq. (3.32) is recovered if we take $\theta_{s_i} = \phi_i / f_{s_i}$ as explained below, by setting

$$\tilde{\Lambda}^4 = \frac{2W_0}{\mathcal{V}^2} a_{s_2} \tau_{s_2} A_{s_2} e^{-a_{s_2}\tau_{s_2}} \,, \tag{3.56}$$

and by requiring the prefactors of the two mixed cosines to be equal.

Let us now discuss how to incorporate the $\mathbb{Z}_2$-symmetry breaking. For this, we need to keep in

mind that we need stacks of at least two coincident D7-branes for each instanton effect to generate a superpotential and in turn the scalar potential above. Hence, we have that $a_{s_i} = 2\pi/N_{s_i}$ with $N_{s_i} \geq 2$ in the cosine terms of the scalar potential. The effective coefficients of the two axion fields in the two cosine terms in the scalar potential thus read

$$\begin{aligned} c_1^+ &\equiv \frac{2\pi}{f_{s_1}} \frac{n^1_{s_1}}{N_{s_1}}, \qquad & c_1^- &\equiv \frac{2\pi}{f_{s_1}} \frac{n^1_{s_2}}{N_{s_2}}, \\ c_2^+ &\equiv \frac{2\pi}{f_{s_2}} \frac{n^2_{s_1}}{N_{s_1}}, \qquad & c_2^- &\equiv \frac{2\pi}{f_{s_2}} \frac{n^2_{s_2}}{N_{s_2}}, \end{aligned} \tag{3.57}$$

where for simplicity we assume that the string compactification has produced diagonal kinetic terms for the two axions of the form $\mathcal{L}_{kin} = \frac{1}{2} f_{s_1}^2 (\partial\theta_{s_1})^2 + \frac{1}{2} f_{s_2}^2 (\partial\theta_{s_2})^2$, implying canonically normalized axion fields $\theta_{s_i} = \phi_i / f_{s_i}$. Hence, maximizing the field range of the inflaton ϕ_2 and thus r while keeping $f_{s_2} \leq M_P$ sub-Planckian implies a relation between wrapping numbers and gauge group ranks: $n^2_{s_i} = N_{s_i}/2\pi$. The simplest choice achieving this would be $N_{s_1} = N_{s_2} = 6$ which produces $c_2^{\pm} \simeq 1$.

Next, maintaining inflationary dynamics behaving nearly like exact hybrid inflation requires a mass hierarchy between $m_{\phi_1} \gg H \gg m_{\phi_2}$ and a small amount of $\mathbb{Z}_2$-symmetry breaking by setting $c_1^{\pm} = c_1 \pm \delta_c$ with $\delta_c \ll c_1$ as in Section 3.4.2. The first condition requires $c_1^{\pm} \gtrsim 10$, implying $n^1_{s_i} \gtrsim 10\, n^2_{s_i}$. Since the $n^2_{s_i}$ are integers, their smallest difference $\delta_c = 1$ implies a 10%-level $\mathbb{Z}_2$-symmetry breaking. A level of 1% $\mathbb{Z}_2$-breaking is possible for the same δ_c for a choice of $N_{s_1} = N_{s_2} = 60$ and wrapping numbers $n^1_{s_1} = 100 + \delta_c$, $n^1_{s_2} = 100 - \delta_c$ and $n^1_{s_i} \approx 10\, n^2_{s_i}$, for $n^2_{s_i} = 10$, while maintaining the ϕ_2 field range and ϕ_1-ϕ_2 mass hierarchy.

We now discuss a second scenario for generating the potential (3.32). The C_2-axions present in CY orientifolds with $h^{1,1}_- > 0$ can acquire a periodic scalar potential if the relevant stack of D7-branes present in the compactification is magnetized [96]. Then, the gauge kinetic function is modified and depends holomorphically also on the $h^{1,1}_-$ axion multiplets G^a. In this way, the continuous shift symmetry of the odd axion c^a is broken to a discrete one at the level of the superpotential W when we consider also its non-perturbative corrections. The other axions θ_i can be stabilized at a higher scale than c^a by considering one additional unmagnetized stack wrapping another representative of the homology class. With this setup, gaugino condensation on different D7-branes stacks gives rise to the non-perturbative corrections of the form

$$W_{np} = \sum_{\zeta} A_\zeta e^{-a_\zeta \left(T_\zeta + i k_{\zeta mn} F^m_\zeta \left(G^n + \frac{\tau}{2} F^n_\zeta\right)\right)} . \tag{3.58}$$

Here, $k_{\zeta mn}$ are the triple intersection numbers between the divisors $\zeta = D_1 \dots D_3$, and the odd 2-cycles $\Sigma^{(-)}_{m/n}$, $m, n = 1, \dots, h^{1,1}_-$ and ζ runs over the wrapped divisors $D_1, \dots, D_{h^{1,1}_+}$, while $F^m_{D_i}$ are the fluxes each stack on the divisor D_i carries, but they also refer to only one (m) of the two C_2-axions each time.

In this setup, we shall consider $h^{1,1}_- = 2$ and $h^{1,1}_+ = 3$. As before, consider the complex structure moduli to be stabilized at a higher scale. Assume also that the τ_{D_i}, θ_{D_i} and b^m are stabilized by a combination of the LVS mechanism, string-loop corrections and/or higher order F-term contributions, D-terms and by unmagnetized D-branes, and that the $b^a = 0$ are at their minimum. Next, assume that both odd cycles $\Sigma^{(-)}_{1,2}$ intersect with the divisors corresponding to τ_{D_1} and τ_{D_2} while only $\Sigma^{(-)}_2$ intersects with the divisor corresponding to τ_{D_3}. These are conditions on the non-vanishing intersection numbers. They combine with the splitting of the intersection numbers indices k_{ABC}, $k = 1 \dots 5$ into the even indices $A = (\zeta, m)$ and the restructuring of the 2-cycle volume moduli into 4-cycle $\mathcal{N} = 1$ Kähler moduli containing 4-cycle volumes τ_ζ and the 2-form axion chiral multiplets G^m. If the inversion relation between the 2-cycles v^A and the (τ_ζ, G^m) can be performed explicitly, this may result in a

volume schematically of the form

$$\mathcal{V} \sim \left(\tau_{D_1} + k^{D_1}_{mn} b^m b^n\right)^{3/2} - \left(\tau_{D_2} + k^{D_2}_{mn} b^m b^n\right)^{3/2} - \left(\tau_{D_3} + k^{D_3}_{22} (b^2)^2\right)^{3/2} , \tag{3.59}$$

where $m, n = 1, 2$. In this case, the potential for the c^m axions takes the form

$$\begin{aligned} V &= \sum_{\zeta} \Lambda^4_{\zeta} \left[1 - \cos\left(a_\zeta k^{\zeta}_{mn} F^m_{\zeta} c^n\right)\right] \\ &= \Lambda^4_{D_1} \left[1 - \cos\left(\left(a_{D_1} k^{D_1}_{11} F^1_{D_1} + a_{D_1} k^{D_1}_{21} F^2_{D_1}\right) c^1 + \left(a_{D_1} k^{D_1}_{12} F^1_{D_1} + a_{D_1} k^{D_1}_{22} F^2_{D_1}\right) c^2\right)\right] \\ &\quad + \Lambda^4_{D_2} \left[1 - \cos\left(\left(a_{D_2} k^{D_2}_{11} F^1_{D_2} + a_{D_2} k^{D_2}_{21} F^2_{D_2}\right) c^1 + \left(a_{D_2} k^{D_2}_{12} F^1_{D_2} + a_{D_2} k^{D_2}_{22} F^2_{D_2}\right) c^2\right)\right] \\ &\quad + \Lambda^4_{D_3} \left[1 - \cos\left(a_{D_3} k^{D_3}_{22} F^2_{D_3} c^2\right)\right] . \end{aligned} \tag{3.60}$$

Next, the fact that the stacks of N_{D_i} D7-branes are wrapped on each divisor D_i producing the instanton contributions in W implies that $a_{D_i} = 2\pi/N_{D_i}$. The intersection numbers k^{ζ}_{mn} are fixed numerical quantities for a given CY manifold, while the fluxes $F^m_{D_i}$ are integers. Finally, canonically normalizing the axions c^m will replace c_1, c_2 with ϕ_1/f_1, ϕ_2/f_2, where f_1, f_2 represent the axion decay constants of the canonically normalized axion fields ϕ_1, ϕ_2. Hence, the resulting terms

$$\begin{aligned} \left(a_{D_1} k^{D_1}_{11} F^1_{D_1} + a_{D_1} k^{D_1}_{21} F^2_{D_1}\right) \frac{\phi_1}{f_1} &\equiv c_1^+ \phi_1 \\ \left(a_{D_2} k^{D_2}_{11} F^1_{D_2} + a_{D_2} k^{D_2}_{21} F^2_{D_2}\right) \frac{\phi_1}{f_1} &\equiv c_1^- \phi_1 \\ \left(a_{D_1} k^{D_1}_{12} F^1_{D_1} + a_{D_1} k^{D_1}_{22} F^2_{D_1}\right) \frac{\phi_2}{f_2} &\equiv c_2^+ \phi_2 \\ \left(a_{D_2} k^{D_2}_{12} F^1_{D_2} + a_{D_2} k^{D_2}_{22} F^2_{D_2}\right) \frac{\phi_2}{f_2} &\equiv c_2^- \phi_2 \end{aligned} \tag{3.61}$$

will typically have $c_1^+ \neq c_1^-$ and $c_2^+ \neq c_2^-$ (unless particular combinations of the $a_{D_{1,2}}$, the triple intersection numbers, and the gauge flux quanta appearing in (3.61) are chosen in very particular combinations). At most, they typically can be tuned by choosing the flux integers to be nearly the same to some finite accuracy, leading automatically to the situation of Section 3.4.2. Hence, embedding harmonic hybrid inflation into string theory along these lines *generically* avoids the hybrid inflation domain wall problem. Thus, by tuning appropriately the triple intersection numbers and the flux quanta, the potential in (3.41) can be recovered. The perks of using the C_2-axions instead of C_4-axions are that one has more freedom in tuning parameters to recast the needed potential, and that interestingly they are better for phenomenological purposes as well.

3.5 Winding inflation and de Sitter uplift

We would like now to go back to large field inflation and introduce a new and rather little studied class of models which goes under the name of winding inflation [178]. This time, the inflationary sector and dynamics arise from two complex structure moduli u, v of a CY orientifold compactification of type IIB. At the leading order, all other $h^{2,1}(X) - 2$ moduli are stabilized at their minimum by fluxes. The same happens for the imaginary parts of u and v as well as the real part of a particular linear combination of these two moduli, $\mathrm{Re}\,(Mu + Nv)$, with $N \gg M$ (M and N being integer flux numbers).[9]

[9] We are using a different convention with respect to the one in [178], instead we are using the convention of [66]. One can restore the convention of [178] setting $M = 1$, $N \to -N$ and $z \to 2\pi z$.

However, $\mathrm{Re}\,(u)$ is a flat direction in the superpotential, and it is lifted by the exponential terms coming from the small instanton corrections. This term induces a cosine potential for this field, which then displays the effective dynamics of a single slow-rolling axion-like field and realises natural inflation. Therefore, the field $\mathrm{Re}\,(u)$ is moving along a winding trajectory, whose length is parameterized by the linear combination $\mathrm{Re}\,(Mu + Nv)$.

Including also the non-perturbative corrections for the complex structure moduli sector, the Kähler potential for the complex structure moduli is (cf. (2.19))

$$\begin{aligned} K = -\ln\Bigg(& -\frac{4}{3}\kappa_{ijk}\mathrm{Im}\,(z^i)\mathrm{Im}\,(z^j)\mathrm{Im}\,(z^k) + ic \\ & - 2\sum_{\beta_1,\beta_2}^{\infty} n_{\beta_1,\beta_2}\left(\mathrm{Li}_3\left(e^{i\beta_i z^i}\right) + \mathrm{Li}_3\left(e^{-i\beta_i \overline{z}^i}\right)\right) \\ & -2\sum_{\beta_1,\beta_2}^{\infty} n_{\beta_1,\beta_2}\beta_i\mathrm{Im}\,(z^i)\left(\mathrm{Li}_2\left(e^{i\beta_i z^i}\right) + \mathrm{Li}_2\left(e^{-i\beta_i \overline{z}^i}\right)\right)\Bigg)\,. \end{aligned} \tag{3.62}$$

Here, κ_{ijk} are the triple intersection numbers of $\tilde{X}$, while $c = -\frac{i}{4\pi}\zeta(3)\chi(X)$, where $\chi(X)$ is the Euler characteristic of the compactification manifold X and $\mathrm{Li}_n(x)$ is the polylogarithm function. The quantities n_{β_1,β_2} in (3.62) are the genus 0 GV invariants, counting the number of holomorphic curves of genus 0 in a given homology class $[\beta] = [\beta_1, \beta_2]$ of $\tilde{X}$. Such quantities will play a prominent role in our proposal. For reviews see [31, 32].

A few comments about the above Kähler potential are in order. The $4d$ $\mathcal{N} = 1$ Kähler potential in (3.62) is obtained by a projection of the underlying $4d$ $\mathcal{N} = 2$ Kähler potential to the orientifold-even subsector. The underlying $\mathcal{N} = 2$ Kähler potential itself is obtained in a large complex structure (LCS) limit by mirror symmetry considering the instantonic quantum corrections. It is now important to note that the truncated Kähler potential in (3.62) is tree-level with respect to genuine $\mathcal{N} = 1$ quantum corrections. For a general $\mathcal{N} = 1$ orientifold background, such $\mathcal{N} = 1$ quantum corrections will mix Kähler and complex structure moduli space. Indeed, the factorization is only preserved at tree-level [34]. Once quantum corrections are taken into account, there are mixing terms that break the factorization. These string loop corrections to the tree-level Kähler potential K_0 are suppressed inverse powers of the volume of the compactification space (see for instance [46, 47, 179, 180]). Moreover, they possess a particular structure and scaling property which leads to Kähler potential corrections $\delta K \sim \mathcal{V}^{-p}$ appearing in the scalar potential as $\delta V \sim \mathcal{V}^{-2-2p}$ instead of the expected scaling $\sim \mathcal{V}^{-2-p}$. This automatic cancellation of the $\sim \mathcal{V}^{-2-p}$-terms in the scalar potential is called 'extended no-scale'. Next, the string loop corrections do depend in their coefficients on the complex structure moduli. These functions become large for parametrically large values of the moduli. However, the full loop correction coefficients are also suppressed by the usual $1/(16\pi^2)$ loop factors. Hence, as long as the dynamics of winding inflation is realized using stabilized values at *moderately* LCS (corresponding to $\langle \mathrm{Im}\,(z_i)\rangle \gtrsim \mathcal{O}(1)$), then the extended no-scale structure of the string loop corrections ensures that, already for quite moderate values of the stabilized volume $\mathcal{V}$, the induced scalar potential terms are subdominant to any parts of V induced from fluxes, non-perturbative corrections and/or α'-corrections used for moduli stabilization and the winding complex structure axion dynamics. Hence, provided these conditions are satisfied, we can neglect the string loop corrections which would spoil the factorization of the moduli space.

We can now introduce the usual GVW superpotential (2.26), which we write as

$$W = (N_F - SN_H)^T \cdot \Sigma \cdot \Pi \,, \tag{3.63}$$

where $N_F, N_H \in \mathbb{Z}$ are flux integers coming from the integration of F_3 and H_3 on a symplectic integral base of the 3-cycles of the orientifold CY, τ is the 10d axio-dilaton and

$$\Sigma = \begin{pmatrix} 0 & -\mathbb{1} \\ \mathbb{1} & 0 \end{pmatrix} . \tag{3.64}$$

Π is the period vector with entries (2.17)

$$\Pi = \begin{pmatrix} 1 \\ z^i \\ \frac{1}{2}\kappa_{ijk} z^j z^k + \frac{1}{2} a_{ij} z^j + b_i - \sum\limits_{\beta_1,\beta_2}^{\infty} n_{\beta_1,\beta_2} \beta_i \mathrm{Li}_2\left(e^{i\beta_i z^i}\right) \\ -\frac{1}{3!}\kappa_{ijk} z^i z^j z^k + b_i z^i + \frac{c}{2} + 2i \sum\limits_{\beta_1,\beta_2}^{\infty} n_{\beta_1,\beta_2} \mathrm{Li}_3\left(e^{i\beta_i z^i}\right) - \sum\limits_{\beta_1,\beta_2}^{\infty} n_{\beta_1,\beta_2} \beta_i z^i \mathrm{Li}_2\left(e^{i\beta_i z^i}\right) \end{pmatrix} . \tag{3.65}$$

Here a_{ij} are related to the triple intersection numbers, while b_i are related to the intersections of the second Chern class and the divisors of $\tilde{X}$.

The model proposed in [178] achieves a long winding trajectory by working in a regime of LCS for some complex structure moduli. By arranging the desired ratios of complex structure moduli VEVs via tuning 3-form fluxes, it is possible to generate controlled left-over flat quasi-axion directions in complex structure moduli space near the LCS point from the instanton contributions encoded by the GV invariants. Moreover, [178] shows that properly choosing the fluxes can generate flat axion valleys with a large path length on a small fundamental domain, which allows generating inflationary dynamics once the long flat valley is lifted by the GV-controlled instanton effects. Hence, in order for the winding trajectory to exist, the authors require that the F-term conditions stabilize u and v such that

$$e^{-\mathrm{Im}\,(u)} \ll e^{-\mathrm{Im}\,(v)} \ll 1 \,. \tag{3.66}$$

As another assumption, they choose appropriate flux integers so that u and v appear only linearly in the superpotential and include only the instantonic contribution coming from v. The authors proceed defining an expansion parameter $\varepsilon = e^{-\mathrm{Im}\,(v)}$, and expand the Kähler potential and the superpotential at leading order in ε. The point is that the F-term conditions stabilize in general all complex structure moduli and the axio-dilaton, but the presence of $\mathrm{Re}\,(Mu + Nv)$ in the superpotential breaks one of the two remaining shift symmetries of u and v. The shift symmetry parameterized by $\mathrm{Re}\,(u)$ (which does not appear neither in the Kähler potential nor in the superpotential) is a flat direction before introducing the corrections proportional to ε. Such corrections generate an oscillating potential, responsible for the inflationary period. We argue that there is another interesting way to realize this hierarchy, by exploiting some properties of the geometry of the extra dimensions. In the following, we develop this idea.

We consider a type IIB CY orientifold X with $h^{2,1}_{-}(X) = 2$ complex structure moduli $\{z^i\}$ and $h^{1,1}_{+}$ Kähler moduli. X has a mirror $\tilde{X}$ with $\tilde{h}^{1,1}_{+} = 2$. We assume further that the stabilization of the complex structure moduli, the axio-dilaton and the Kähler moduli proceed in hierarchical steps with the following characteristics

- We supplement the CY orientifold compactification with quantized 3-form fluxes [38]. These gen-

erate a scalar potential for the complex structure moduli and the axio-dilaton, stabilizing them at mass scales typically somewhat below the KK scale. At this level, the Kähler moduli remain a flat direction in a so-called $4d$ $\mathcal{N}=1$ no-scale compactification.

- Taking into account both perturbative and non-perturbative quantum corrections, we stabilize the Kähler moduli at a lower mass scale in either a supersymmetric (KKLT [51]) or supersymmetry breaking (LVS [52]) AdS vacuum. The stabilization of the Kähler moduli must proceed such, that large enough values for the 4-cycle volumes (the individual Kähler moduli) as well as the total CY volume are obtained to guarantee decoupling of the volume moduli stabilization from the flux stabilization of the complex structure moduli.
- A final step of controlled further supersymmetry breaking and uplifting (a positive contribution to vacuum energy) is needed to generate classical stable dS vacuum at the end (see e.g. [51]).

Our analysis will show that our model is expected to work in any string vacuum satisfying the above generic characteristics are met.

3.5.1 Inflationary sector

To begin with, in our setup we assume that the F-term conditions stabilize $z_1 = u$ and $z_2 = v$ in such a way that their imaginary parts are comparable, i.e. $\mathrm{Im}\,(u) \sim \mathrm{Im}\,(v)$. The hierarchy needed for a winding trajectory is then realized by considering

$$n_{1,0} e^{-\mathrm{Im}\,(u)} \ll n_{0,1} e^{-\mathrm{Im}\,(v)} \ll 1\,, \tag{3.67}$$

provided that the corresponding GV invariants $n_{0,1}$ and $n_{1,0}$ satisfy $n_{0,1} \gg n_{1,0}$. In order for this hierarchy to be not spoiled by higher instanton effects, we further need to require that

$$\mathrm{Im}\,(u) \sim \mathrm{Im}\,(v) \gg \ln \frac{n_{0,2}}{n_{0,1}}\,, \tag{3.68}$$

and

$$\mathrm{Im}\,(u) \gg \ln \frac{n_{1,1}}{n_{0,1}} \quad \text{and} \quad \mathrm{Im}\,(v) \gg \ln \frac{n_{1,1}}{n_{1,0}}\,. \tag{3.69}$$

If Eqs. (3.68) and (3.69) are satisfied, all other contributions coming from higher order GV invariants are suppressed by the exponential terms and we can disregard them. We now need to identify a small ε parameter to get the inflationary potential via a perturbative expansion, namely we define

$$\varepsilon = n_{0,1} e^{-\mathrm{Im}\,(v)}\,. \tag{3.70}$$

Eq. (3.70) gives another condition on the values that $\mathrm{Im}\,(v)$ (and $\mathrm{Im}\,(u)$) can assume, since we want $\varepsilon \ll 1$. Notice that requiring $\varepsilon \ll 1$ implies that $\mathrm{Im}\,(u)$ and $\mathrm{Im}\,(v)$ are stabilized at LCS. In general, this condition alone is sufficient to satisfy all previous ones.

It is then possible to proceed as in the original model. At leading order $\mathrm{Im}\,(u)$, $\mathrm{Im}\,(v)$, the axio-dilaton as well as the linear combination $\mathrm{Re}\,(Mu + Nv)$ are stabilized at the minimum. The only remaining flat direction is aligned with $\mathrm{Re}\,(u)$. It is convenient to reparameterise the fields as

$$\phi \equiv u \quad \text{and} \quad \psi \equiv Mu + Nv\,, \tag{3.71}$$

and we thus require $N > M$ to have one of the winding directions which is longer than the other. In

this way, the expansion parameter becomes

$$\varepsilon = n_{0,1} e^{-\mathrm{Im}\,(v)} = n_{0,1} e^{-\frac{\mathrm{Im}\,(\psi) - M\mathrm{Im}\,(\phi)}{N}}\,, \tag{3.72}$$

and

$$n_{0,1} e^{iv} = n_{0,1} e^{i\frac{\psi - M\phi}{N}} = \varepsilon\, e^{i\frac{\mathrm{Re}\,(\psi) - M\mathrm{Re}\,(\phi)}{N}}\,. \tag{3.73}$$

By choosing appropriately the fluxes and introducing the term $W_0(\tau)$ which includes all the fields already stabilized at leading order by the F-terms, we can write the superpotential as

$$W = W_0(\tau) + f(\tau)\psi + \varepsilon\, g_{0,1}(\tau, \psi, \mathrm{Im}\,\phi)\, e^{-i\frac{M\mathrm{Re}\,\phi}{N}} + \mathcal{O}(\varepsilon^2)\,, \tag{3.74}$$

where $g_{0,1}(\tau, \psi, \mathrm{Im}\,\phi)$ is a function of all stabilized fields. We can repeat the same discussion for the Kähler potential, obtaining

$$K = K_0(\tau, \psi, \mathrm{Im}\,(\phi)) + \varepsilon\, \tilde{g}_{0,1}(\tau, \psi, \mathrm{Im}\,(\phi))\, e^{-i\frac{M\mathrm{Re}\,\phi}{N}} + \mathcal{O}(\varepsilon^2)\,. \tag{3.75}$$

The scalar potential for the complex structure moduli and the axio-dilaton is given by

$$V = e^K K^{I\bar{J}} D_I W D_{\bar{J}} \overline{W}\,. \tag{3.76}$$

At zeroth order in ε, $D_I W = 0$ sets τ, ψ, $\mathrm{Im}\,(\phi)$ to their minimum and we are left with a flat direction parameterized by $\varphi = \mathrm{Re}\,(\phi)$. This flat direction is lifted by the first order corrections in ε to K_0 and W_0, which induce a shift in the VEVs of the other moduli. To see this, it is useful to write the structure of the F-terms as

$$D_I W = D_I|_0 W_0 + K_{0,I} \Delta W_{GV} + \Delta K_{GV,I} W_0 \equiv D_I W|_0 + \Delta D_I W|_{GV}\,. \tag{3.77}$$

Since on the supersymmetric flux vacua we have $D_i W|_0 = 0$, this entails that the scalar potential along φ is lifted by the GV corrections at $\mathcal{O}(\varepsilon^2)$, because the non-vanishing potential at the supersymmetry locus of all other fields is given by

$$V_{\mathrm{inf}} \sim e^{K_0} (K^0)^{I\bar{J}} \Delta D_I W|_{GV} \Delta D_{\bar{J}} \bar{W}|_{GV}\,. \tag{3.78}$$

To give an explicit expression for the effective inflationary axion-like potential in (3.78), in [178] the authors make an orthogonal transformation on (3.76) to diagonalize the Kähler metric. Hence, the potential, separated in real and imaginary parts of the moduli, takes the following form

$$V = e^{K_0} \sum_{\alpha=1}^{6} \tilde{w}_\alpha^2\,, \quad \text{where} \quad \tilde{w}_\alpha = \tilde{a}_\alpha + \varepsilon \left[\tilde{b}_\alpha \cos\left(\frac{M\varphi}{N}\right) + \tilde{c}_\alpha \sin\left(\frac{M\varphi}{N}\right) \right] \tag{3.79}$$

with $\tilde{a}_\alpha$, $\tilde{b}_\alpha$ and $\tilde{c}_\alpha$ being functions of all moduli. From the classical F-terms, $\tilde{a}_\alpha = 0$ for all values of α. However, considering the $\mathcal{O}(\varepsilon)$ corrections coming from the GV invariants, the VEVs of $\tilde{a}_\alpha$, $\tilde{b}_\alpha$ and $\tilde{c}_\alpha$ get shifted. Since eq. (3.79) is proportional to $\tilde{w}_\alpha^2$ and we are interested in a potential up to order $\mathcal{O}(\varepsilon^2)$, it is sufficient to consider order 1 corrections in ε only for $\tilde{a}_\alpha$, while keeping at leading order $\tilde{b}_\alpha$ and $\tilde{c}_\alpha$. A further rotation and a change of basis in the fields cancel all six terms but one combination,

which is the inflaton potential

$$V_{\rm inf}\left(\varphi\right) \sim e^{K_0}\kappa\,\varepsilon^2\left[\sin\left(\frac{M}{N}\varphi+\theta\right)\right]^2 \sim e^{K_0}\kappa\,\varepsilon^2\left[1-\cos\left(2\frac{M}{N}\varphi+2\theta\right)\right]\,, \tag{3.80}$$

where κ encodes numerical and τ-independent factors and θ is a phase.

We would like now to comment about the interplay among Kähler moduli stabilization and the complex structure axion winding potential. Stabilizing the Kähler moduli e.g. as prescribed in the KKLT or LVS scenarios leads to a mass hierarchy between the two class of moduli (which is more pronounced for the LVS) as well as a hierarchy between the terms of the flux scalar potential fixing the complex structure moduli at $\mathcal{O}\left(\mathcal{V}^{-2}\right)$ and the volume moduli scalar potential at $\mathcal{O}\left(|W_0|\mathcal{V}^{-2}\right)$ for KKLT, and $\mathcal{O}\left(\mathcal{V}^{-3}\right)$ for LVS (see the discussion in [52]). Next, the terms of the winding scalar potential are controlled by the GV invariants and the VEVs of the complex structure moduli. However, these VEVs were determined by the 3-form flux scalar potential and hence receive only suppressed corrections from the stress-energy sources driving Kähler moduli stabilization by virtue of the above hierarchies. We conclude that the Kähler moduli stabilizing part of the moduli scalar potential, which indeed does in general spoil factorization of the moduli space, will not affect the axion winding potential at leading order.

3.5.2 De Sitter uplift

Further investigations of this winding mechanisms showed that it is possible to use it also to construct a de Sitter uplift [66]. By tuning the flux quanta, the authors were able to generate an oscillating potential for the complex structure moduli, involving several cosines. This potential has a sequence of minima of increasing positive vacuum energy contribution, which are responsible for the controlled supersymmetry breaking. Choosing the parameters of this potential such that the difference between two adjacent minima is smaller than the depth of the scalar potential produced by the stabilization of the Kähler moduli, for instance, in LVS [52], it is possible to realize an uplift of either a KKLT-type or LVS-type AdS vacuum to a de Sitter vacuum. Here, we will focus only on LVS-type vacua and differently from [66], we will again exploit the relations among the GV invariants.

In order for the uplift to work, this time we have to require that

$$\varepsilon = n_{0,1}e^{-{\rm Im}\,(v)} \sim n_{1,0}e^{-{\rm Im}\,(u)}\,, \tag{3.81}$$

with a relative magnitude given by

$$\alpha \propto \frac{n_{1,0}}{n_{0,1}}e^{{\rm Im}\,(v)-{\rm Im}\,(u)} \sim \mathcal{O}(1)\,. \tag{3.82}$$

By performing a similar analysis as in the previous case and spelled out in details in [3], we get a potential with the form

$$V_{\rm dS}(\varphi) = e^{K_0}\kappa\,\varepsilon^2\left[\cos\left(\varphi+\theta_1\right)-\alpha\cos\left(\frac{P}{Q}\varphi+\theta_2\right)\right]^2\,. \tag{3.83}$$

Here, κ encodes numerical and τ-independent factors, $\theta_{1,2}$ are phases and α is the $\mathcal{O}(1)$ parameter introduced in (3.82).

By tuning the phases to zero, the potential has a stationary point at

$$\begin{aligned} V_{\rm dS}(0) &= e^{K_0}\kappa\,\varepsilon^2(1-\alpha)^2\,, \\ V''_{\rm dS}(0) &= 2e^{K_0}\kappa\,\varepsilon^2(1-\alpha)\left(\frac{P^2}{Q^2}\alpha-1\right)\,, \end{aligned} \tag{3.84}$$

which is a minimum for $Q^2/P^2 < \alpha < 1$, provided that $P/Q > 1$. The LVS AdS minimum is given in (2.38). We can consider the superposition of the LVS potential with (3.83) and tune the parameters to get a controlled supersymmetry breaking and an uplift from AdS to Minkowski or dS vacuum as

$$V(\mathcal{V},\varphi) = V_{\rm LVS}(\mathcal{V}) + \frac{g_s}{\mathcal{V}^2}\kappa\,\varepsilon^2\left[\cos\left(\varphi+\theta_1\right) - \alpha\cos\left(\frac{P}{Q}\varphi+\theta_2\right)\right]^2\,. \tag{3.85}$$

Finally, it is possible to scan the flux landscape and to tune α to make an uplift from the AdS vacuum to a dS one, imposing at the stationary point the relation for (3.83)

$$\kappa\,\varepsilon^2(1-\alpha)^2 = \mathcal{O}(1)\frac{|W_0|^2\sqrt{\ln\left(\mathcal{V}\right)}}{\mathcal{V}}\,. \tag{3.86}$$

Let us stress that this method provides a new way to uplift AdS vacua, which potentially avoid the problems affecting e.g. the most used anti-D-brane mechanism [62, 181] (see however [182] for a partial solution).

3.5.3 Combining inflation and uplift

Finally, we could check if it is possible to combine an inflationary sector with the uplift, both arising from similar winding effects. The idea is to generalize the examples presented before by considering a case with more complex structure moduli. To simplify the example, we choose a manifold X whose mirror is a CY with $\tilde{h}^{1,1} = 4$. Let us call the complex structure moduli u_1, v_1, u_2 and v_2. At the minimum, their imaginary parts, the axio-dilaton, $\mathrm{Re}\left(Mu_1 + Nv_1\right)$ and $\mathrm{Re}\left(Pu_2 + Qv_2\right)$ are stabilized, but $\mathrm{Re}\left(u_1\right)$ and $\mathrm{Re}\left(u_2\right)$ are flat directions when we do not consider the exponential terms. By tuning the fluxes, we can choose

$$\phi_1 = u_1\,, \quad \psi_1 = Mu_1 + Nv_1 \tag{3.87}$$

and define the expansion parameter

$$\varepsilon_1 = n_{0,1,0,0}e^{-\mathrm{Im}\left(v_1\right)} = n_{0,1,0,0}e^{-\frac{\mathrm{Im}\left(\psi_1\right)-M\mathrm{Im}\left(\phi_1\right)}{N}}\,. \tag{3.88}$$

Here, the hierarchy among the GV invariants must be

$$n_{1,0,0,0}e^{-\mathrm{Im}\left(u_1\right)} \ll n_{0,1,0,0}e^{-\mathrm{Im}\left(v_1\right)}\,. \tag{3.89}$$

Therefore, we can neglect the contributions coming from the instantonic corrections for u_1. The idea is once again to generate an inflationary potential provided that (3.88) is smaller than 1.

A similar discussion can be carried out for the other two moduli u_2 and v_2, by introducing

$$\phi_2 = u_2\,, \quad \psi_2 = Pu_2 + Qv_2 \tag{3.90}$$

and

$$\varepsilon_2 = n_{0,0,1,0} e^{-\mathrm{Im}\,(v_2)} = n_{0,0,1,0} e^{-\frac{\mathrm{Im}\,(\psi_2) - P\,\mathrm{Im}\,(\phi_2)}{Q}} \sim n_{0,0,0,1} e^{-\mathrm{Im}\,(u_2)} = n_{0,0,0,1} e^{-\mathrm{Im}\,(\phi_2)}\,. \tag{3.91}$$

This time, the instanton contributions coming from both the moduli u_2 and v_2 are comparable and must be both kept in the expansion. Such conditions can be obtained by tuning the expectation values and fluxes, but it is also possible to construct such hierarchy and the condition in (3.91) with the invariants.

Another condition that must be guaranteed is the one controlling the order in which inflation and uplift must happen. We ask that ε_1 controls the dynamics of the inflationary regime at an energy smaller than the one used for the uplift controlled by ε_2. Crucially, we should require that $\varepsilon_1 \ll \varepsilon_2$. Since we also want the two regimes to happen (almost) independently, we can assume that the effects of the two expansions are just a superposition of the single effects. The superpotential and the Kähler potential after these reparametrizations are

$$\begin{aligned} W =& W_0(\tau,\psi_1,\psi_2) + \varepsilon_1\, g_{0,1,0,0}(\tau,\psi_1,\mathrm{Im}\,\phi_1) e^{-i\frac{M}{N}\mathrm{Re}\,(\phi_1)} + \\ &+ \varepsilon_2 \left[g_{0,0,1,0}(\tau,\psi_2,\mathrm{Im}\,\phi_2) e^{-i\frac{P}{Q}\mathrm{Re}\,(\phi_2)} + h_{0,0,1,0}(\tau,\mathrm{Im}\,\phi_2) e^{i\mathrm{Re}\,(\phi_2)} \right] + \mathcal{O}(\varepsilon^2)\,, \\ K =& K_0(\tau,\psi_1,\psi_2,\mathrm{Im}\,\phi_1,\mathrm{Im}\,\phi_2) + \varepsilon_1\, \tilde{g}_{0,1,0,0}(\tau,\psi_1,\mathrm{Im}\,\phi_1) e^{-i\frac{M}{N}\mathrm{Re}\,(\phi_1)} + \\ &+ \varepsilon_2 \left[\tilde{g}_{0,0,1,0}(\tau,\psi_2,\mathrm{Im}\,\phi_2) e^{-i\frac{P}{Q}\mathrm{Re}\,(\phi_2)} + \tilde{h}_{0,0,1,0}(\tau,\mathrm{Im}\,\phi_2) e^{i\mathrm{Re}\,(\phi_2)} \right] + \mathcal{O}(\varepsilon^2)\,. \end{aligned} \tag{3.92}$$

In the previous equations we are neglecting all terms of order ε_1^2, ε_2^2 and $\varepsilon_1\varepsilon_2$. Let us spend some more words about this approximation. Suppose we want to realize the situation described in [66] and reviewed in our set-up in [3]. The potential is found after having integrated out the heavy complex structure moduli. Similar to the discussion above, the F-terms split as

$$\begin{aligned} D_I W &= D_I|_0 W_0 + K_{0,I} \Delta W_{GV}^{(\phi_1)} + \Delta K_{GV,I}^{(\phi_1)} W_0 + K_{0,I} \Delta W_{GV}^{(\phi_2)} + \Delta K_{GV,I}^{(\phi_2)} W_0 \\ &\equiv D_I W|_0 + \Delta D_I W|_{GV}^{(\phi_1)} + \Delta D_I W|_{GV}^{(\phi_2)}\,. \end{aligned} \tag{3.93}$$

Hence, the total scalar potential at $\mathcal{O}(\varepsilon^2)$ scales as

$$V_{\mathrm{tot}} \sim e^{K_0} (K^0)^{I\bar{J}} \left(\Delta D_I W|_{GV}^{(\phi_1)} + \Delta D_I W|_{GV}^{(\phi_2)} \right) \left(\Delta D_{\bar{J}} \overline{W}|_{GV}^{(\phi_1)} + \Delta D_{\bar{J}} \overline{W}|_{GV}^{(\phi_2)} \right)\,. \tag{3.94}$$

This scalar potential has three pieces

$$V_{\mathrm{tot}} \sim V_{\mathrm{inf}}^{\mathcal{O}(\varepsilon_1^2)} + V_{\mathrm{dS}}^{\mathcal{O}(\varepsilon_2^2)} + \sqrt{V_{\mathrm{inf}}} \sqrt{V_{\mathrm{dS}}} \Big|^{\mathcal{O}(\varepsilon_1\varepsilon_2)}\,, \tag{3.95}$$

where $V_{\mathrm{inf}}^{\mathcal{O}(\varepsilon_1^2)}$ and $V_{\mathrm{dS}}^{\mathcal{O}(\varepsilon_2^2)}$ read

$$V_{\mathrm{inf}}(\varphi_1) = e^{K_0} \kappa\, \varepsilon_1^2 \left[\sin\left(\frac{M}{N} \varphi_1 + \theta_1 \right) \right]^2\,, \tag{3.96}$$

$$V_{\mathrm{dS}}(\varphi_2) = e^{K_0} \kappa\, \varepsilon_2^2 \left[\cos\left(\varphi_2 + \theta_{2,1}\right) - \alpha_2 \cos\left(\frac{P}{Q} \varphi_2 + \theta_{2,2} \right) \right]^2\,, \tag{3.97}$$

and we have defined $\varphi_1 \equiv \mathrm{Re}\,(\phi_1)$ and $\varphi_2 \equiv \mathrm{Re}\,(\phi_2)$. It is easy to see from (3.95) that $\sqrt{V_{\mathrm{inf}}} \sqrt{V_{\mathrm{dS}}} \big|^{\mathcal{O}(\varepsilon_1\varepsilon_2)}$ has the same stationary points with respect to φ_2 of $V_{\mathrm{dS}}^{\mathcal{O}(\varepsilon_2^2)}$. The hierarchy $\varepsilon_1 \ll \varepsilon_2$ may thus enable us to stabilize into dS using $V_{\mathrm{dS}}^{\mathcal{O}(\varepsilon_2^2)}$ while having a slow-roll inflation valley given by the suppressed

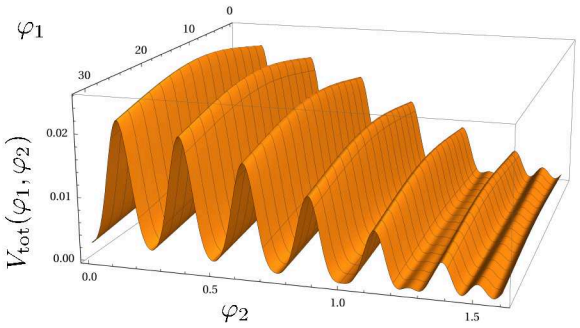

Figure 3.11: An example of the potential $V_{\rm tot}$ in (3.95). We use $M/N = 1/10$, $P/Q = 25$, all the phases set to zero, $\alpha_2 = 1$, $\varepsilon_1 = 0.02$, $\varepsilon_2 = 0.1$.

cross-term $\sqrt{V_{\rm inf}}\sqrt{V_{\rm dS}}\big|^{\mathcal{O}(\varepsilon_1\varepsilon_2)}$ modulated by the far stronger suppressed term $V_{\rm inf}^{\mathcal{O}(\varepsilon_1^2)}$.

Very interestingly, the effective inflaton potential is no longer of the pure natural inflation type. For instance, a Fourier decomposition of the effective scalar potential $V_{\rm eff}^{\rm valley}(\varphi_1)$ in a φ_1-valley defined by the condition $(\partial_{\varphi_2} V)(\varphi_1) = 0$ will generically have the form

$$V_{\rm eff}^{\rm valley}(\varphi_1) \sim \left[1 - \cos\left(2\frac{M}{N}\varphi_1 + 2\theta_1\right)\right] + \sum_{n\geq 2} c_n \cos(\omega_n \varphi_1)\,, \tag{3.98}$$

with rapidly decreasing c_n, frequencies ω_n being multiples of $2M/N$. Therefore, we expect the predictions for CMB observables like the spectral tilt n_s and the tensor-to-scalar ratio r to deviate from pure natural inflation. We leave an analysis of the ensuing phenomenology for future work.

A natural question one can ask when looking at fig. 3.11 is how likely it is for the two axions to undergo a tunneling transition between two local minima of the potential $V_{\rm tot}$. To avoid complications coming from considering a CdL tunneling [173] with two fields, we restricted ourselves to compute the probability for the field φ_2 to undergo tunneling, for a fixed value of φ_1. Indeed, we set φ_1 to the value where the largest probability of tunneling is expected, i.e. on the plane where eq. (3.95) has a local maximum for φ_1. This happens for $\varphi_1 = 5\pi + 10n\pi$, with $n \in \mathbb{Z}$. Looking at the sections of the potential at fixed φ_1 we can apply the well-known formulas for the decay probability for a single field [173]:

$$\Gamma = \exp(-B) \quad \text{with} \quad B = B_0\, r(x,y) \equiv \left(\frac{27\pi^2 T^4}{2(\Delta V)^3}\right) r(x,y)\,. \tag{3.99}$$

Here B is the bounce action and T is the tension of the domain wall. We have also defined the field theoretic bounce B_0 and its gravitational correction

$$r(x,y) = 2\frac{1 + xy - \sqrt{1+2xy+x^2}}{x^2(y^2-1)\sqrt{1+2xy+x^2}}\,, \tag{3.100}$$

with

$$x = \frac{3T^2}{4M_P^2 \Delta V}\,, \quad y = \frac{V_f + V_t}{\Delta V} \text{ and } \Delta V = V_f - V_t\,. \tag{3.101}$$

We have denoted the values of the potential in the false and true vacuum, respectively, with $V_f \equiv V_{\rm tot}(5\pi, \varphi_2 = \varphi_f)$ and $V_t \equiv V_{\rm tot}(5\pi, \varphi_2 = \varphi_t)$. In particular, we choose $\varphi_f \sim 0.25$ and $\varphi_t \sim 0.50$, for the plots shown in fig. 3.12. It is clear from those that the decay rate is highly suppressed for a value of $x \gtrsim 0.004$. An important comment is now due: so far, we have not canonically normalized the kinetic term for the φ_2 axion. By doing so, the canonically normalized field space distance between the true

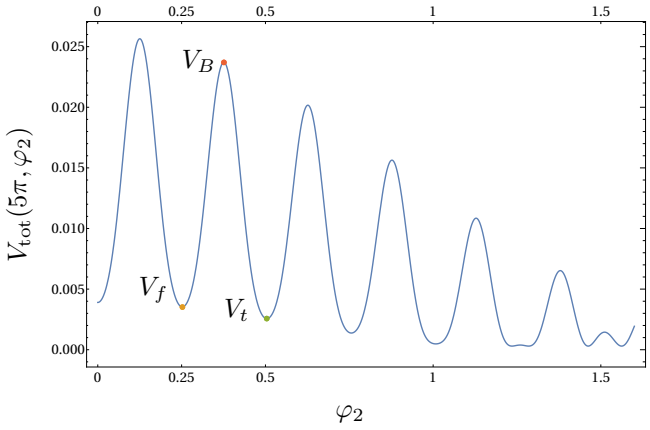

(a) We show the profile for the potential of Figure 3.11 at $\varphi_1 = 5\pi$. The orange and the green dots correspond to the values of the potential at the two local minima, respectively at $\varphi_2 \sim 0.25$ and $\varphi_2 \sim 0.50$. The red dot is the value of the potential at the local maximum, i.e. $\varphi_2 \sim 0.38$. This plot is given for $f = 1$.

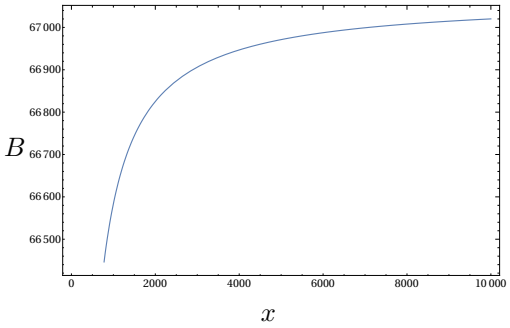

(b) B defined in (3.99) as a function of x.

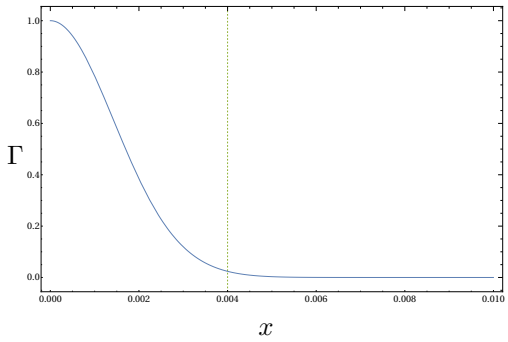

(c) Γ defined in (3.99) as a function of x.

Figure 3.12: In fig. 3.12a we show the potential at the fixed value of $\varphi_1 = 5\pi$. We notice that since $V_B - V_f \gg V_f - V_t$, the thin-wall approximation can be used to compute the domain wall tension T. From Figures 3.12b and 3.12c we can find a critical value of $x \sim 0.004$ for which the tunneling probability is enough suppressed.

vacuum φ_t and the false vacuum φ_f will depend on the axion decay constant f for the φ_2 field. We define then

$$\Delta\Phi = (\varphi_t - \varphi_f) f \sim 0.25 f \,. \tag{3.102}$$

We further call the difference of the potential between the red and green dots in Figure 3.12a as $\Delta V_B = V_B - V_f$, i.e. ΔV_B is the height of the barrier between the two minima. Since $\Delta V_B \gg \Delta V$, the thin-wall approximation is well justified in our context. In this approximation, the tension of the domain wall reads

$$T = \int_{\Phi_t}^{\Phi_f} \mathrm{d}\Phi \sqrt{2\left(V_{\rm tot}(5\pi,\Phi/f) - V_{\rm tot}(5\pi,\Phi_f/f)\right)} \sim \sqrt{2\Delta V_B}\,\Delta\Phi \sim 0.35 f \sqrt{\Delta V_B}\,. \tag{3.103}$$

From the definition of x in (3.101), we can find a parametric dependence between x and f, i.e.

$$x \sim \frac{f^2}{M_P^2}\frac{\Delta V}{V_t}\,. \tag{3.104}$$

In order for the tunneling probability to be sufficiently suppressed, we require B to be larger than an order $\mathcal{O}(100)$ number.

In a full model with moduli stabilization consistent with an inflationary sector producing the right

CMB-scale curvature perturbation, the typical scale of moduli and inflationary scalar potential will be fixed for large-field models where the slow-roll parameter is $\varepsilon \sim 0.01$ to be $\left|V_{\text{eff}}^{\text{valley}}\right| \sim 10^{-10}$. Rescaling the scalar potential in fig. 3.12a to these values and reevaluating the bounce action, we get

$$B \sim 10^2 \left(\frac{f}{M_P}\right)^2 \frac{1}{V_t}\,. \tag{3.105}$$

The longevity requirement $B \gtrsim 100$ thus translates in a lower bound on f, given by

$$\frac{f}{M_P} \gtrsim \sqrt{V_t} \gtrsim 10^{-5}\,. \tag{3.106}$$

Hence, guaranteeing sufficient longevity of a given inflationary valley places a lower bound on the axion decay constant of the axion direction responsible for generating the valley structure of $f \gtrsim 10^{-5} M_P$.

To sum up, we have shown that the combined sector providing a mechanism for both inflation and uplifting works along the same lines as the individual mechanisms discussed in the previous sections. It is an interesting task for the future to apply this setup to an explicit model.

3.6 Discussion

Postulating an early epoch of accelerated expansion called inflation solves many conceptual problems originating from e.g. the observation of the CMB and its anisotropies. However, so far we have no proof for the presence of such early dynamics. Nevertheless, since theoretically inflation appears to be a solid proposal, it is worth exploring which models could be the right ones in explaining the accelerated expansion while producing all the cosmological features we observe in the sky. In fact, it is possible to connect the theory with experiments via a number of observable quantities; this gives a beautiful way to test the inflationary proposal as well as the properties of a theory of Quantum Gravity such as String Theory.

In this chapter, we have discussed how inflation and String Theory are tightly related, and how one can benefit from the other. In particular, String Theory predicts the existence of axion fields, which are excellent inflatons candidates. The leading proposals for axions inflation are axion alignment and axion monodromy, which we reviewed with their pros and cons. For axion monodromy inflation, we supplied the discussion with new bounds on the observables quantities coming from weak gravity arguments on the infrared theory of string axions.

In addition, we have presented two new models of axion inflation. *Harmonic hybrid inflation* is a mechanism for realizing hybrid inflation using two axion fields with a purely non-perturbatively generated scalar potential. We analysed the influence of initial condition choices on the occurrence of successful inflation, showing that this model generates observationally viable slow-roll inflation for a wide range of initial conditions. The structure of the scalar potential is highly constrained by the discrete shift symmetries of the axions.

We showed that it generates observationally viable slow-roll inflation for a wide range of initial conditions. This is possible while accommodating certain Swampland conjectures, namely $f \lesssim M_P$ and $\Delta\phi_{60} \lesssim M_P$ on the axion periodicity and slow-roll field range, respectively. Moreover, the cosine form of the scalar potential in our model leads to a limited violation of the Lyth bound, as already noticed [183] in models of hybrid natural inflation involving a single axion [184]. We saw that harmonic hybrid inflation is capable of producing a tensor to scalar ratio $r \sim 10^{-4}$. We also note the recent model of hybrid monodromy inflation [185] which rather complementarily employs axion monodromy [143]

from massive 4-forms [147, 186] to realize the mechanism of 'mutated hybrid inflation' [187]. Moreover, it was recently pointed out how hybrid inflation could avoid overproduction of dark radiation while providing a setup where the inflationary sector is not sequestered and the construction support the presence of a viable QCD axion [188].

Then, we discussed controlled $\mathbb{Z}_2$-symmetry breaking of the adjacent axion vacua as a means of avoiding cosmological domain wall problems. Including a minimal form of $\mathbb{Z}_2$-symmetry breaking into the minimally tuned setup leads to a prediction of primordial tensor modes with the tensor-to-scalar ratio in the range $10^{-4} \lesssim r \lesssim 0.01$, directly accessible to upcoming CMB observations. Moreover, we found that the presence of an inflationary saddle point produces a regime of quantum diffusion driven slow-roll eternal inflation as long as the $\mathbb{Z}_2$-symmetry breaking parameter is small enough. As a finite amount of symmetry breaking is necessary to avoid the domain wall problem, this may indicate that harmonic hybrid inflation shrinks the field space region available for eternal inflation and might conceivably even favour its absence.

Finally, we outlined several avenues towards realizing harmonic hybrid inflation in type IIB String Theory, which are thus testable with upcoming observations. We provide arguments that the relevant scalar potential can arise either from C_4 axions via multiple-wrapped D7-brane stacks or from C_2-axions acquiring a scalar potential from D7-brane stacks magnetized by quantized gauge flux. Let us note that the fine-tuning of initial conditions needed to generate enough inflation quickly increases once we choose the larger of the two axion decay constants to be sub-Planckian by a significant amount. As this implies rather $f_{\text{inflaton}} \lesssim M_P$ instead of $f_{\text{inflaton}} \ll M_P$, a concrete realization of our mechanism needs to check if higher instanton harmonics with instanton actions of e.g. gravitational instantons generically scaling as $S_{\text{inst}} \sim nM_P/f_{\text{inflaton}}$ remain sufficiently suppressed (see e.g. [20, 147, 189]). We leave a more detailed analysis, clearly dependent on UV input, for future more complete string theory realizations.

The other inflationary model we have presented is a large-field model provided by the phases of the complex structure moduli. In particular, we have showed that it is possible to realize winding inflation [178] (and winding de Sitter uplift [66]) by a hierarchy of the GV invariants of the underlying CY threefold along tuning the VEVs of the complex structure moduli as in the original proposal.[10] The non-perturbative quantum corrections encoded by the invariants can provide a controlled lifting of flat directions left over in the complex structure moduli space by properly choosing fluxes in type IIB String Theory CY orientifold flux compactifications. In particular, we can use CYs with a built-in hierarchy of the lowest-degree GV invariants to collaborate with the tuning of moduli VEV hierarchies in controlling the instanton contributions to the scalar potential, and in some cases remove the need to tune the VEVs at all. This provides explicit examples for the mechanism outlined in [66, 178] to generate both dS vacua and natural-inflation-like slow-roll inflation with the complex structure moduli sector from fluxes and GV-invariant controlled quantum corrections alone.

However, for the inflationary model, we found that our setup still satisfies the no-go theorem for aligned winding trajectories with two moduli proposed in [191]. The issues found in [191] for obtaining a super-Planckian decay constant are still present in our construction, even if we can avoid a hierarchy among the VEVs of the moduli.

In addition to the inflationary model, we presented a mechanism involving a sector of four moduli which can realize both supersymmetry-breaking vacua and positive vacuum energy contribution and (in absence of the no-go theorem) large-field inflation. Upon combination with a proper CY realizing full moduli stabilization in an AdS vacuum, this may lead to the construction of dS vacua with an

[10] To show that CY threefolds with the prescribed hierarchy actually exist, we created a database of genus 0 GV invariants up to total degree 10 for the CICYs up to Picard number 9, based on the use of `INSTANTON` [190]. The database can be found at the following link.

inflationary sector in type IIB string theory. While the no-go theorem still presents obstacles for this type of setup, which relies on two out of four axions to arrange for inflation, we use the relative simplicity of this setup to show that the dS vacuum sector operates rather decoupled from the inflaton sector. This in turn makes it plausible that extending the inflaton sector to more axions to avoid the no-go theorem can still co-exist with the dS sector. We leave for future research the task of working out a full model along these lines. Finally, we estimated the life-time of the inflationary valleys in our combined mechanism due to CdL tunneling to neighbouring valleys. Interestingly, guaranteeing sufficient longevity of a given inflationary valley places a lower bound on the axion decay constant of the axion direction responsible for generating the valley structure of $f \gtrsim 10^{-5} M_P$.

Chapter 4

Fuzzy Dark Matter from String Axions

Walking forwards with no sight
'Cause the rhythm leaves you blind
Walking forwards with no sight
Yeah it's dark as night.

— Blood Red Shoes, *Colours Fade*

String Theory has been claimed to give rise to natural fuzzy dark matter (FDM) candidates in the form of ultralight axions. In this chapter, we revisit this claim by a detailed study of how moduli stabilisation reviewed in Section 2.1.3 affects the masses and decay constants of different axion fields which arise in type IIB flux compactifications. We find that obtaining a considerable contribution to the observed dark matter abundance without tuning the axion initial misalignment angle is not a generic feature of $4d$ string models since it requires a mild violation of the WGC bound. Our analysis singles out C_4-axions, C_2-axions and thraxions as the best candidates to realise FDM in String Theory. For all these ultralight axions we provide predictions which can be confronted with present and forthcoming observations. Before turning to the details of these results, we review the problem of the missing mass in the universe and how dark matter could solve it. Then we give an overview of the different types of DM candidates and finally explain why FDM is an intriguing proposal both for phenomenology but also to relate String Theory with observations.

4.1 Basics of dark matter

Let us start by considering the first Friedmann equation (3.2). The value of k can be determined experimentally by measuring the parameter Ω, defined as the ratio of the energy density of our universe $\rho(t)$ and the critical density $\rho_{\rm crit}\,(t)$,

$$\Omega\,(t) \equiv \frac{\rho\,(t)}{\rho_{\rm crit}\,(t)}\,, \quad \text{where} \quad \rho_{\rm crit}\,(t) \equiv 3H^2\,. \tag{4.1}$$

Hence, Ω measures the energy density in units of H^2 and is therefore called the *density parameter*. With this definition, the first Friedmann equation (3.2) can be rewritten as

$$\Omega - 1 \equiv \frac{k}{a^2 H^2} \equiv \frac{k}{\dot{a}}\,, \tag{4.2}$$

from which we see that a flat universe ($k = 0$) corresponds to $\Omega = 1$, whereas an open ($k = -1$) and closed ($k = 1$) universe lead to $\Omega < 1$ and $\Omega > 1$ respectively. Therefore, we can understand the geometry of our universe also by comparing $\rho(t_0)$ with $\rho_{\rm crit}\,(t_0)$, where t_0 corresponds to the present time. In the case of multiple contributions to the energy density of the universe, we will have $\Omega = \sum_i \Omega_i$. We have seen in Section 3.1 that we can treat our universe as a perfect fluid. In particular, we can divide it into four components:

- non-relativistic (pressure-less) matter which dilutes with the volume growth of the spatial slices as $\rho_m = \rho_m(t_0)a^{-3}$
- relativistic matter and radiation which are red-shifted and therefore their energy densities decrease more rapidly, i.e. $\rho_r = \rho_r(t_0)a^{-4}$
- the spatial curvature in (4.2) also plays a role and its energy density dilutes as $\rho_k = \rho_k(t_0)a^{-2}$
- the cosmological constant Λ with energy and pressure related as $\rho_\Lambda = -p_\Lambda$, which are constant over time.

We can now write the second Friedmann equation (3.2) as

$$\left(\frac{H}{H(t_0)}\right)^2 = \Omega_r a^{-4} + \Omega_m a^{-3} + \Omega_k a^{-2} + \Omega_\Lambda\,. \tag{4.3}$$

Evaluating this equation today implies that $\sum_i \Omega_i + \Omega_k = 1$. Most importantly, observations of the CMB and the large-scale structure found that the universe is flat, with $\Omega_k < 0.2\%$, and composed of [192]

$$\Omega_m \simeq 0.31\,, \quad \Omega_\Lambda \simeq 0.68\,. \tag{4.4}$$

However it turns out that the visible matter (*baryonic* matter) constitute only the 5% of the content of the universe!

In 1933, the astronomer Fritz Zwicky first noted that a certain amount of matter was 'missing'. He published a pioneering paper where he studied the mass of the Coma cluster, finding that the velocity dispersion of galaxies was so high that, to keep the system stable, the average mass density of the cluster had to be much higher than the one deduced from the baryonic matter. He first proposed the existence of unseen, *dark matter*. In the following decades, many more clusters were found to have the same mass discrepancy, but the proposals to solve this issue were many. In 1970, in their study of rotation curves of the Andromeda nebula, Vera Rubin and Kent Ford showed that the mass profile as computed from both the distribution of stars in the galactic spiral and the mass-to-light ratio in the stellar disk, did not match with the masses derived from the observed rotation curves [193]. From Kepler's Laws, the rotation velocities were expected to decrease with the distance from the galactic centre. Instead, rotation curves remained flat as the galactic radius increased: the galaxy had much more mass than the visible one, and this mass was gravitationally interacting. It was not until 1974, when James Peebles, Jeremiah Ostriker and Amos Yahil, in their search for the mass density of the universe Ω, synthesized for the first time the two problems of galaxies and clusters into a single issue, stating that they were both due to a lack of

mass in the universe [194]. In particular, they found that the galactic masses had been underestimated by a factor of 10 or more. However, despite long model building efforts, the origin and nature of dark matter remains one of the biggest puzzles in Physics and Astronomy.

Today, we know experimentally that the dark matter (DM) contribution to the total mass of the universe is way more significant than that of baryonic matter. In the years, many proposals of possible DM candidates were put forward, however so far we have been able only to rule some out. We can divide the candidates into three major groups on the basis of their physical features:

- baryonic and non-baryonic DM. By baryonic DM we refer to objects that are made of known constituents, such as Standard Model particles and the ordinary matter in general, but that are not visible either because their light is too faint or because their presence can only be inferred indirectly. On the contrary, non-baryonic DM is made of brand-new particles from completions of the Standard Model, and their interaction with photons is so weak that they are not visible.

- thermal and non-thermal DM: based on the way DM constituents are produced. If a DM particle is in thermal equilibrium with the other components of the universe and suddenly it decouples, then this particle is said to be produced thermally. Instead, a non-thermal particle is produced via a dynamical mechanism, in such a way that it may not be in thermal equilibrium with the universe at the moment of its production.

- hot and cold DM: this distinction depends on the velocity the particles have when they decouple from the primordial plasma. A particle species is said to be hot DM (HDM) if the velocity dispersion of these particles is relativistic. Instead, cold DM (CDM) is made of particles having a very slow velocity dispersion compared to the speed of light. Usually, in the term CDM also non-thermal DM is included.

The distinction between hot and cold is of extreme importance because HDM and CDM decouple from radiation before ordinary matter, and in turn they give rise to two different scenarios of structure formation in the early universe. In particular, the CMB showed that at high redshift the fist primordial structures to appear are the smallest ones, which subsequently converge and form bigger structures. This depends on the value of the Jeans mass[1] of the DM present during the epoch of structure formation. It turns out that this scenario of structure formation is actually possible only in a CDM background, where also small matter fluctuations can grow. Therefore, HDM has long been ruled out from being a possible DM candidate, and the Standard Model of cosmology is also called ΛCDM from its main constituents, CDM and the dark energy Λ.

In CDM models, dark matter is made out of weakly interacting non-relativistic particles with a small initial velocity dispersion relation inherited from interactions in the early universe that do not erase structures on galactic and sub-galactic scales. Despite its success in explaining the large scale structure of the universe, ΛCDM was believed to suffer from some problems related to galaxy formation [195] that may be actually explained with unaccounted baryonic feedback mechanisms or to new exotic dark matter physics on small scales [196–200] but a final and exhaustive solution is still lacking. Regardless of the veracity of small-scale problems, Weakly Interacting Massive Particles (WIMPs) having mass $\sim \mathcal{O}(100)$ GeV that were considered the most promising CDM candidates have continuously eluded whatever kind of experimental measurement as collider searches and direct/indirect detection experiments.

[1] The Jeans mass is a reference mass indicating whether a perturbation of matter can grow (if its mass is bigger than the Jeans mass of the DM) or must fade away (if on the contrary its mass is smaller than the Jeans mass of the DM). the Jeans mass scales with the cube of the free-streaming velocity, so that for HDM it is $\sim \mathcal{O}(10)$ bigger than for CDM.

These concerns about ΛCDM and WIMPs led to the study of alternative DM models. Among those, in recent years the idea of bosonic ultralight CDM, also called Fuzzy Dark Matter (FDM), has been proposed [101,102,201,202]. In one of its prominent versions, DM is made of ultralight axion-like particles that form halos as Bose-Einstein condensates. In this theory, each axionic particle can develop structures on the scale of de Broglie wavelength thanks to gravitational interactions. This is an ensemble effect given by the mean properties of every single axion field. A prominent soliton, i.e. a state where self-gravity is balanced by the effective pressure arising from the uncertainty principle, develops at the centre of every bound halo. The soliton properties depend on the axion mass, but usually its extension is assumed to be much smaller than the galaxy or galaxy cluster size. In the original proposal, an axion having mass around 10^{-22} eV and decay constant $f \sim 10^{16\div17}$ GeV was pointed out as the best candidate to represent the dominant part of CDM in the universe since the wave nature of such a particle can suppress kiloparsec-scale cusps in DM halos and reduce the abundance of low mass halos [102,201,203].

Recent studies put severe constraints on the vanilla FDM model without self-interactions, where the usual cosine axionic potential is approximated as $1-\cos(\phi/f) \sim \phi^2/2f^2$. Various analyses of Lyman-α forest, satellite galaxies formation, dwarf galaxies, the Milky Way core and Black Hole superradiance [204–211] leave as the only viable mass windows $m_\phi \sim 10^{-24}$ eV and $m_\phi \sim 10^{-15}$ eV, although certain of these bounds could be relaxed and open a window near 10^{-21} eV also. These experimental bounds imply that FDM cannot solve the alleged small-scale problems affecting ΛCDM, as the Jeans mass (representing the lower bound on DM halos mass production) rapidly decreases at increasing ultralight boson masses [209]. Nevertheless, even in this case, these problems can be solved by baryonic physics and a better understanding of galaxy formations may allow us to discriminate between standard CDM and FDM models. Indeed, it was proven that small-mass halos suppression in the FDM model causes a delay in the onset of Cosmic Dawn and the Epoch of Reionization. Future experiments, such as the HERA survey, will measure the neutral hydrogen (HI) 21 cm line power spectrum at high statistical significance across a broad range of redshifts [206, 209] and their findings may be able to discriminate between standard WIMP and FDM scenarios. Since experimental bounds and simulations strongly constrain the original FDM model with negligible self-interaction, many extensions of it have been studied. It was shown that for large initial misalignment angles, ALPs self-interactions can affect the baryonic structure and accelerate star formation in the early universe or induce oscillon formation that can give rise to detectable low frequency stochastic gravitational waves [212]. Other authors suggest that FDM may not represent the entirety of DM [213] or that FDM may not be given by a single component, being made out of multiple ultralight ALPs [214].

The almost-Planckian decay constant together with the possible multiple axionic nature of FDM have been claimed to be a possible sign in favour of the string *axiverse* [102, 215], where a plenitude of axion-like particles (ALPs) naturally emerge from 4D effective theories. However, in this chapter, we point out that obtaining a FDM axion with the correct mass and decay constant is not automatic in String Theory. Indeed, even if one would naively think that ultralight axions generically emerge from String Theory equipped with naturally high decay constants, reproducing the right relic abundance turns out to be hard and provides sharp predictions for fundamental microscopical parameters. We carry out a detailed analysis, studying the general features of closed and open string ALPs coming from type IIB string theory. Focusing on simple extra-dimensions geometries and using the most common moduli stabilisation prescriptions, for each class of ALPs we provide in what follows general predictions for the expected mass, decay constant and dark matter abundance. We discuss the settings of the microscopical parameters that lead to ultralight axions representing non-negligible fractions of DM, and we estimate how these requirements put stringent predictions for the relevant energy scales of the 4D effective field

theory, such as the KK scale, the gravitino mass and the scale of inflation. Finally, we compare our predictions for FDM ALPs with current observational constraints, and we highlight which stringy FDM candidates occupy a region of the parameter space that will be probed by next generation experiments.

Let us point out that we will only consider the simplest setups, thus neglecting the effects that may arise from considering numerous axionic fields. Indeed, we assume that the axionic potential does not create local minima, and that there are no turns in the field dynamics when they start to oscillate at times when $m \sim H$. We also neglect the possibility of having axion alignment, as this is not the most common situation and its implementation often involves a considerable amount of tuning. Despite our simple assumptions, we believe the results presented below remain true also for more general extradimensional geometries. Indeed, we find that among closed string axions only those related to large cycles can be good FDM candidates. Although it is not possible to write the most generic volume of a CY, the number of moduli entering the volume with a positive sign must be finite.

4.2 String origin of ultralight axionic DM candidates

Since the number of ALPs is related to the number of moduli, which can easily reach the value of several hundreds, we can have many ultralight axion candidates which create the so called axiverse [18]. On the other hand, it is essential to note that, although string compactifications carry plenty of candidates for axion and axion-like weakly interacting particles, there are several known mechanisms by which they can be removed from the low energy spectrum. The low energy spectrum below the compactification scale generically contains many axion-like particles which arise either as closed string axions, which are the KK zero modes of $10d$ antisymmetric tensor fields, or as the phase of open string modes. While the number of closed string axions is related to the topology of the internal manifold, the number of open string axions is more model dependent since their existence relies upon the brane setup. We will briefly describe the main properties of both closed and open string axions, trying to understand what conditions are required in order to reproduce viable FDM particles. In particular, we dedicated Section 2.2 on closed string axions.

Let us focus here on the most relevant features that our axion fields need to satisfy in order to be good FDM candidates. Considering for simplicity a single axion, a commonly used set of conventions is

$$\mathcal{L} = \frac{1}{2} f^2 (\partial\theta)^2 - A e^{-S} \cos(\theta)\,, \tag{4.5}$$

where f is the axion decay constant and S represents the instanton action that gives rise to the axion potential. From the above expression, where we set the instanton charge to one for simplicity, we see that the axion mass is given by

$$m_\phi^2 = A M_P^4 e^{-S}/f^2\,. \tag{4.6}$$

Using this notation the axion periodicity is $2\pi/f$ and the value for Sf corresponding to (half of) a Giddings-Strominger wormhole (for a review see [189]) is

$$Sf = \frac{\sqrt{6}\pi}{8} \simeq 0.96\,. \tag{4.7}$$

Given that FDM particles have to be produced through the misalignment mechanism and that a GUT scale decay constant implies that the PQ symmetry is broken before the inflationary stage, the DM

abundance of the physical ALP particle, $\phi = f\theta$, can be expressed as [18]:

$$\frac{\Omega_\phi h^2}{0.112} \simeq 2.2 \times \left(\frac{m_\phi}{10^{-22}\text{eV}}\right)^{1/2} \left(\frac{f}{10^{17}\text{GeV}}\right)^2 \theta_{mi}^2 \sim 1\,, \tag{4.8}$$

where $\theta_{mi} \in [0, 2\pi]$ is the initial misalignment angle with respect to the minimum of the potential.[2] In (4.8) we are considering small field initial displacement, large misalignment will be briefly treated in Appendix D.4. Therefore, assuming an initial misalignment angle $\theta_{mi} \sim \mathcal{O}(1)$, a prefactor $A \sim \mathcal{O}(1)$, and imposing the right value for the axion mass and decay constant, $m_\phi \sim 10^{-22}$ eV and $f \sim 10^{-2} M_P$, we have that

$$Sf = -f \ln\left(\frac{m_\phi^2 f^2}{A M_P^4}\right) \gtrsim 1\,. \tag{4.9}$$

This means that the existence of a FDM candidate tends to slightly violate the WGC [189,216]. Hence, in the next sections we are going to check the most generic closed string axion candidates in terms of their ability to reach a regime where they acquire their mass from an instanton with $Sf = \mathcal{O}(\text{a few})$ as indicated by eq. (4.9). What we find is summarised in table 4.1, showing that only few candidates, C_2 axions and thraxions, and to some extent also C_4 in certain limits, can violate the bound $Sf \lesssim 1$, thus potentially allowing for all dark matter to be FDM. We would like to point out that since the axion mass has an exponential dependence on the instanton action S, the accordance with or the violation of the WGC crucially depends on the precise extremality bound, i.e. on the value of α entering the formulation of the WGC in (2.44). It appears indeed quite interesting that experiments constraining the parameter space of FDM ALPs may be able to probe the upper limit of the axionic WGC, thus shedding some light on the underlying theory of Quantum Gravity.

The axionic content of the theory coming from closed string modes is given by the fields C_0, c_α, b_α, d_i, whose number depends on the geometrical structure of the extra dimensions (cf. Sections 2.1.3 and 2.2). Moreover, a new class of ultralight axions coming from flux compactification of type IIB string theory was recently discovered [76]: thraxions are axionic modes living at the tip of warped multi-throats of the compact manifold, near a conifold transition locus in complex structure moduli space. As shown in [76], at the tip of such throats there exists a $4d$ mode c that can be thought of as the integral of the two-form C_2 over the S^2 collapsing at the conifold point, as measured far away from that point. Although so far no study has been carried out on the phenomenology of such axions, it was shown in [88] that they do exist in a quite interesting fraction of orientifolds of the known compact manifolds realised as complete intersections of polynomial equations in products of projective spaces, also known as CICYs [217]. More in general, it is expected that Klebanov-Strassler throats with tiny warp factor are widely present in type IIB CY orientifolds or F-theory models [218–220]. Therefore, in this work we study how they behave as possible FDM candidates, as they are known theoretically to be ultralight, and they possess a flux-enhanced decay constant.

Being interested in axions that can nearly saturate the WGC bound, we analyse some simple setups that allow us to estimate the maximum value of Sf. These results are summed up in table 4.1 and further details can be found in Appendix D.1. From our analysis, it turns out that C_2, C_4 axions and thraxions are the best candidates to satisfy the constraint (4.9). To study the behaviour of C_4 axions having $Sf \sim \mathcal{O}(1)$, we consider two different CY geometries: the Swiss-cheese case and the fibred case, where the overall volume of the extra dimensions is parametrised by a single or by two degrees of freedom

[2] Given that $\frac{\Omega_\phi h^2}{0.112} \propto e^{-S/4} f^{3/2}$, we see that the representation fraction of every axion in the DM halo changes depending on its value of S and/or f. In general, for the same value of f, axions with smaller S are more represented, hence the DM abundance is dominated by the heavier axions (cf. (4.6)). For axions with the same S, those with larger f have a larger DM abundance and (cf. (4.6)) are also lighter. This last case is less generic.

Axion	Sf
C_0	$1/\sqrt{2}\, M_P$
B_2	$< M_P$
C_2	$\begin{cases} S_{ED1} f \lesssim M_P \\ S_{ED3} f \lesssim \sqrt{g_s}\, \mathcal{V}^{1/3} M_P \end{cases}$
C_4 (1 dof)	$\lesssim \sqrt{3/2}\, M_P$
C_4 (2 dof)	$\lesssim M_P$
$C_{2,\text{thrax}}$	$S_{\text{eff}} f_{\text{eff}} \lesssim \frac{3\pi M^3 \sqrt{g_s}}{\mathcal{V}^{1/3}} M_P$

Table 4.1: Bounds on Sf for different classes of closed string axions. These results arise from the study of simple extra-dimensions geometries. Further details are contained in Appendix D.1. Our simple explicit constructions here saturate these bounds ('$\sim$'), while we expect more general compactifications to satisfy them ('$<$'). C_0 and B_2 are listed for completeness, but generically they cannot be FDM candidates as they get very high masses from flux stabilisation.

(dof) respectively. Then, we study C_2 axions in the Swiss-cheese geometry. These fields can be viable FDM candidates in case they get a mass through non-perturbative effects coming from pure ED1 and ED3/ED1 instanton corrections. In the former case the bound on Sf is similar to the C_4-axion case but these axions tend to be naturally lighter. In presence of ED3/ED1 corrections, it seems that the strong version of WGC can be slightly violated, as in LVS $Sf \sim \mathcal{V}^{1/3}/\sqrt{\ln(\mathcal{V})} > 1$. Nevertheless, it may be not appropriate to apply the WGC in this case as this is a hybrid setup where we are effectively comparing the C_2-axion decay constant with the C_4 ED3 instanton action. These results are in agreement with what previously stated in the literature about the construction of explicit models and in works where a full mathematical analysis has been carried out for specific axion classes [71]. Indeed, no cases have been reported for C_4 and C_2 axions, where it was possible to clearly violate the constraint of the WGC even in its weak form while keeping the theory under control.

Concerning thraxions, we analyse both the case in which their mass is independent of the stabilisation of Kähler moduli and also when it gets lifted by their presence. Since their existence relies only on the presence of multi-throats and fluxes inside such throats, we do not have to specify any type of geometry for the compact manifold as thraxion features only depend on in its volume size $\mathcal{V}$. As shown in table 4.1, we are also concerned with K, M, the flux numbers coming from the integral of the H_3, F_3 field strengths over $\mathcal{B}$-type and $\mathcal{A}$-type 3-cycles respectively, and the string coupling g_s. Thraxions will acquire a potential due to the constituting warped-down 3-form flux energy density at the IR end of a throat, as well as from ED1 instanton contributions. As we discuss in Section 4.2.3, the former case is more appropriate for our purpose, and we will show how to rewrite the intrinsic flux-generated thraxion potential in terms of an effective 'instanton' action S_{eff} which we can arrange to be dominant compared to ED1 effects. To clear the physical meaning and the values of the parameters used in the following sections, we summarize them in table 4.2.

Besides looking at the constraint on Sf, we also need to consider that a good FDM axion must be extremely light. The current techniques developed to perform moduli stabilisation in type IIB are able to exclude already some possible candidates. The axio-dilaton, together with complex structure moduli, are stabilised at high energies by background fluxes, so that they are naturally too heavy to represent FDM. The same conclusion is true for the orientifold-odd B_2 axions which are usually much heavier than the overall volume modulus [221, 222]. The remaining candidates are given by C_2, C_4 axions and

	description	LVS range	KKLT range
W_0	tree-level superpotential	$1 \div 10^2$	$\exp\left(-\frac{2\pi}{N}\mathcal{V}^{2/3}\right)$
g_s	string coupling	$(\ln \mathcal{V})^{-1}$	$10^{-2} \div 0.2$
A	non-perturbative correction prefactor	$10^{-4} \div 10^4$	$10^{-4} \div 10^4$
N	number of D7-branes	$1 \div 10$	$30 \div 60$
M, K	flux numbers from F_3, H_3	≥ 10	≥ 10

Table 4.2: Description of microscopic parameters and their associated ranges considered in the study of closed string axions in LVS and KKLT moduli stabilisation. Where we provide a functional form, i.e. g_s in LVS or W_0 in KKLT, no a priori range can be given. For instance, W_0 cannot be interpreted as a parameter in KKLT as its value fixes the whole stabilisation. The same reasoning applies to g_s in LVS.

thraxions that we analyse in the following sections.

4.2.1 LVS: FDM from C_4 axions

We start our study by considering C_4 axions in LVS, which we reviewed in Section 2.1.3. If the CY volume in (2.36) is parametrised by a single Kähler modulus, i.e. ($f_{3/2} = \tau_1^3$) LVS is able to stabilise all the real part of Kähler moduli. If this is not the case, i.e. ($f_{3/2} = \tau_1\sqrt{\tau_2}$ or $f_{3/2} = \sqrt{\tau_1\tau_2\tau_3}$) we will be left with some flat directions in the Kähler moduli space. A potential for these fields can be generated at lower energies by e.g. higher order α' and g_s-loop corrections. Once these fields get stabilised, the scalar potential for the axions associated to volume cycles is induced by non-perturbative terms as in (2.29). The field dependence of the decay constant associated to C_4 axions is given by [18]

$$f \sim \begin{cases} \frac{M_P}{\tau} & \text{volume axion,} \\ \frac{M_P}{\sqrt{\mathcal{V}}} & \text{blow-up axion.} \end{cases} \tag{4.10}$$

Moreover, in this setup the instanton action appearing in the axion potential (4.5) is given by $S = a\tau$. By looking for a particle having a high decay constant and an extremely small mass, we immediately see from (4.10) that a FDM particle is more likely represented by axions related to large cycles parametrising the overall volume. In fact, while blow-up axion seem to have a higher decay constant ($\sim \mathcal{V}^{-1/2}$) compared to volume axion ($\sim \mathcal{V}^{-2/3}$), LVS stabilisation requires that $\mathcal{V} \sim e^{a_s\tau_s}$. This implies that matching the right FDM mass value tunes the overall volume too large ($\mathcal{V} \sim \exp(220)$) making the match between m and f unfeasible and, above all, this would cause the string scale to be much lower than eV where the theory is no longer under control. In addition, from the τ dependence of the decay constant, the axion mass and the total amount of FDM, eq. (4.8), we can easily conclude that in the presence of multiple volume axions, the heavier particles will represent a higher percentage of DM. By assuming that all the other parameters and the initial misalignment angle are the same for every axion, we have that $\frac{\Omega_\theta}{0.112} \sim e^{-S/4} \propto m_\theta^{1/2}$. In what follows, we are going to analyse two simple examples of concrete $4d$ effective models coming from type IIB string theory: Swiss-cheese and fibred CY threefolds.

Swiss-cheese geometry: Consider a CY with the typical Swiss-cheese shape for the volume, namely

$$\mathcal{V} = \alpha\left(\tau_{\mathcal{V}}^{3/2} - \lambda_s\tau_s^{3/2}\right), \tag{4.11}$$

	$N=1$	$N=2$	$N=10$
$\mathcal{V}$	$200 \div 300$	$500 \div 800$	$6000 \div 9000$

Table 4.3: Predicted overall volumes for different values of N imposing 100% of FDM.

where α and λ_s are positive real coefficients of order one. After LVS stabilisation, all Kähler moduli but the overall volume axion $d_{\mathcal{V}}$ are stabilised. This will represent our FDM candidate, with mass given by

$$m_{d_{\mathcal{V}}}^2 = \frac{8\kappa S_{\mathcal{V}}^3 A_{\mathcal{V}} W_0 e^{-S_{\mathcal{V}}}}{3\mathcal{V}^2} M_P^2 \,, \qquad S_{\mathcal{V}} = a_{\mathcal{V}} \tau_{\mathcal{V}} \,, \tag{4.12}$$

while its decay constant is

$$f_{\mathcal{V}} = \sqrt{\frac{3}{2}} \frac{M_P}{S_{\mathcal{V}}} \,. \tag{4.13}$$

The previous relations are based on the assumption that both the kinetic Lagrangian and the mass matrix associated to C_4 axions are diagonal. Working in the large volume limit, this can be safely assumed, as the off-diagonal terms of the Kähler matrix are suppressed by powers of $\tau_s/\tau_b \ll 1$ while the off-diagonal terms of the mass matrix are exponentially suppressed. In what follows, we try to understand which requirements are needed to match the FDM prescriptions. Supposing to have no prior knowledge on the cosmological history of the universe, we assume a constant axion field distribution. Given a uniform probability density on the range $[0; 2\pi]$, the mean value of $d_{\mathcal{V}}$ is given by π and its standard deviation is $\sigma_d^2 = \pi^2/3$, therefore we consider a misalignment angle $d_{mi} = \pi/\sqrt{3}$ as it represents the most likely value. This assumption is supported by [223] where it was shown that for any inflationary scale $H \gtrsim 1$ keV, the misalignment angle distribution becomes flat through stochastic diffusion. The most stringent constraint on inflationary model building in FDM models comes from isocurvature perturbation bounds, as we briefly describe in Appendix D.4.

In the Swiss-cheese geometry, the amount of DM depends only on the instanton action $S_{\mathcal{V}}$. This implies that once we fix the required amount of DM, we can immediately compute the natural value of mass and decay constant the FDM axion candidate needs to have. Knowing the shape of the instanton action, we can write $\mathcal{V} \simeq (S_{\mathcal{V}}/a_{\mathcal{V}})^{3/2}$, being $a_{\mathcal{V}} = 2\pi/N$, so that the formula for the DM abundance, eq. (4.8), becomes:

$$\frac{\Omega_\theta h^2}{0.112} \simeq 6.36 \times 10^{27} a_{\mathcal{V}}^{3/4} (c\, g_s)^{1/4} \frac{e^{-S_{\mathcal{V}}/4}}{S_{\mathcal{V}}^2} \,, \qquad \text{where} \qquad c = W_0 A_{\mathcal{V}} \,. \tag{4.14}$$

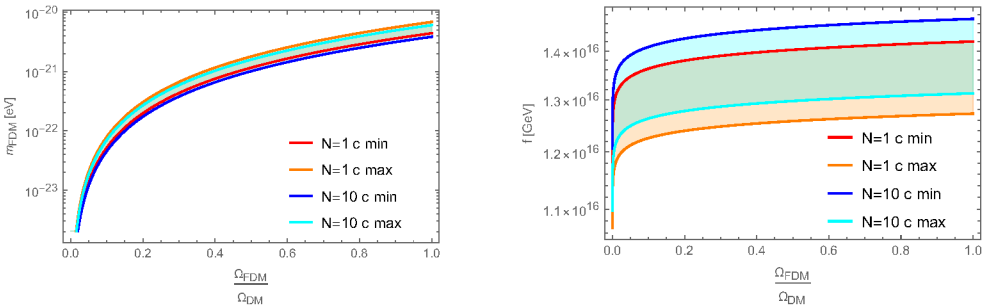

Figure 4.1: Predictions for axion mass (left) and decay constant (right) varying the percentage of axionic FDM and the non-perturbative effects giving rise to the ALP potential.

Given that the value of the parameters may vary across different models, we decide to fix the maximum and minimum values that they may acquire and we choose different values of $N = \{1, 2, 10\}$. Moreover, we use the LVS relation between the string coupling and the overall volume: $\mathcal{V} \sim e^{g_s^{-1}}$ to reduce the amount of fine-tuning. The extrema of the values we consider are listed in table 4.2.

Looking at the previous formula it is clear that once we fix the upper and lower bounds for W_0, $A_\mathcal{V}$ and the fraction of FDM $\frac{\Omega_{FDM}}{\Omega_{DM}}$, we can easily determine the mass and decay constant values of our axion candidate. The natural amount of axionic DM with the right mass and decay constant range can be found in fig. 4.1. While the predictions for the decay constant are not significantly influenced by changing the parameters, the particle mass can vary across different setups. As shown in table 4.3, these setups put strong constraints on the predicted overall volume $\mathcal{V}$. The lightest DM particles representing a considerable fraction of FDM have $m \lesssim 10^{-20}$ eV. It is worth noticing that neither the mass nor the decay constant value seem to be sensitive to the gauge theory on the brane stack.

Concerning the implications related to this FDM model, let us now estimate what the relevant energy scales are going to be. The KK scales, i.e. the maximum energies at which a 4D treatment of the theory is allowed, that are associated with bulk KK modes and KK replicas of open string modes living on D7-branes wrapping 4-cycles are given by

$$M_{KK}^{(i)} = \frac{\sqrt{\pi} M_P}{\sqrt{\mathcal{V}} \tau_i^{1/4}} \,. \tag{4.15}$$

This implies that for the Swiss-cheese geometry $M_{KK} = \frac{\sqrt{\pi} M_P}{\mathcal{V}^{2/3}} \sim 10^{15} \div 10^{16}$ GeV. Moreover, we have that the blow-up moduli which are stabilised through LVS prescription receive masses comparable to the gravitino mass, $m_{3/2} = M_P W_0 / \mathcal{V} \sim 10^{14} \div 10^{16}$ GeV. The last relevant energy scale is given by the inflationary scale. Looking at the ALP decay constant and mass, we can estimate what are the predictions for inflation that would arise from the ultralight C_4 axion detection. These are mainly due to isocurvature perturbations constraint and imply that the Hubble parameter during inflation, H_I, needs to be low, $H_I < 5 \cdot 10^{11}$ GeV, giving rise to undetectable stochastic gravitational waves, being the tensor-to-scalar ratio $r < 10^{-6}$. An extended derivation of these results can be found in Appendix D.4. We conclude this paragraph by stressing that since FDM needs to be the dominant DM component, the mass spectrum of the theory between the inflationary scale and the FDM scale should be nearly empty. In particular, as we already stressed, since heavier axions naturally represent higher DM fractions, the axion spectrum in the aforementioned range needs to be exactly empty.

Fibred geometry: Consider a fibred CY, whose volume can be written as

$$\mathcal{V} = \alpha \left(\tau_b \sqrt{\tau_f} - \lambda_s \tau_s^{3/2} \right) , \tag{4.16}$$

where τ_f parametrises the volume of a K3-fibre over a $\mathbb{P}^1$ base whose volume is controlled by τ_b, and τ_s represents the volume of a rigid del Pezzo divisor. Again, α and λ_s are positive real coefficients of order one. After LVS stabilisation, the fibre modulus is still a flat direction and requires additional corrections to be stabilised. These are usually taken to be α' corrections or KK and winding g_s loop corrections [46–48,179,180,224]. In this setup, the two good FDM candidates are the closed string axions

related to the base and the fibre modulus. The decay constants and the masses are given by

$$\begin{cases} f_{d_b} = \frac{M_P}{a_b \tau_b} = \frac{M_P}{S_b}\,, \quad m_{d_b}^2 \simeq \frac{4\kappa S_b^3 A_b W_0\, e^{-S_b}}{\mathcal{V}^2} M_P^2 \\ f_{d_f} = \frac{M_P}{\sqrt{2} a_f \tau_f} = \frac{1}{\sqrt{2}} \frac{M_P}{S_f}\,, \quad m_{d_f}^2 \simeq \frac{8\kappa S_f^3 A_f W_0\, e^{-S_f}}{\mathcal{V}^2} M_P^2\,. \end{cases} \tag{4.17}$$

Again, these relations are based on the assumption that both the kinetic Lagrangian and the mass matrix associated to C_4 axions are diagonal. As the field-space metric related to τ_f and τ_b is exactly diagonal, the same considerations provided in the Swiss-cheese geometry apply. Without loss of generality we can consider the case where $\alpha = 1$ so that

$$\mathcal{V} = \tau_b \sqrt{\tau_f} = \frac{S_b \sqrt{S_f}}{a_b \sqrt{a_f}}\,. \tag{4.18}$$

The masses of the two axions become

$$\begin{aligned} m_{d_f}^2 &\simeq c_f a_b^2 a_f \frac{S_f^2}{S_b^2} e^{-S_f} M_P^2\,, \qquad c_f = 2 g A_f \\ m_{d_b}^2 &\simeq c_b a_b^2 a_f \frac{S_b}{S_f} e^{-S_b} M_P^2\,, \qquad c_b = g A_b \end{aligned} \tag{4.19}$$

where $g = 4\kappa W_0$. By fixing the ratio between the two decay constants to be $q = f_{d_b}/f_{d_f}$, we immediately see that the ratio between the abundance of DM components is given by

$$\frac{\Omega_b}{\Omega_f} \simeq 1.09 \left(\frac{c_b}{c_f}\right)^{1/4} q^{5/4} e^{-\frac{M_P}{4 f_b}\left(1 - \frac{q}{\sqrt{2}}\right)}\,. \tag{4.20}$$

This result highlights that we can face two opposite scenarios. Isotropic compactification ($q \simeq \sqrt{2}$) implies that the two axions have similar masses and represent similar percentages of DM. On the other hand, given the exponential sensitivity of Ω_b/Ω_f on the parameter q, in anisotropic compactifications ($q \ll 1$ or $q \gg 1$) just one axion can play the rôle of the FDM particle. As already mentioned in the previous sections, also in case of nearly isotropic compactifications, the heavier axion will naturally

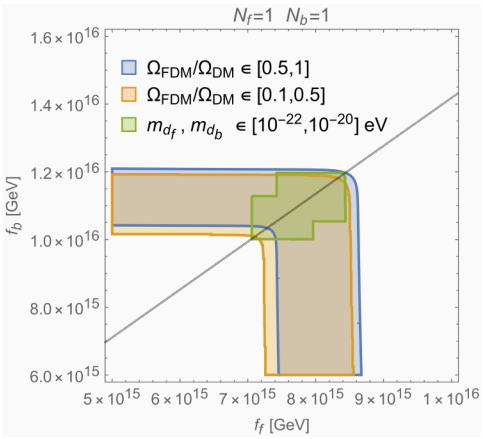

Figure 4.2: Allowed percentages of axionic DM as a function of the axion decay constants. The coloured areas satisfy the constraint $\frac{\Omega_b h^2}{0.112} + \frac{\Omega_f h^2}{0.112} \leq 1$. The blue and yellow areas refer to regions where ultralight axionic DM represents different percentages of the total amount of DM of the universe. The green area identifies the region where we have two FDM axions. The black line is given by $q = f_b/f_f = \sqrt{2}$.

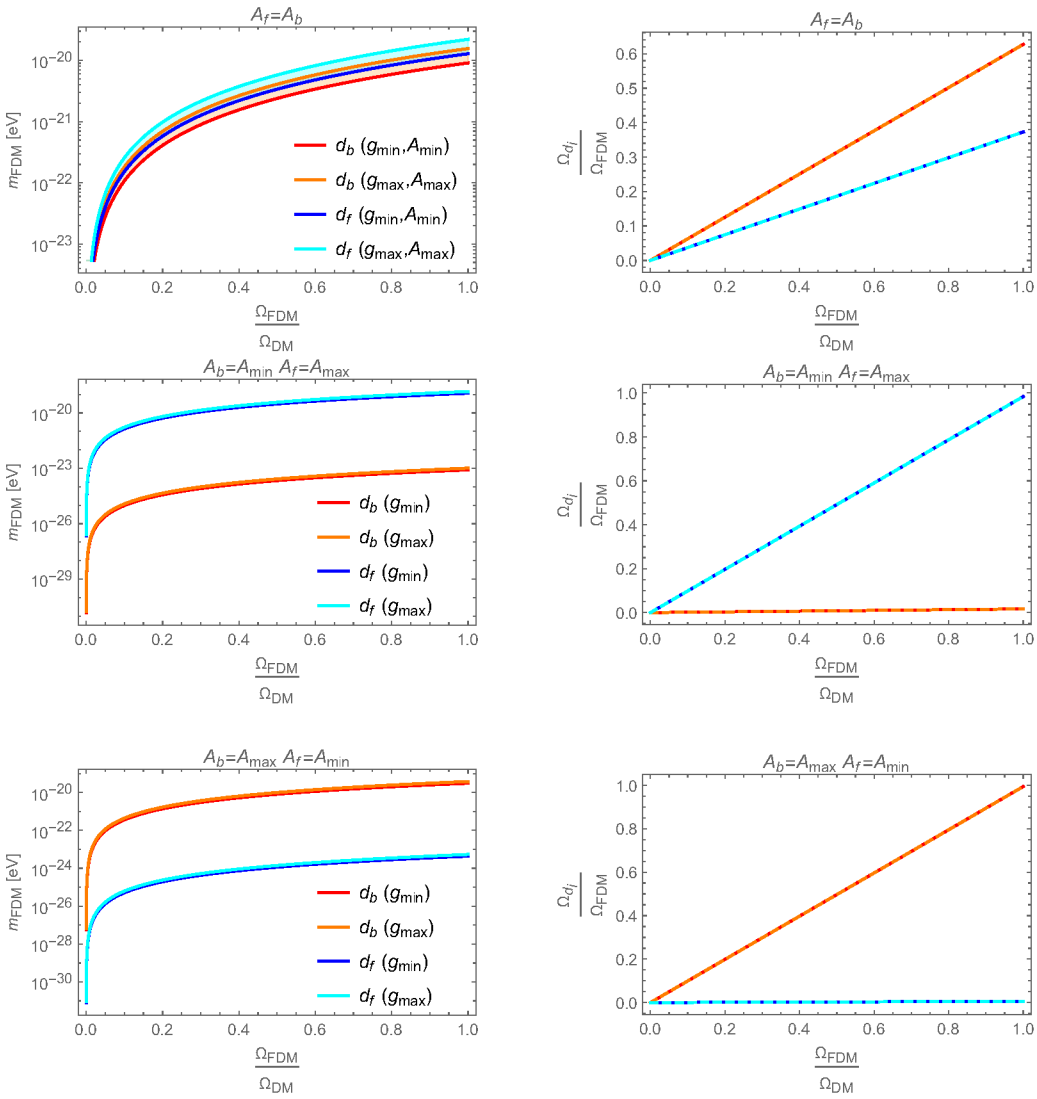

Figure 4.3: Left: d_f and d_b axion masses as a function of the total ultralight axion fraction of DM. Right: Relative contributions to Ω_{DM} coming from d_f and d_b axions. Top panels are referred to equal values of the perturbative corrections prefactors A_i, $i = f, b$. Central and bottom panels contain the results related to the cases where $A_f = A_{max} \gg A_b = A_{min}$ and $A_f = A_{min} \ll A_b = A_{max}$ respectively. The extreme values A_{min} and A_{max} can be read from table 4.2.

represent the higher fraction of DM. Let us consider for W_0, and A_i, $i = b, f$, the same parameter range as described in table 4.2. Moreover, given that the mass range of the two particles will follow the same behaviour as in the Swiss-cheese geometry, we us focus on the case where $N_f = N_b = 1$. Also considering the whole parameter space, we can already dramatically restrict the predictions for the allowed decay

	$\mathcal{V}$
$q = 0.01$	$(2.4 \div 3.6) \cdot 10^4$
$q = 0.1$	$(2.5 \div 3.8) \cdot 10^3$
$q = \sqrt{2}$	$(1.9 \div 2.9) \cdot 10^2$
$q = 10$	$(4.9 \div 7.3) \cdot 10^2$
$q = 100$	$(1.5 \div 2.3) \cdot 10^3$

Table 4.4: Overall volume of the extra-dimensions for different values of q. The range of the values was chosen so that both τ_b and τ_f get stabilised at values $\gg 1$, in accordance with instanton expansion and EFT prescriptions.

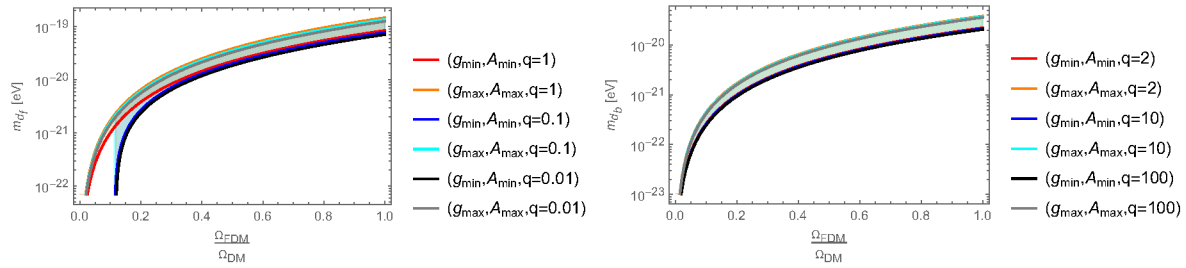

Figure 4.4: m_{d_b} and m_{d_f} as functions of the axion DM fraction varying the ratio between the decay constants $q = f_b/f_f$. Top: When $q \leq 1$ the contributions coming from d_b are negligible and its mass becomes $\ll 10^{-40}$ eV. Bottom: When $q \geq 2$ the contributions coming from d_f are negligible and its mass becomes $\ll 10^{-40}$ eV. The maximum and minimum values of the parameters used to compute the allowed mass range can be found in table 4.2. In these plots, we assumed for simplicity that $A_f = A_b$ given that, considering small and large q values, a relative variation of these parameters does not have any impact on the predictions.

constants. The results of this analysis are represented in fig. 4.2. From this plot, we can identify the narrow region where we have two suitable FDM candidates. Let us now fix the decay constant ratio q in order to inspect the green central area and understand what will be the composition and the mass of the two axions. The results obtained fixing $q = \sqrt{2}$ are represented in Fig. 4.3. If we fix $A_b = A_f$, we find two different axions having mass $\sim 10^{-20}$ representing similar percentages of DM. If A_f and A_b get different values, one of the axions becomes much lighter than 10^{-22} eV representing a negligible fraction of DM.

We now consider the effect coming from an anisotropic compactification. Also in this case, the predictions for the mass of the two candidates are quite robust. Indeed, as we show in Fig. 4.4, choosing different values of $q = \{0.01, 0.1, 1, 2, 10, 100\}$ the results about the mass and DM fraction do not change. For large values of q, d_b is the FDM axion which represents a significant fraction of DM when it acquires a mass $m \gtrsim 10^{-20}$ eV, while d_f is much lighter ($\ll 10^{-44}$ eV) and has a negligible impact on DM abundance. On the other hand, when q is fixed to small values, d_f is the right FDM candidate representing a large amount of DM when its mass is given by $m \sim 10^{-19}$ eV, while the contribution coming from d_b is negligible. The predictions for the overall volume $\mathcal{V}$ for different values of q and varying parameters are listed in table 4.4.

For what concerns the relevant energy scales of the model, i.e. KK masses, eq. (4.15) and the gravitino mass, the results found for the Swiss-cheese geometry are still valid in presence of CY fibrations in the isotropic compactification limit. Anisotropic compactifications may lead to different results depending on the overall volume considered. The ratio between the KK masses related to τ_f and τ_b 4-cycles scales as $M_{KK}^{(b)}/M_{KK}^{(f)} \sim q^{1/4}$. In this setup, the inflationary scale and the tensor-to-scalar ratio are suppressed compared to the Swiss-cheese geometry. For both isotropic and anisotropic compactifications and for any value of initial misalignment angles, we have that the inflationary scale $H_I < 10^{11}$ GeV and the tensor-to-scalar ratio $r < 10^{-7}$. Further details can be found in Appendix D.4.

4.2.2 LVS: FDM from C_2 axions

Our discussion at the beginning of Sec. 4.2 made it clear that it is the C_2-axions which can lay claim to be the best candidates of the type IIB O3/O7 orientifold closed string axion sector. This is so because their shift symmetry remains protected even under orientifolding, and they acquire a potential from non-perturbative effects less easily than C_4-axions, as we now summarise (see e.g. [100, 225]). In the absence of branes [144] or flux monodromy [147, 186, 226], scalar potentials for C_2 axions arise either via

ED1-brane instantons, via bound states of ED3/ED1-brane instantons or via gaugino condensation on stacks of 4-cycle-wrapping D7-branes with gauge flux as follows:

- The C_2 axion potential can be generated by ED1-branes wrapped on 2-cycles. Such effects induce non-perturbative contributions to the metric of R-R two-forms axions themselves, but cannot contribute to the superpotential in our setup [22, 144]. In the following, we will use that both KKLT and LVS can be arranged to stabilize the B_2 axion at vanishing VEV at high mass scale. In this case, Kähler potential corrections scale like $\exp(-2\pi t_+/\sqrt{g_s})$ where t_+ represents the Einstein frame volume of the orientifold-even 2-cycle, Σ_2^+ wrapped by the ED1-brane. These are easily suppressed by considering modest t_+ volumes potentially giving rise to light C_2 fields.

- The structure of the ED3/ED1-bound state instanton contribution to the superpotential is given by a modular theta function. For large enough real argument, this becomes exponentially damped. In our cases, the total scalar potential results in stabilising $b = 0$ so no extra damping from a finite b-VEV arises in the exponential in W. The suppression of the C_2-cosine potential comes from $\exp(-T)$ dependence of the ED3-parent instanton. Hence in total, if you have an ED3 that has a dissolved ED1 [22] this gives a non-perturbative correction to W like $\exp(-T-G)$. Formally, the G-dependence of the ED1 dissolved inside the ED3 arises as an ED3 magnetised by 2-form gauge flux threading 2-cycles in the ED3-wrapped 4-cycles. As the ED3-brane itself is a purely Euclidean instanton effect, the path integral enforces summation over the unmagnetised ED3 and all magnetised ED3/ED1-bound states, mandating the appearance of the G-dependence in W for ED3 contributions to 4-cycles intersecting with orientifold-odd 2-cycle combinations.

- If you use instead a D7-brane stack to stabilise the T moduli, magnetisation of the D7-brane stack is a choice of compactification data (no path integral forces you to sum over magnetised D7-brane states, since unlike a purely euclidean instanton the full D7-brane fills $4d$ spacetime as well). Thus, by avoiding putting gauge fluxes on the D7-branes you prevent single-suppressed $\exp(-T-G)$ terms in W from arising [37,94–96,227]. However, the path integral will generate contributions from ED3/ED1-bound state instantons to the gauge kinetic function. Such a correction to the gauge kinetic function of the 7-brane stack scaling like $\exp(-T-G)$ in turn induces a superpotential correction of order $\exp(-2T-G)$ [144]. Compared to the scale of the superpotential terms $\exp(-T)$ stabilising the T moduli, this leads to a double suppression of the potential for the C_2 axion.

We shall now summarise the scaling of the scalar potential for the C_2 axion arising from these non-perturbative effects in the concrete scenarios of KKLT and LVS stabilisation of the volume moduli on Swiss-cheese CY orientifolds with two volume moduli:

- We first look at KKLT: if a harmonic zero-mode C_2 axion counted by $h^{1,1}_-$ acquires a single suppressed non-perturbative scalar potential from ED3/ED1-bound state instantons, then in KKLT it is too heavy to form FDM. Even if its potential comes from the double suppressed contribution of an unmagnetised 7-brane stack, the C_2 axion remains too heavy to constitute FDM. The reason is that in KKLT the lowest volume moduli masses $\sim \exp(-T)$ are always around the gravitino mass scale. Since this in turn is bounded from below by $\mathcal{O}(\text{ TeV})$ the resulting C_2 mass scale $\sim \exp(-2T)$ is still too heavy. On the other hand, if this axion receives a mass through pure ED1 contributions appearing in the Kähler potential, it may represent a good FDM candidate. Indeed, in this setup, the C_2 axion can become much lighter than the C_4 one and its mass would scale as $\exp(-2T-\sqrt{T/g_s})$.

- In LVS we should always have a CY manifold with a volume form such that it has at least two volume moduli appearing in the Swiss-cheese form. For a C_2 axion we can now consider intersection couplings with either the small LVS blow-up or the CY volume-carrying big cycle. We begin by looking at the case of C_2 intersecting with the small cycle. If you have a double suppressed term in W from an unmagnetised 7-brane stack on a small cycle, the term in the exponent would scale as $2(2\pi/N)\tau_s$. For $N = 2$ this scales like a single ED3/ED1-bound state instanton wrapping the small cycle. Moreover, in this case $N = 2$ is the most favourable setup for a potential FDM role as the volume needs to be $\mathcal{V} \sim \exp(100)$, while it would be even large for $N > 2$ driving the EFT out of the controlled regime. Also the case of ED1 branes wrapped around a blow-up cycle does not lead to good FDM candidates. Indeed, being $\tau_s \sim g_s^{-1}$, Kähler potential corrections scale like $\exp(-2\pi/g_s)$ and matching the right mass value requires $\mathcal{V} \gtrsim 10^{20}$ making the axion decay constant, $f \sim M_P/\sqrt{\mathcal{V}} \sim 10^8$ GeV, way too small. Hence, C_2-FDM cannot arise in LVS from the LVS blow-up cycle or similarly small blow-up cycles.

- Conversely, in LVS a D7-brane stack wrapped around the large volume cycle induces a double suppressed mass term that would imply either a too light axion or volume too small for control of the α'-expansion.

- What thus remain are the cases of an ED3/ED1-bound state instanton in LVS or an ED1-instanton wrapping the volume cycle in both KKLT and LVS. In the first case, the resulting single-suppressed cosine potential for C_2 on the big cycle leads to a borderline situation and the relation between the C_4 and C_2 masses, the decay constants and the FDM abundances requires further investigation. Also the second case of a pure ED1-instanton may lead to interesting results as the Kähler potential corrections scaling as $\exp(-\mathcal{V}^{1/3}/\sqrt{g_s})$ can give rise to sufficiently light C_2 fields for both stabilisation prescriptions under study.

In what follows we consider the simple setup where we have a single orientifold-odd modulus G, the extradimensional geometry is Swiss-cheese and there is are non-vanishing intersection number between the pair of 2-cycles projected by the O7-action onto t_+ and a harmonic C_2 axion, and the large volume 4-cycle. While extensions to multiple odd moduli lead so similar results, moving towards more complex geometries is highly non-trivial. Given that we are only interested in the overall scaling of the mass and the decay constant, we leave this analysis for future work. We separately study the cases where the C_2 axion gets a mass from pure ED1 (in K) or ED3/ED1 instanton effects (in W). In both cases, the Kähler potential is given by (2.30) (in what follows we consider only leading α' corrections) where $\mathcal{V} = \mathcal{V}(T_i, G, S)$ is the volume of the compact dimensions.

Pure ED1 effects in LVS: Let us consider the case where the ED1 wraps a 2-cycle t_b parametrizing the overall volume. For simplicity, we assume that the volume dependence on t_b is given by $\mathcal{V} \supset \kappa_{bbb}\, t_b^3/6$, where κ_{bbb} is the big cycle self-intersection number.[3] If this condition is satisfied, the 2-cycle volume can be written as $t_b = ((T_b + \bar{T}_b)/\kappa_{bbb})^{1/2}$. In the simplest Swiss-cheese setup, the CY volume is given by [144]:

$$\mathcal{V}/\alpha \simeq \left[T_b + \bar{T}_b - \kappa_b (G - \bar{G})^2 + C e^{-\frac{2\pi}{\sqrt{g_s}}\sqrt{\frac{(T_b+\bar{T}_b)}{\kappa_{bbb}}}} \mathrm{Re}\left[e^{i\pi G}\right] \right]^{3/2} - (T_s + \bar{T}_s)^{3/2}\,, \tag{4.21}$$

[3] Similar results hold for more complex intersection polynomials once we go to the LVS limit, where one of the 2-cycles dominates over the other ones.

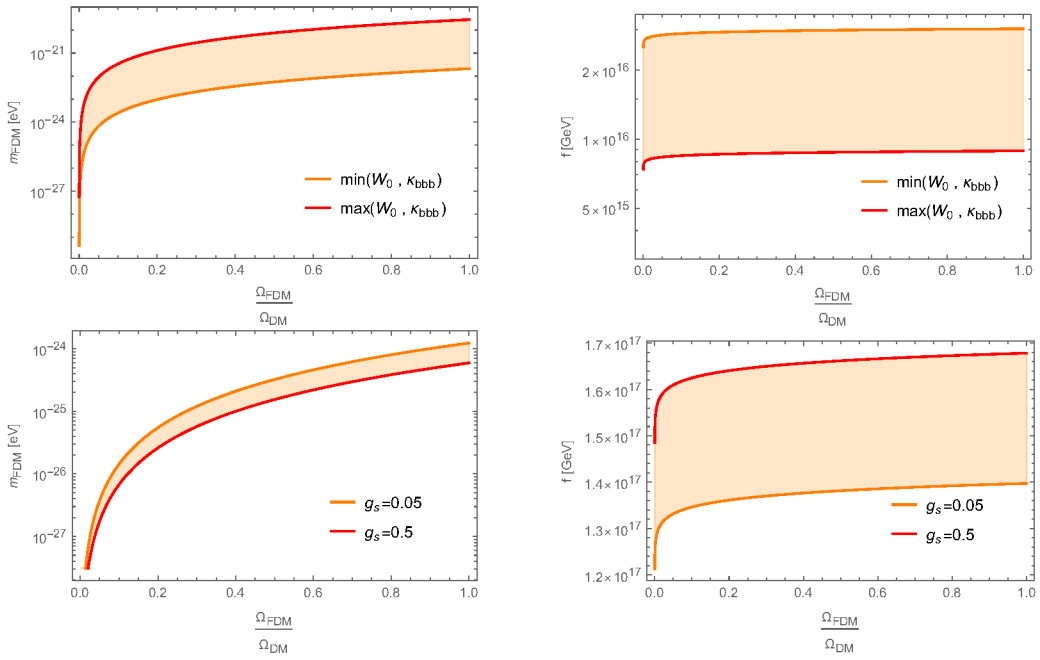

Figure 4.5: Predictions for C_2-axion mass (left) and decay constant (right) in LVS (top) and KKLT (bottom) scenarios. The axion receives a mass through ED1 instanton effects coming from an ED1-brane wrapping the volume 2-cycle.

where $\alpha = \frac{1}{3}(2/\kappa_{bbb})^{1/2}$, $\kappa_b = \kappa_{b--}g_s/4$ being κ_{b--} the intersection number of the big divisor with the odd cycle and $\mathrm{Re}(e^{iG}) = e^{i\pi(G-\bar{G})}\cos\left[\pi(G+\bar{G})\right]$. We further assume the small blow-up 4-cycle Σ_s to be wrapped by an ED3 instanton or a small D7-brane stack generating the following non-perturbative correction to the superpotential:

$$W = W_0 + A_s e^{-a_s T_s}\,. \tag{4.22}$$

Assuming stabilisation of the B_2 axion at $\langle b\rangle = 0$, the C_2 axion decay constant is given by [34]:

$$2\pi f = M_P\sqrt{\frac{g_s t_b|\kappa_{b--}|}{2\mathcal{V}}}\,, \tag{4.23}$$

where $\kappa_{b--} \leq 0$. The action for the ED1 wrapped around t_b is

$$S_{ED1} = \frac{2\pi\, t_b}{\sqrt{g_s}}\,. \tag{4.24}$$

Hence the WGC relation becomes

$$Sf = \sqrt{\frac{t_b^3|\kappa_{b--}|}{2\mathcal{V}}}M_P \quad \xrightarrow[t_b\gg1]{\text{LVS}} \quad \sqrt{\frac{3|\kappa_{b--}|}{\kappa_{bbb}}}M_P\,, \tag{4.25}$$

where on the right side we took the LVS limit. The scalar potential for C_2 arising from the aforementioned corrections to K and W is suppressed compared to the LVS terms and scales like

$$\delta V \simeq -\frac{C\,W_0^2}{g_s^{1/2}\mathcal{V}^{11/3}}e^{-2\,\pi\gamma\frac{\mathcal{V}^{1/3}}{\sqrt{g_s}}}\cos\left(2\pi c\right)\,, \qquad \text{where} \qquad \gamma = \frac{3^{1/3}}{2^{1/6}\kappa_{bbb}^{1/3}}\,, \tag{4.26}$$

and we assumed LVS stabilization for τ_b, τ_s and d_s. Finally, the axion mass is given by

$$m_c^2 \simeq \frac{C\,W_0^2}{|\kappa_{b--}| g_s^{3/2}\mathcal{V}^3} e^{-2\,\pi\gamma\frac{\mathcal{V}^{1/3}}{\sqrt{g_s}}}\,M_P^2\,. \tag{4.27}$$

For simplicity from now on we fix $\kappa_{b--} = -1$ and $C = 1$ as their tuning does not really affect our final predictions. We let W_0 and κ_{bbb} vary in $W_0 \in [1, 10^2]$ and $\kappa_{bbb} \in \{1, \ldots, 10\}$ while we set $g_s = \ln^{-1}(\mathcal{V})$ according to LVS prescription. Our results are shown in Fig. 4.5 where we see that the C_2 axion coming from an ED1-brane wrapping the volume 2-cycle can actually represent a good FDM candidate. Just as in the previous cases, the decay constant is not sensitive to the variation of the microscopical parameters.Instead, here the variation of the mass is more pronounced. We have in fact that the C_2 axion can represent a considerable percentage of DM if it gets a mass $m \sim [7 \cdot 10^{-22}, 10^{-19}]$ eV corresponding to volumes of about $\mathcal{V} \sim [10^4, 10^5]$ and string couplings $g_s \sim [0.08, 0.1]$.

Pure ED1 effects in KKLT: Here we consider the simplest case where $h^{1,1}_+ = 1$. The overall volume, the C_2 axion decay constant and the ED1-instanton action coincide with those listed in the previous section if we neglect the blow-up field contributions. The correction to the superpotential is given by:

$$W = W_0 + A_b e^{-a_b T_b}\,. \tag{4.28}$$

Assuming again that $\langle b\rangle = 0$, the C_2 scalar potential arising from ED1 corrections to K and W is suppressed compared to the KKLT AdS scale and reads:

$$\delta V \simeq \frac{C\,a_b^2 A_b^2 g_s}{\tau_b^2} e^{-2a_b\tau_b - 2\pi\sqrt{2\frac{\tau_b}{g_s\kappa_b}}} \cos(2\pi c)\,. \tag{4.29}$$

The axion mass is given by:

$$m_c^2 \simeq \frac{C\,a_b^2 A_b^2}{\tau_b \kappa_{b--}} e^{-2a_b\tau_b - 2\pi\sqrt{2\frac{\tau_b}{g_s\kappa_b}}} M_P^2\,. \tag{4.30}$$

For simplicity from now on we fix $|\kappa_{b--}| = \kappa_{bbb} = 1$, $C = A_b = 1$, $a_b = 0.1$ as their tuning does not significantly affect our final predictions. We let W_0 and g_s vary in $W_0 \in [10^{-12}, 10^{-2}]$ and $g_s \in [0.05, 0.5]$ while we set $\tau_b = -\ln(W_0)/a_b$ according to the KKLT prescription. Our results are shown in Fig. 4.5 where we see that the C_2 axion can be extremely light in the KKLT scenario, actually too light to represent FDM. In this case, both the decay constant and the mass are not very sensitive to the variation of the microscopical parameters. The decay constant is $f \sim 10^{17}$ GeV while the mass $m \sim 10^{-24}$ eV. Low mass values correspond to $W_0 \sim 10^{-10}$, high values to $W_0 \sim 10^{-2}$.

ED3/ED1 effects: If the axions acquire a mass via ED3/ED1-instanton contributions, the superpotential receives leading order non-perturbative corrections given by

$$W = W_0 + A_s\, e^{-a_s T_s} + A_b\, e^{-a_b T_b} + C e^{-a_b(T_b + iG)}\,. \tag{4.31}$$

These corrections tend to make the volume C_4 axion and the C_2 axion degenerate in mass. After LVS and b axion stabilisation, which we assume to take place at $\langle b\rangle = 0$, we are left with two ultralight axion candidates, namely d_b and c. The field space metric associated to these fields is diagonal

$$\mathcal{L}_{kin} = \frac{1}{2}\left[\frac{3}{2\tau_b^2}(\partial d_b)^2 - \frac{6\kappa_b}{\tau_b}(\partial c)^2\right]\,, \tag{4.32}$$

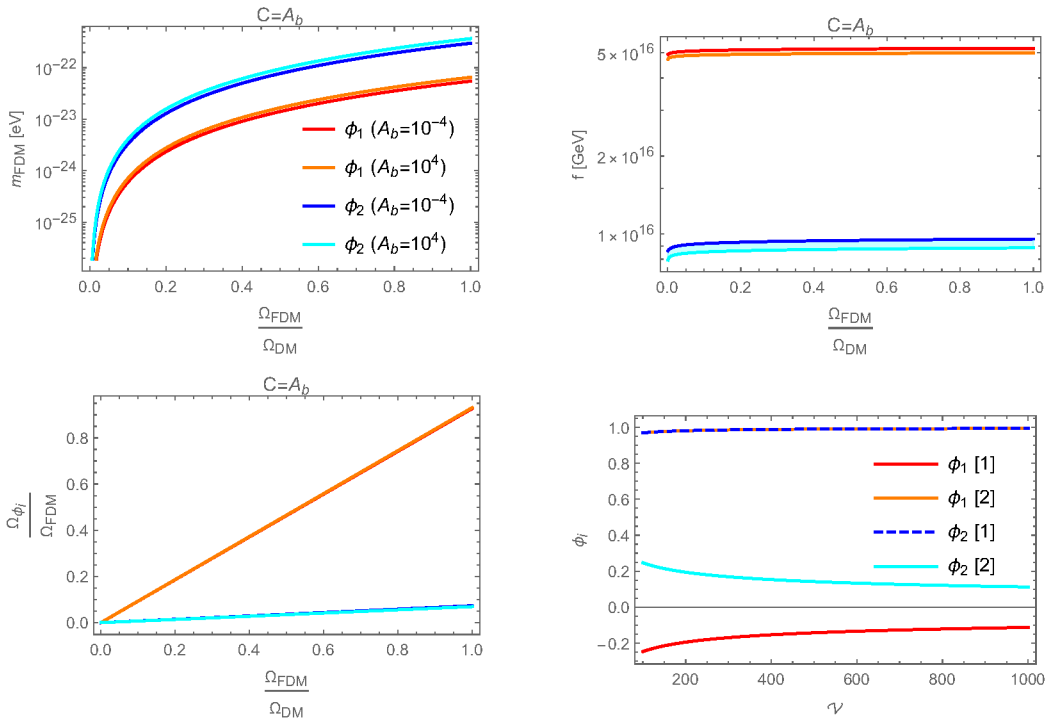

Figure 4.6: Results for C_2 and C_4 axionic FDM from ED3/ED1-bound state instanton effects wrapping the overall volume cycle in the Swiss-cheese geometry. The results are given in terms of the mass matrix eigenvectors ϕ_1 and ϕ_2, eq. (4.39). Top: axion masses (left) and decay constants (right) as a function of the total ultralight axionic DM fraction. Bottom-left: relative abundance of the axionic DM particles. Bottom-right: eigenvectors components as a function of the overall volume $\mathcal{V}$. At small volumes the eigenvectors of the mass matrix ϕ_1 and ϕ_2 are mainly given by the C_2 and C_4 axion respectively.

while their scalar potential is given by

$$V_F \supset \frac{a_b \kappa W_0}{2\tau_b^2} e^{-a_b\tau_b} \left(A_b \cos(a_b d_b) + C \cos\left[a_b\left(d_b + c\right)\right]\right) . \tag{4.33}$$

In terms of the canonically normalised fields it becomes

$$V_F \supset \frac{a_b \kappa W_0}{2\tau_b^2} e^{-a_b\tau_b} \left(A_b \cos\left(\frac{\hat{d}_b}{g_{d_b}}\right) + C \cos\left[\left(\frac{\hat{d}_b}{g_{d_b}} + \frac{\hat{c}}{g_c}\right)\right]\right) , \tag{4.34}$$

where

$$g_{d_b} = \sqrt{\frac{3}{2}}\frac{1}{a_b\tau_b} , \qquad g_c = \frac{1}{a_b}\sqrt{\frac{6|\kappa_b|}{\tau_b}} . \tag{4.35}$$

As we will show below, we cannot identify g_{d_b} and g_c with the decay constants, as the physical fields are given by the mass matrix eigenvectors that may not be aligned with d_b and c. Let us consider for simplicity the case where $A_b = C$. The minimum of the scalar potential is given by

$$\frac{\hat{d}_b}{g_{d_b}} = (2k+1)\pi , \qquad \frac{\hat{c}}{g_c} = 2m\pi , \qquad m, k \in \mathbb{Z} \tag{4.36}$$

so that the mass matrix in a neighbourhood of the minimum becomes

$$M = \Lambda \bar{M} = \Lambda \begin{pmatrix} \frac{2}{g_{d_b}^2} & \frac{1}{g_{d_b} g_c} \\ \frac{1}{g_{d_b} g_c} & \frac{1}{g_c^2} \end{pmatrix} \quad \text{where} \quad \Lambda = \frac{a_b A_b \kappa W_0}{2\tau_b^2} e^{-a_b \tau_b} \,. \tag{4.37}$$

The eigenvalues, λ_i, and eigenvectors, ϕ_i, of $\bar{M}$ are

$$\lambda_1 = \frac{g_{d_b}^2 + 2g_c^2 - \sqrt{g_{d_b}^4 + 4g_c^4}}{2g_{d_b}^2 g_c^2} \,, \qquad \lambda_2 = \frac{g_{d_b}^2 + 2g_c^2 + \sqrt{g_{d_b}^4 + 4g_c^4}}{2g_{d_b}^2 g_c^2} \tag{4.38}$$

$$\phi_1 = \frac{1}{|g_-|} \begin{pmatrix} \frac{2g_c^2 - g_{d_b}^2 - \sqrt{g_c^4 + 4g_{d_b}^4}}{2g_c g_{d_b}} \\ 1 \end{pmatrix} , \qquad \phi_2 = \frac{1}{|g_+|} \begin{pmatrix} \frac{2g_c^2 - g_{d_b}^2 + \sqrt{g_c^4 + 4g_{d_b}^4}}{2g_c g_{d_b}} \\ 1 \end{pmatrix} \tag{4.39}$$

where $|g_\pm| = 1 + \left(\frac{2g_c^2 - g_{d_b}^2 \pm \sqrt{g_c^4 + 4g_{d_b}^4}}{2g_c g_{d_b}} \right)^2$ is just a normalisation factor so that $|\phi_i| = 1$. Using these results, we can write the decay constants and the masses of the physical axions as

$$f_{\phi_i} = \frac{1}{\sqrt{\lambda_i}} \,, \quad m_{\phi_i}^2 = \Lambda \lambda_i \,. \tag{4.40}$$

Here we note, that in the limit of large $\tau_b \sim \mathcal{V}^{2/3}$ we find that the lightest axion ϕ_1 has $f_{\phi_1} \sim g_c \sim \sqrt{g_s/\tau_b}$ and thus $S_{ED3} f_{\phi_1} \sim \sqrt{g_s \tau_b}$ confirming with our summary in Table 4.1. This implies a violation of certain strong forms of the WGC.

Also in this case, we find that FDM particles naturally arise from string compactification only if the overall volume of the extra dimensions is small. For simplicity, in this section we fix $W_0 = 1$ while we let A_b vary in $A_b \in [10^{-4}, 10^4]$. The overall volumes which are compatible with having 100% of ultralight axionic DM are $\mathcal{V} \in 200 \div 300$. The results related to this setup are shown in Fig. 4.6. Despite the relation $\phi_1 \equiv c$ and $\phi_2 \equiv \hat{d}_b$ only holds at $\mathcal{V} \to \infty$, the eigenvectors ϕ_1 and ϕ_2 are mainly given by the C_2 and C_4 axion respectively. Although the shape of the potential in (4.34) may suggest some mass degeneracy, the hierarchy in the mass scales and in the abundances of the two fields is apparent. While the two decay constants are comparable and their values lie in the expected range $\sim 10^{16}$ GeV, the C_2 axion is much lighter and more represented than the C_4. The reason why in this context the lighter axion can represent a higher fraction of DM is that the two fields acquire a mass through instanton corrections that have a different nature. In this way, they do not share the same dependence of the mass and the decay constant on the instanton action. The C_2 axion field, that would represent the prominent FDM candidate in this setup, exhibits a mass that is lighter than the original FDM estimate, $m_c < 10^{-22}$ eV. In this section we are relying again on LVS moduli stabilisation, hence the same energy scales that we have shown in the case of C_4 axions in the Swiss-cheese geometry remain valid.

4.2.3 FDM from Thraxions: KKLT & LVS?

In the KKLT scenario, it is difficult to realise ultralight axions. In this case, axions get stabilised at the same energy level as their moduli partners by the same non-perturbative effect to W. This is a consequence of the fact that KKLT AdS vacuum is supersymmetric. Their masses then are generically of the same order as the gravitino mass. Therefore, axions coming from KKLT moduli stabilisation behave just like the axionic partner of the small-cycle volume moduli in LVS, they are too heavy to be FDM candidates.

However, there is a way out: we could have a viable FDM candidate if the underlying internal manifold admits the presence of *thraxions* [76]. Thraxions occupy a special corner of the axion landscape as their mass is exponentially suppressed by powers of the warp factor $\omega \sim \exp(-S/3)$ of the throat. At the level of complex structure moduli stabilisation via fluxes of [38], their squared mass scales as [76]

$$\frac{m^2}{M_P^2} \sim \frac{4\, g_s\, e^{-2S}}{\sqrt{3}\, S^{3/2}\, \mathcal{V}^{2/3} M^2}\,, \tag{4.41}$$

where $\mathcal{V}$ is the volume of the bulk CY and M is a flux quantum coming from the integral of a 3-form field strength F_3 over the $\mathcal{A}$-type 3-cycle of the deformed side of the conifold transition. Note that here, compared to the axions studied so far, the dependence on the instanton action S is enhanced by a factor of 2, resulting in a bigger suppression of the mass. In principle, we should consider also the possibly present effects of ED1 instantons coming from ED1-branes wrapping the 2-cycle, which contribute an action

$$S_{ED1} \sim \sqrt{\frac{KM}{g_s}}\,, \tag{4.42}$$

where K is another flux quantum defined as the integral of the 3-form field strength H_3 over the $\mathcal{B}$-type 3-cycle. The effective instanton action generating the thraxion potential reads

$$S_{\text{eff}} \sim \frac{2\pi K}{g_s M}\,. \tag{4.43}$$

Note, that $\omega \ll 1$ is ensured when $K > g_s M$. The ED1-brane instanton effects come with a shorter periodicity. Yet, they can remain subdominant in the thraxion scalar potential while satisfying the WGC in its mild version. We should therefore require ED1-contributions to be suppressed compared to the flux-backreaction induced thraxion scalar potential scale. This can be achieved by requiring the following hierarchy among fluxes:

$$M \gtrsim \sqrt{\frac{K}{M g_s}}\,. \tag{4.44}$$

In this way, we are satisfying a milder version of the WGC. The effective decay constant reads

$$f_{\text{eff}} \sim \frac{3\sqrt{g_s} M}{2\mathcal{V}^{1/3}} M_P\,, \tag{4.45}$$

which is enhanced by a factor M compared to the standard f (cf. [76]). Hence, the WGC relation reads

$$S_{\text{eff}} f_{\text{eff}} \sim \frac{3\pi K}{\sqrt{g_s}\, \mathcal{V}^{1/3}} M_P\,. \tag{4.46}$$

We can turn eq. (4.46) into an upper bound on $S_{\text{eff}} f_{\text{eff}}$ by using the relation (4.44) among the flux numbers. This brings the value displayed in Table 4.1, namely

$$S_{\text{eff}} f_{\text{eff}} \lesssim \frac{3\pi M^3 \sqrt{g_s}}{\mathcal{V}^{1/3}} M_P\,. \tag{4.47}$$

The presence of no-scale breaking terms, which are necessary to stabilise the Kähler moduli sector, *generically* induces cross terms between the thraxion and the moduli in the total potential, as we discussed in Section 2.4. These new terms generate a mass for the thraxion which scales as $\exp(-S)$. Hence, the mass loses the double suppression, and the thraxion potentially becomes slightly heavier

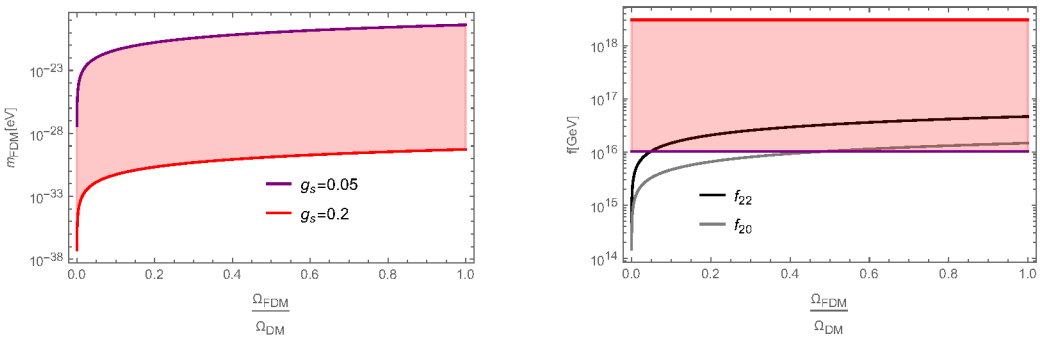

Figure 4.7: Predictions for the thraxion mass and decay constant as functions of the FDM abundance. All plots are drawn fixing $M = 10$: increasing M makes the thraxions lighter. We choose a conservative approach which allows us to have a wider phenomenology, given that the flux distribution in the landscape is an open field of investigation. For LVS, the volume scales as $\mathcal{V} \sim \exp(1/g_s)$, hence allowing us to deal with only one free parameter (as we consider $W_0 \sim \mathcal{O}(1)$).

than in (4.41). The mass squared now reads

$$\begin{aligned} \frac{m^2}{M_P^2} &\sim \frac{4\, g_s\, e^{-S}}{3^{5/4}\, S^{3/4}\, \mathcal{V}^{2/3} M^2} \frac{|W_0|}{\mathcal{V}^{4/3}} \qquad \text{for KKLT stabilisation}\,, \\ \frac{m^2}{M_P^2} &\sim \frac{4\, g_s\, e^{-S}}{3^{5/4}\, S^{3/4}\, \mathcal{V}^{2/3} M^2} \frac{\ln \mathcal{V}}{\mathcal{V}^3} \qquad \text{for LVS stabilisation}\,, \end{aligned} \tag{4.48}$$

where we distinguished between KKLT and LVS moduli stabilisation procedures. The decay constant remains the same as in (4.45), as it is dominated by the physics in the UV. However, for the KKLT case we should impose the consistency condition that $\omega^3 > W_0^2$ [2]. This relation comes from requiring that gaugino condensation effects in the bulk CY do not become comparable with background fluxes at the IR end of the throat [104]. Since for FDM the scalar potential should scale as $\sim 10^{-100}$ in Planck units, we find an upper bound for $|W_0|$, namely $|W_0| < 10^{-50}$. Even if we might be able to engineer such values in the landscape, their presence is highly suppressed by the statistics of the flux vacua distribution. Thus, we prefer to keep the discussion general and conclude that it is very unlikely that thraxions in KKLT can behave as FDM.[4]

We display the results for thraxions as FDM candidates in LVS in Fig. 4.7. First, we point out that we allowed the parameters to vary between the biggest and smallest values compatible with a consistent compactification, regardless of FDM astrophysical constraint. Then, it is indeed remarkable that for a certain parameter space we cover the FDM window. Hence, for the LVS case the thraxion is a viable candidate. The main difference with the other harmonic axions is that now larger values for the total volume $\mathcal{V}$ are preferred: in Fig. 4.7 we are plotting $10^2 \leq \mathcal{V} \leq 5\times 10^8$, where the upper bound corresponds to the purple line. The fact that thraxions should rely on large volumes of the extra dimensions to lie in the FDM range may turn out to be a drawback. As we will discuss in Sec. 4.3, large values of the CY volume may be statistically less represented in the landscape of string vacua.

As explained in Section 2.4, in certain geometries it can happen that the cross terms with the Kähler moduli vanish. Hence, the mass scales substantially again as in (4.41). We checked also these setups, and we found that there is no appreciable difference with the results given in fig. 4.7.

We are now able to estimate the mass of the warped KK modes living inside the warped-throat systems hosting the thraxion. Indeed, they will be heavier than the thraxion, as their masses scales

[4]Note that also in the cases where the six-fold warp factor suppression can be restored, the value of $|W_0|$ would anyway remain too low to be fully trusted.

linearly with the warp factor ω as

$$\frac{m_{w,KK}}{M_P} \sim \frac{\omega}{R} \sim \frac{\omega}{\mathcal{V}^{1/6}\sqrt{\alpha'}}\,, \tag{4.49}$$

where R is the throat radius which can be rewritten in terms of the bulk CY volume and the parameter α'. The KK masses change drastically from the double to the single suppression case, as we shall discuss below. We can express $m_{w,KK}$ in terms of the variables of our setup as

$$m_{w,KK}^{(s,\mathrm{LVS})} \simeq 2\times 10^{-3}\, g_s^{3/4} e^{5/(9g_s)} \left(\frac{m}{10^{-22}\ \mathrm{eV}}\right)^{2/3} K^{1/4} M^{5/12}\ \mathrm{eV}\,, \tag{4.50a}$$

$$m_{w,KK}^{(d)} \simeq 304\, g_s^{7/12} \left(\frac{10^4}{\mathcal{V}}\right)^{5/9} \left(\frac{m}{10^{-22}\ \mathrm{eV}}\right)^{1/3} K^{1/4} M^{1/12}\ \mathrm{GeV}\,, \tag{4.50b}$$

where the index s stand for the single suppressed case. We can give a rough estimate of $m_{w,KK}$ for 10^{-22} eV $\leq m \leq 10^{-19}$ eV by plugging the other parameters accordingly. Hence, we find

$$50\ \mathrm{eV} \lesssim m_{w,KK}^{(s,\mathrm{LVS})} \lesssim 300\ \mathrm{eV}\,, \tag{4.51a}$$

$$0.4\ \mathrm{GeV} \lesssim m_{w,KK}^{(d,\mathrm{LVS})} \lesssim 8\ \mathrm{GeV}\,. \tag{4.51b}$$

Note that we expect these modes, which live at the IR ends of the thraxion-carrying multi-throat, to be nearly completely sequestered. Hence, their interactions with standard model particles are suppressed. At this point we would like to discuss an intriguing possibility regarding the warped KK modes arising from the single-suppressed case. With the scaling found above, a warped KK mode might behave as standard CDM. Therefore, in the single-suppression case we may envision a scenario where the thraxion represents part of the total DM abundance as FDM, while the warped KK mode may constitute the rest. We leave this possibility for future work.

In this setup, the bulk energy scales strongly depend on the moduli stabilisation prescription that we use. In LVS we have that the bulk KK scale ranges in $M_{KK}^{bulk} \in 10^{12} \div 10^{17}$ GeV while the gravitino mass is $m_{3/2} \in 10^{9} \div 10^{16}$ GeV. The constraints on inflation coming from isocurvature perturbations bounds can be shown to be comparable to those related to C_4 and C_2 axions, implying low inflationary scale and undetectable tensor modes.

Finally, we must point out that the results above rely on the internal manifold to be (almost) CY. This is true when the throats in the multi-throat system are all symmetrical and host one thraxion only: in this particular case the thraxion minimises at vanishing vacuum energy. If this symmetry is not met by the system, the thraxion will not necessarily minimise at zero, and thus it could break the CY condition. Moreover, the single-suppressed terms introduced by Kähler moduli stabilisation induce an additional shift on the thraxion vacuum which pushes it further away from the vanishing VEV. This tends to increase the amount of CY breaking and could lead also to a non-supersymmetric vacuum. The fact that vacua at non-zero thraxion VEV break the CY condition implies that the use of the effective 4D supergravity action derived by compactifying type IIB string theory on CY orientifolds is questionable in this situation. However, we could be entitled to keep using the results based on the CY-derived 4D EFT if the CY breaking does not change the EFT (too) drastically. This could happen, for instance, if the thraxion VEV is sufficiently small, so that the manifold is 'close to' the original conformal CY and the CY-based 4D supergravity approach still gives at least the qualitatively right behaviour. Alternatively, the CY-breaking effect of a non-vanishing thraxion VEV may turn out to be largely 'decoupled' from the bulk CY (leaving the largest part of the Laplacian eigenvalue spectrum qualitatively unchanged compared to the actual CY) and stays sequestered in the throats.

4.3 Overall predictions and comparison with experimental constraints

In what follows we wrap up all the results coming from the previous sections and we compare our findings with current and future experimental constraints. As already mentioned, empirical bounds coming from Lyman-α forest, black hole superradiance and ultra-faint dwarf galaxies that are DM dominated put strong constraints on the vanilla FDM model, ruling out a non-negligible area of the parameter space [204–211]. We sum up these bounds together with our results in Fig. 4.8. We show the contributions to DM of our light axionic candidates in the mass spectrum $[10^{-34}, 10^{-10}]$ eV. The DM abundance in (4.8) applies only to axions in the mass range $m \gtrsim 10^{-28}$ eV, i.e. to axions which oscillate before matter-radiation equality. The abundance of the axions oscillating after equality (10^{-33} eV $\lesssim m \lesssim 10^{-28}$ eV) and of those ones that have not yet begun to oscillate ($m \lesssim 10^{-33}$ eV) is taken from [228]. Our analysis was able to provide some sharp relations between the mass and the abundance of ultralight ALPs coming from type IIB string theory. We found that non-negligible fractions of DM can only be given by C_2 and C_4 ALPs or thraxions under the following conditions:

- C_4: 4-form axions can be good FDM candidates in LVS stabilisation only if the ALPs are related to cycles parametrising the overall volume. The overall extra-dimensions volume needs to be small $\mathcal{V} \in 10^2 \div 10^4$ and $g_s \sim 0.2$. We considered for simplicity the case where the ALP mass is given by non-perturbative corrections coming from ED3-instanton and gaugino condensation on a stack of $N \leq 10$ branes. Results coming from higher numbers of branes do not show any significant difference and are highly constrained by Eridanus-II and black hole superradiance bounds. These particles can represent $\sim$10% of DM when their mass is $m \sim 10^{-22}$ eV.

- C_2: they can represent FDM in LVS when there is non-vanishing intersection between the harmonics C_2 and the volume cycle in the extra dimensions. In LVS, if the C_2 axions acquire a mass through ED3/ED1 bound state instantons, these particles can represent nearly 50% of DM when their mass is around 10^{-23} eV. In this case the overall extra-dimension volume needs to be small $\mathcal{V} \sim \mathcal{O}(10^2)$. If, on the other hand, these axions gain mass due to pure ED1 effects, in LVS they can represent 20% of DM if their mass $\sim 10^{-21}$ eV (for volumes $\mathcal{V} \sim 10^4 \div 10^5$), while in KKLT they can represent up to 100% of DM for masses $m \sim 10^{-25} \div 10^{-24}$ eV (for volumes $\mathcal{V} \sim 10^2 \div 10^3$). Therefore, we can conclude that C_2 axions in KKLT are too light to be FDM.

- Thraxions: these particles can be FDM candidates in LVS only. Here the allowed parameter region is wider compared to the previous cases. The CY volume can vary between $\mathcal{V} \in 10^2 \div 10^8$ and thus $g_s \in 0.05 \div 0.2$. These ALPs can represent 20% of DM if $m \sim 10^{-21}$ eV and 100% of DM when $m \in 10^{-25} \div 10^{-23}$ eV.

Note that scaling the WGC relation up or down amounts to shifting a given axion abundance band up or down.[5] Generically, this implies that the bands coming from string axions satisfying but not saturating the WGC constraint will place below the C_4 constraint band in Fig. 4.8 (which also means, most stringy axions except the ones considered in this work will give negligible FDM abundance). Given

[5]Consider an axion satisfying $Sf = \alpha M_P$ with $0 < \alpha < \infty$. Given the axion mass in Eq. 4.6, we see that

$$S = -2\log(m) + \mathcal{O}(\log^2(m), \log(\alpha))\,,$$

and the axion DM abundance in Eq. (4.8) satisfies

$$\frac{\Omega_\phi h^2}{0.112} \propto m^{1/2} f^2 = m^{1/2}\frac{\alpha^2}{S^2} \sim \frac{m^{1/2}}{(\log(m))^2} \times \alpha^2 \left(1 + \mathcal{O}(\log^2(m), \log(\alpha))\right)\,.$$

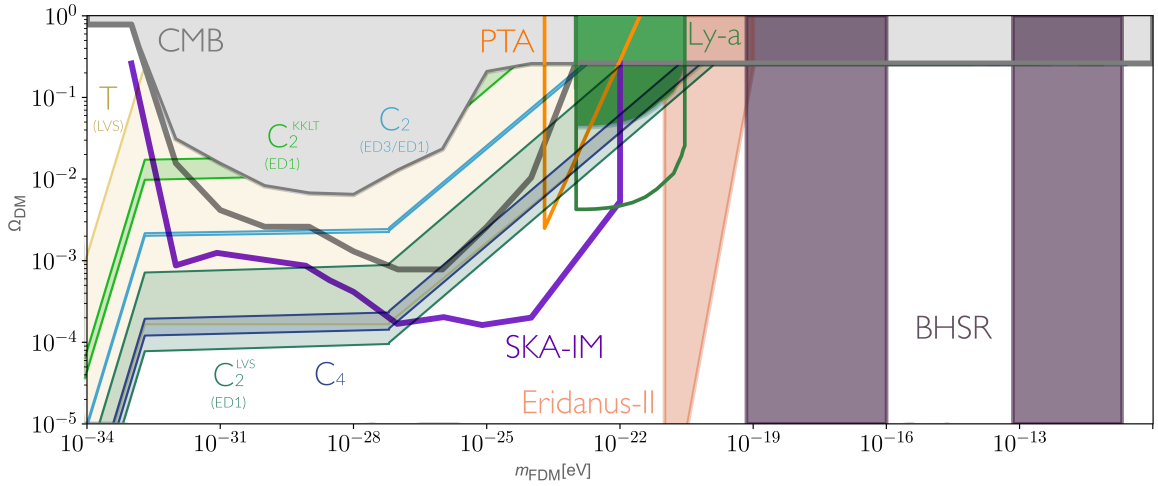

Figure 4.8: Mass and total DM abundance predictions for large cycles C_4 axions (blue stripe), C_2 axions (light blue stripe for ED3/ED1 effects, dark/light green stripe for pure ED1 effects in LVS/KKLT), and thraxions in LVS (sand stripe) stabilisation. These results are compared to the current experimental bounds coming from CMB (solid grey area), Lyman-α forest (solid red), Eridanus II (solid pink area) observations and with theoretical predictions based on Black Hole Superradiance (solid purple area). Future experimental bounds coming from CMB (grey), Lyman-α forest detection (red), Square Kilometre Array (brown) and Pulsar Timing Arrays (orange) are identified with solid lines. The reported experimental bounds were adapted from the recent review on ultralight bosonic dark matter [211]. We refer the reader to that text and to the references therein for more details and extended bibliography. Note that axions moderately evading the WGC (thraxions and C_2 axions) are those representing the lightest FDM candidates.

the variety of possible ultralight axionic DM candidates, it is natural to ask whether some of them are more probable than others. Recent works have been analysing the relation between the distribution of string vacua, the axion masses and the decay constants [229, 230]. Despite this is far beyond the scope of this discussion, we try to provide a very short description of how the number of vacua varies across our FDM candidates. In LVS, the relation between the overall volume and the string coupling leads to the following differential relation

$$\mathrm{d}\mathcal{V} \simeq -\frac{e^{1/g_s}}{g_s^2}\mathrm{d}g_s\,. \tag{4.52}$$

Given that the distribution of g_s was shown to be uniform [229, 231] we can write $\mathrm{d}g_s \sim \mathrm{d}N$, N being the number of flux vacua, so that

$$\mathrm{d}N \sim \mathrm{d}\left(\ln\mathcal{V}\right)^{-1}\,. \tag{4.53}$$

Instead, in KKLT the relation between the tree-level superpotential and the overall volume (considering a single Kähler modulus for simplicity) leads to

$$\mathrm{d}\mathcal{V} \sim -\frac{3}{2a}\frac{\mathcal{V}^{1/3}}{W_0}\mathrm{d}W_0\,. \tag{4.54}$$

The W_0 distribution is assumed to be uniformly distributed in the complex plane so that $\mathrm{d}|W_0|^2 \sim |W_0|\mathrm{d}|W_0| \sim \mathrm{d}N$ for standard values of W_0 [219] while it scales as $|W_0| \sim e^{-1/g_s}$ for exponentially suppressed values of W_0 [232–234]. This implies that in KKLT

$$\mathrm{d}N \sim \mathrm{d}\left[e^{-2a\mathcal{V}^{2/3}}\right] \qquad \text{for not too small } |W_0|\,,$$

$$\mathrm{d}N \sim \mathrm{d}\left[\mathcal{V}^{-2/3}\right] \qquad \text{for exponentially small } |W_0| \ .$$

The relation between the overall volume and the axion mass for large cycles C_4 axions, C_2 axions and thraxions in KKLT scenario scales as $m \sim \exp(-\frac{a}{2}\mathcal{V}^{\alpha})$, $\alpha = 1/3,\, 2/3$. Instead, for thraxions in LVS it reads $m \sim c/\mathcal{V}^{11/6}$, $c \in \mathbb{R}^+$. This implies that the relation between the number of vacua and the mass of the ALP is given by:

$$\begin{aligned}
&\mathrm{d}N \sim \mathrm{d}\left[\ln\left(\frac{2}{a}\ln(m^{-1})\right)\right]^{-1} && \text{for } C_2/C_4 \text{ axions in LVS}\,,\\
&\mathrm{d}N \sim \mathrm{d}\left[\ln(m^{-1})\right]^{-1} && \text{for thraxions in LVS}\,,\\
&\mathrm{d}N \sim \mathrm{d}\left[m^4\right] && \text{for thraxions in KKLT}\,,\\
&\mathrm{d}N \sim \mathrm{d}\left[\frac{2}{a}\ln(m^{-1})\right]^{-1} && \text{for thraxions in KKLT } (W_0 \sim e^{-1/g_s})\,.
\end{aligned}$$

where we listed only those results corresponding to viable FDM candidates. We can conclude that ALPs relying on LVS stabilisation do not show a strongly preferred mass value, given that here the number of vacua distribute at most logarithmic with respect to the thraxion mass. On the contrary, thraxions living in the KKLT setup show a polynomial distribution for fairly large values of W_0, stating that higher thraxion masses are more likely to appear in the string landscape. This distribution then flattens out towards a logarithmic distribution for exponentially suppressed W_0 values.

We would like to stress that our results provide scaling relationships for the simple setups analysed here. A more complete and general treatment of the problem as e.g. the number of moduli increases, also considering different geometries, is well beyond the scope of this discussion. Nonetheless, we would like to give a hint about why we believe our results do not substantially change as the complexity of the extra dimensions increases. Thraxion fields depend on the CY geometry only via the overall volume, therefore changing the compactification manifold do not significantly affect their result. On the other hand, C_4 axions can be good FDM candidates if and only if they are the axion partners of Kähler moduli parametrising the overall volume $\mathcal{V}$ so that they nearly saturate the WCG bound. Although it is not possible to write the most generic volume of a CY in terms of 4-cycles (the change from 2-cycle variables to 4-cycle volumes enforced by the O7-orientifold action is in general not feasible analytically), the number of moduli entering the volume with a positive sign must be finite. Furthermore, the Kähler cone conditions tend to create a hierarchy between the volumes of the 2-cycles thus reducing the number of very large cycles. Moreover, the presence of many moduli will have to lower the value of Sf, as they increase the value of the total volume [235]. It is therefore quite reasonable to think that as the complexity of the extra dimensions increases, the C_4 axions are naturally moved towards lower masses, away from the desired value to represent FDM that was shown to be exponentially sensitive to $\mathcal{V}$. Similar arguments also apply to the case of C_2 coupled to C_4 through ED3/ED1-instanton interactions. In fact, this effect tends to make C_4 and C_2 axions almost degenerate in mass.

4.4 Discussion

In this chapter, we systematically dissect the long-standing lore that string axions can represent viable FDM candidates. We focus on the string axiverse coming from type IIB string theory compactified down to $4d$ on a CY orientifold with O3/O7-planes. After studying the properties of the whole axionic spectrum, we restrict the discussion to those axions that can represent good FDM candidates. In simple

setups without alignment, tuned parameters and other non-trivial dynamical effects, we find that this request is closely related to the WGC for axions and implies that FDM saturates the bound $Sf \sim M_P$. The best candidates turn out to be C_2, C_4 closed string axions and thraxions.

LVS stabilisation naturally gives rise to ultralight C_4 and C_2 axions. Indeed, being the LVS vacuum non-supersymmetric, these axions can be many orders of magnitude lighter than their volume modulus partners. On the contrary, KKLT stabilisation can only give rise to ultralight C_2 axions in presence of ED1-instanton corrections but an accurate computation reveals that these particles are too light to be FDM. Thraxions are axionic modes which stay ultralight regardless of the moduli stabilisation prescription chosen, given that their mass scaling is mostly dominated by the warp factor of the multi-throat systems they live in.

Our results show that string axions can exist in the FDM window allowed by experiments, but this translates into requiring specific properties of the compactification. As mentioned before, for this aim LVS is the preferred stabilisation procedure. For the harmonic zero mode C_2 and C_4 axions to fit the FDM window, the results suggest that the CY volume should be 'smallish' (with respect to LVS standard volumes). The masses and decay constants are basically insensitive to all the other microscopical parameters, making our predictions quite sharp. We also checked the scenario where more C_4 ultralight axions are present by considering a fibred CY. While in general cases heavier axions represent considerably higher DM fractions, in case of isotropic compactifications if we choose similar internal parameters for all the axions, i.e. same rank of gauge group and prefactor coming from complex structure moduli stabilisation, we end up having multiple FDM particles. In this specific case, the relative abundance of the FDM particles is determined by their Sf value. Axions that come closer to saturating the WGC bound will represent higher percentages of DM.

For the C_2 axions, the situation is more involved. After checking many possibilities which can give rise to ultralight masses for these modes, we find that the only viable FDM scenarios are the case of a pure ED1 or an ED3/ED1-bound state instanton wrapping the cycle supporting the CY volume. In the former case we have that a FDM C_2 axion is compatible with volumes $\mathcal{V} \sim 10^4$, implying that an eventual DM contribution coming from the volume axion would be suppressed, this particle being parametrically lighter (potentially constituting dark radiation). In the case of ED3/ED1 effects, C_2 axions can be ultralight only in presence of very light C_4 axions. Due to different instanton properties, this setup allows for a moderate mass hierarchy such that here the heavier particle, i.e. the C_4 axion, constitutes the subdominant FDM fraction in the DM halo.

Then, we analyse the predictions for the masses and decay constants as a function of the DM abundance for the thraxions. These axionic modes allow for a wider range of masses, making them easier to fit the FDM window. We study both Kähler moduli stabilisation scenarios (KKLT and LVS), as well as the two possible regimes arising there: i) the thraxion mass keeps its double-suppression from warping even after Kähler moduli stabilisation; or ii) it receives corrections from Kähler moduli stabilisation which cut the power of the warp factors suppressing the thraxion mass by half. Surprisingly, our results for thraxion FDM partially decouple from these details, but show that only in LVS thraxions can behave as FDM. The most prominent requirement is that in LVS the volume of the bulk CY should be rather big, as opposite to the cases discussed previously. A few caveats are in order concerning our results for thraxion FDM. Hence, while they appear to span a large portion of the parameter space in Fig. 4.8, we leave questions as to their generality for the future.

Finally, we compared our results with current astrophysical and experimental bounds. For each scenario analysed, we discussed the relation between our predictions and the exclusion bands. Moreover, we provided a preliminary discussion of the vacuum distribution for the mass of such axions in the

string landscape. The results show that our FDM candidates from String Theory have a very flat mass distribution for almost all cases studied. It is particularly exciting that our predictions show overlap with the regions in reach of future experiments. Hence, if at some point axions were to be found at these mass scales, we may be able to learn from the data about the type of axion detected, as well as its couplings, and potentially even something about their underlying microscopic theory.

Given this comparison, we wish to comment in passing on a further observation. Take a final look at the FDM abundance $\Omega_{\rm FDM} \sim \sqrt{m_\phi} f^2 \theta^2 \sim e^{-S/4} f^{3/2} \theta^2$. From this expression we see that for all axions with $f > H$ during inflation, which get populated via the misalignment mechanism $\langle \theta^2 \rangle \sim \pi^2/3$, generically heavier axions acquiring their mass from instantons roughly saturating the WGC bound $Sf \lesssim M_P$ dominate the DM content. An exception arises if e.g. two different axions acquire masses such that the heavier of the two acquires its mass from an instanton which does not saturate the WGC ($Sf < M_P$), while the instanton giving mass to the lighter axion saturates it ($Sf \simeq M_P$). A simple example for the generic case would be e.g. the two C_4 axions from the large and the blow-up 4-cycle of a 2-moduli LVS compactification, while the exception is seen e.g. for the case of the C_4-C_2 2-axion system arising from the ED3-ED1 bound state instanton on the volume 4-cycle. From this, it becomes clear that for the generic case the heavier axion states would completely dominate the dark matter content. An eventual detection of a sizable FDM fraction would therefore imply one of two possible predictions for the high-scale setup of a UV model: i) all the heavier WGC saturating axion states have $m > H$ during inflation, and there is a desert of axion states between the FDM mass scale and the inflationary H. ii) Avoiding the desert requires either fast decay of the heavy $m < H$ axion states significantly before BBN, or an anthropically selected very small heavy axion misalignment angle. Hence, a detection of FDM would put serious constraints on the structure of the allowed UV completion.

Chapter 5

Conclusions and Outlook

String Theory is the best candidate we have for a theory of Quantum Gravity. So far, it has proven to be a solid framework from which we can attempt to explain the phenomena that do not find a solution in the Standard Model alone. In this thesis, we explored its phenomenology, in order to understand both how we could detect string-theoretical signatures in the sky, and also what consequences experimental bounds would imply for the UV-completed theory. For this purpose, we provided a detailed comparison between the predicted parameter space for ultralight axions coming from type IIB string theory and the current astrophysical bounds on fuzzy dark matter [1]. Most interestingly, it turns out that a large portion of this space will be inspected by the next generation of experiments. Indeed, this is very exciting and fascinating, not only because a possible detection would favour String Theory as the right UV theory, but also because it would give us hints to understand the right way to connect String Theory with our world. By this we mean in particular the features that the right compactification should have, and how the supersymmetric partners of the axions should be stabilised.

To widen the possibilities of this search, we initiated the systematics for the phenomenology of thraxions [2, 76], studying how they fit in the low-energy EFT when all moduli receive a potential. These axionic modes are even lighter than closed string axions, allowing for new features in the axiverse phenomenology. So far, we have inspected how they behave as dark matter candidates [1], but given their unique properties they could serve as dark radiation or dark energy as well.

String Theory also plays a crucial role during the early history of our universe, where Quantum Gravity effects kick in. In particular, it should be able to explain the accelerated expansion the universe underwent some fractions of seconds after the initial singularity. While we have evidence for this inflationary epoch, we lack the precise model (and in particular the field) responsible for such effect. Axions have long been pointed out as good inflaton candidates because of their shift symmetry, which allows for prolonged slow-roll inflation while protecting the axion mass from radiative corrections. In this spirit, we have proposed a new model of small-field axion inflation [4] which builds up from Linde's original proposal called hybrid inflation. Moreover, we have pointed out how the topological data of the compactification space can help create a good inflationary trajectory, as well as possibly a de Sitter uplift of AdS vacua [3]. This is based on the winding inflation model of [178, 191], there the inflationary direction is realised along a winding trajectory in the field space of two axionic fields originating from the complex structure moduli sector. It would be of great interest to build an explicit model in the context of LVS stabilisation [52], where an inflationary sector together with the uplift to positive cosmological constant can be realised following [3].

Recently, the Swampland program has put constraints on large-field models of inflation (and also on

the possibility to derive de Sitter from String Theory at all). These conjectures also apply to axions, and one of their major consequences is the restriction of the decay constant to sub-Planckian values. However, there are some ways in which (some of) these conjectures can be evaded, as we argue in [1, 2], by relying on the *effective* decay constant. Indeed, a sub-Planckian decay constant would limit the phenomenology of axions, hence parametrically extending it via e.g. flux-enhancement or monodromy gives more space for model building. For example, a future detection of axions evading the strong forms of these conjectures would confirm experimentally that to have a UV-completable EFT, one needs the presence of *at least* one axion satisfying them.

Complementary to this, we propose a *lower* bound on the decay constant based on the Festina Lente bound [72, 73], which depends on the Hubble parameter and is valid in a quasi-de Sitter background, namely during inflation and at the present time. Our bound shows how the decay constant of a fundamental axion can never vanish in a consistent EFT, supporting existing arguments based on distances in moduli spaces [11]. Moreover, our result has consequences on inflationary observables of some axion inflation models, as e.g. axion monodromy inflation.

We conclude by stressing how important it is to keep proposing connections between String Theory and observational signatures. The recent detection of gravitational waves opened up a brand-new window that is going to be intensively explored in the next years, and Stage 4 of ground based CMB surveys as well as the LiteBird satellite will allow studying in great details the early history of our universe. It is an exciting time and a huge opportunity for string phenomenology. Moreover, the swampland program is helping understand the most plausible ways to carry out UV-completable model building. I believe that in the near future, astrophysical data and theoretical motivations will converge and point out the best UV-completed candidate theory for our universe. I am looking forward to that moment.

Acknowledgments

Alexander, thank you for giving me this opportunity and for constantly believing in me. The time we spent together was always interesting, both remotely and especially in person. Thanks for sharing your insights on String Theory, inflation, society and Sci-Fi: discussing with you is always fascinating.

Alessandro and Federico, thank you for our collaborations and for the uncountable hours spent online together. Federico, I am truly in debt for the amount of things you explained to me, especially during my first months at DESY. Alessandro, thanks for being the most amazing unofficial officemate, and for always finding the time to listen to me, would it be about physics or life. I am extremely grateful for the many ways you helped me and for your friendship, you made my last year at DESY memorable. Unfortunately, I am not good with rhymes.

Jacob, thank you for sharing your million ideas. Your curiosity is marvellous and your perseverance is a source of inspiration for me. I am so in debt for all you taught me and for making me passionate about modular forms. You made it in the end.

Rafael, thank you for our tea breaks and for your small seminars about random topics, discussions with you are always the most enjoyable. I am glad our paths crossed in my last year.

Veronica, thank you for keeping me always with a foot in real life, and for providing me with a different perspective, not only on physics. I will remember our night in Florence forever.

I would also like to thank Cesar, Craig, Daniel and Timo. You made every lunch break amusing and every exchange of ideas fascinating. It was a pleasure for me to share ideas and jokes with you. In particular, thanks Daniel for translating the abstract, and thanks Timo for sharing your knowledge and your thoughts with me when I needed help.

Thank you Gerben, Michele and Yvette for our collaborations, I am grateful for our discussions and their outcomes, it was a pleasure working with you.

Finally, I would like to thank all the Theory Group at DESY, in particular the PhD students and my officemate Philine. Our time together was short, but still we managed to have amazing adventures.

Grazie mamma e papà, tutto questo non sarebbe stato possibile senza il vostro costante supporto e la vostra fiducia nelle mie scelte. Grazie Carlotta e Echo per rallegrarmi in ogni momento. Nonostante la lontananza, siete sempre incredibilmente vicini.

Enrico, grazie per aver preso quell'aereo. Grazie di tutto.

Appendix A

Complete Intersection Calabi-Yaus

In this appendix, we firstly review some relevant facts about complete intersection Calabi-Yau manifolds in an ambient space $\mathcal{A}$ given by the product of projective spaces $\mathbb{P}^{n_1} \times ... \times \mathbb{P}^{n_s}$ [236, 237]. A projective space of $\dim_{\mathbb{C}} = n$ is defined as

$$\mathbb{CP}^n \simeq \frac{\mathbb{C}^{n+1} \setminus \{0\}}{[z_1, ..., z_{n+1}] \sim \lambda [z_1, ..., z_{n+1}]}, \tag{A.1}$$

where $z_1, ..., z_{n+1}$ are $n+1$ homogeneous coordinates of $\mathbb{C}^{n+1}$ and $\lambda \in \mathbb{C}^\star$. The quotient is an equivalence relation which can be used to rescale the homogeneous coordinates and set them to a certain value. This means that in a given patch $U_i \simeq \{z_i \neq 0\}$, $i = 1, ..., n+1$ we can perform the rescaling

$$[z_1, ..., z_{i-1}, z_i, z_{i+1}, ..., z_{n+1}] \sim \left[\frac{z_1}{z_i}, ..., \frac{z_{i-1}}{z_i}, 1, \frac{z_{i+1}}{z_i}, ..., \frac{z_{n+1}}{z_i}\right] = [x_1, ..., x_n]\,. \tag{A.2}$$

The x_i coordinates on the r.h.s. are called affine coordinates. The projective space is equipped with the Fubini-Study metric, which is defined as

$$g_{i\bar{j}} = \frac{1}{(1 + |\mathbf{x}|^2)^2} \begin{pmatrix} 1 + |\mathbf{x}|^2 - |x_1|^2 & -\bar{x}_1 x_2 & \cdots & -\bar{x}_1 x_n \\ -\bar{x}_2 x_1 & 1 + |\mathbf{x}|^2 - |x_2|^2 & \cdots & -\bar{x}_2 x_n \\ \vdots & \vdots & \ddots & \vdots \\ -\bar{x}_n x_1 & -\bar{x}_n x_2 & \cdots & 1 + |\mathbf{x}|^2 - |x_n|^2 \end{pmatrix}, \tag{A.3}$$

where we have set the Kähler modulus to one. Note that for $\mathbb{CP}^n$, $\mathrm{d}J = 0$, that is the projective space is Kähler. This can be proven by considering a patch, computing the associated Fubini-Study metric and applying the exterior derivative to J, remembering that $\mathrm{d} = \partial + \bar{\partial}$ since the Kähler form is a complex one. Then it goes that if for one patch we find that $\mathrm{d}J = 0$, then this is true for every other patch.

An useful property of the Fubini-Study metric is that, in this normalization, the integral over the manifold $\mathcal{M}$ of the Käler form J is always equal to one. Therefore, computing the volume of the manifold becomes rather easy, as it is defined as

$$\mathcal{V} = \int_{\mathcal{M}} J \wedge ... \wedge J. \tag{A.4}$$

We saw that projective spaces are Kähler, now we want to understand whether they can be CY or not. One requisite for a manifold to be CY is to have vanishing first Chern class. For this purpose, we should first introduce the definition of Chern class for a given manifolds. The k-th Chern class $c_k(\mathcal{M})$

is an element of the cohomology $H^k_d(\mathcal{M})$ defined from the expansion of the total Chern class

$$c(\mathcal{M}) = 1 + \sum_j c_j(\mathcal{M}) = \det(1+\mathcal{R}) = 1 + \mathrm{tr}\mathcal{R} + \mathrm{tr}(\mathcal{R}\wedge\mathcal{R} - 2(\mathrm{tr}\mathcal{R})^2) + ... \tag{A.5}$$

where $\mathcal{R}$ is the matrix valued curvature 2-form $\mathcal{R} = R^i_{jk\bar{l}}\mathrm{d}x^k \wedge \mathrm{d}\bar{x}^{\bar{l}}$. It is direct to see that if the manifold X has vanishing Ricci tensor, then the first Chern class, being the trace of the curvature 2-form, also vanishes. The other direction, that is if a manifold has vanishing first Chern class then it admits a Ricci-flat metric, is ensured by Yau's theorem. This is the point that is useful for us, because one can show that for $\mathbb{CP}^n$, the Chern class is given by

$$c\left(\mathbb{CP}^n\right) = (1+J)^{n+1} = 1 + (n+1)\,J + ... \tag{A.6}$$

where the sum goes on until the n-th form. From (A.6) one can directly see that for $\mathbb{CP}^n$ the first Chern class never vanishes. Then, a projective space for any n is never a CY.

Before moving forward and studying how to build proper CY manifolds starting from projective spaces, let us introduce another useful definition. First, by top Chern class we refer to the highest class that one can have on a given manifold, so that it has the maximum dimension a form can have on that manifold. Thus, if we integrate the top Chern class, we have to do it over the whole manifold. This in turn gives a topological invariant called the Euler characteristic

$$\chi\left(M_n\right) = \int_{M_n} c_n\left(M\right)\,. \tag{A.7}$$

Given the ambient space $\mathcal{A} = \prod_i \mathbb{P}^{n_i}$, where $i = 1, \ldots, s$, a compact Kähler 3-fold can be constructed as the zero-locus of k homogeneous polynomials $p_j\left(z\right)$ in $\mathcal{A}$, subject to the constraint

$$\sum_{i=1}^{s} n_i - k = 3\,. \tag{A.8}$$

Each p_j is characterized by its multi-degree q^i_j, where $j = 1, \ldots, k$, which specifies the degree in the homogeneous coordinates of each $\mathbb{P}^{n_i}$. A CY constructed in this way is referred to as Complete Intersection Calabi-Yau, or CICY. A convenient way to encode the above information is by means of the configuration matrix

$$\left[\begin{array}{c|ccc} \mathbb{P}^{n_1} & q^1_1 & \cdots & q^1_k \\ \mathbb{P}^{n_2} & q^2_1 & \cdots & q^2_k \\ \vdots & \vdots & \ddots & \vdots \\ \mathbb{P}^{n_s} & q^s_1 & \cdots & q^s_k \end{array}\right]\,. \tag{A.9}$$

If we require the zero-locus of the p_j to be a CY manifold, the vanishing condition for the first Chern class imposes

$$n_i + 1 = \sum_{j=1}^{k} q^i_j \quad \forall\, i = 1, ...s\,. \tag{A.10}$$

Let X be a CICY with ambient space $\mathcal{A}$. A configuration matrix representing a CY X for which $h^{1,1}(X) = h^{1,1}(\mathcal{A})$ is said to be favourable. When this happens, all the divisors of the CICY X descend directly from the ones of the ambient space $\mathcal{A}$.

One could think that the construction outlined above leads to infinitely many topologically distinct CYs, as one could in principle increase both the number of $\mathbb{P}^{n_i}$ factors and their dimensions, and add

more equations accordingly. However, this is false. It was shown [238] that all topologically distinct CYs realizable with this construction can be obtained from ambient spaces for which both the number s of $\mathbb{P}^{n_i}$ factors and the size of the n_i is bounded from above. Therefore, the full set of topologically distinct CICYs can be obtained from a set of finitely many configuration matrices. A database of 7890 configuration matrices was famously built in [217] and it was shown that such a database is complete, in the sense that any other configuration matrix not present in the database will describe a CY topologically equivalent to the one already present in the list.

However, not all the 7890 configuration matrices in the old CICY database are favourable, just 4896 of them are. Favorability is not an intrinsic property of the CY X itself, but rather depends on the choice of the configuration matrix used to describe X. In the work of [239] the old CICY database was improved: for almost all non-favourable configuration matrices in the old CICY database, a new configuration matrix representing the same CY was found, such that the new configuration matrix is now favourable. This was achieved by chains of ineffective splittings, performed on the old configuration matrix [239]. The number of favourable configurations was then pushed up to 7842. The remaining CICYs, which still does not admit a favourable configuration matrix, admit nevertheless a completely different description as a single hypersurface in a product of two del Pezzo surfaces, $\mathrm{dP}_m \times \mathrm{dP}_n$ and a theorem by Kollár [240] guarantees that such description is favourable. Furthermore, out of the 7842 favourable CICYs, 22 of them are either 6-tori, or direct products of K3 and 2-tori. A new database was created by keeping only the 7820 favourable and non-product CICYs.

New Manifolds from Splitting Matrices: In the following, we will briefly describe how to get new configuration matrices from old ones via chains of contractions and splittings. We can exchange one configuration matrix with another by means of the determinant splitting/contracting, which can be summarized as

$$\left[\begin{array}{c|cccc} \mathbb{P}^n & 1 & 1 & \cdots & 1 & 0 \\ X & u_1 & u_2 & \cdots & u_{n+1} & M \end{array}\right] \longleftrightarrow \left[\begin{array}{c|cc} X & \sum_{a=1}^{n+1} u_a & M \end{array}\right], \tag{A.11}$$

where X is an arbitrary product of projective factors, u_a are column vectors with as many entries as the factors in X, and M is a matrix. Let us call the manifold on the r.h.s. $\mathcal{M}$ with Euler number χ and the manifold on the l.h.s. $\widetilde{\mathcal{M}}$ with Euler number $\tilde{\chi}$. One can show that after splitting a configuration matrix, we have a relation between their Euler numbers which reads $|\tilde{\chi}| \leq |\chi|$. When the two Euler numbers are equal, we have an ineffective splitting, that is $\mathcal{M}$ and $\widetilde{\mathcal{M}}$ are actually the same manifold. Instead, when after the splitting of a configuration matrix we find that $|\tilde{\chi}| < |\chi|$, we made an effective splitting, which in turn means that $\mathcal{M}$ and $\widetilde{\mathcal{M}}$ are topologically district manifolds. This was recognized to be a conifold transition between the two manifolds [77, 78, 241]. This is the reason why $|\tilde{\chi}|$ is always smaller than $|\chi|$: $\tilde{\mathcal{M}}$ is the resolved side of the conifold transition, during which some 3-cycles of $\mathcal{M}$ have shrinken and were replaced by 2-cycles.

Redundancies in the CICYs: A natural question that can be asked is when two CY manifolds are the same. In this discussion, every time we say that two CY are the same, we mean that they are diffeomorphic as real manifolds. A famous theorem by Wall [242] implies that two simply-connected, closed Calabi-Yau 3-folds X and Y are isomorphic as real manifolds, if

1. The Hodge numbers agree, namely $h^{1,1}(X)$=$h^{1,1}(Y)$ and $h^{2,1}(X)$=$h^{2,1}(Y)$.

2. There exists a choice of base in $H^4(X, \mathbb{Z})$ given by D_i, $i = 1, \ldots h^{1,1}(X)$, and a choice of base

in $H^4(Y,\mathbb{Z})$ given by $\hat{D}_i$, $i = 1,\dots h^{1,1}(Y)$ such that $\int_{D_i} c_2(X) = \int_{\hat{D}_i} c_2(Y)$, where $c_2(X)$ (resp $c_2(Y)$) is the second Chern class of (the tangent bundle) of X (resp Y).

3. With the same choice of base of the point above for $H^4(X,\mathbb{Z})$ and $H^4(Y,\mathbb{Z})$ the triple intersection numbers agree, namely $\int_X D_i \cdot D_j \cdot D_k = \int_Y \hat{D}_i \cdot \hat{D}_j \cdot \hat{D}_k, \quad \forall i,j,k = 1,\dots h^{1,1}(X) = h^{1,1}(Y)$.

Clearly, if two real manifolds are diffeomorphic, then this implies that also they will be homeomorphic as topological spaces, therefore topologically equivalent.

It is worth stressing that the choice of a configuration matrix for a given CICY X is not unique, in the sense of Wall's theorem stated above. The same CY manifold X can be realized in multiple ways by different configuration matrices. Nevertheless, different choices of the configuration matrix for the same CICY X can make more explicit (or hide) different features of the CY itself. For example, the number of complex structure deformations visible as versal deformations of the polynomial equations, and the fibrations trivially visible from the configuration matrices, both depend on the choice of the configuration matrix for X.

The new CICY database, despite being maximally favourabilised, is still not a list of unique Calabi-Yau manifolds. It is therefore important to check for redundancies, to provide for a minimal list of topologically distinct and favourable CICYs. On the other hand, the existence of redundancies in the original CICY database was realized many years ago [30,78,243,244], and many of them were identified in [245], within the subset of the 4896 favourable CICYs of the old database. In such case, the check of the redundancies was done using Wall's theorem [242]: the authors of [245] checked whether given two CICYs X and Y with identical Hodge numbers, they could find a change of basis in $H^4(X,\mathbb{Z})$ and $H^4(Y,\mathbb{Z})$ such that also the second Chern classes and triple intersection numbers agree. In particular, they focused on the change of variables given by permutations of the divisors.[1]

We perform a similar scan within the new CICY database. Given two CICYs with different configuration matrices, the first trivial check is to look at their Hodge numbers. If they agree, we can check if a permutation of the basis elements of $H^4(X,\mathbb{Z})$ could exist, such that the second Chern class and the triple intersection numbers of X computed in the new basis agree with those of Y. We find that there are three qualitatively distinct cases:

1. The CICYs that already have Hodge numbers equal, (the integrals of) c_2 (over the base elements of H^4) equal, and also the intersection numbers equal. No change of basis is needed, and Wall's theorem trivially applies.

2. The CICYs that have all Hodge numbers equal and (the integrals of) c_2 (over the base elements of H^4) equal. The triple intersection numbers can be made equal with a permutation of the basis elements of H^4 that leaves (the integrals of) c_2 (over the basis elements of H^4) unchanged.

3. Finally, the CICYs that have only Hodge numbers equal, but both (the integrals of) c_2 (over the basis elements of H^4) and the intersection numbers can be made equal with a permutation of the basis elements of H^4. These are the most general set.

We list the tuples of redundant CICYs, divided by $\tilde{h}^{1,1}$, in appendix C of [3]. In such a list, each parenthesis contains all CICYs that are redundant by a permutation of the basis elements in H^4. For

[1] An alternative way to select redundant CICYs was also proposed in [246]. There, not only permutations of the basis elements of $H^4(X,\mathbb{Z})$ and $H^4(Y,\mathbb{Z})$ were considered, but also linear transformations with rational coefficients. This allowed the authors to claim the existence of some other redundancies, by finding a suitable new basis for $H^4(X,\mathbb{Q})$ and $H^4(Y,\mathbb{Q})$, which would now match the triple intersection number and second Chern class. However, it is not clear to us why Wall's theorem immediately applies in this case. For this reason, we decided to stick to linear changes of basis with integer coefficients, and only work with integral cohomology. Even less generally, we restrict ourselves to looking for permutations of the divisors.

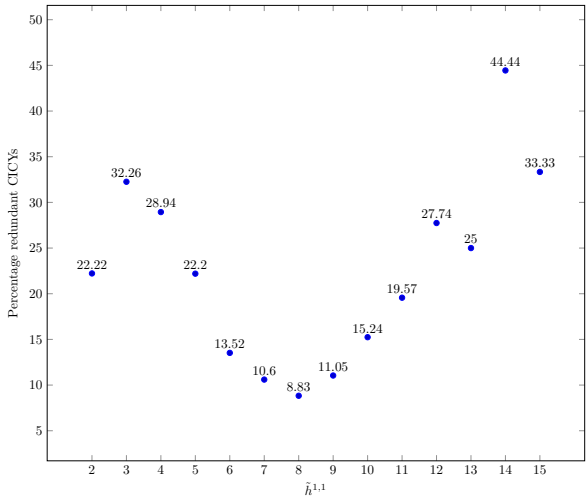

Figure A.1: Distribution of redundant CICYs per $h^{1,1}$ normalized for the number of favourable CICYs at fixed $h^{1,1}$.

some of the CICYs in the cases above, we also give the explicit change of basis matrix. The list of such matrices can be accessed at link.

We found all redundancies up to $h^{1,1} = 13$. We have not been able to check the most general transformations for the CICYs with $h^{1,1} = 15$ (which are 15) and for those with $(h^{1,1}, \tilde{h}^{2,1}) = (14, 16)$ (which are 14). However, even for $h^{1,1} = 14, 15$ we managed to find the right change of basis also for these CICYs belonging to the case 2 above.

We find around 536 equivalence classes involving a total of 1169 non-product favourable CICYs. This can be compared with the number of equivalence classes found in [245] and in [246]. We find a larger number of redundancies, essentially for two reasons. Firstly, we consider the new CICY database, while in [245] the authors perform this scan on the old CICY database. Since more CICYs X_i are now favourable, it is easier to study change of basis in $H^4(X_i)$, since now $H^4(X_i) \simeq H^4(\mathcal{A}_i)$. Secondly, we push our scan to $h^{1,1} = 13$ while the authors of [246] stopped at $h^{1,1} = 6$.Therefore, we conclude that at least 6651 CICYs are topologically distinct, and thus could lead to phenomenologically distinct models.

Normalizing the number of redundant non-product favourable CICYs per $h^{1,1}$ by the number of total non-product favourable CICYs with the same $h^{1,1}$ we get the percentage of redundant CICYs in the plot shown in Figure A.1. It is very tempting to speculate that for some reasons the percentage number of redundant CICYs per $h^{1,1}$ lies on a parabola with minimum at $h^{1,1} = 8$. This is also beautifully consistent with the following fact. Right now we are only considering redundancies in the set of favourable CICYs, however, for $h^{1,1} = 19$ there are 15 non-favourable CICYs which are well known to be all redundant, and all of them are the Schoen manifold [239]. Therefore, the percentage of redundant CICYs at $h^{1,1} = 19$ is 100%. Adding to Figure A.1 this extra case, we would have a point that exactly lies on the interpolating parabola found from the points in the plot.

We stress the fact that for $h^{1,1} = 15$ we have not checked all possible combinations to find redundancies. It is possible that there are more redundant CICYs than the 5 we have found. Looking at Figure A.1, the interpolation of the shape of the distribution would suggest that there might be over 50% of the CICYs with $h^{1,1} = 15$ which are redundant. There are also 14 CICYs with $(h^{1,1}, h^{2,1}) = (14, 16)$ that have not been scanned completely for a generic transformation (i.e. the one belonging to the case 3 in the previous list), but, using the same argument of the interpolation, we may expect that there are no more redundancies in that sector.

It is also possible that some more redundancies can be found by allowing for a more general linear change of base, and not just permutations. This could maybe improve the situation of points at $h^{1,1} = 2, 13, 15$ in Figure A.1. However, it is also perfectly possible that there is no actual distribution of the redundancies and the percentage is smaller than the one naively expected by fitting the data with a parabola.

Appendix B

Concrete Calabi-Yau Orientifolds Supporting Thraxions

In this appendix, we discuss explicit examples of CY orientifolds which support multi-throat systems hosting thraxions. We work with the set of manifolds known as CICYs [217]. For a review, see appendix A. In the following, we restrict ourselves to work with favourable CICYs only.

An explicit database listing all the $\mathbb{Z}_2$ actions on CICY manifolds which admit fixed loci of codimension 1 and 3, and that descend from involutions of $\mathcal{A}$ was produced in [88]. One important comment is that at a generic point in complex structure moduli space, a CICY will not admit any geometric $\mathbb{Z}_2$ symmetry which could be used in order to define an orientifold projection. However, at special points in complex structure moduli space, such symmetry exists. Due to this complex structure tuning, $\mathbb{Z}_2$ symmetric CYs will generically contain conifold singularities that lie on the fixed locus of the $\mathbb{Z}_2$ action. Being located on top of an O-plane, these singularities cannot be deformed in a way that is compatible with the $\mathbb{Z}_2$ action. However, they can be resolved, just as the usual conifold: they can be resolved in two different ways, related by a flop. After the orientifold projection, these singularities are called *frozen conifold singularities*. We stress that this feature is extremely generic: in Figure B.1 we show the percentage of CICY orientifolds for which there exists at least one frozen conifold with respect to all CICY orientifolds, as a function of the Hodge numbers.

We wish now to comment about some aspects of the orientifolds admitting frozen conifolds. From Figure B.1 we see clearly that, regardless the presence of thraxions, only $\mathcal{O}(1)\%$ of all orientifolds are free of frozen conifolds. While the CICYs comprise only a comparatively small set of CY manifolds, this outcome raises the possibility that a sizable fraction of all O7-orientifolds of CYs may contain frozen conifolds.

If this is the case, this poses the question of understanding in more details the resolution branches of the frozen conifold singularities. This is especially important for phenomenological applications. By entering the resolved phase of a frozen conifold singularity, $h^{1,1}_+$ increases by $\Delta h^{1,1}_{+,\text{f.c.}}$. Thus, new divisors will be present in the resolved phase, compared to the divisors of the double-cover, i.e. the original CY before the orientifold quotient is taken. In turn, this implies that the simple splitting of the $H^{1,1}(\text{CY})$-eigenspace of the parent CY into $\mathbb{Z}_2$-even and odd subspaces to compute the purely even sector and even-odd-odd sector intersection numbers will generically fail to be correct in the resolved phase. Furthermore, such computation is of dubious meaning at the singular point, as the Dolbeault cohomology is not well-defined for singular varieties. Hence, achieving an understanding of the structure and ubiquity of singular CY orientifolds characterized by the presence of frozen conifolds, as well as their resolutions, forms a

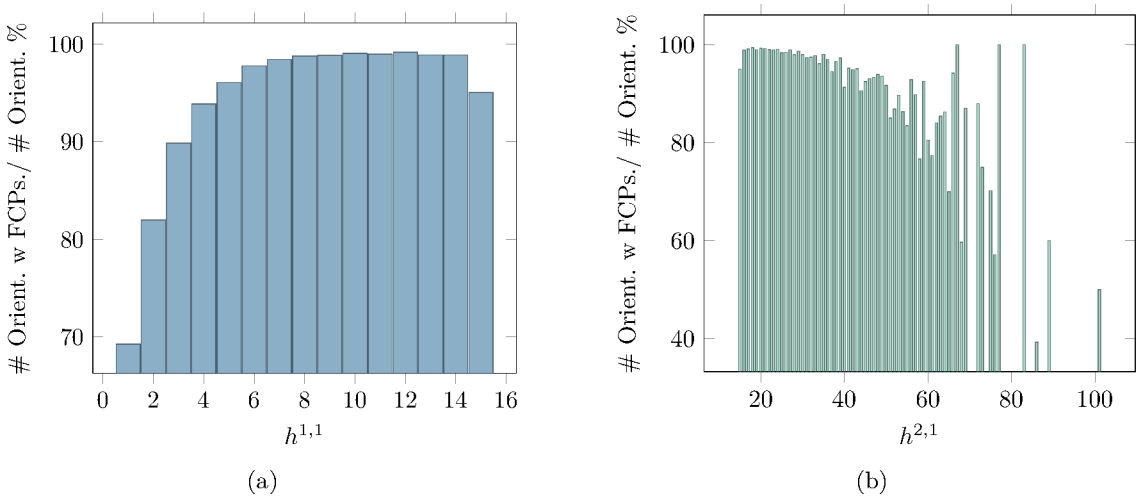

Figure B.1: Percentage of orientifolds admitting frozen conifold points, with respect of the total number of orientifolds, distributed by $h^{1,1}$ and $h^{2,1}$. We remark that we are only analyzing favorable CICYs, therefore the cutoff at $h^{1,1} = 15$.

pressing task for the future.

We would like now to bring the attention back to the set of CICY orientifolds constructed in [88]. A subset of them consists of geometries hosting multi-conifolds and therefore thraxions. We immediately stress that these multi-conifolds are *not* the frozen ones discussed in the previous paragraph, as thraxions are defined in the deformed phase. We will explain this point in more details later. In order for a CICY orientifold to allow for the presence of thraxions, two conditions must be satisfied:

1. In the double cover, it must be possible to cross a conifold transition locus in a way that preserves the $\mathbb{Z}_2$ symmetry that one uses to define the orientifold. As a consequence, the resolved side must have $h^{1,1}_{+}$ larger than the deformed side.

2. The set of axions that appears in the resolved side must not be fully projected out by the O7-orientifold projection. This means that $h^{1,1}_{-}$ must also increase in the resolved side.

The two conditions together imply the following: at the $\mathcal{N} = 2$ level, there are two sets of multi-conifolds, each one with the same number of conifold points in it, the same number of homology relations, and the orientifold swaps them. We note that, despite the multi-conifolds do not lie on the $\mathbb{Z}_2$ fixed locus, in principle other sets of conifold singularities can, and generically will, lie on top of the orientifold plane. Therefore, resulting in frozen conifolds. We depict this in Figure B.2.

Let $\mathcal{M}$ be the set of $319,521$ thraxions transitions. With this we mean couples of resolved and deformed geometries associated with a conifold transition used to define a thraxion. Equivalently, $\mathcal{M}$ is the set of all the possible multi-throat systems that can appear in the CICY orientifold database. We note that it is possible that the same deformed side of the CY orientifold has more than one multi-throat, and therefore has more than one resolved phase. We define three interesting subsets of $\mathcal{M}$ as follows. First, we consider a set $\mathcal{M}_1$ of multi-throats such that the position and number of O3/O7-planes is the same both in the deformed phase and the resolved one, related by the conifold transition used to define the thraxions themselves. We find that $\mathcal{M}_1$ consists of $11,533$ elements. In addition to this, we further restrict to orientifolds that do not have frozen conifolds. This leaves us with a subset $\mathcal{M}_2 \subset \mathcal{M}_1$ of $1,279$ examples satisfying both conditions. Finally, we consider only orientifolds that do admit both O7-planes and O3-planes. This generates a subset $\mathcal{M}_3 \subset \mathcal{M}_2 \subset \mathcal{M}_1$ of 57 examples satisfying all three conditions.

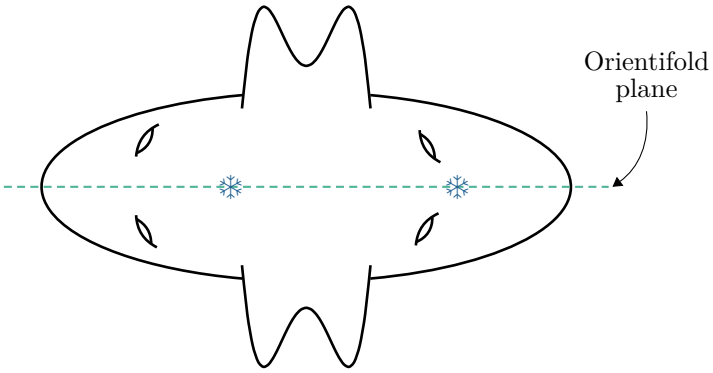

Figure B.2: A representation of the orientifold projection acting on a CY manifold with two double throats. The blue dashed line represent the fixed locus of the projection. The double throats are mapped to each other by the $\mathbb{Z}_2$ symmetry. Snowflakes depict frozen conifolds.

The reason why we restrict to these subsets is the following. For CY orientifolds in $\mathcal{M}\backslash\mathcal{M}_1$ the number and position of orientifold planes varies in a discontinuous way when crossing the transition locus. This means that in the proximity of the transition locus, some O-planes are very close to either merging or splitting. This implies that some extra degrees of freedom become very light in such a region of the moduli space. We leave the study of this very interesting situation for future work. For CY orientifolds in $\mathcal{M}_1 \setminus \mathcal{M}_2$ the number and position of O-planes in the two sides of the transition agree, but there are frozen conifold points on at least one of the O7-planes. While these models are in principle viable for phenomenology, the presence of frozen conifolds makes it hard to compute topological quantities needed for writing the low energy effective action, as for example the triple intersection numbers. Finally, CY orientifolds in $\mathcal{M}_2 \setminus \mathcal{M}_3$ are free of the two possible problems remarked before. However, all orientifolds in this set have either no O7-planes, or no O3-planes. Therefore, using them for phenomenology can be challenging or also completely impossible.

We compiled a new database, listing all the couples of deformed/resolved CICY orientifolds contained in $\mathcal{M}_2$. This database is explicitly available at this link. Every element of the database takes the following form:

$$\{\{\text{Resolved CICY info}\}, \{\text{Deformed CICY info}\}, \#\text{ thraxions}, \#\text{ Conifold pts.}\}\ . \tag{B.1}$$

The last two entries are the number of thraxions and the number of conifold points, computed as:

$$\#\text{ thraxions} \coloneqq \left|\Delta h^{1,1}_{-}\right|\ , \quad \#\text{ Conifold pts.} \coloneqq \frac{1}{4}\left|\Delta\chi\right|\ , \tag{B.2}$$

with χ the Euler number of the two CYs. The first two components contain some useful information about the orientifold:

1. The number of the CICY following the numeration given in [239].
2. $h^{1,1}$ and $h^{2,1}$ of the CICY before the orientifold action.
3. A configuration matrix of the CICY.
4. The triple intersection polynomial of the CICY.[1]
5. The number of the orientifold given in [88].

[1] This is computed with respect to a divisor basis given by the pullbacks of the hyperplane classes of the various $\mathbb{P}^{n_i} \in \mathcal{A}$.

6. The rows in the configuration matrix that have to be swapped in order to define the thraxion transition.

7. $h^{1,1}_{-}$ and $h^{2,1}_{-}$ of the CICY orientifold.

8. The triple intersection polynomial of the CICY orientifold computed as in [225].

9. The data relative to the number of O7-planes, number of O3-planes, number of frozen conifolds on each O7-plane, following the notation of [88].

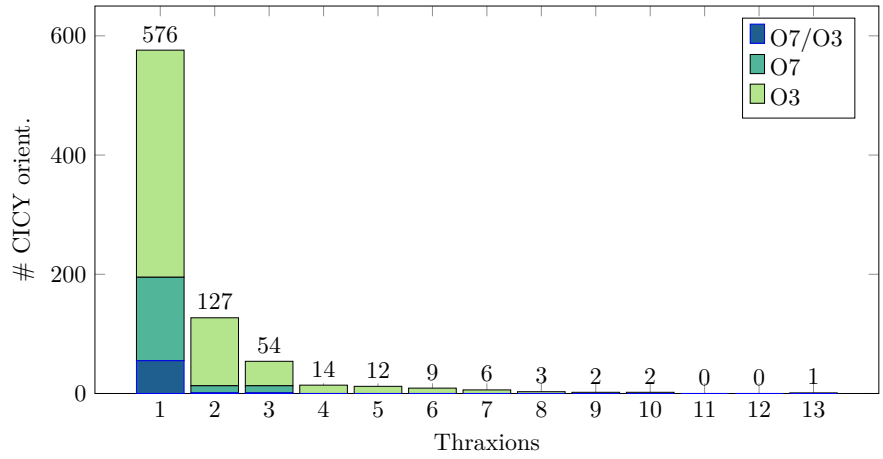

Figure B.3: Number of CICY orientifolds in $\mathcal{M}_2$ for given number of thraxions. The different colors show the presence of both O7/O3-planes, or only O7- or O3-planes.

Essentially, by construction, for every multi-throat system there is just one thraxion.[2] However, it does happen that the same CICY orientifold admits *multiple* multi-throats, therefore allowing for multiple thraxions, still one per multi-throat system. We display in figure B.3 the number of multi-throats (and therefore the number of thraxions) within the database $\mathcal{M}_2$ discussed above.

If we instead consider the set $\mathcal{M}_1$, we find a much larger number of orientifolds supporting thraxions. We report this in fig. B.4.

Note that since in every multi-throat system there is a single homology relation giving rise to a single thraxion, when we study the moduli stabilisation problem we are in the situation described in Section 2.4.4. Therefore, it is possible to argue that with a certain amount of tuning of the fluxes, the thraxion potential does not receive order $\mathcal{O}(\varepsilon)$ contributions from the stabilisation of the Kähler moduli. Such needed tuning involves a democratic distribution of the fluxes in the throats and as a result the thraxion mass is still six-times-warped suppressed. However, if the number of throats in a given multi-throat system is equal to 2, the tuning of the fluxes is minimal. For this reason, in Figure B.5 we show the multi-throats in $\mathcal{M}_2$ for a given number of throats. In the database we provide, there are, then, 110 multi-throats that have only 2 conifold points. We leave for further study the question of which exact flux choice must be made so that the discussion in Section 2.4.4 can be realized.

[2] We stress that this needs not to be the case in general, it is just an artefact of the way in which thraxions transitions were discovered in [88].

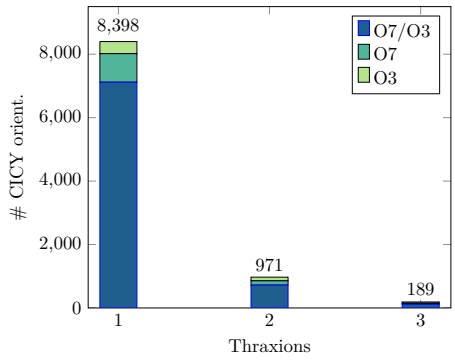

(a) Number of CICY orientifolds that admit up to 3 thraxions.

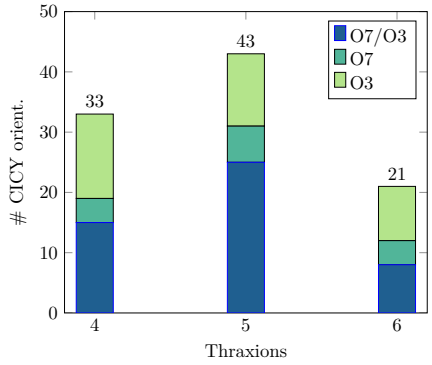

(b) Number of CICY orientifolds that admit from 4 to 6 thraxions.

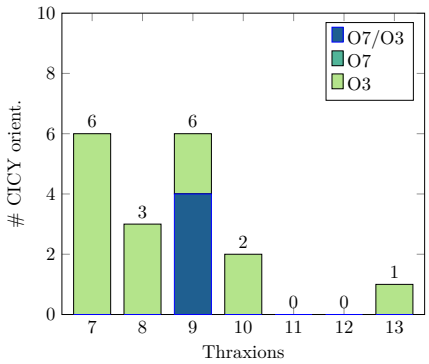

(c) Number of CICY orientifolds that admit from 7 to 13 thraxions.

Figure B.4: Number of CICY orientifolds in $\mathcal{M}_1$ for given number of thraxions. The different colors show the presence of both O7/O3-planes, or only O7 or O3-planes.

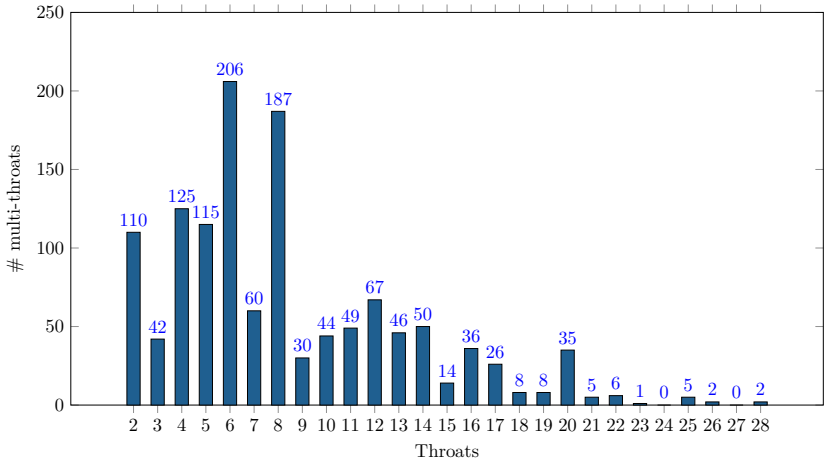

Figure B.5: Number of multi-throats in $\mathcal{M}_2$ that admit from 2 to 28 throats.

Appendix C

A database of GV invariants for CICYs

In this appendix, we recall the usual technique to compute the genus 0 GV invariants of Calabi-Yau threefolds, as explained in [247, 248]. By using this technique, we created a database of GV invariants for the set of favourable CICYs, searching for compactification spaces showing the required hierarchy of invariants to make viable the models of Section 3.5. Suppose we want to compute the GV invariants of a given CICY $\tilde{X}$. Let t_i, $i = 1, \dots \tilde{h}^{1,1}$, be the number of Kähler moduli of such manifold. By mirror symmetry, there will exist a mirror manifold X with complex structure moduli z_i, $i = 1, \dots, h^{2,1} = \tilde{h}^{1,1}$.[1] The main idea of the algorithm will be to explicitly compute the period vector in the mirror side X, and then from this extract the quantum corrected triple intersection numbers of the CICY $\tilde{X}$. The general expression for the configuration matrix of $\tilde{X}$ is given in (A.9). From the generators of the Mori cone of the mirror manifold X, it is possible to define vectors $l^{(i)}$, given by

$$l^{(i)} = \left(-q_1^{(i)}, \dots - q_k^{(i)}\,; \dots, 0, 1, \dots, 1, 0, \dots\right) \equiv \left(\left\{l_{0j}^{(i)}\right\}\,;\, \left\{l_r^{(i)}\right\}\right)\,, \tag{C.1}$$

where $i = 1, \dots, h^{2,1}$ and $j = 1, \dots, k$ and the number of 1's in $\left\{l_r^{(i)}\right\}$ are equal to $n_i + 1$ at a position corresponding to the $\mathbb{P}^{n_i}$ that has been considered. The period vector $\Pi(z)$ for X is a vector with $2h^{2,1} + 2$ components. The first component, also called the *fundamental period*, is given by

$$w_0(z) = \sum_{n_1 \geq 0} \dots \sum_{n_{h^{2,1}} \geq 0} c(n) \prod_{i=1}^{h^{2,1}} z_i^{n_i}\,, \quad \text{where} \quad c(n) = \frac{\prod_j \Gamma\left(1 - \sum_{s=1}^{h^{2,1}} l_{0j}^{(s)} n_s\right)}{\prod_i \Gamma\left(1 + \sum_{s=1}^{h^{2,1}} l_i^{(s)} n_s\right)}\,. \tag{C.2}$$

Note in particular that it is possible to write down the fundamental period of X, just from the information encoded in the configuration matrix of $\tilde{X}$. One then extends such solution of the Picard-Fuchs equations for arbitrary values of $h^{2,1}$ parameters ρ_i, defining

$$w_0(z, \rho) = \sum_{n_1 \geq 0} \dots \sum_{n_{h^{2,1}} \geq 0} c(n + \rho) \prod_{i=1}^{h_{2,1}} z_i^{n_i + \rho_i}\,. \tag{C.3}$$

[1] Following the convention introduced in the main text, we denote $h^{1,1}(\tilde{X})$ as $\tilde{h}^{1,1}$.

In terms of (C.3), the full period vector $\Pi(z)$ can be defined as

$$\Pi(z) = \begin{pmatrix} w_0(z) \\ \left.\frac{\partial}{\partial\rho_i} w_0(z,\rho)\right|_{\rho=0} \\ \left.\frac{1}{2}\kappa^0_{ijk}\frac{\partial}{\partial\rho_j}\frac{\partial}{\partial\rho_k} w_0(z,\rho)\right|_{\rho=0} \\ \left.-\frac{1}{6}\kappa^0_{ijk}\frac{\partial}{\partial\rho_i}\frac{\partial}{\partial\rho_j}\frac{\partial}{\partial\rho_k} w_0(z,\rho)\right|_{\rho=0} \end{pmatrix}, \tag{C.4}$$

where κ^0_{ijk} are the classical triple intersection numbers of $\tilde{X}$. At this point one has obtained the GV invariants for X, but in order to extract them, one needs to rewrite such period vector in terms of the Kähler moduli of $\tilde{X}$, which are defined by the mirror map

$$t^i(z) = \frac{w_i(z)}{w_0(z)}\,, \tag{C.5}$$

where

$$w_i(z) = \sum_{n_1\geq 0}\cdots\sum_{n_{h^{2,1}}\geq 0} \left.\frac{1}{2\pi i}\frac{\partial}{\partial\rho_i} c(n+\rho)\right|_{\rho=0} \prod_{i=1}^{h^{2,1}} z_i^{n_i} + w_0(z)\frac{\ln z_i}{2\pi i}\,. \tag{C.6}$$

At the technical level, the most complicated point of the algorithm is the inversion of eq. (C.5) to get the complex structure moduli z as a function of t. This is the part which limits the most every attempted implementation of the code.

The quantum-corrected triple intersection numbers κ_{ijk} can be expressed as

$$\kappa_{ijk}(t) = \frac{\partial}{\partial t_i}\frac{\partial}{\partial t_j}\frac{\left.\frac{1}{2}\kappa^0_{kab}\frac{\partial}{\partial\rho_a}\frac{\partial}{\partial\rho_b} w_0(z,\rho)\right|_{\rho=0}}{w_0(z)}(t)\,, \tag{C.7}$$

where it is clear that the fraction is computed first as a function of the complex structure moduli z_i, then, one substitutes the inverse of (C.5), and takes the last two derivatives with respect to the Kähler moduli t_i.

Let us introduce $q_i = \exp(2\pi i t_i)$ and the general expression for κ_{ijk} as

$$\kappa_{ijk} = \kappa^0_{ijk} + \sum_{d_1\geq 0}\cdots\sum_{d_{\tilde{h}^{1,1}}\geq 0} n_{d_1,\ldots,d_{\tilde{h}^{1,1}}}\, d_i d_j d_k \frac{\prod_{l=1}^{\tilde{h}^{1,1}} q_l^{d_l}}{1-\prod_{l=1}^{\tilde{h}^{1,1}} q_l^{d_l}}\,. \tag{C.8}$$

Matching the coefficients of the series expansion in q_i for both Eqs. (C.7) and (C.8), it is possible to extract the GV invariants $n_{d_1,\ldots d_{\tilde{h}^{1,1}}}$ for a given CICY.

The algorithm, schematically reviewed above, was coded in the Mathematica program `INSTANTON` [190]. By using such a program, we collected all genus 0 GV invariants for all the favourable CICYs listed by [239] up to $\tilde{h}^{1,1} = 9$. For any CICY in this subset, we computed all GV invariants such that the sum of their degrees is smaller or equal than 10.

We wish now comment on some empirical properties of the GV invariants in the database, and some

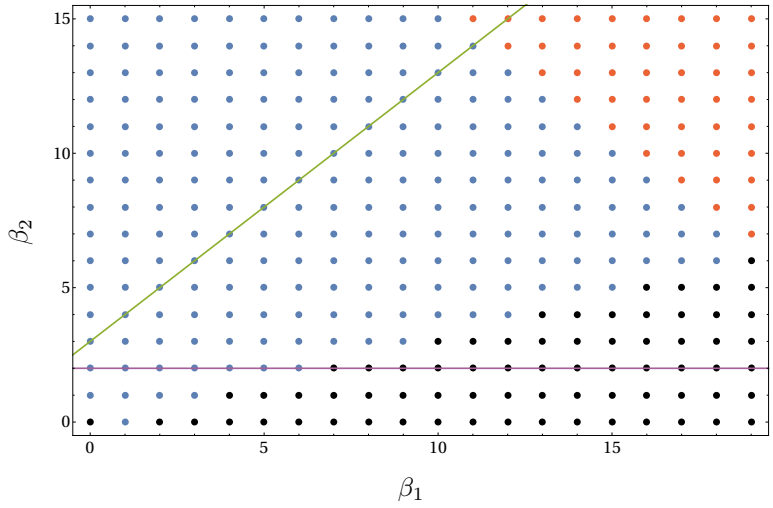

Figure C.1: Occupation sites for the CICY 7858.

patterns which we recognized. For any given favourable CICY $\tilde{X}$ the Mori cone will be $\tilde{h}^{1,1}$ dimensional. For every integer point in the Mori cone, there corresponds a curve class $[\beta]$, and one can compute the genus 0 GV invariants for this curve class. One can then move further away in the following sense. Pick any line passing through $[\beta]$, with rational angular coefficient. Such a line will hit the boundary of the Mori cone on one side, but will continue indefinitely towards infinity on the other side. In particular, it will intersect infinitely many integer points inside the Mori cone, each corresponding to a curve class. One can then compute the GV invariants for curve classes lying on such line. There are three qualitatively different ways in which the GV invariants behave when moving towards infinity in the Mori cone, in a specific direction. For some choices of the direction, the GV invariants will grow indefinitely and exponentially. We will call such directions *exponentially infinite rays*.

Much more interesting is a second type of behavior, in which for some specific directions the GV invariants will eventually become zero. We will call these directions *vanishing rays*. An important role is played by those vanishing rays which are normal to a boundary of the Mori cone. As already pointed out in [77, 78, 248] for the CICYs and in [98] in the context of the Kreuzer-Skarke database, the existence of such vanishing rays signals the presence of a conifold transition, or a flop.In particular the GV invariants of a CY $\tilde{Y}$ connected to $\tilde{X}$ by a conifold transition can be recovered by summing all the GV invariants of $\tilde{X}$ in each of those vanishing ray. We illustrate this in the context of the CICY 7858, which is connected by a conifold transition to the quintic.

In Figure C.1 we plot the Mori cone of the CICY 7858. We put a blue dot for every curve class $[\beta]$ for which we computed that $n_{[\beta]} \neq 0$. We put a red dot for all curve classes for which we have not computed the GV invariant, but we strongly believe it is going to be non-zero. We finally put a black dot for all curve classes such that $n_{[\beta]} = 0$. We can clearly see that, for example, the ray given by $(0,3)+\text{Span}(1,1)$ (corresponding to the green line in Figure C.1) is an infinite ray. On the other hand, the ray given by $(0,2) + \text{Span}(1,0)$ (corresponding to the purple line in Figure C.1) is a vanishing ray. We see that in general, in this example, all rays of the form $(0,n) + \text{Span}(1,0)$, for all $n \in \mathbb{N}$ are vanishing rays.

The Mori cone of the quintic is then identified with the vertical axis in the figure, and the GV invariants of the quintic of degree i, can be found by summing over all GV invariants corresponding to

the same vanishing ray normal to the boundary of the Mori cone, namely,

$$n_i = \sum_{j=1}^{\infty} n_{j,i} \,. \tag{C.9}$$

Although we discussed just one specific example here, we observe that this phenomenon is generic in the CICY database and can be regarded as a confirmation of the well-known fact that all CICYs are connected by conifold transitions [78]. For every couple of CICYs connected by a single conifold transition, the GV invariants of the two manifolds are related in the manner discussed above. This behavior is expected, as, to access a conifold transition from the resolved side, one shrinks some $\mathbb{P}^1$ curves, and therefore projects the Mori cone onto one of its boundaries.

We now move to a third type of interesting direction in the Mori cone, which we call *infinite periodic ray*. Along these directions, the GV invariants continue to be always non-vanishing, but they do not grow exponentially. Instead, they will repeat periodically. We observe this phenomenon, for example, in 13 $\tilde{h}^{1,1} = 2$ CICYs, in particular for the GV invariants $n_{0,m}$. We do not have an argument for why such periodicity arises. However, we note empirically that this is related to the presence of $\mathbb{P}^2$ factors in the ambient space geometry. A peculiar example of this is the bi-cubic CICY (7884), where the invariants repeat along both the $[1, 0]$ and the $[0, 1]$ direction of the Mori cone and are $\mathbb{Z}_2$ symmetric. One can find that infinite periodic rays also exist for $\tilde{h}^{1,1} = 3$, anytime a $\mathbb{P}^3$ is present in the configuration matrix. We conjecture that this phenomenon is generic. However, as we go to a larger $\tilde{h}^{1,1}$, it is more difficult to study such behaviour.

The last thing that we note from our database is the fact that the numerical values of degree 1 GV invariants tend to decrease with $\tilde{h}^{1,1}$. For example, the quintic has $\tilde{h}^{1,1} = 1$ and its degree 1 GV invariant is $n_1 = 2875$, the largest one in the whole database. On the other hand, the degree 1 GV invariants of the CICY number 7858 of Figure C.1 are $n_{0,1} = 366$, $n_{1,0} = 36$. We wish to address these empirical properties in a future work.

Appendix D

String Axion Appendices

D.1 Closed string axions: Sf computations

C_0 axion: The C_0 axion is part of the axio-dilaton field $\mathcal{S} = \frac{i}{g_s} + C_0$, and its periodicity is defined as $C_0 \equiv C_0 + 1$. The decay constant can be read from the kinetic part of the 4D Lagrangian arising from the Kähler potential:

$$K \supset -\ln(\mathcal{S} - \bar{\mathcal{S}}) + \cdots . \tag{D.1}$$

This implies

$$\mathcal{L} = K_{\mathcal{S}\bar{\mathcal{S}}} |\partial \mathcal{S}|^2 + \cdots = -\frac{1}{(\mathcal{S} - \bar{\mathcal{S}})^2} (\partial C_0)^2 + \cdots = \frac{g_s^2}{4} (\partial C_0)^2 + \cdots . \tag{D.2}$$

From the conventions given in Eq. (4.5), this means that $2\pi f = g_s/\sqrt{2}$. Based on analyticity and periodicity, the instanton contribution (if present) to the superpotential is $\sim \exp(2\pi i \mathcal{S})$, such that the instanton action reads $S = 2\pi/g_s$. Thus,

$$Sf = \frac{1}{\sqrt{2}} . \tag{D.3}$$

B_2 axions: Let us consider the $\mathcal{N} = 1$ description of a CY geometry in which Kähler moduli are encoded in 2-cycle superfields, with the real part being the B_2 axion b. Note that the results derived in what follows do not directly apply to an orientifold of type IIB with D3/D7 branes since we are using the wrong $\mathcal{N} = 1$ part of the original $\mathcal{N} = 2$ SUSY of the CY model. However, the calculation for the two moduli t_1, t_2 gives the correct value for Sf in a type IIB $\mathcal{N} = 2$ model which is 'ready' for the geometric projection associated with $t_1 \leftrightarrow t_2$. This includes the restriction to the combined t_1/t_2 instanton which will survive the projection. Thus, since Sf does not depend on which SUSY will eventually survive but merely characterises the real axion b_-, we can trust our result also for the orientifolded D3/D7 case.

In the simplest case with one 2-cycle, the overall CY volume is given by

$$\mathcal{V} = \frac{1}{6} \kappa_{111} v^3 , \tag{D.4}$$

where $t = iv + b$, and $b \equiv b + 1$. The Kähler potential reads

$$K \supset -3 \ln(t - \bar{t}) + \cdots . \tag{D.5}$$

The structure of the exponential terms in the non-perturbative corrections is $\sim \exp(2\pi i t)$, such that the

only difference with the C_0 axion case is the famous no-scale prefactor 3. Thus,

$$Sf = \sqrt{\frac{3}{2}}\,. \tag{D.6}$$

Now let us generalise to the case of two moduli t_1, t_2. The standard form of the volume is given by

$$\mathcal{V} = \frac{1}{6}\kappa_{ijk}v^i v^j v^k\,. \tag{D.7}$$

We require that an orientifolding with $\mathbb{Z}_2$ action $t_1 \leftrightarrow t_2$ is possible. This imposes symmetry constraints on the triple intersection numbers κ_{ijk} such that the volume becomes

$$\mathcal{V} = \frac{1}{6}\left(\kappa_{111}\left[(v^1)^3 + (v^2)^3\right] + 3\kappa_{112}\left[(v^1)^2 v^2 + v^1(v^2)^2\right]\right)\,. \tag{D.8}$$

Changing variables to $t^\pm \equiv t^1 \pm t^2$ gives

$$\begin{aligned}\mathcal{V} &= \frac{1}{24}\left[(\kappa_{111}+3\kappa_{112})(v^+)^3 + 3(\kappa_{111}-\kappa_{112})(v^+)(v^-)^2\right] \\ &\equiv \frac{1}{24}\left[\kappa_{+++}(v^+)^3 + 3\kappa_{+--}v^+(v^-)^2\right]\,.\end{aligned} \tag{D.9}$$

We are interested only in the kinetic term for b^-, at the locus where $v^- = 0$. For this, we need

$$K_{--} = -\frac{\partial}{\partial t^-}\frac{\partial}{\partial \bar{t}^-}\ln\mathcal{V}(v_\pm) \qquad \text{with} \qquad v_\pm = -i(t_\pm - \bar{t}_\pm)/2\,. \tag{D.10}$$

This leads to

$$K_{--} = -\frac{1}{4}\frac{\partial^2}{\partial(v^-)^2}\ln\mathcal{V}(v_\pm) = -\frac{1}{4}\,\frac{6\kappa_{+--}}{\kappa_{+++}(v^+)^2}\,. \tag{D.11}$$

Since κ_{+++} must be positive for positive volume, we learn that κ_{+--} is negative.

The leading instanton for b^- is the product of the instantons coupling to t^1 and t^2. This is enforced by the $\mathbb{Z}_2$ symmetry. The action of this double instanton is $2\pi(v^1+v^2) = 2\pi v^+$ and the corresponding phase factor is $\exp(2\pi i(b^1+b^2)) = \exp(2\pi i b^+)$.

Now everything looks very similar to the C_0 axion case discussed before. One difference is the factor

$$\sqrt{\frac{6|\kappa_{+--}|}{\kappa_{+++}}}\,, \tag{D.12}$$

affecting f. The other is the replacement $g_s \to 1/v^+$, but this factor drops out in the end anyway. Thus, since we originally had $Sf = 1/\sqrt{2}$, we now arrive at

$$Sf = \sqrt{\frac{3|\kappa_{+--}|}{\kappa_{+++}}}\,. \tag{D.13}$$

The crucial question is how large the ratio

$$\frac{|\kappa_{+--}|}{\kappa_{+++}} = \frac{\kappa_{112}-\kappa_{111}}{3\kappa_{112}+\kappa_{111}} \tag{D.14}$$

can become. If κ_{111} and κ_{112} are non-negative, then the maximal value of $1/3$ is attained for $\kappa_{111}/\kappa_{112} = 0$, leading to $Sf = 1$. As $\kappa_{111}/\kappa_{112}$ grows, Sf falls.

C_2 axions: In the case of type IIB superstring theory with D3/D7 branes, the b_- axion is paired with the corresponding c_- axion coming from C_2. The value of Sf for the latter is most easily inferred by noting that, first, the 10D kinetic term changes according to

$$(\partial B_2)^2/g_s^2 \quad \to \quad (\partial C_2)^2\,, \tag{D.15}$$

and, second, the tension changes between the fundamental string and the euclidean D1-brane as $1/(2\pi\alpha') \to 1/(2\pi\alpha' g_s)$. Thus, $f \to f g_s$ and $S \to S/g_s$, leading to

$$Sf = \sqrt{\frac{3|\kappa_{+--}|}{\kappa_{+++}}} \leq 1\,. \tag{D.16}$$

where the upper bound in this simple case comes from the discussion around Eq. (D.14).

C_4 axions For a single (or one dominant) Kähler modulus in type IIB with D3/D7 branes one has

$$K \supset -3\ln(T+\bar{T}) + \cdots\,, \qquad T = \tau + id\,, \qquad d \equiv d+1\,. \tag{D.17}$$

The non-perturbative term in W is $\sim \exp(-2\pi T)$, such that everything is analogous to the B_2 axion without orientifolding:

$$Sf = \sqrt{\frac{3}{2}}\,. \tag{D.18}$$

Let us now consider the case of a fibred geometry. In the simplest fibred geometry, e.g. K3 over S^2, one has

$$K \supset -2\ln\mathcal{V} + \cdots = -2\ln(T_1\sqrt{T_2}) + \cdots\,. \tag{D.19}$$

Relative to the C_0 axion, one reads off factors 2 and 1 in f^2. Thus, one finds for the fibre T_1, $Sf = 1$ and for the base T_2, $Sf = \frac{1}{\sqrt{2}}$.

D.2 Open string axions computations

In the following, we focus on an open string complex scalar matter field $C = |C|e^{i\sigma}$ which lives on a collapsed cycle. The general form of the Kähler potential and superpotential which describe the theory for the shrinked cycle near the singularity are given by [249]

$$K = -2\ln\left(\mathcal{V} + \frac{\hat{\xi}}{2}\right) + \lambda_{seq}\frac{\tau_{seq}^2}{\mathcal{V}} + K_{matter}\,, \tag{D.20}$$

$$W = W_0 + \sum_{i=1}^{h_{1,1}} A_i\, e^{-a_i T_i} + W_{matter}\,, \tag{D.21}$$

where W_{matter} and K_{matter} are related to the matter sector contributions depending on the field C. In presence of more than one matter field the general form of K_{matter} is given by [250]

$$K_{matter} = \mathcal{K}_\gamma(T_i, \bar{T}_i) C^\gamma \bar{C}^{\bar{\gamma}}\,. \tag{D.22}$$

In order to understand the properties of the ultralight axion candidate, σ, we have to study the moduli stabilisation procedure in the sequestering scenario [251]. The leading order contribution to the scalar

potential, after dilaton and the complex moduli fields stabilisation, comes from the D-term which takes the following form:

$$V_{D_{D3}} = \frac{1}{Re(f_{seq})}\Big(q_C \frac{\partial K}{\partial |C|}|C| - \xi_{seq}\Big)^2 , \tag{D.23}$$

where q_C is the charge of the matter field, f_{seq} is the gauge kinetic function related to the U(1) symmetry while $\xi_{seq} = -\frac{q_{seq}}{4\pi}\frac{\partial K}{\partial T_{seq}}$ and τ_{seq} is the cycle on which the U(1) charge is located. Working near the singularity, $T_{seq} = \tau_{seq} + id_{seq}$, we have that $\tau_{seq} \to 0$ and the gauge kinetic function

$$f_{seq} = S + q_{seq}\, T_{seq}\,.$$

Since we want to find an axion, that is a pseudo Nambu-Goldstone field σ with translational symmetry, we want the following conditions to be satisfied

- a Peccei-Quinn mechanism related to the breakdown of the U(1) symmetry of the potential related to $|C|$, i.e. $\langle |C| \rangle \neq 0$.
- a minimum for the scalar potential which provides an extremely small value of $\langle \tau_{seq} \rangle \ll 1$ in order to support the collapsed cycle assumption.

Working with the canonically normalised matter field, $|\hat{C}|$, the D-terms becomes:

$$V_{D_{D3}} = \frac{1}{Re(f_{seq})}\Big(q_C|\hat{C}|^2 + \frac{q_{seq}}{8\pi}\frac{\partial K}{\partial \tau_{seq}}\Big)^2 . \tag{D.24}$$

Since the D-term has the same volume dependence as the flux generated F-term potential used to fix both the dilaton and the complex moduli, we have to set it to zero in order to have a consistent stabilisation procedure and preserve supersymmetry at this order in the expansion in inverse powers of $\mathcal{V}$. This implies

$$|\hat{C}|^2 = \frac{q_{seq}}{8\pi\, q_C}\frac{\partial K}{\partial \tau_{seq}} \sim \frac{\partial K}{\partial \tau_{seq}}\,. \tag{D.25}$$

This relation fixes one direction in the $(|C|, \tau_{seq})$ plane which corresponds to the supersymmetric partner of the axion which is eaten up by the relative anomalous U(1) gauge boson in the process of anomaly cancellation. The axion which becomes the longitudinal component of the massive gauge boson is a combination of an open and a closed string axion. The mass of the Abelian gauge boson is given by [251]

$$m^2_{\mathrm{U}(1)} \simeq g^2_{seq}\Big[(f_\sigma)^2 + (f_{d_{seq}})^2\Big]\,, \tag{D.26}$$

where g_{seq} is the gauge kinetic coupling of the theory living on the sequestered cycle.
If we focus on the U(1) charged complex scalar field C living on a D3-brane at a singularity ($\tau_{seq} \ll 1$), we will have that the open axion decay constant will be

$$f^2_\sigma = |\hat{C}|^2 = \frac{q_{seq}\,\lambda_{seq}}{8\pi\, q_C}\frac{\tau_{seq}}{\mathcal{V}}M_P^2 \sim \frac{\tau_{seq}M_P^2}{\mathcal{V}} \ll M_s^2\,. \tag{D.27}$$

On the other hand, the decay constant associated to the closed string axion related to the sequestered cycle is just $f_{d_{seq}} = \frac{\partial^2 K}{\partial \tau_{seq}\partial \tau_{seq}} = \frac{\lambda_{seq}}{\mathcal{V}}$. We see that, in this case the open string axion is eaten up by the gauge boson while the open string axion is still a dynamical field. the same process applies to anomalous U(1) on D7-brane stacks in the geometric regime. In that case, the open string axion is the degree of freedom which is eaten up and we are left with just the closed string axion. Coming back to the sequestered scenario, after D-term stabilisation, we can still consider the open string axion σ as a

flat direction, while the moduli τ_{seq} and d_{seq} are fixed and the gauge boson acquires a mass of the order of the string scale, namely

$$M_{\mathrm{U}(1)} \sim \frac{M_P}{\sqrt{\mathcal{V}}} \sim M_s \,. \tag{D.28}$$

The matter field $|C|$ acquires a mass through sub-leading soft terms which look like [251]

$$V_F(|\hat{C}|) = r_2 \frac{|\hat{C}|^2}{\mathcal{V}^{\alpha_2}} + r_3 \frac{|\hat{C}|^3}{\mathcal{V}^{\alpha_3}} + \left(\frac{r_4}{\mathcal{V}^{\alpha_4}} - \frac{\gamma_4}{\mathcal{V}}\right) |\hat{C}|^4 \,. \tag{D.29}$$

The terms proportional to c_i come from the expansion of the scalar potential in powers of $|\hat{C}|$, while the one depending on γ_4 comes from the breaking of the no-scale structure by τ_{seq}. If $r_2 > 0$, the matter field has a vanishing VEV and, thanks to the D-term stabilisation condition $\langle \tau_{seq} \rangle = 0$. If instead $|C|$ shows a tachyonic mass from supersymmetry breaking, i.e. $r_2 < 0$, then, depending on the signs of the different coefficients, $|\hat{C}|$ can develop a non-vanishing VEV. One may think that, given the relation between $\langle |\hat{C}| \rangle$ and $\langle \tau_{seq} \rangle$, the collapsed cycles get stabilised at values larger than the string scale, resolving in this way the singularity. It was shown that in models with just fractional D3-branes, the cycle is still sequestered, being $\alpha_3 = 2$, $\alpha_4 = 1$ and either $\alpha_2 = 3$ or $\alpha_2 = 4$ depending on the moduli dependence of the Kähler metric from matter field. The stabilisation of the matter field gives

$$\langle |\hat{C}| \rangle = \frac{2 r_2}{3 r_3} \frac{1}{\mathcal{V}^{\alpha_2 - 2}} \,, \qquad \langle \tau_{seq} \rangle = \frac{p}{\mathcal{V}^{2\alpha_2 - 5}} \,, \tag{D.30}$$

where $p = \frac{32\pi\, q_C\, r_2^2}{9 q_{seq}\, \lambda_{seq}\, r_3^2}$ depends on soft terms and on the terms breaking the no-scale structure. We see that for both values of α_2 we are still in sequestered scenario as

$$\begin{aligned} &f_\sigma \propto \tfrac{1}{\mathcal{V}} \,, \qquad \tau_{seq} \propto \tfrac{1}{\mathcal{V}} \qquad \text{when } \alpha_2 = 3 \\ &f_\sigma \propto \tfrac{1}{\mathcal{V}^2} \,, \qquad \tau_{seq} \propto \tfrac{1}{\mathcal{V}^3} \qquad \text{when } \alpha_2 = 4 \,. \end{aligned} \tag{D.31}$$

At this level of approximation σ is still a flat direction. This field receives a mass through hidden sector strong dynamics effects as described in the main text.

D.3 Additional corrections for C_4 axions

In order to understand whether there can be some more involved constructions leading to a C_4 FDM candidate with mass around 10^{-22} eV, we examined several setups that we list below.

Non-vanishing 2-form fluxes: Let us consider the fibred geometry described in section 4.2.1 as, having two Kähler moduli, it is more flexible compared to the Swiss-cheese case. The overall volume is given by:

$$\mathcal{V} = \frac{2}{3} t_2^3 + t_1 t_2^2 = \frac{\sqrt{\tau_1}\, \tau_2}{2} - \frac{\tau_1^{3/2}}{3} \,. \tag{D.32}$$

Let us turn on gauge fluxes as $\mathcal{F} = m^i \omega_i + \dots$ where $m^i = 2\pi n_i$, $n_i \in \mathbb{Z}$, where ω_j are orientifold-even 2-forms, $i = 1, \dots, h^{1,1}_+$. The presence of non-trivial gauge fluxes $\mathcal{F}$ can induce a U(1)-charge q_i for the i-th Kähler modulus together with a flux-dependent correction to the gauge kinetic function f_j of the form

$$q_i = \int_X \mathcal{F} \wedge \omega_i \wedge \omega_j \tag{D.33}$$

$$f_i = T_i - h_i(\mathcal{F})\, S\,, \quad \text{where} \quad h_i(\mathcal{F}) = \int_{\rm CY} \mathcal{F}\wedge\mathcal{F}\wedge\omega_i = k_{ijk}\, m_j\, m_k\,, \tag{D.34}$$

and k_{ijk} are the intersection numbers. Considering the simple fibred geometry of eq. (D.32) with just two divisors, the Kähler form is $J = t_1\omega_1 + t_2\omega_2$ while the intersection numbers are $k_{122} = 2$, $k_{222} = 4$. In this setup, we consider the most general flux form, $\mathcal{F} = m_1\,\omega_1 + m_2\,\omega_2$ and we compute the corrections to the gauge kinetic couplings and the induced charges

$$\begin{aligned} &h_1(\mathcal{F}) = 2\,m_2^2\,, \quad h_2(\mathcal{F}) = 4\,m_2(m^2 + m^1)\,, \\ &q_{22} = 2\,m_1 + 4\,m_2\,, \quad q_{21} = 2\,m_2\,. \end{aligned} \tag{D.35}$$

The non-perturbative corrections to the superpotential induced by non-vanishing worldvolume gauge fluxes are given by:

$$W_{\rm n.p.} = A_i\, e^{-a_i f_i} = A_1\, e^{-a_1\left(T_1 + \frac{2}{g_s}\, m_2^2\right)} + A_2\, e^{-a_2\left(T_2 + \frac{4 f_2}{g_s}\,(m_2+m_1)\right)}\,. \tag{D.36}$$

We see that gauge fluxes can induce an extra suppression in the axion mass. On the other hand, being interested in the perturbative regime of the theory, we need $g_s \ll 1$. This implies that the contributions to W coming from gauge fluxes will induce an $\exp(-\mathcal{O}(10))$ correction that can produce considerably lighter FDM candidates. Nevertheless, the correction coming from 2-form fluxes cannot disrupt the predictions given in the main text and its precise contribution is model dependent. For this reason, in the body of this paper we treat the simplest case neglecting gauge flux effects.

Ample divisors: We focus again on the fibred geometry discussed above. In this section we consider the case where the fibred CY contains an ample divisor of the form $\tau_D = \tau_f + \tau_b$ so that the superpotential receives non-perturbative corrections of the form [176]:

$$W = W_0 + A e^{-a(T_f + T_b)}\,. \tag{D.37}$$

The leading order contributions to the F-term scalar potential are given by:

$$V_F \supset \Lambda_2 \cos\left(\frac{\phi_f}{f_{f_{mix}}} + \frac{\phi_b}{f_{b_{mix}}}\right)\,, \quad \text{where} \quad \Lambda_2 \simeq \frac{4\kappa\, a A W_0(\tau_f + \tau_b)}{\mathcal{V}^2}\, e^{-a(\tau_f+\tau_b)}\,. \tag{D.38}$$

The eigenvalues of the mass matrix are:

$$m_\lambda^2 = \left\{0, \left(\frac{1}{f_{f_{mix}}^2} + \frac{1}{f_{b_{mix}}^2}\right)\Lambda_2\right\}\,, \tag{D.39}$$

so that the effective decay constant of the massive axion is then given by

$$\bar{f} = \frac{f_{f_{mix}} f_{b_{mix}}}{\sqrt{f_{f_{mix}}^2 + f_{b_{mix}}^2}}\,. \tag{D.40}$$

A numerical inspection of this setup reveals that the natural amount of DM having mass $\sim 10^{-22}$ eV is around 1%, while the most likely values of the mass and of the decay constant are $\sim 10^{-19}$ eV and 10^{15} GeV respectively. We can therefore conclude that the presence of ample divisors does not affect the predictions given in the main text.

Poly-instantons: For completeness, we now check the possibility of getting FDM through poly-instanton corrections. For instance let us consider let us consider the following corrections to the super potential given by an Euclidean D3-instanton wrapping the cycle τ_p yielding to non-perturbative corrections to the gauge kinetic functions of the condensing gauge group on τ_i [252]:

$$W = W_0 + Ae^{-a_i T_i + Ce^{-2\pi T_p}} \simeq W_0 + Ae^{-a_i T_i} + A\,C e^{-a_i T_i - 2\pi T_p}\,. \tag{D.41}$$

Let us assume that T_i is a blow up cycle which can be stabilised in the usual LVS fashion and that the real part of T_p is stabilised through g_s loops. In this way there is no explicit relation between the overall volume stabilisation and the VEV of τ_p. The axion d_p receives mass contributions only through these n.p. corrections. Then the potential related to d_p will scale as

$$V(d_p) \sim V_{\rm LVS} e^{-2\pi\langle\tau_p\rangle} \sim \mathcal{O}(\mathcal{V}^{-3-p})\,, \tag{D.42}$$

where the value of p depend on the geometry of the cycle T_p and is usually of order unity. The decay constant of d_p also depends on the geometry, for instance is τ_p is a rigid blow-up cycle or the fibre modulus, we have

$$f_{d_p} \sim \begin{cases} \frac{M_P}{2\pi}\frac{1}{\sqrt{\mathcal{V}}} & \text{blow up} \\ \frac{M_P}{2\pi\tau_p} & \text{fibre} \end{cases} \tag{D.43}$$

then we see that in the first case, in order to satisfy the condition on the decay constant, we have to deal with an extremely small overall volume, in which case it is not possible to get the desired tiny mass for the axion d_p. In the second case there can be a chance of getting extra mass suppression with respect to the results presented in the main text. Nevertheless, given that this setup is more model dependent and we cannot provide sharp predictions for the exact mass of the FDM candidate, we consider the examples provided in the main text as the most general predictions.

D.4 Anharmonicity and isocurvature bounds

All the results presented in the main text assume that ALP self-interaction can be neglected. This is valid for small misalignment angles $\theta_{mi} \lesssim 1$. In the most general case, assuming that the PQ symmetry is broken before inflation, $f >> H_I$, we can have an enhanced axion density which depends on the form factor function $F(\theta)$ as follows [253]:

$$\frac{\Omega_\theta h^2}{0.112} \simeq 1.4 \times \left(\frac{m}{10^{-22}\text{eV}}\right)^{1/2} \left(\frac{f}{10^{17}\text{GeV}}\right)^2 \theta_{mi}^2\, F(\theta_{mi})\,, \tag{D.44}$$

where $F(\theta_{mi}) \to 1$ for $\theta \sim 1$ and $F(\theta_{mi}) \to \infty$ for $\theta \sim \pm\pi$. This function has been found to be given by [254]

$$F(\theta_{mi}) = \left[\ln\left(\frac{e}{1-\theta_{mi}^4/\pi^4}\right)\right]\,. \tag{D.45}$$

Let us now focus for simplicity on C_4 ALPs in Swiss-cheese geometry. We can estimate the misalignment angle value that correspond to a FDM particles with mass $\sim 10^{-22}$ eV representing 100% of DM without fine-tuning any of the microscopical parameters $W_0 = 1$ and $A_i = 1$. This is given by a value that is extremely near to the maximum of the axion potential, namely $\theta_{mi} \simeq 0.99\pi$. For an extended treatment of the phenomenology arising in this last regime see [255].

Such a large value for θ_{mi} may lead to the over-closure of the universe through the domain wall

problems. In order to check whether different vacua, separated by domain walls, are populated in space, we need to compare quantum fluctuations and the classical initial field displacement. Domain walls problem can be avoided if

$$\Delta\theta_{in} \gg H_I/(2\pi f) \qquad \text{where} \qquad \Delta\theta_{in} \simeq 10^{-2}\pi\,, \tag{D.46}$$

which for C_4 in Swiss-cheese geometry implies $H_I \ll 0.1f \sim 10^{15}$ GeV that does not significantly impact on model building.

Indeed, the most stringent inflationary constraint related to FDM models comes from the experimental boundaries on isocurvature perturbation. This looks like:

$$\Delta^2_{\mathcal{S}} = \Delta^2_{\mathcal{R}} \frac{\beta_{iso}}{1-\beta_{iso}} < 5.6 \times 10^{-11}\,, \tag{D.47}$$

where the scalar power spectrum $\Delta^2_{\mathcal{R}}$ and the isocurvature parameter β_{iso} have been constrained to be $\Delta^2_{\mathcal{R}} \simeq 2\times 10^{-9}$ and $\beta_{iso} \lesssim 2.6\times 10^{-2}$ at a pivot scale $k^* = 0.05\text{Mpc}^{-1}$ [111]. When the PQ symmetry is broken before inflation, the isocurvature perturbations produced by the axion field are given by [254,256]:

$$\Delta^2_S = \left(\frac{H_I}{\pi\theta_{mi} f}\right)^2 \left(1 + \frac{\theta_{mi}}{2}\frac{F'(\theta_{mi})}{F(\theta_{mi})}\right)^2 . \tag{D.48}$$

Given the experimental constraint on $\Delta^2_{\mathcal{S}}$, the previous equation induces an upper bound on the inflationary scale. This bound is strongly related to the assumption that the ALP is decoupled from the inflaton dynamics. In string theory this is not always the case as the field space turns out to be curved and the shape of the scalar potential is highly non-trivial. Nevertheless, whatever kind of coupling, both kinetic or in the potential, heavily depends on the inflationary model under study. For this reason, we decide to focus on the simplest assumption.

Using the bound on the inflationary scale, we can derive a rough estimate of the bound on the tensor-to-scalar ratio, r that can be expressed as

$$r = \frac{\Delta^2_t}{\Delta^2_{\mathcal{R}}} \simeq \frac{2}{\Delta^2_s \pi^2}\frac{H_I^2}{M_P^2}\,. \tag{D.49}$$

In [1] we derive the constraints on the inflationary scale and the tensor-to-scalar ratio coming from the setups discussed in the main text. We consider both the harmonic approximation and the tuned initial misalignment angle case with $\theta_{mi} = 0.99\pi$. In general, we observe that tensor modes that are produced during inflation will be undetectable and, as expected, a large misalignment angle is compatible with lower axion masses. On the other hand, this tuned initial condition implies stronger constraints on H_I and r.

In this section we saw that the requirement of having a FDM particle with the standard FDM mass coming from C_4 axions leads to heavy fine-tuning of either the microscopical parameters, or the misalignment angle. Since from a statistical perspective it is not clear how to justify the tuning on θ_{mi} and the parameters tuning may lead the EFT out of the controlled regime, we decided to focus on the most likely cases where the ALP is heavier and the axion self-interactions can be ignored at leading order.

Bibliography

[1] M. Cicoli, V. Guidetti, N. Righi and A. Westphal, *Fuzzy Dark Matter Candidates from String Theory*, 2110.02964.

[2] F. Carta, A. Mininno, N. Righi and A. Westphal, *Thraxions: towards full string models*, *JHEP* **01** (2022) 082 [2110.02963].

[3] F. Carta, A. Mininno, N. Righi and A. Westphal, *Gopakumar-Vafa hierarchies in winding inflation and uplifts*, *JHEP* **05** (2021) 271 [2101.07272].

[4] F. Carta, N. Righi, Y. Welling and A. Westphal, *Harmonic hybrid inflation*, *JHEP* **12** (2020) 161 [2007.04322].

[5] G. 't Hooft, *Computation of the Quantum Effects Due to a Four-Dimensional Pseudoparticle*, *Phys. Rev. D* **14** (1976) 3432.

[6] R. D. Peccei and H. R. Quinn, CP *conservation in the presence of pseudoparticles*, *Phys. Rev. Lett.* **38** (1977) 1440.

[7] S. Weinberg, *A new light boson?*, *Phys. Rev. Lett.* **40** (1978) 223.

[8] F. Wilczek, *Problem of strong p and t invariance in the presence of instantons*, *Phys. Rev. Lett.* **40** (1978) 279.

[9] C. Vafa and E. Witten, *Parity Conservation in QCD*, *Phys. Rev. Lett.* **53** (1984) 535.

[10] M. Reece, *Photon Masses in the Landscape and the Swampland*, *JHEP* **07** (2019) 181 [1808.09966].

[11] H. Ooguri and C. Vafa, *On the Geometry of the String Landscape and the Swampland*, *Nucl. Phys. B* **766** (2007) 21 [hep-th/0605264].

[12] S.-J. Lee, W. Lerche and T. Weigand, *Emergent strings from infinite distance limits*, *JHEP* **02** (2022) 190 [1910.01135].

[13] N. Arkani-Hamed, L. Motl, A. Nicolis and C. Vafa, *The String landscape, black holes and gravity as the weakest force*, *JHEP* **06** (2007) 060 [hep-th/0601001].

[14] B. Heidenreich, M. Reece and T. Rudelius, *Sharpening the Weak Gravity Conjecture with Dimensional Reduction*, *JHEP* **02** (2016) 140 [1509.06374].

[15] B. Heidenreich, M. Reece and T. Rudelius, *Evidence for a sublattice weak gravity conjecture*, *JHEP* **08** (2017) 025 [1606.08437].

[16] D. Harlow, B. Heidenreich, M. Reece and T. Rudelius, *The Weak Gravity Conjecture: A Review*, 2201.08380.

[17] C. Vafa, *The String landscape and the swampland*, hep-th/0509212.

[18] M. Cicoli, M. Goodsell and A. Ringwald, *The type IIB string axiverse and its low-energy phenomenology*, *JHEP* **10** (2012) 146 [1206.0819].

[19] J. de Swart, G. Bertone and J. van Dongen, *How Dark Matter Came to Matter*, *Nature Astron.* **1** (2017) 0059 [1703.00013].

[20] T. Banks, M. Dine, P. J. Fox and E. Gorbatov, *On the possibility of large axion decay constants*, *JCAP* **06** (2003) 001 [hep-th/0303252].

[21] P. Svrcek and E. Witten, *Axions In String Theory*, *JHEP* **06** (2006) 051 [hep-th/0605206].

[22] T. W. Grimm, *Axion inflation in type II string theory*, *Phys. Rev. D* **77** (2008) 126007 [0710.3883].

[23] A. Arvanitaki, S. Dimopoulos, S. Dubovsky, N. Kaloper and J. March-Russell, *String Axiverse*, *Phys. Rev. D* **81** (2010) 123530 [0905.4720].

[24] LIGO Scientific Collaboration and Virgo Collaboration collaboration, *Observation of gravitational waves from a binary black hole merger*, *Phys. Rev. Lett.* **116** (2016) 061102.

[25] V. M. Mehta, M. Demirtas, C. Long, D. J. E. Marsh, L. McAllister and M. J. Stott, *Superradiance in string theory*, *JCAP* **07** (2021) 033 [2103.06812].

[26] C. Vafa, *Evidence for F theory*, *Nucl. Phys. B* **469** (1996) 403 [hep-th/9602022].

[27] D. R. Morrison and C. Vafa, *Compactifications of F theory on Calabi-Yau threefolds. 1*, *Nucl. Phys. B* **473** (1996) 74 [hep-th/9602114].

[28] D. R. Morrison and C. Vafa, *Compactifications of F theory on Calabi-Yau threefolds. 2.*, *Nucl. Phys. B* **476** (1996) 437 [hep-th/9603161].

[29] T. Weigand, *F-theory*, *PoS* **TASI2017** (2018) 016 [1806.01854].

[30] P. Candelas and X. de la Ossa, *Moduli Space of Calabi-Yau Manifolds*, *Nucl. Phys. B* **355** (1991) 455.

[31] S. Hosono, A. Klemm and S. Theisen, *Lectures on mirror symmetry*, *Lect. Notes Phys.* **436** (1994) 235 [hep-th/9403096].

[32] K. Hori, S. Katz, A. Klemm, R. Pandharipande, R. Thomas, C. Vafa et al., *Mirror symmetry*, vol. 1 of *Clay mathematics monographs*. AMS, Providence, USA, 2003.

[33] B. R. Greene and M. Plesser, *Duality in {Calabi-Yau} Moduli Space*, *Nucl. Phys. B* **338** (1990) 15.

[34] T. W. Grimm and J. Louis, *The Effective action of N = 1 Calabi-Yau orientifolds*, *Nucl. Phys. B* **699** (2004) 387 [hep-th/0403067].

[35] P. S. Aspinwall and J. Louis, *On the ubiquity of K3 fibrations in string duality*, *Phys. Lett. B* **369** (1996) 233 [hep-th/9510234].

[36] S. Kachru and C. Vafa, *Exact results for N=2 compactifications of heterotic strings*, *Nucl. Phys. B* **450** (1995) 69 [hep-th/9505105].

[37] H. Jockers and J. Louis, *The Effective action of D7-branes in N = 1 Calabi-Yau orientifolds*, *Nucl. Phys. B* **705** (2005) 167 [hep-th/0409098].

[38] S. B. Giddings, S. Kachru and J. Polchinski, *Hierarchies from fluxes in string compactifications*, *Phys. Rev. D* **66** (2002) 106006 [hep-th/0105097].

[39] S. Gukov, C. Vafa and E. Witten, *CFT's from Calabi-Yau four folds*, *Nucl. Phys. B* **584** (2000) 69 [hep-th/9906070].

[40] E. Cremmer, S. Ferrara, C. Kounnas and D. V. Nanopoulos, *Naturally Vanishing Cosmological Constant in N=1 Supergravity*, *Phys. Lett. B* **133** (1983) 61.

[41] M. Dine and N. Seiberg, *Nonrenormalization theorems in superstring theory*, *Phys. Rev. Lett.* **57** (1986) 2625.

[42] A. M. Uranga, *D-brane instantons and the effective field theory of flux compactifications*, *JHEP* **01** (2009) 048 [0808.2918].

[43] L. Gorlich, S. Kachru, P. K. Tripathy and S. P. Trivedi, *Gaugino condensation and nonperturbative superpotentials in flux compactifications*, *JHEP* **12** (2004) 074 [hep-th/0407130].

[44] E. Witten, *Nonperturbative superpotentials in string theory*, *Nucl. Phys. B* **474** 343 [hep-th/9604030].

[45] K. Becker, M. Becker, M. Haack and J. Louis, *Supersymmetry breaking and alpha-prime corrections to flux induced potentials*, *JHEP* **06** (2002) 060 [hep-th/0204254].

[46] M. Berg, M. Haack and B. Kors, *String loop corrections to Kahler potentials in orientifolds*, *JHEP* **11** (2005) 030 [hep-th/0508043].

[47] M. Berg, M. Haack and E. Pajer, *Jumping Through Loops: On Soft Terms from Large Volume Compactifications*, *JHEP* **09** (2007) 031 [0704.0737].

[48] M. Cicoli, J. P. Conlon and F. Quevedo, *Systematics of String Loop Corrections in Type IIB Calabi-Yau Flux Compactifications*, *JHEP* **01** (2008) 052 [0708.1873].

[49] R. Minasian, T. G. Pugh and R. Savelli, *F-theory at order α'^3*, *JHEP* **10** (2015) 050 [1506.06756].

[50] V. Balasubramanian and P. Berglund, *Stringy corrections to Kahler potentials, SUSY breaking, and the cosmological constant problem*, *JHEP* **11** (2004) 085 [hep-th/0408054].

[51] S. Kachru, R. Kallosh, A. D. Linde and S. P. Trivedi, *De Sitter vacua in string theory*, *Phys. Rev. D* **68** (2003) 046005 [hep-th/0301240].

[52] V. Balasubramanian, P. Berglund, J. P. Conlon and F. Quevedo, *Systematics of moduli stabilisation in Calabi-Yau flux compactifications*, *JHEP* **03** (2005) 007 [hep-th/0502058].

[53] S. Kachru, R. Kallosh, A. D. Linde, J. M. Maldacena, L. P. McAllister and S. P. Trivedi, *Towards inflation in string theory*, *JCAP* **10** (2003) 013 [hep-th/0308055].

[54] C. P. Burgess, R. Kallosh and F. Quevedo, *De Sitter string vacua from supersymmetric D terms*, *JHEP* **10** (2003) 056 [hep-th/0309187].

[55] R. Kallosh and T. Wrase, *Emergence of Spontaneously Broken Supersymmetry on an Anti-D3-Brane in KKLT dS Vacua*, *JHEP* **12** (2014) 117 [1411.1121].

[56] E. A. Bergshoeff, K. Dasgupta, R. Kallosh, A. Van Proeyen and T. Wrase, $\overline{\text{D3}}$ *and dS*, *JHEP* **05** (2015) 058 [1502.07627].

[57] R. Kallosh, F. Quevedo and A. M. Uranga, *String Theory Realizations of the Nilpotent Goldstino*, *JHEP* **12** (2015) 039 [1507.07556].

[58] L. Aparicio, F. Quevedo and R. Valandro, *Moduli Stabilisation with Nilpotent Goldstino: Vacuum Structure and SUSY Breaking*, *JHEP* **03** (2016) 036 [1511.08105].

[59] I. n. García-Etxebarria, F. Quevedo and R. Valandro, *Global String Embeddings for the Nilpotent Goldstino*, *JHEP* **02** (2016) 148 [1512.06926].

[60] M. P. Garcia del Moral, S. Parameswaran, N. Quiroz and I. Zavala, *Anti-D3 branes and moduli in non-linear supergravity*, *JHEP* **10** (2017) 185 [1707.07059].

[61] J. Moritz, A. Retolaza and A. Westphal, *Toward de Sitter space from ten dimensions*, *Phys. Rev. D* **97** (2018) 046010 [1707.08678].

[62] C. Crinò, F. Quevedo and R. Valandro, *On de Sitter String Vacua from Anti-D3-Branes in the Large Volume Scenario*, *JHEP* **03** (2021) 258 [2010.15903].

[63] M. Cicoli, F. Quevedo and R. Valandro, *De Sitter from T-branes*, *JHEP* **03** (2016) 141 [1512.04558].

[64] M. Cicoli, A. Maharana, F. Quevedo and C. P. Burgess, *De Sitter String Vacua from Dilaton-dependent Non-perturbative Effects*, *JHEP* **06** (2012) 011 [1203.1750].

[65] D. Gallego, M. C. D. Marsh, B. Vercnocke and T. Wrase, *A New Class of de Sitter Vacua in Type IIB Large Volume Compactifications*, *JHEP* **10** (2017) 193 [1707.01095].

[66] A. Hebecker and S. Leonhardt, *Winding Uplifts and the Challenges of Weak and Strong SUSY Breaking in AdS*, *JHEP* **03** (2021) 284 [2012.00010].

[67] N. Arkani-Hamed, L. Motl, A. Nicolis and C. Vafa, *The String landscape, black holes and gravity as the weakest force*, *JHEP* **06** (2007) 060 [hep-th/0601001].

[68] T. Rudelius, *Constraints on Axion Inflation from the Weak Gravity Conjecture*, *JCAP* **09** (2015) 020 [1503.00795].

[69] J. Brown, W. Cottrell, G. Shiu and P. Soler, *Fencing in the Swampland: Quantum Gravity Constraints on Large Field Inflation*, *JHEP* **10** (2015) 023 [1503.04783].

[70] A. Hebecker, F. Rompineve and A. Westphal, *Axion Monodromy and the Weak Gravity Conjecture*, *JHEP* **04** (2016) 157 [1512.03768].

[71] M. Demirtas, C. Long, L. McAllister and M. Stillman, *Minimal Surfaces and Weak Gravity*, *JHEP* **03** (2020) 021 [1906.08262].

[72] M. Montero, T. Van Riet and G. Venken, *Festina Lente: EFT Constraints from Charged Black Hole Evaporation in de Sitter*, *JHEP* **01** (2020) 039 [1910.01648].

[73] M. Montero, C. Vafa, T. Van Riet and G. Venken, *The FL bound and its phenomenological implications*, 2106.07650.

[74] H. Nariai, *On Some Static Solutions of Einstein's Gravitational Field Equations in a Spherically Symmetric Case*, *General Relativity and Gravitation* **31** (1999) 945.

[75] L. J. Romans, *Supersymmetric, cold and lukewarm black holes in cosmological Einstein-Maxwell theory*, *Nucl. Phys. B* **383** (1992) 395 [hep-th/9203018].

[76] A. Hebecker, S. Leonhardt, J. Moritz and A. Westphal, *Thraxions: Ultralight Throat Axions*, *JHEP* **04** (2019) 158 [1812.03999].

[77] P. Candelas and X. C. de la Ossa, *Comments on Conifolds*, *Nucl. Phys. B* **342** (1990) 246.

[78] P. Candelas, P. S. Green and T. Hubsch, *Rolling Among Calabi-Yau Vacua*, *Nucl. Phys. B* **330** (1990) 49.

[79] P. Candelas, X. C. De La Ossa, P. S. Green and L. Parkes, *A Pair of Calabi-Yau manifolds as an exactly soluble superconformal theory*, *Nucl. Phys. B* **359** (1991) 21.

[80] P. Candelas, P. S. Green and T. Hübsch, *Finite distance between distinct calabi-yau manifolds*, *Phys. Rev. Lett.* **62** (1989) 1956.

[81] M. Reid, *The moduli space of 3-folds with $k = 0$ may nevertheless be irreducible.*, *Mathematische Annalen* **278** (1987) 329.

[82] T.-m. Chiang, B. R. Greene, M. Gross and Y. Kanter, *Black hole condensation and the web of Calabi-Yau manifolds*, *Nucl. Phys. B Proc. Suppl.* **46** (1996) 82 [hep-th/9511204].

[83] A. C. Avram, M. Kreuzer, M. Mandelberg and H. Skarke, *The Web of Calabi-Yau hypersurfaces in toric varieties*, *Nucl. Phys. B* **505** (1997) 625 [hep-th/9703003].

[84] V. V. Batyrev, *Dual polyhedra and mirror symmetry for Calabi-Yau hypersurfaces in toric varieties*, *J. Alg. Geom.* **3** (1994) 493 [alg-geom/9310003].

[85] V. Batyrev and M. Kreuzer, *Constructing new Calabi-Yau 3-folds and their mirrors via conifold transitions*, *Adv. Theor. Math. Phys.* **14** (2010) 879 [0802.3376].

[86] M. Lynker and R. Schimmrigk, *Conifold transitions and mirror symmetries*, *Nucl. Phys. B* **484** (1997) 562 [hep-th/9511058].

[87] V. V. Batyrev, I. Ciocan-Fontanine, B. Kim and D. van Straten, *Conifold transitions and mirror symmetry for Calabi-Yau complete intersections in Grassmannians*, *Nucl. Phys. B* **514** (1998) 640 [alg-geom/9710022].

[88] F. Carta, J. Moritz and A. Westphal, *A landscape of orientifold vacua*, *JHEP* **05** (2020) 107 [2003.04902].

[89] S. Sethi, C. Vafa and E. Witten, *Constraints on low dimensional string compactifications*, *Nucl. Phys. B* **480** (1996) 213 [hep-th/9606122].

[90] I. R. Klebanov and A. A. Tseytlin, *Gravity duals of supersymmetric SU(N) x SU(N+M) gauge theories*, *Nucl. Phys. B* **578** (2000) 123 [hep-th/0002159].

[91] I. R. Klebanov and M. J. Strassler, *Supergravity and a confining gauge theory: Duality cascades and chi SB resolution of naked singularities*, *JHEP* **08** (2000) 052 [hep-th/0007191].

[92] L. Randall and R. Sundrum, *A Large mass hierarchy from a small extra dimension*, *Phys. Rev. Lett.* **83** (1999) 3370 [hep-ph/9905221].

[93] M. Grana, *Flux compactifications in string theory: A Comprehensive review*, *Phys. Rept.* **423** (2006) 91 [hep-th/0509003].

[94] H. Jockers and J. Louis, *D-terms and F-terms from D7-brane fluxes*, *Nucl. Phys. B* **718** (2005) 203 [hep-th/0502059].

[95] T. W. Grimm, M. Kerstan, E. Palti and T. Weigand, *On Fluxed Instantons and Moduli Stabilisation in IIB Orientifolds and F-theory*, *Phys. Rev. D* **84** (2011) 066001 [1105.3193].

[96] C. Long, L. McAllister and P. McGuirk, *Aligned Natural Inflation in String Theory*, *Phys. Rev. D* **90** (2014) 023501 [1404.7852].

[97] J. Moritz, *On accelerated expansion in string theory*, Ph.D. thesis, Hamburg U., 2019. 10.3204/PUBDB-2019-02649.

[98] M. Demirtas, M. Kim, L. Mcallister and J. Moritz, *Conifold Vacua with Small Flux Superpotential*, 2009.03312.

[99] X. Gao and P. Shukla, *F-term Stabilization of Odd Axions in LARGE Volume Scenario*, *Nucl. Phys. B* **878** (2014) 269 [1307.1141].

[100] M. Cicoli, A. Schachner and P. Shukla, *Systematics of type IIB moduli stabilisation with odd axions*, 2109.14624.

[101] W. Hu, R. Barkana and A. Gruzinov, *Cold and fuzzy dark matter*, *Phys. Rev. Lett.* **85** (2000) 1158 [astro-ph/0003365].

[102] L. Hui, J. P. Ostriker, S. Tremaine and E. Witten, *Ultralight scalars as cosmological dark matter*, *Phys. Rev. D* **95** (2017) 043541 [1610.08297].

[103] S. Gandhi, L. McAllister and S. Sjors, *A Toolkit for Perturbing Flux Compactifications*, *JHEP* **12** (2011) 053 [1106.0002].

[104] D. Baumann, A. Dymarsky, S. Kachru, I. R. Klebanov and L. McAllister, *D3-brane Potentials from Fluxes in AdS/CFT*, *JHEP* **06** (2010) 072 [1001.5028].

[105] S. Andriolo, D. Junghans, T. Noumi and G. Shiu, *A Tower Weak Gravity Conjecture from Infrared Consistency*, *Fortsch. Phys.* **66** (2018) 1800020 [1802.04287].

[106] S. Kachru, J. Pearson and H. L. Verlinde, *Brane / flux annihilation and the string dual of a nonsupersymmetric field theory*, *JHEP* **06** (2002) 021 [hep-th/0112197].

[107] I. Bena, E. Dudas, M. Graña and S. Lüst, *Uplifting Runaways*, *Fortsch. Phys.* **67** (2019) 1800100 [1809.06861].

[108] I. Bena, J. Blåbäck, M. Graña and S. Lüst, *The Tadpole Problem*, 2010.10519.

[109] M. Kreuzer and H. Skarke, *Complete classification of reflexive polyhedra in four-dimensions*, *Adv. Theor. Math. Phys.* **4** (2002) 1209 [hep-th/0002240].

[110] WMAP collaboration, *Nine-Year Wilkinson Microwave Anisotropy Probe (WMAP) Observations: Cosmological Parameter Results*, *Astrophys. J. Suppl.* **208** (2013) 19 [1212.5226].

[111] Planck collaboration, *Planck 2018 results. X. Constraints on inflation*, *Astron. Astrophys.* **641** (2020) A10 [1807.06211].

[112] BICEP2, Keck Array collaboration, *BICEP2 / Keck Array x: Constraints on Primordial Gravitational Waves using Planck, WMAP, and New BICEP2/Keck Observations through the 2015 Season*, *Phys. Rev. Lett.* **121** (2018) 221301 [1810.05216].

[113] D. Scolnic et al., *The Complete Light-curve Sample of Spectroscopically Confirmed SNe Ia from Pan-STARRS1 and Cosmological Constraints from the Combined Pantheon Sample*, *Astrophys. J.* **859** (2018) 101 [1710.00845].

[114] DES collaboration, *Dark Energy Survey year 1 results: Cosmological constraints from galaxy clustering and weak lensing*, *Phys. Rev. D* **98** (2018) 043526 [1708.01530].

[115] A. de Mattia et al., *The Completed SDSS-IV extended Baryon Oscillation Spectroscopic Survey: measurement of the BAO and growth rate of structure of the emission line galaxy sample from the anisotropic power spectrum between redshift 0.6 and 1.1*, 2007.09008.

[116] A. H. Guth, *The Inflationary Universe: A Possible Solution to the Horizon and Flatness Problems*, *Phys. Rev. D* **23** (1981) 347.

[117] A. D. Linde, *A New Inflationary Universe Scenario: A Possible Solution of the Horizon, Flatness, Homogeneity, Isotropy and Primordial Monopole Problems*, *Phys. Lett. B* **108** (1982) 389.

[118] A. Albrecht and P. J. Steinhardt, *Cosmology for Grand Unified Theories with Radiatively Induced Symmetry Breaking*, *Phys. Rev. Lett.* **48** (1982) 1220.

[119] Planck collaboration, *Planck 2018 results. I. Overview and the cosmological legacy of Planck*, *Astron. Astrophys.* **641** (2020) A1 [1807.06205].

[120] D. Baumann, *Inflation*, in *Theoretical Advanced Study Institute in Elementary Particle Physics: Physics of the Large and the Small*, pp. 523–686, 2011, 0907.5424, DOI.

[121] D. Baumann and L. McAllister, *Inflation and String Theory*, Cambridge Monographs on Mathematical Physics. Cambridge University Press, 2015, 10.1017/CBO9781316105733, [1404.2601].

[122] Planck collaboration, *Planck 2018 results. X. Constraints on inflation*, *Astron. Astrophys.* **641** (2020) A10 [1807.06211].

[123] A. A. Starobinsky, *Spectrum of relict gravitational radiation and the early state of the universe*, *JETP Lett.* **30** (1979) 682.

[124] D. H. Lyth, *What would we learn by detecting a gravitational wave signal in the cosmic microwave background anisotropy?*, *Phys. Rev. Lett.* **78** (1997) 1861 [hep-ph/9606387].

[125] N. Stebor et al., *The Simons Array CMB polarization experiment*, *Proc. SPIE Int. Soc. Opt. Eng.* **9914** (2016) 99141H.

[126] Simons Observatory collaboration, *The Simons Observatory: Science goals and forecasts*, *JCAP* **02** (2019) 056 [1808.07445].

[127] H. Hui et al., *BICEP Array: a multi-frequency degree-scale CMB polarimeter*, *Proc. SPIE Int. Soc. Opt. Eng.* **10708** (2018) 1070807 [1808.00568].

[128] CMB-S4 collaboration, *CMB-S4 Science Book, First Edition*, 1610.02743.

[129] K. Abazajian et al., *CMB-S4 Science Case, Reference Design, and Project Plan*, 1907.04473.

[130] K. Abazajian et al., *CMB-S4 Decadal Survey APC White Paper*, *Bull. Am. Astron. Soc.* **51** (2019) 209 [1908.01062].

[131] A. Kogut et al., *The Primordial Inflation Explorer (PIXIE): A Nulling Polarimeter for Cosmic Microwave Background Observations*, *JCAP* **07** (2011) 025 [1105.2044].

[132] M. Hazumi et al., *LiteBIRD: A Satellite for the Studies of B-Mode Polarization and Inflation from Cosmic Background Radiation Detection*, *J. Low Temp. Phys.* **194** (2019) 443.

[133] H. Sugai et al., *Updated Design of the CMB Polarization Experiment Satellite LiteBIRD*, *J. Low Temp. Phys.* (2020) [2001.01724].

[134] E. J. Copeland, A. R. Liddle, D. H. Lyth, E. D. Stewart and D. Wands, *False vacuum inflation with Einstein gravity*, *Phys. Rev. D* **49** (1994) 6410 [astro-ph/9401011].

[135] A. Westphal, *String cosmology — Large-field inflation in string theory*, *Int. J. Mod. Phys. A* **30** (2015) 1530024 [1409.5350].

[136] E. Pajer and M. Peloso, *A review of Axion Inflation in the era of Planck*, *Class. Quant. Grav.* **30** (2013) 214002 [1305.3557].

[137] D. Baumann and L. McAllister, *Inflation and String Theory*, Cambridge Monographs on Mathematical Physics. Cambridge University Press, 5, 2015, 10.1017/CBO9781316105733, [1404.2601].

[138] K. Freese, J. A. Frieman and A. V. Olinto, *Natural inflation with pseudo - Nambu-Goldstone bosons*, *Phys. Rev. Lett.* **65** (1990) 3233.

[139] J. E. Kim, H. P. Nilles and M. Peloso, *Completing natural inflation*, *JCAP* **01** (2005) 005 [hep-ph/0409138].

[140] T. Banks and N. Seiberg, *Symmetries and Strings in Field Theory and Gravity*, *Phys. Rev. D* **83** (2011) 084019 [1011.5120].

[141] S. Dimopoulos, S. Kachru, J. McGreevy and J. G. Wacker, *N-flation*, *JCAP* **08** (2008) 003 [hep-th/0507205].

[142] T. Rudelius, *On the Possibility of Large Axion Moduli Spaces*, *JCAP* **04** (2015) 049 [1409.5793].

[143] E. Silverstein and A. Westphal, *Monodromy in the CMB: Gravity Waves and String Inflation*, *Phys. Rev. D* **78** (2008) 106003 [0803.3085].

[144] L. McAllister, E. Silverstein and A. Westphal, *Gravity Waves and Linear Inflation from Axion Monodromy*, *Phys. Rev. D* **82** (2010) 046003 [0808.0706].

[145] L. McAllister, E. Silverstein, A. Westphal and T. Wrase, *The Powers of Monodromy*, *JHEP* **09** (2014) 123 [1405.3652].

[146] F. Marchesano, G. Shiu and A. M. Uranga, *F-term Axion Monodromy Inflation*, *JHEP* **09** (2014) 184 [1404.3040].

[147] N. Kaloper and L. Sorbo, *A Natural Framework for Chaotic Inflation*, *Phys. Rev. Lett.* **102** (2009) 121301 [0811.1989].

[148] R. Flauger, L. McAllister, E. Silverstein and A. Westphal, *Drifting Oscillations in Axion Monodromy*, *JCAP* **10** (2017) 055 [1412.1814].

[149] R. Flauger and E. Pajer, *Resonant Non-Gaussianity*, *JCAP* **01** (2011) 017 [1002.0833].

[150] Planck collaboration, *Planck 2018 results. IX. Constraints on primordial non-Gaussianity*, *Astron. Astrophys.* **641** (2020) A9 [1905.05697].

[151] A. D. Linde, *Hybrid inflation*, *Phys. Rev.* **D49** (1994) 748 [astro-ph/9307002].

[152] J. Garcia-Bellido and A. D. Linde, *Preheating in hybrid inflation*, *Phys. Rev. D* **57** (1998) 6075 [hep-ph/9711360].

[153] L. Kofman, *Tachyonic preheating*, in *8th International Symposium on Particles Strings and Cosmology*, pp. 167–182, 2001, hep-ph/0107280.

[154] M. A. Amin, M. P. Hertzberg, D. I. Kaiser and J. Karouby, *Nonperturbative Dynamics Of Reheating After Inflation: A Review*, *Int. J. Mod. Phys. D* **24** (2014) 1530003 [1410.3808].

[155] D. G. Figueroa and F. Torrenti, *Gravitational wave production from preheating: parameter dependence*, *JCAP* **10** (2017) 057 [1707.04533].

[156] M. Gleiser, N. Graham and N. Stamatopoulos, *Generation of Coherent Structures After Cosmic Inflation*, *Phys. Rev. D* **83** (2011) 096010 [1103.1911].

[157] G. N. Felder, J. Garcia-Bellido, P. B. Greene, L. Kofman, A. D. Linde and I. Tkachev, *Dynamics of symmetry breaking and tachyonic preheating*, *Phys. Rev. Lett.* **87** (2001) 011601 [hep-ph/0012142].

[158] G. N. Felder, L. Kofman and A. D. Linde, *Tachyonic instability and dynamics of spontaneous symmetry breaking*, *Phys. Rev. D* **64** (2001) 123517 [hep-th/0106179].

[159] T. Asaka, W. Buchmuller and L. Covi, *False vacuum decay after inflation*, *Phys. Lett. B* **510** (2001) 271 [hep-ph/0104037].

[160] E. J. Copeland, S. Pascoli and A. Rajantie, *Dynamics of tachyonic preheating after hybrid inflation*, *Phys. Rev. D* **65** (2002) 103517 [hep-ph/0202031].

[161] D. H. Lyth, *Contribution of the hybrid inflation waterfall to the primordial curvature perturbation*, *JCAP* **07** (2011) 035 [1012.4617].

[162] Y. Zeldovich, I. Kobzarev and L. Okun, *Cosmological Consequences of the Spontaneous Breakdown of Discrete Symmetry*, *Zh. Eksp. Teor. Fiz.* **67** (1974) 3.

[163] A. Vilenkin, *Cosmic Strings and Domain Walls*, *Phys. Rept.* **121** (1985) 263.

[164] V. Mukhanov, *Physical Foundations of Cosmology*. Cambridge University Press, Oxford, 2005.

[165] L. Kofman, A. D. Linde and A. A. Starobinsky, *Reheating after inflation*, *Phys. Rev. Lett.* **73** (1994) 3195 [hep-th/9405187].

[166] L. Kofman, A. D. Linde and A. A. Starobinsky, *Towards the theory of reheating after inflation*, *Phys. Rev. D* **56** (1997) 3258 [hep-ph/9704452].

[167] M. Dias, J. Frazer and D. Seery, *Computing observables in curved multifield models of inflation—A guide (with code) to the transport method*, *JCAP* **12** (2015) 030 [1502.03125].

[168] P. J. Steinhardt, *NATURAL INFLATION*, in *Nuffield Workshop on the Very Early Universe*, pp. 251–266, 7, 1982.

[169] A. Vilenkin, *The Birth of Inflationary Universes*, *Phys. Rev. D* **27** (1983) 2848.

[170] A. D. Linde, *Eternally Existing Selfreproducing Chaotic Inflationary Universe*, *Phys. Lett. B* **175** (1986) 395.

[171] A. D. Linde, *Particle physics and inflationary cosmology*, vol. 5. 1990, [hep-th/0503203].

[172] A. H. Guth, *Eternal inflation and its implications*, *J. Phys. A* **40** (2007) 6811 [hep-th/0702178].

[173] S. R. Coleman and F. De Luccia, *Gravitational Effects on and of Vacuum Decay*, *Phys. Rev. D* **21** (1980) 3305.

[174] M. Cicoli, S. Krippendorf, C. Mayrhofer, F. Quevedo and R. Valandro, *D-Branes at del Pezzo Singularities: Global Embedding and Moduli Stabilisation*, *JHEP* **09** (2012) 019 [1206.5237].

[175] J. P. Conlon, F. Quevedo and K. Suruliz, *Large-volume flux compactifications: Moduli spectrum and D3/D7 soft supersymmetry breaking*, *JHEP* **08** (2005) 007 [hep-th/0505076].

[176] K. Bobkov, V. Braun, P. Kumar and S. Raby, *Stabilizing All Kahler Moduli in Type IIB Orientifolds*, *JHEP* **12** (2010) 056 [1003.1982].

[177] R. Blumenhagen, S. Moster and E. Plauschinn, *Moduli Stabilisation versus Chirality for MSSM like Type IIB Orientifolds*, *JHEP* **01** (2008) 058 [0711.3389].

[178] A. Hebecker, P. Mangat, F. Rompineve and L. T. Witkowski, *Winding out of the Swamp: Evading the Weak Gravity Conjecture with F-term Winding Inflation?*, *Phys. Lett. B* **748** (2015) 455 [1503.07912].

[179] G. von Gersdorff and A. Hebecker, *Kahler corrections for the volume modulus of flux compactifications*, *Phys. Lett. B* **624** (2005) 270 [hep-th/0507131].

[180] M. Cicoli, J. P. Conlon and F. Quevedo, *General Analysis of LARGE Volume Scenarios with String Loop Moduli Stabilisation*, *JHEP* **10** (2008) 105 [0805.1029].

[181] D. Junghans, *LVS de Sitter Vacua are probably in the Swampland*, 2201.03572.

[182] X. Gao, A. Hebecker, S. Schreyer and G. Venken, *The LVS Parametric Tadpole Constraint*, 2202.04087.

[183] A. Hebecker, S. C. Kraus and A. Westphal, *Evading the Lyth Bound in Hybrid Natural Inflation*, *Phys. Rev. D* **88** (2013) 123506 [1305.1947].

[184] G. G. Ross and G. German, *Hybrid natural inflation from non Abelian discrete symmetry*, *Phys. Lett. B* **684** (2010) 199 [0902.4676].

[185] N. Kaloper, M. Koenig, A. Lawrence and J. H. Scargill, *On Hybrid Monodromy Inflation (Hic Sunt Dracones)*, 2006.13960.

[186] N. Kaloper, A. Lawrence and L. Sorbo, *An Ignoble Approach to Large Field Inflation*, *JCAP* **03** (2011) 023 [1101.0026].

[187] E. D. Stewart, *Mutated hybrid inflation*, *Phys. Lett. B* **345** (1995) 414 [astro-ph/9407040].

[188] A. Hebecker, J. Jaeckel and M. Wittner, *Axions in String Theory and the Hydra of Dark Radiation*, 2203.08833.

[189] A. Hebecker, T. Mikhail and P. Soler, *Euclidean wormholes, baby universes, and their impact on particle physics and cosmology*, *Front. Astron. Space Sci.* **5** (2018) 35 [1807.00824].

[190] A. Klemm and M. Kreuzer, "Instanton (1.0)." http://hep.itp.tuwien.ac.at/~kreuzer/pub/prog/inst.m, 2001.

[191] A. Hebecker, D. Junghans and A. Schachner, *Large Field Ranges from Aligned and Misaligned Winding*, *JHEP* **03** (2019) 192 [1812.05626].

[192] Planck collaboration, *Planck 2018 results. VI. Cosmological parameters*, *Astron. Astrophys.* **641** (2020) A6 [1807.06209].

[193] V. C. Rubin and J. Ford, W. Kent, *Rotation of the Andromeda Nebula from a Spectroscopic Survey of Emission Regions*, *APJ* **159** (1970) 379.

[194] J. P. Ostriker, P. J. E. Peebles and A. Yahil, *The Size and Mass of Galaxies, and the Mass of the Universe*, *APJL* **193** (1974) L1.

[195] J. S. Bullock and M. Boylan-Kolchin, *Small-scale challenges to the lambda-cdm paradigm*, *Annual Review of Astronomy and Astrophysics* **55** (2017) 343–387.

[196] A. M. Brooks, M. Kuhlen, A. Zolotov and D. Hooper, *A baryonic solution to the missing satellites problem*, *The Astrophysical Journal* **765** (2013) 22.

[197] D. N. Spergel and P. J. Steinhardt, *Observational evidence for selfinteracting cold dark matter*, *Phys. Rev. Lett.* **84** (2000) 3760 [astro-ph/9909386].

[198] J. I. Read, M. G. Walker and P. Steger, *Dark matter heats up in dwarf galaxies*, *Mon. Not. Roy. Astron. Soc.* **484** (2019) 1401 [1808.06634].

[199] P. Colin, V. Avila-Reese and O. Valenzuela, *Substructure and halo density profiles in a warm dark matter cosmology*, *Astrophys. J.* **542** (2000) 622 [astro-ph/0004115].

[200] P. Salucci, *The distribution of dark matter in galaxies*, *Astron. Astrophys. Rev.* **27** (2019) 2 [1811.08843].

[201] H.-Y. Schive, T. Chiueh and T. Broadhurst, *Cosmic Structure as the Quantum Interference of a Coherent Dark Wave*, *Nature Phys.* **10** (2014) 496 [1406.6586].

[202] L. Hui, *Wave Dark Matter*, 2101.11735.

[203] H.-Y. Schive, M.-H. Liao, T.-P. Woo, S.-K. Wong, T. Chiueh, T. Broadhurst et al., *Understanding the Core-Halo Relation of Quantum Wave Dark Matter from 3D Simulations*, *Phys. Rev. Lett.* **113** (2014) 261302 [1407.7762].

[204] D. J. Marsh and J. C. Niemeyer, *Strong Constraints on Fuzzy Dark Matter from Ultrafaint Dwarf Galaxy Eridanus II*, *Phys. Rev. Lett.* **123** (2019) 051103 [1810.08543].

[205] K. Hayashi, E. G. M. Ferreira and H. Y. J. Chan, *Narrowing the Mass Range of Fuzzy Dark Matter with Ultrafaint Dwarfs*, *Astrophys. J. Lett.* **912** (2021) L3 [2102.05300].

[206] D. Jones, S. Palatnick, R. Chen, A. Beane and A. Lidz, *Fuzzy Dark Matter and the 21cm Power Spectrum*, *Astrophys. J.* **913** (2021) 7 [2101.07177].

[207] DES collaboration, *Milky Way Satellite Census. III. Constraints on Dark Matter Properties from Observations of Milky Way Satellite Galaxies*, *Phys. Rev. Lett.* **126** (2021) 091101 [2008.00022].

[208] L. Zu, L. Feng, Q. Yuan and Y.-Z. Fan, *Stringent constraints on the light boson model with supermassive black hole spin measurements*, *Eur. Phys. J. Plus* **135** (2020) 709 [2007.03222].

[209] O. Nebrin, R. Ghara and G. Mellema, *Fuzzy dark matter at cosmic dawn: new 21-cm constraints*, *Journal of Cosmology and Astroparticle Physics* **2019** (2019) 051–051.

[210] A. Maleki, S. Baghram and S. Rahvar, *Constraint on the mass of fuzzy dark matter from the rotation curve of the Milky Way*, *Phys. Rev. D* **101** (2020) 103504 [2001.04454].

[211] D. J. E. Marsh and S. Hoof, *Astrophysical Searches and Constraints on Ultralight Bosonic Dark Matter*, 2106.08797.

[212] A. Arvanitaki, S. Dimopoulos, M. Galanis, L. Lehner, J. O. Thompson and K. Van Tilburg, *Large-misalignment mechanism for the formation of compact axion structures: Signatures from the QCD axion to fuzzy dark matter*, *Phys. Rev. D* **101** (2020) 083014 [1909.11665].

[213] B. Schwabe, M. Gosenca, C. Behrens, J. C. Niemeyer and R. Easther, *Simulating mixed fuzzy and cold dark matter*, *Phys. Rev. D* **102** (2020) 083518 [2007.08256].

[214] H. N. Luu, S.-H. H. Tye and T. Broadhurst, *Multiple Ultralight Axionic Wave Dark Matter and Astronomical Structures*, *Phys. Dark Univ.* **30** (2020) 100636 [1811.03771].

[215] L. Visinelli and S. Vagnozzi, *Cosmological window onto the string axiverse and the supersymmetry breaking scale*, *Phys. Rev. D* **99** (2019) 063517 [1809.06382].

[216] R. Alonso and A. Urbano, *Wormholes and masses for Goldstone bosons*, *JHEP* **02** (2019) 136 [1706.07415].

[217] P. Candelas, A. M. Dale, C. A. Lutken and R. Schimmrigk, *Complete Intersection Calabi-Yau Manifolds*, *Nucl. Phys. B* **298** (1988) 493.

[218] S. Ashok and M. R. Douglas, *Counting flux vacua*, *JHEP* **01** (2004) 060 [hep-th/0307049].

[219] F. Denef and M. R. Douglas, *Distributions of flux vacua*, *JHEP* **05** (2004) 072 [hep-th/0404116].

[220] A. Hebecker and J. March-Russell, *The Ubiquitous throat*, *Nucl. Phys. B* **781** (2007) 99 [hep-th/0607120].

[221] X. Gao and P. Shukla, *F-term stabilization of odd axions in large volume scenario*, *Nuclear Physics B* **878** (2014) 269–294.

[222] K. Hristov, *Axion stabilization in type iib flux compactifications*, *Journal of High Energy Physics* **2009** (2009) 046–046.

[223] P. W. Graham and A. Scherlis, *Stochastic axion scenario*, *Phys. Rev. D* **98** (2018) 035017 [1805.07362].

[224] M. Berg, M. Haack and B. Kors, *Loop corrections to volume moduli and inflation in string theory*, *Phys. Rev. D* **71** (2005) 026005 [hep-th/0404087].

[225] X. Gao and P. Shukla, *On Classifying the Divisor Involutions in Calabi-Yau Threefolds*, *JHEP* **11** (2013) 170 [1307.1139].

[226] X. Dong, B. Horn, E. Silverstein and A. Westphal, *Simple exercises to flatten your potential*, *Phys. Rev. D* **84** (2011) 026011 [1011.4521].

[227] H. Jockers, *The Effective Action of D-branes in Calabi-Yau Orientifold Compactifications*, *Fortsch. Phys.* **53** (2005) 1087 [hep-th/0507042].

[228] D. J. E. Marsh, *Axion Cosmology*, *Phys. Rept.* **643** (2016) 1 [1510.07633].

[229] I. Broeckel, M. Cicoli, A. Maharana, K. Singh and K. Sinha, *Moduli stabilisation and the statistics of axion physics in the landscape*, *Journal of High Energy Physics* **2021** (2021) .

[230] V. M. Mehta, M. Demirtas, C. Long, D. J. E. Marsh, L. Mcallister and M. J. Stott, *Superradiance Exclusions in the Landscape of Type IIB String Theory*, 2011.08693.

[231] J. J. Blanco-Pillado, K. Sousa, M. A. Urkiola and J. M. Wachter, *Towards a complete mass spectrum of type-IIB flux vacua at large complex structure*, *JHEP* **04** (2021) 149 [2007.10381].

[232] M. Demirtas, M. Kim, L. McAllister and J. Moritz, *Vacua with small flux superpotential*, *Physical Review Letters* **124** (2020) .

[233] M. Demirtas, M. Kim, L. McAllister and J. Moritz, *Conifold vacua with small flux superpotential*, *Fortschritte der Physik* **68** (2020) 2000085.

[234] R. Álvarez-García, R. Blumenhagen, M. Brinkmann and L. Schlechter, *Small Flux Superpotentials for Type IIB Flux Vacua Close to a Conifold*, 2009.03325.

[235] M. Demirtas, C. Long, L. McAllister and M. Stillman, *The Kreuzer-Skarke Axiverse*, *JHEP* **04** (2020) 138 [1808.01282].

[236] T. Hubsch, *Calabi-Yau manifolds: A Bestiary for physicists*. World Scientific, Singapore, 1994.

[237] L. B. Anderson and M. Karkheiran, *TASI Lectures on Geometric Tools for String Compactifications*, *PoS* **TASI2017** (2018) 013 [1804.08792].

[238] P. Green and T. Hubsch, *Calabi-yau Manifolds as Complete Intersections in Products of Complex Projective Spaces*, *Commun. Math. Phys.* **109** (1987) 99.

[239] L. B. Anderson, X. Gao, J. Gray and S.-J. Lee, *Fibrations in CICY Threefolds*, *JHEP* **10** (2017) 077 [1708.07907].

[240] J. Kollar, *Deformations of elliptic Calabi-Yau manifolds*, 1206.5721.

[241] P. Candelas and X. de la Ossa, *Moduli space of Calabi-Yau manifolds*, in *XIII International School of Theoretical Physics: The Standard Model and Beyond*, pp. 215–242, 9, 1989.

[242] C. T. C. Wall, *Classification Problems in Differential Topology. V. On Certain 6-Manifolds.*, *Inventiones Mathematicae* **1** (1966) 355.

[243] A. Avram, P. Candelas, D. Jancic and M. Mandelberg, *On the connectedness of moduli spaces of Calabi-Yau manifolds*, *Nucl. Phys. B* **465** (1996) 458 [hep-th/9511230].

[244] P. Candelas, X. de la Ossa, Y.-H. He and B. Szendroi, *Triadophilia: A Special Corner in the Landscape*, *Adv. Theor. Math. Phys.* **12** (2008) 429 [0706.3134].

[245] L. B. Anderson, Y.-H. He and A. Lukas, *Monad Bundles in Heterotic String Compactifications*, *JHEP* **07** (2008) 104 [0805.2875].

[246] A.-m. He and P. Candelas, *On the Number of Complete Intersection {Calabi-Yau} Manifolds*, *Commun. Math. Phys.* **135** (1990) 193.

[247] S. Hosono, A. Klemm, S. Theisen and S.-T. Yau, *Mirror symmetry, mirror map and applications to Calabi-Yau hypersurfaces*, *Commun. Math. Phys.* **167** (1995) 301 [hep-th/9308122].

[248] S. Hosono, A. Klemm, S. Theisen and S.-T. Yau, *Mirror symmetry, mirror map and applications to complete intersection Calabi-Yau spaces*, *AMS/IP Stud. Adv. Math.* **1** (1996) 545 [hep-th/9406055].

[249] J. P. Conlon, A. Maharana and F. Quevedo, *Towards Realistic String Vacua*, *JHEP* **05** (2009) 109 [0810.5660].

[250] J. P. Conlon, D. Cremades and F. Quevedo, *Kahler potentials of chiral matter fields for Calabi-Yau string compactifications*, *JHEP* **01** (2007) 022 [hep-th/0609180].

[251] M. Cicoli, D. Klevers, S. Krippendorf, C. Mayrhofer, F. Quevedo and R. Valandro, *Explicit de Sitter Flux Vacua for Global String Models with Chiral Matter*, *JHEP* **05** (2014) 001 [1312.0014].

[252] R. Blumenhagen and M. Schmidt-Sommerfeld, *Power Towers of String Instantons for N=1 Vacua*, *JHEP* **07** (2008) 027 [0803.1562].

[253] L. Visinelli and P. Gondolo, *Dark Matter Axions Revisited*, *Phys. Rev. D* **80** (2009) 035024 [0903.4377].

[254] L. Visinelli, *Light axion-like dark matter must be present during inflation*, *Phys. Rev. D* **96** (2017) 023013 [1703.08798].

[255] M. Reig, *The Stochastic Axiverse*, *JHEP* **09** (2021) 207 [2104.09923].

[256] N. Kitajima and F. Takahashi, *Resonant conversions of QCD axions into hidden axions and suppressed isocurvature perturbations*, *JCAP* **01** (2015) 032 [1411.2011].